

Reactivity of sodium pentaphospholide
towards $C\equiv E$ (E = C, N, P, As) triple bonds

A Dissertation

Submitted in Partial Fulfilment of the Requirements for the
Degree of *Doctor Rerum Naturalium* (*Dr. rer. nat.*)

to the Department of Biology, Chemistry, Pharmacy
of Freie Universität Berlin

by

Andrey Petrov

Berlin, 2022

Supervisor: Prof. Dr. Christian Müller

Second examiner: Prof. Dr. Sebastian Hasenstab-Riedel

Date of defense: 28.11.2022

The described work was carried out within the period between April 2019 and June 2022 at Freie Universität Berlin under the supervision of Prof. Dr. Christian Müller.

Acknowledgement

First of all, I would like to thank Prof Dr. Christian Müller for the opportunity to join his group and perform a research project under his supervision. I am very grateful for all kinds of support and advice I received within the last 3 years.

I would like to thank Prof. Dr. Sebastian Hasenstab-Riedel for being the second reviewer of my dissertation.

I thank Dr. Nathan Coles and Dr. Jelena Wiecko for their support and precious advises. Special thanks to Manuela Weber for the help with the SC-XRD analysis of the single crystals and Lea Dettling for the DFT calculations. I am thankful to Dr. Simon Steinhauer and Dr. Friedrich Wossidlo for the assistance with the special NMR experiments.

I am very grateful to Dr. Sebastien Lapointe, Dr. Jelena Wiecko for the proof-reading of the thesis. I would like to thank Sabrina and Moritz for their help. Special thanks to my old chemistry faculty friends Airat, Aidar, and Ilya for their comments on my dissertation.

I would like to thank my colleagues Dr. Steven Giese, Dr. Daniel Frost, Tim Görlich, Jinxiong Lin, Lea Dettling, Lara Šibila, Luise Sander, Richard Kopp, Moritz Ernst, Dorian Reich, and Markus Peschke for the help, ideas, jokes, peaceful atmosphere in the lab and for the good time we spent together. I thank my bachelor and intern students Dina and Lawrence.

This work would be impossible without 24/7 support of my dear wife Liliia (Tsmok!) and my big family: Irina, Vladimir, Kirill, Zifa and Rifgat.

I am very grateful to my first flatmate in Berlin, Svjetlana Mur, who I miss very much. I would always remember you as an example of the brave and very positive person. I would like to thank my friends Tim Görlich and Timur Bulatov for helping me with the first steps in Berlin.

Special thanks to Asian Snack for helping me to survive in 2020 when Mensa was closed.

Declaration of independence

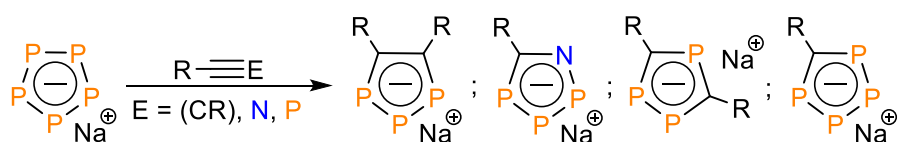
I hereby confirm that I have written my dissertation independently and I have not used any sources other than those I have specified. Intellectual property of other authors has been marked accordingly. I also declare that I have not applied for an examination procedure at any other institution and that I have not submitted the dissertation in this or any other form to any other faculty as a dissertation.

*Dedicated to my grandparents
Aleksi Tokranov and Petr Kozlov.*

Abstract

White phosphorus (P_4) reacts with two equivalents of sodium in refluxing diglyme to give the sodium salt of the aromatic pentaphospholide anion $[cyclo-P_5]^-$, which is considered as the inorganic analog of the classical cyclopentadienyl anion $[Cp]^-$. Indeed, $[cyclo-P_5]^-$ forms sandwich complexes with the η^5 -coordination mode similar to isolobal $[Cp]^-$. However, due to the presence of the energetically and sterically accessible lone pairs on the phosphorus atoms, an additional η^1 -coordination is also feasible. Apart from the coordination to different transition metal centers little is known about the chemical behavior of $[cyclo-P_5]^-$.

In this work, the reactivity of the pentaphospholide anion towards alkynes, nitriles, phosphalkynes, and arsaalkynes is studied (**Scheme I**). The reaction of $[cyclo-P_5]^-$ with the unsaturated compounds results in the formation of novel or barely explored five-membered 6π -electron aromatic heterocycles: 1,2,3-triphospholide anions, 1,2,4-triphospholide anions, 1,2,3,4-tetraphospholide anions, and 1-aza-2,3,4-triphospholide anions. These heterocycles react with $[CpFe(\eta^6\text{-Toluene})]PF_6$ or $FeCl_2(DME)$ to give the corresponding (aza)phosphaferrocenes. The novel compounds are characterized by multinuclear NMR spectroscopy, single-crystal X-ray diffraction analysis (SC-XRD) and cyclic voltammetry. Additionally, the selected species are analyzed quantum chemically.

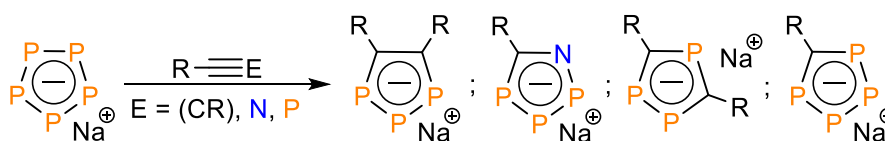


Scheme I. Reactivity of sodium pentaphospholide towards triple bonds.

Zusammenfassung

P_4 reagiert mit zwei Äquivalenten Natrium in refluxierendem Diglyme zum Natriumsalz des aromatischen Pentaphospholid-Anions [*cyclo*- P_5]⁻, welches als anorganisches Analogon zum klassischen Cyclopentadien-Anion [Cp]⁻ angesehen wird. Tatsächlich formt [*cyclo*- P_5]⁻ Sandwichkomplexe im η^5 -Koordinationsmodus, welcher klassischerweise vom isolobalen [Cp]⁻ bekannt ist. Zusätzlich können jedoch durch die energetisch und sterisch zugänglichen, freien Elektronenpaare an den Phosphoratomen - auch Komplexverbindungen in η^1 -Koordinationsmodus zugänglich gemacht werden. Abgesehen von der Koordination an verschiedenen Übergangsmetallzentren ist wenig über das chemische Verhalten von [*cyclo*- P_5]⁻ bekannt.

In der vorliegenden Arbeit wurde die Reaktivität des Pentaphospholid-Anions gegenüber Alkinen, Nitrilen, Phosphoralkinen und Arsaalkinen untersucht (**Schema I**). Die Interaktion zwischen [*cyclo*- P_5]⁻ mit ausgewählten ungesättigten Systemen führt zur Bildung neuer, oder kaum erforschter, fünfgliedriger aromatischer 6π -Elektronen-Heterocyklen: 1,2,3-Triphospholid-Anionen, 1,2,4-Triphospholid-Anionen, 1,2,3,4-Tetraphospholid-Anionen und 1-Aza-2,3,4-triphospholid-Anionen. Die neuen Heterocyklen reagieren mit [$CpFe(\eta^6$ -Toluene)] PF_6 oder $FeCl_2(DME)$ zu den jeweiligen (Aza)Phosphaferrocenen. Die erhaltenen Verbindungen wurden mittels NMR-Spektroskopie, Einkristall-Röntgendiffraktometrie und Cyclovoltammetrie charakterisiert. Zusätzlich wurden ausgewählte Strukturen quantenchemisch untersucht.



Schema I. Reaktivität von Natrium Pentaphospholid gegenüber Dreifachbindungen.

List of publications

Erlin Yue, Andrey Petrov, Daniel S. Frost, Lea Dettling, Lawrence Conrad, Friedrich Wossidlo, Nathan T. Coles, Manuela Weber, and Christian Müller, **Highly flexible phosphabenzenes: a missing coordination mode of 2,4,6-triaryl- λ^3 -phosphinines**, *Chem. Commun.* **2022**, 58, 6184–6187; DOI: <https://doi.org/10.1039/D2CC01817A>.

Andrey Petrov, Lawrence Conrad, Nathan T. Coles, Manuela Weber, Dirk Andrae, Almaz Zagidullin, Vasili Miluykov, and Christian Müller, **Reactivity of sodium pentaphospholide towards $C\equiv E$ (E=C, N, P) triple Bonds**, *to be submitted*.

Andrey Petrov, Nathan T. Coles, Manuela Weber, and Christian Müller, **Synthesis of the tetraphospholide anions**, *to be submitted*.

Table of contents

Chapter 1. Introduction.....	13
1.1 Synthesis of phosphorus-containing compounds	14
1.2 General physical and chemical properties of P ₄	15
1.3 Activation of P ₄ by alkali metals. Polyphosphide anions	16
1.4 Pentaphospholide anion	19
1.5 Chemical properties of pentaphospholide anion	21
1.6 Phospholide anions	25
1.7 Phosphametallocenes	31
1.8 Motivation of this study	32
Chapter 2. Reactivity of the pentaphospholide anion towards C≡C triple bonds. Synthesis of 1,2,3-triphospholide anions.....	34
2.1 Introduction.....	35
2.1.1 1,2,3-triphospholide anions	35
2.2 Results and discussion.....	36
2.2.1 Synthesis of sodium 4,5-dialkyl-1,2,3-triphospholides	36
2.2.2 Synthesis of 4,5-dialkyl-1,2,3-triphosphaferrocenes	42
2.2.3 Synthesis of 1,2,3-triphospholides with the heteroatom-functionalized substituents	46
2.3 Conclusions.....	54
2.4 Experimental part.....	55
2.4.1 General remarks.....	55
2.4.2 Synthesis of alkynes	57
2.4.3 Synthesis of sodium pentaphospholide Na[cyclo-P ₅] (2)	61
2.4.4 Synthesis of sodium 1,2,3-triphospholides	61
2.4.5 Synthesis of 1,2,3-triphosphaferrocenes	65
2.4.6 Crystallographic data for all compounds	68
Chapter 3. Reactivity of the pentaphospholide anion towards C≡N triple bonds. Synthesis of 1-aza-2,3,4-triphospholide anions.	70
3.1 Introduction.....	71
3.1.1 Azaphospholide anions.	71
3.2 Results and discussion.....	74

3.2.1 Synthesis of sodium 1-aza-2,3,4-triphospholides	74
3.2.2 DFT study of the parent 1-aza-2,3,4-triphospholide anion.....	80
3.2.3 Synthesis of 1-aza-2,3,4-triphosphaferrocenes	83
3.3 Conclusions.....	87
3.4 Experimental part.....	88
3.4.1 General remarks.....	88
3.4.2 Synthesis of sodium 1-aza-2,3,4-triphospholides	90
3.4.3 Synthesis of sodium 1-aza-2,3,4-triphospholides	90
3.4.4 Synthesis of 1-aza-2,3,4-triphosphaferrocenes	93
3.4.5 Crystallographic data for all compounds	94
Chapter 4. Reactivity of the pentaphospholide anion towards $C\equiv P$ and $C\equiv As$ triple bonds. Synthesis of 1,2,3,4-tetraphospholide anions.....	96
4.1 Introduction.....	97
4.1.1 Phosphaalkynes.....	97
4.1.2 1,2,3,4-tetraphospholide anions.....	99
4.2 Results and discussion.....	101
4.2.1 Synthesis of sodium 1,2,4-triphospholides and 1,2,3,4-tetraphospholides	101
4.2.2 Synthesis of 1,2,3,4-tetraphospholide anions	106
4.2.3 Synthesis of 1,2,4-triphosphaferrocenes and 1,2,3,4-tetraphosphaferrocenes	110
4.2.4 Arsaalkynes.....	119
4.2.5 Arsaphospholides	120
4.2.6 Test reaction between $Na[cyclo-P_5]$ and supermesitylarsaalkyne.....	121
4.3 Conclusions.....	123
4.4 Experimental part.....	124
4.4.1 General remarks.....	124
4.4.2 Synthesis of starting materials	126
4.4.3 Synthesis of sodium 1,2,4-triphospholides and 1,2,3,4-tetraphospholides	129
4.4.4 Synthesis of sodium 5-R-1,2,3,4-tetraphospholides	132
4.4.5 Synthesis of 1,3,4-triphosphaferrocenes and 1,2,3,4-tetraphosphaferrocenes	135
4.4.6 Synthesis 5-R-1,2,3,4-tetraphosphaferrocenes	137
4.4.7 Test reaction with supermesitylarsaalkyne	139
4.4.8 Crystallographic data for all compounds	139
Summary	142

List of abbreviations	148
References.....	151

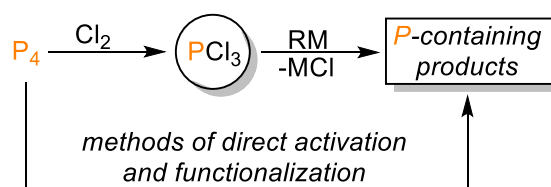
Chapter 1. Introduction

1.1 Synthesis of phosphorus-containing compounds

White phosphorus (P_4) is the most reactive allotrope of elemental phosphorus and the major commercial P-atom source in the synthesis of numerous phosphorus-containing compounds utilized by the chemical industry. P_4 is produced directly from the naturally abundant phosphate rock in a so-called "thermal process" that involves a reduction in a furnace with carbon and silica (as oxygen acceptor).^[1] The availability of white phosphorus and its high reactivity made widespread use of this compound possible. However, P_4 itself has no significant direct applications and is mainly converted to PCl_3 through chlorination with Cl_2 gas. A subsequent functionalization of PCl_3 *via* reduction or salt metathesis reactions gives an access to the desired compounds (**Scheme 1**).^[2]

PCl_3 exploitation in the synthesis generates stoichiometric amounts of halide waste and is exposed to unselective reactions.^[3] Thus, from a safety, economic and ecological standpoint, alternative strategies of a P-atom incorporation that exclude corrosive PCl_3 and troublesome Cl_2 from the sequence are of great interest.

The most drastic attempt to solve the problem of an effective P-atom incorporation is the use of phosphate materials like phosphoric acid (H_3PO_4) as a precursor.^[4,5] H_3PO_4 is produced on an incomparably larger scale than P_4 from the phosphate ore in a so-called "wet process" that does not require high energy inputs as the production of white phosphorus. Despite potential benefits in fine chemicals synthesis, the use of phosphoric acid is still very limited and challenging. Therefore, P_4 remains the major industrially viable precursor (**Scheme 1**).



Scheme 1. Synthesis of phosphorus-containing compounds.

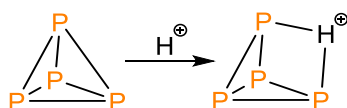
An attractive alternative to a present practice would be a direct transfer of P_4 to valuable products.^[6,7] These methods allow to bypass manipulations with potentially hazardous and corrosive intermediates. However, the scope of such reactions is limited due to the low selectivity and unpredictable behavior of P_4 . Significant efforts are directed to study a

selective P₄ cage activation by various substrates to overcome these difficulties. Interestingly, some activated phosphorus species possess structural and electronic features suitable for further functionalization. At the present stage, P₄ activation is a well-established field as showcased in a diversity of the currently known chemistry.^[8,9,10]

1.2 General physical and chemical properties of P₄

Under normal conditions, white phosphorus is a waxy material of a complicated cubic crystal structure that consists of rotationally disordered P₄ tetrahedrons (α -P₄ modification). Single crystals suitable for analysis of the structure of white phosphorus (β -P₄ modification) can be obtained at low temperatures.^[11] The P—P bond length of the white phosphorus regular tetrahedron was measured with different techniques (electron diffraction of gaseous P₄,^[12] Raman spectroscopy,^[13] SC-XRD^[11]) that yielded different results. Due to experimental uncertainties, the calculated bond length of 2.194 Å is considered as the standard.^[9] Despite a suggested high bond strain energy caused by acute 60° bond angles, P₄ is more stable than cages with up to ten P atoms and more obtuse angles. The remarkable stability of the tetrahedral P₄ cage has been attributed to a reduced lone pair repulsion due to geometric features.^[14] Another contributing factor is the stabilization of P₄ through delocalized bonding.^[15] Moreover, the highly negative NICS (Nucleus Independent Chemical Shift) value in the center of the tetrahedron suggest a spherical aromaticity in the P₄ cage.^[16]

Although P₄ possesses four lone pairs, it shows a weak nucleophilicity on the assumption that the lone pair on each P atom is spherically distributed around the nucleus (3s orbital) and does not outstretch towards the outer sphere.^[17] Thus, electrophiles, such as the proton, react with P₄ at the edge of the tetrahedron (**Scheme 2**) because the HOMO has a significant orbital coefficient above the line that connects two adjacent atoms (**Figure 1**).^[18]



Scheme 2. P₄ interaction with the electrophile.

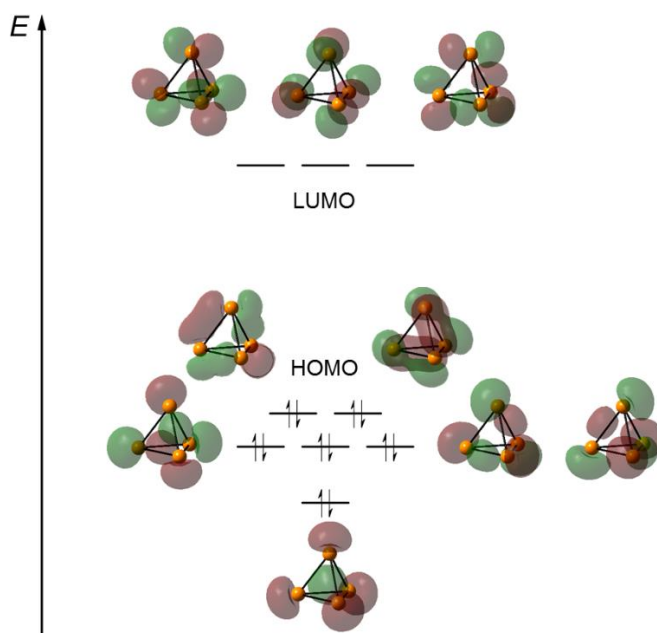
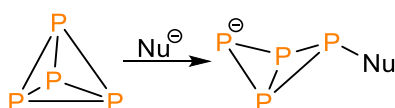


Figure 1. Frontier molecular orbitals of P_4 . Calculated at the B3LYP/def2-TZVP level of theory.

A distorted structure of the reduced $[P_4]^-$ anion is only 119 kJ/mol higher in energy than the neutral P_4 , while the oxidated form is higher for more than 1000 kJ/mol.^[9] This is in line with numerous experimental evidences showing a pronounced electrophilicity of P_4 . Usually, the electrophilicity of P_4 is attributed to the high bond strain energy,^[19] despite that the QTAIM (Quantum Theory of Atoms in Molecules) analysis did not reveal any significant P—P bond bending.^[20] Formally, the nucleophilic attack occurs at one of the phosphorus atoms *via* the interaction of a nucleophile with one of the three degenerate LUMOs of the P_4 tetrahedron (**Figure 1**).^[18] This interaction results in the disruption of one P—P bond under the formation of a butterfly-like bicyclo[1.1.0]tetraphosphabutane species (**Scheme 3**).^[9]



Scheme 3. P_4 interaction with a nucleophile.

1.3 Activation of P_4 by alkali metals. Polyphosphide anions

A reaction of phosphorus with the group I elements leads to various alkali metal salts of negatively charged P-clusters called polyphosphides. The reaction between alkali metals and

phosphorus can be performed either in a solid-state or in a liquid-phase.^[21] Solid-state techniques require more stable allotropes of phosphorus, such as red phosphorus (P_{red}), and usually yield insoluble and thermodynamically very stable polyphosphides. On the other hand, the majority of solution-based methods employ P_4 , which has a good solubility in common organic solvents and liquid ammonia. In contrast to solid-state methods, the interaction of P_4 with alkali metals in a liquid phase is controlled kinetically, rather than thermodynamically, resulting in very reactive species of moderate solubility. The outcome of this seemingly simple reaction depends on the reaction conditions, the solvent, the alkali metal, and the atomic ratio (M/P) between starting compounds. By varying these parameters, a simple phosphide $[P]^{3-}$, cage, or cyclic (aromatic) polyphosphides $[P_n]^{x-}$ can be obtained (Figure 2).^[19]

It is assumed, that the first step of the P_4 cage activation with an alkali metal is a formal one or two-electron transfer followed by the P—P bond cleavage and a formation of a butterfly-like radical anion or dianion structure.^[19] A reaction of P_4 with a large excess of alkali metal in organic solvents usually leads to a simple phosphide $[P]^{3-}$.^[22] Reducing the M/P ratio leads to the formation of polyphosphides (Figure 2).

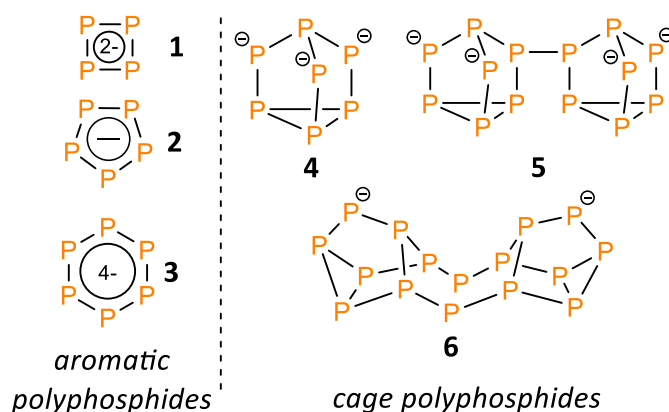
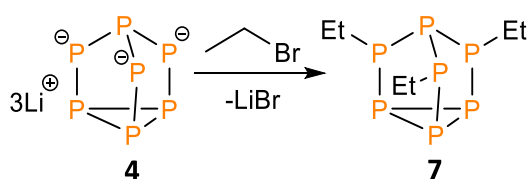


Figure 2. Selected examples of polyphosphide anions

As an example, the reaction between Na or K with P_4 in THF and in a molar ratio of 1:2 leads to a mixture of M_3P_{19} , $M_2(6)$, M_3P_{21} , M_4P_{26} , $M_3(4)$, and $M_4(5)$ ($M = \text{Na}, \text{K}$).^[23] Interestingly, the addition of catalytic amounts of naphthalene to the Na and P_4 mixture (3:1.75 molar ratio) gives $Na_3(4)$ exclusively.^[24]

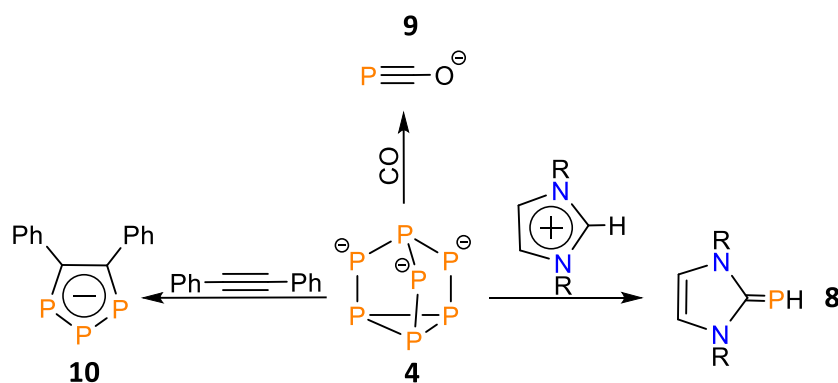
Highly reactive Cs tends to form small polyphosphide cages and cycles. For instance, *Korber et al.* showed that P₄ activation with Cs leads to the 6π electron aromatic Cs₂(**1**).^[25] While the reaction with Li leads to phosphorus-rich cage polyphosphide Li₄(**6**).^[26] As a rule, the use of organic solvents that has a lower boiling point than the melting point of the selected alkali metal yields higher aggregated polyphosphides. Thus, it is a common practice to exploit Na/K alloys in THF or DME when it is necessary to avoid a formation of higher polyphosphides.^[19]

In contrast to neutral P₄, negatively charged polyphosphides act as typical nucleophiles and, for example, react with aliphatic halides (**Scheme 4**).^[27]



Scheme 4. Reaction between polyphosphide and aliphatic halide.

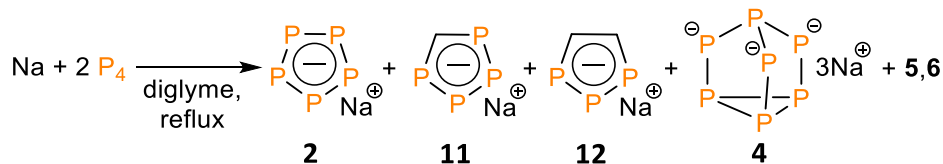
Simple M_{3-x}H_xP phosphides are used to generate PH₃, P(TMS)₃, and other phosphines in laboratories.^[22,28] Phosphorus-rich polyphosphides are almost insoluble in organic solvents, thus special attention is given to the small aromatic pentaphospholide anion **2** (discussed in the next section) and the cage heptaphosphide trianion **4**. Polyphosphides can be functionalized by different electrophiles and electron-poor systems. For example, **4** is proved to be a versatile source of one or several phosphorus atoms for the synthesis of imidazolyl phosphinidenes (**8**),^[24] the 2-phosphaethynolate anion (**9**),^[29] and P-heterocycles (**10**)^[30] when treated with electrophiles, CO, or alkynes, respectively (**Scheme 5**). The reactivity towards alkynes is particularly interesting as an example of quick P₄ transfer to P-containing compounds with multiple P—P and P—C bonds, which is not a trivial task *via* the PCl₃ route.^[31]



Scheme 5. Use of **4** in the synthesis.

1.4 Pentaphospholide anion

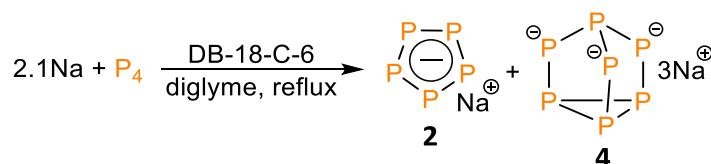
The reaction of Na with two equivalents of P_4 in diglyme under reflux conditions results in the formation of the above-mentioned polyphosphides **4–6** along with the parent 1,2,3,4-tetraphospholide **11** and 1,2,3-triphospholide **12** that indicate the participation of diglyme in the reaction. But what is more important, a detailed analysis of this reaction also revealed the presence of an aromatic polyphosphide species: the pentaphospholide anion **2** (**Scheme 6**).^[32]



Scheme 6. Reaction between Na and two equivalents of P_4 .

The pentaphospholide anion (pentaphosphacyclopentadienide or $[cyclo-P_5]^-$) is a 6π electron aromatic system and an inorganic analog of cyclopentadienide $[Cp]^-$. In contrast to the valence isoelectronic $[cyclo-N_5]^-$ that has been only generated as a transient species,^[33] $[cyclo-P_5]^-$ is persistent in solution. The original method reported by *Baudler et al.* leads to the formation of **2** in 12 % yield.^[34]

Later, *Hey-Hawkins et al.* demonstrated that the reaction between Na and P_4 (in a 2:1 ratio) with DB-18-C-6 (dibenzo-18-crown-6) as the phase-transfer agent substantially increases the yield of $Na[cyclo-P_5]$ up to 22 % and excludes an excessive formation of higher polyphosphides (**Scheme 7**).^[35] The only major by-product of the synthesis is trisodium heptaphospholide **4** which is insoluble in diglyme.



Scheme 7. Improved synthesis of **2**.

$[\text{cyclo-P}_5]^-$ decomposes upon removing the solvent and thus it was never characterized through single crystal X-ray diffraction as a free anion. Nevertheless, the evidence of its aromatic and highly symmetric structure is clear from the ^{31}P NMR spectrum which shows only one singlet resonance with the chemical shift at $\delta = 470.0$ ppm. *Ab initio* calculations of the $[\text{cyclo-P}_5]^-$ cluster also confirm the thermodynamic stability of a D_{5h} planar cyclic structure with a P—P bond length of 2.128 Å. The closest low-lying singlet isomers of $[\text{P}_5]^-$ are a C_s bridged-roof and a C_{2v} pyramid-shaped isomers which are 35 and 40 kcal/mol higher in energy compared to the ground-state D_{5h} isomer, respectively (**Figure 3**).^[36]

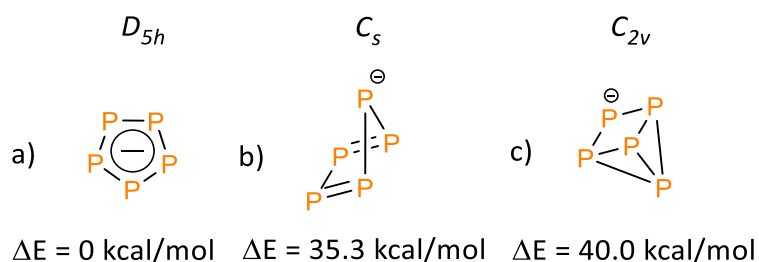


Figure 3. Lowest-lying isomers of $[\text{P}_5]^-$ with their point group symmetries. The relative energies are given at the B3LYP-D3(BJ)/def2-QZVPD level of theory.

DFT calculations on the thermodynamic stability of $M[\text{cyclo-P}_5]$ ($M = \text{Li}, \text{Na}, \text{K}$) salts reveal the pyramidal C_{5v} structures (typical for aromatic species) with ionic bonds as the global minimum (**Figure 4a**). Alternative planar C_{2v} isomers (**Figure 4b**) are higher in energy, although the gap between the two isomers becomes smaller moving from Li^+ (20 kcal/mol) to K^+ (12.3 kcal/mol).^[37] Another planar isomer of $M[\text{cyclo-P}_5]$ with a dicoordinate cation (**Figure 4c**) is a transition state for the metal cation migration from the one ring face to the other.^[38]

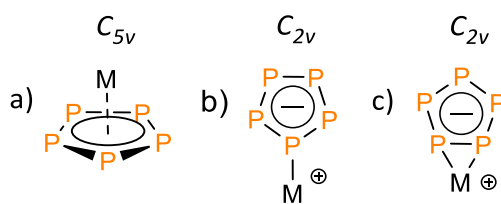


Figure 4. Isomers of $M[\text{cyclo-P}_5]$ salts.

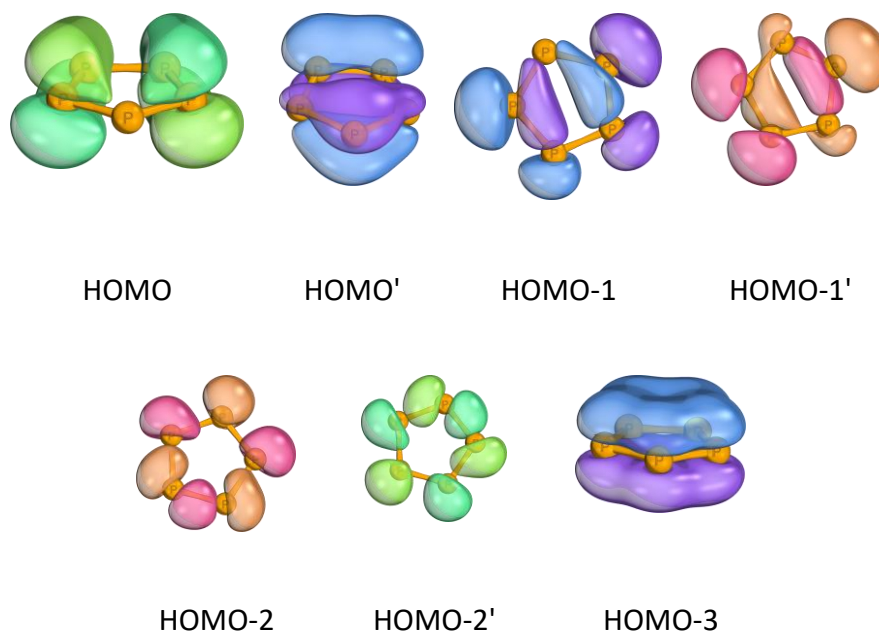


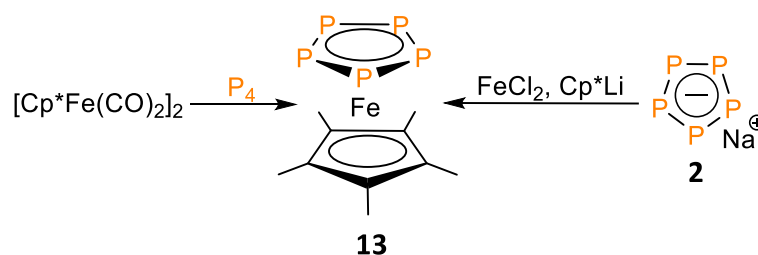
Figure 5. Frontier molecular orbitals of $[\text{cyclo-P}_5]^-$ calculated at the B3LYP-D3/def2-TZVP level of theory.

The structural evidence of the $[\text{cyclo-P}_5]^-$ aromaticity is accompanied by the calculated NICS value of -16.6 ppm in the center of the anion which is reminiscent of $[\text{Cp}]^-$ (-12.7).^[39] The DFT computed frontier molecular orbitals relevant to HOMOs (**Figure 5**) show that $[\text{cyclo-P}_5]^-$ (D_{5h}) possesses 6π electrons (following Hückels rule) localized on two degenerate HOMO (HOMO and HOMO') and HOMO-3 and render the π -aromaticity. Both HOMO-1 and HOMO-2 consist of two degenerate MOs (HOMO-1/HOMO-1' and HOMO-2/HOMO-2') formed from the in-plane s/p orbitals. They represent the σ -bonding MOs as well as the lone-pairs on P-atoms.

1.5 Chemical properties of pentaphospholide anion

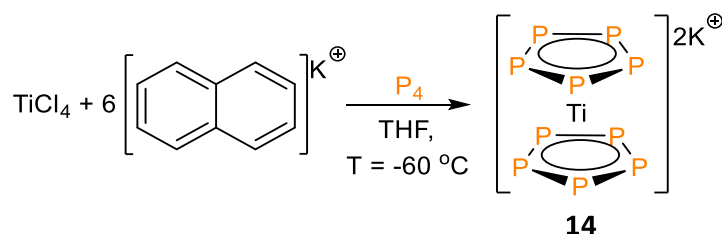
Similar to the classical $[\text{Cp}]^-$, a η^5 -coordination of the pentaphospholide is also favored. A substitution of the CH units in $[\text{Cp}]^-$ scaffold by the isolobal P-atoms results in a decrease of

the LUMO energy and, subsequently, assist in a stabilization of electron-rich metal centers.^[40] The stability of alkali metal salts of $[\text{cyclo-P}_5]^-$ in solution promotes coordination chemistry studies. Analogous to $\text{Na}[\text{Cp}]$, $\text{Na}[\text{cyclo-P}_5]$ also reacts with different Fe(II) precursors to give sandwich pentaphosphaferrocene **13** (**Scheme 8**).^[34,41] But in contrast to classical ferrocene, electron-rich cyclopentadienyl ligands are crucial for the stability of complexes with the η^5 -pentaphospholyl ligand. Some $[\text{cyclo-P}_5]^-$ “cene” complexes are accessible directly from P_4 (**Scheme 8**).^[42]



Scheme 8. Synthesis of pentaphosphaferrocenes **13**.

This approach resulted in the synthesis of the first completely inorganic metallocene system: decaphosphatitanocene **14** (**Scheme 9**) by *Schleyer et al.*^[43]



Scheme 9. Synthesis of decaphosphatitanocene **14**.

Nevertheless, the most interesting feature of many phosphorus aromatic heterocycles, and particularly of the $[\text{cyclo-P}_5]^-$ anion, is the presence of energetically and sterically accessible lone pairs at each P-atom. The ability for a simultaneous η^5 (via the aromatic ring system) and η^1 (via lone pairs) coordination expands the scope of feasible compounds which is in contrast to the classical cyclopentadienyl systems. In the last 20 years, a mixed coordination mode of some air-stable pentaphosphaferrocenes (stabilized by electron-rich or sterically bulky derivatives of cyclopentadiene) has been intensively studied.^[44,45,46] Treating pentaphosphaferrocenes with copper halides gave a rise to supramolecular complexes with

a multidimensional topology. An important milestone in this field was achieved by *Scheer et al.* with the synthesis of spherical inorganic fullerene-like molecules (**15**) through the coordination of the all P-atoms to CuCl (**Figure 6**).^[47] This is an outstanding example that demonstrates a route to other half-shells, nanosized molecules and full-shell structural motifs.^[48,49]

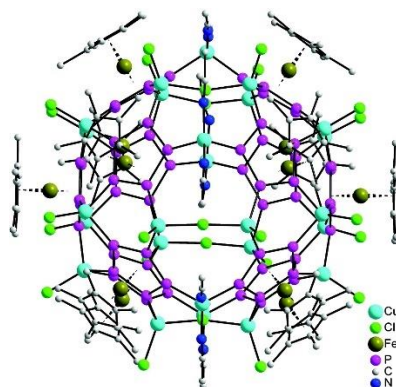
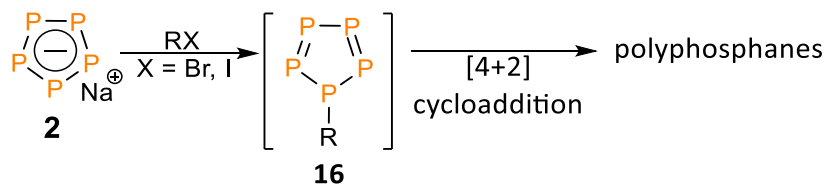


Figure 6. Molecular structure of inorganic fullerene-like molecule based on pentaphosphaferrocene **15**.

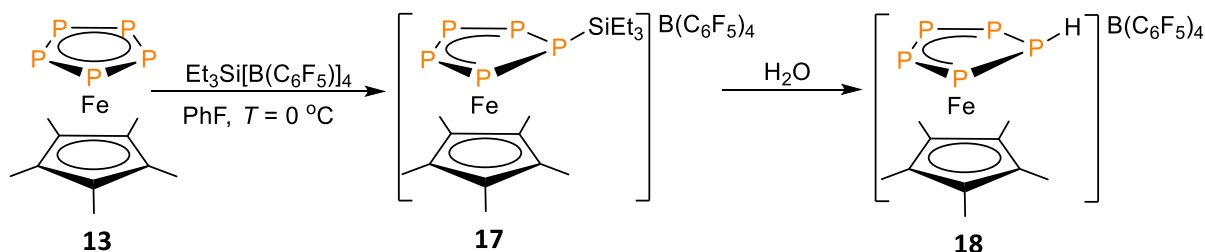
However, apart from the coordination chemistry, only limited information is available concerning the reactivity of the $[\text{cyclo-P}_5]^-$ anion.^[50] Compared to cage polyphosphides with isolated charged centers, pentaphospholide is stable against weak electrophiles due to a delocalization of the negative charge. Attempts to react $\text{M}[\text{cyclo-P}_5]$ ($\text{M} = \text{Li}, \text{Na}$) with stronger electrophiles only led to aggregated polyphosphanes. It is anticipated that the interaction with an electrophile $[\text{R}]^+$ proceeds *via the* formation of 1-*R*-pentaphosphole **16** followed by repeated [4+2] cycloadditions between the reactive P=P double bonds (**Scheme 10**).^[34]



Scheme 10. Reactivity of $[\text{cyclo-P}_5]^-$ towards electrophiles.

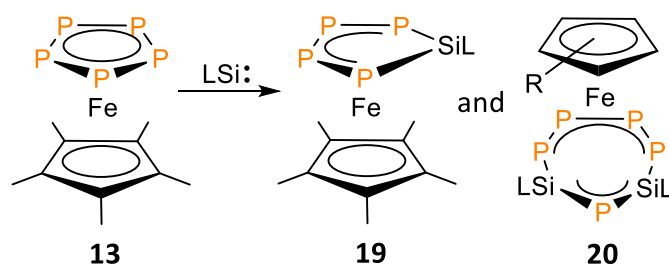
At the same time, the stabilization of $[\text{cyclo-P}_5]^-$ in the coordination sphere of a transition metal promoted studies on the reactivity towards main group elements and compounds. As a result, the otherwise elusive methylated and silylated **17** pentaphospholes have been

successfully synthesized by *Scheer et al.* (**Scheme 11**). Moreover, the selective hydrolysis of P—Si bond yielded a transition metal complex bearing the parent pentaphosphole **18** as a ligand.^[51]



Scheme 11. Synthesis of pentaphospholes in the coordination sphere of Fe(II).

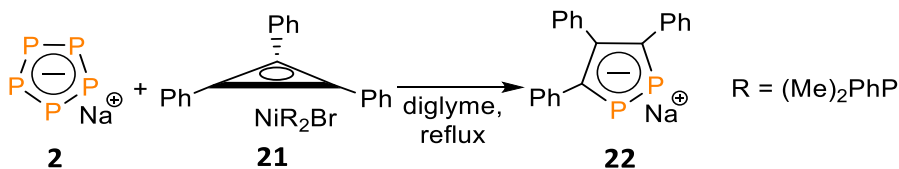
It was also demonstrated that pentaphosphaferrocene undergoes a substitution of one P atom (**19**) with an isoelectronic [LSi] fragment in the reaction with silylenes (**Scheme 12**). Moreover, similar [LSi] units can be inserted *via* a ring expansion into the phosphorus cycle (**20**).^[52]



Scheme 12. Reactivity of pentaphosphaferrocene towards silylenes.

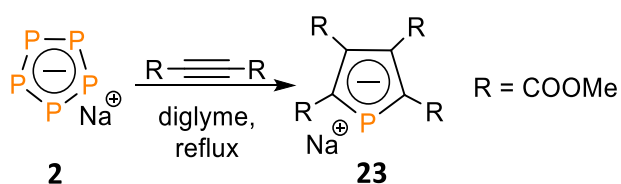
In addition, an insertion into the P-scaffold of pentaphosphaferrocene by low valent Al(I)^[53] and Ge(I)^[54] fragments was reported. The reaction of pentaphosphaferrocene with elemental iodine resulted in the formation of complex polyphosphide species.^[55]

The chemical properties of non-coordinated $[\text{cyclo-P}_5]^-$ are less studied due to uncontrollable interactions with electrophiles (**Scheme 10**) and oxidants. *Hey-Hawkins et al.* showed that $\text{Na}[\text{cyclo-P}_5]$ reacts unusually with the $(\eta^3\text{-cyclopropenyl})\text{-Ni}$ complex **21** to give the 1,2-diphospholide anion ($1,2\text{-}[\text{cyclo}-(\text{PhC})_3\text{P}_2]^-$) **22** instead of the anticipated 18-electron sandwich compound (**Scheme 13**).^[56] The formal elimination of a neutral $[\text{P}_3]$ unit from the $[\text{cyclo-P}_5]$ ring restores aromaticity under the assembly of **22**.



Scheme 13. Synthesis of the 1,2-diphospholide anion **22**.

A similar behavior of $\text{Na}[\text{cyclo-P}_5]$ was observed by *Miluykov et al.* when $[\text{cyclo-P}_5]^-$ was treated with DMAD (Dimethyl acetylenedicarboxylate) (**Scheme 14**). In this case, $[\text{cyclo-P}_5]^-$ acts as a $[\text{P}]^-$ source to build the monophospholide anion 1- $[\text{cyclo}-(\text{RC})_4\text{P}]^-$ **23**.^[57]



Scheme 14. Synthesis of the monophospholide anion **23**.

1.6 Phospholide anions

In the previous section, it was demonstrated that $\text{Na}[\text{cyclo-P}_5]$ **2** reacts with unsaturated hydrocarbons to give the mono- and 1,2-diphospholide anions **23** and **22**, respectively (**Scheme 13** and **Scheme 14**). Compounds **2**, **22**, and **23** belong to the family of phospholide anions $[\text{cyclo}-(\text{CR})_{5-n}\text{P}_n]^-$. As $[\text{cyclo-P}_5]^-$ **2**, the other phospholides (represented in **Figure 7**) can also be described as the heavier analogs of $[\text{Cp}]^-$ in which one or multiple methine units are substituted by the isolobal phosphorus atoms. DFT studies and experiments confirm the aromaticity of these species which is, according to the NICS analysis, reminiscent of $[\text{Cp}]^-$.^[58]

The chemistry of $[\text{cyclo}-(\text{CR})_{5-n}\text{P}_n]^-$ heterocycles was studied unevenly which is clear from a survey of the Cambridge structural database (CSD) (**Figure 7**, inquiry date: 01.12.2018).

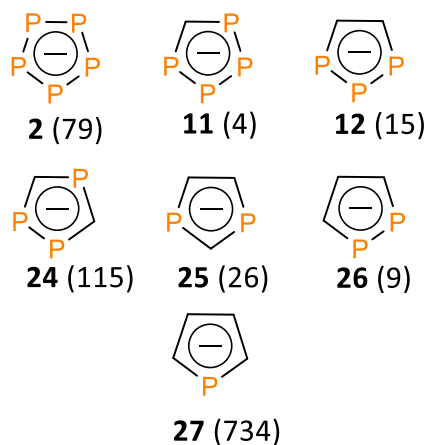
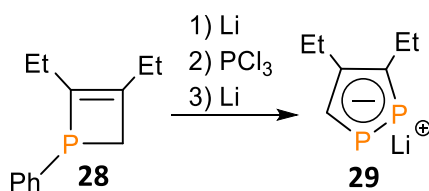


Figure 7. Family of the phospholide anions and the number of structurally authenticated species.

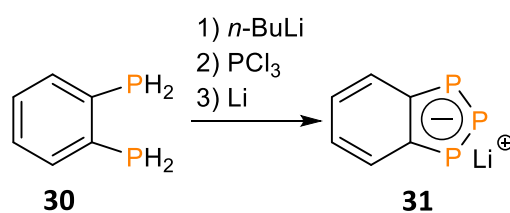
The survey reveals that the number of structurally authenticated monophospholide derivatives (and their complexes) exceeds the number of any other species by far. Moreover, within the pairs **25/26** and **12/24**, the structural isomers with the abstracted phosphorus atoms are better studied than the isomers with the consecutive chain of P-atoms. The revealed trends for $[\text{cyclo}-(\text{CR})_{5-n}\text{P}_n]^-$ are in line with the availability of versatile methods for their synthesis.

While derivatives of monophospholides **27** are easily accessible *via* the standard PCl_3 route,^[59] the synthesis of $[\text{cyclo}-(\text{CR})_{5-n}\text{P}_n]^-$ with $n \geq 2$ is much more difficult. Building a scaffold with several P—P and P—C bonds starting from PCl_3 is a complicated multistep synthesis that includes the isolation of specific, usually unstable organophosphorus precursors.

For instance, 1,2- $[\text{cyclo}-(\text{CR})_3\text{P}_2]^-$ **29** was obtained by *Mathey et al.* *via* a formal insertion of phosphinidenes into 1,2-dihydrophosphetes **28** (**Scheme 15**).^[60] *Russel et al.* showed that the annulated 1,2,3- $[\text{cyclo}-(\text{CR})_2\text{P}_3]^-$ **31** can be synthesized by the reaction between the tetralithium derivative of diphosphenobenzene **30** and PCl_3 (**Scheme 16**).^[31]

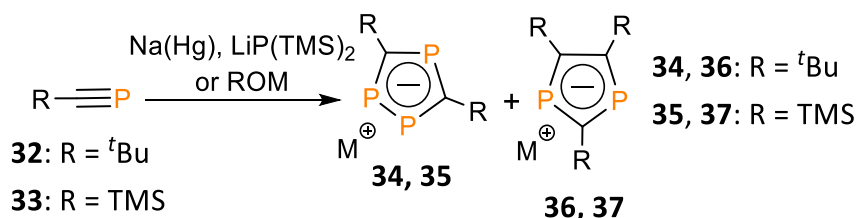


Scheme 15. Synthesis of the 1,2-diphospholide anion **29**.



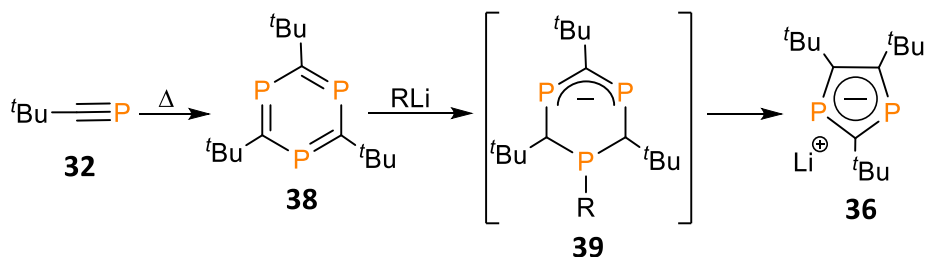
Scheme 16. Synthesis of the annulated 1,2,3-triphospholide anion **31**.

Among numerous organophosphorus precursors, phosphalkynes ($R-C\equiv P$) received a great deal of an interest as versatile blocks for the construction of polyphospholide anions. Initially, it was reported by *Nixon et al.* that ${}^t\text{Bu}-C\equiv P$ (${}^t\text{Bu}$ = *tert*-butyl) **32** and $\text{TMS}-C\equiv P$ (TMS = trimethylsilyl) **33** react with strong nucleophiles to give a mixture of 1,3-[*cyclo*-($C(R)$) $_3P_2$] $^-$ **36**, **37** and 1,2,4-[*cyclo*-($C(R)$) $_2P_3$] $^-$ **34**, **35** (Scheme 17).^[61,62]



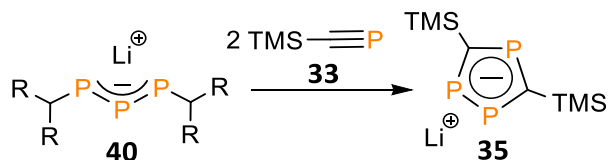
Scheme 17. Synthesis of the 2,4,5-R-1,3-diphospholide **36**, **37** and 3,5-R-1,2,4-triphospholide anions **34**, **35**.

Further studies on the chemistry of phosphalkynes lead to the selective syntheses of the corresponding heterocycles. The exclusive formation of 1,3-[*cyclo*-($C({}^t\text{Bu})$) $_3P_2$] $^-$ **36** is possible when ${}^t\text{Bu}-C\equiv P$ **32** is treated with potassium,^[63] alkyllithium,^[64] or lithium amides.^[65] The reaction proceeds *via* a reduced triphosphabenzene intermediate **39**, which eliminates a phosphinidene fragment (Scheme 18). DFT calculations performed by *Nuylaszi et al.* confirm that the aromaticity of the resulting anions is the driving force of the reaction.^[65]



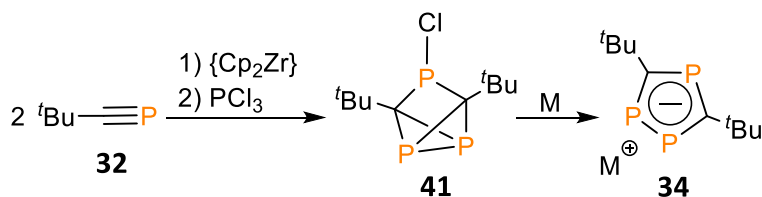
Scheme 18. Mechanism of 1,3-diphospholide anion **1.36** formation.

Schoeller et al. showed that the selective preparation of 1,2,4-[*cyclo*-(C(TMS))₂P₃]⁻ **35** can be achieved *via* a formal [2+2+1] cycloaddition between the lithium salt of persilylated 2,3,4-triphosphapentadienide **40** and TMS—C≡P **33** (Scheme 19).^[66]



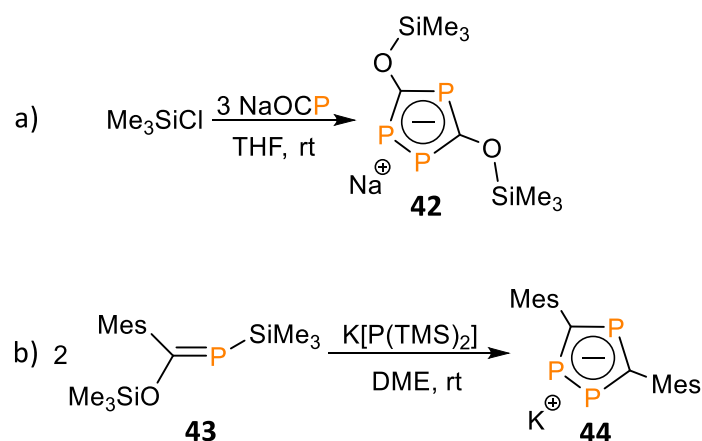
Scheme 19. Synthesis of 1,2,4-triphospholide anion **35**.

Another method, reported by *Regitz et al.*, is based on the multistep synthesis that includes a cyclodimerization of phosphaaalkyne **32** in the coordination sphere of zirconium, followed by a reaction with PCl₃ and a reduction of phosphine derivative **41** with an alkali metal (Scheme 20).^[67]



Scheme 20. Synthesis of 1,2,4-triphospholide anion **34**.

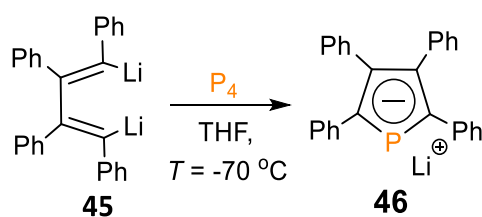
Grützmacher et al. synthesized the 3,5-trimethylsiloxy-1,2,4-triphospholide anion **42** by the reaction between trimethylsilylchloride and sodium phosphaaethynolate.^[68] *Scheer et al.* showed that the mesityl (Mes = 1,3,5-trimethylphenyl) derivative of 1,2,4-triphospholide anion **44** can be obtained by treating the corresponding phosphaaalkene **43** with K[P(TMS)₂]. The exclusive formation of **44** in this reaction was observed most likely due to the presence sterically demanding aryl substituents.^[69]



Scheme 21. a) Synthesis of the 3,5-trimethylsiloxy-1,2,4-triphospholide anion **42**; b) Synthesis of the 3,5-bismesityl-1,2,4-triphospholide anion **44**.

In the last two decades, the concept of P_4 activation and functionalization has emerged as a promising pathway toward P-heterocycles. Under the right cleavage conditions, the P_4 tetrahedron may act as a formal source of $[P_n]$ ($n = 1-4$) units and by this, bypassing elaborate multistep synthesis routes.^[70,71]

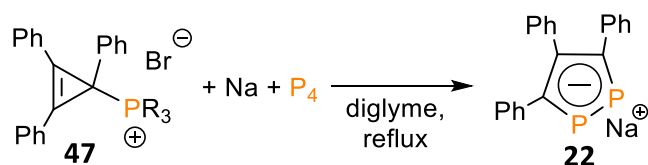
Until now, there is only one example of the direct P_4 functionalization under nucleophilic conditions giving rise to the phospholide anions. Recently, it was reported by *Xi et al.* that 1,4-dilithio-1,3-butadiene **45** reacts with P_4 via a cooperative nucleophilic attack of two $C(sp^2)$ —Li fragments on the P_4 cage to give $[cyclo-(C(Ph))_4P]^-$ **46** in high yields (**Scheme 22**).^[72]



Scheme 22. Synthesis of the monophospholide anion **46**.

On the other hand, polyphosphides, accessible by P_4 activation with alkali metals, allows for the functionalization of the $[P_n]^-$ framework under various electrophilic conditions. This strategy has already been used for the synthesis of some $[cyclo-(CR)_{5-n}P_n]^-$. Several examples of such reactions have been mentioned in the previous paragraphs (**Scheme 5**, **Scheme 13**, **Scheme 14**) as a part of the $[cyclo-P_5]^-$ and $[P_7]^-$ chemistry. It is noteworthy to mention that

the alkali metal activation of P_4 followed by the functionalization is also feasible in a *one-pot* procedure as showed by *Miluykov et al.* (**Scheme 23**). For instance, a three-component reaction between P_4 , Na and cyclopropenylphosphonium salt **47** results in the formation of **22** in high yield.^[73]



Scheme 23. One-pot synthesis of the 3,4,5-triphenyl-1,2-diphospholide anion **22**.

The chemical properties of the phospholides are similar to $[cyclo-P_5]^-$ **2**. They are also capable of forming complexes with the η^5 , η^1 , μ^2 or mixed coordination modes (**Figure 8**) and act as phosphorus-centered nucleophiles.^[74]

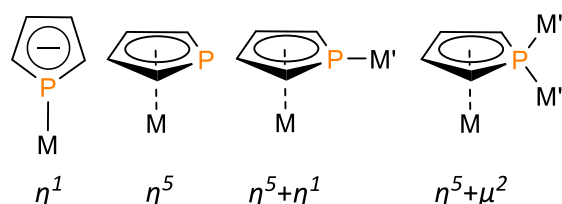
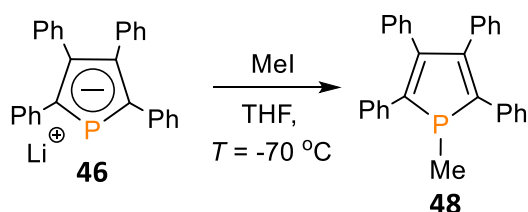


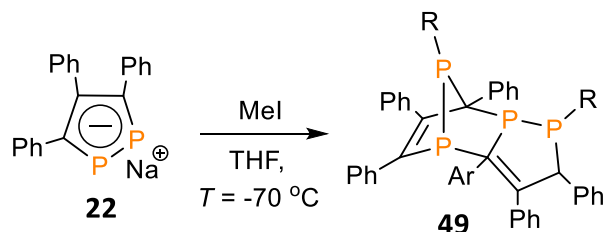
Figure 8. Possible coordination modes of the monophospholide anion.

Bearing in mind that the negative charge is mainly distributed within the P-atoms, the nucleophilicity of $[cyclo-(CR)_{5-n}P_n]^-$ decreases when n approaches five.^[75] The reaction between the phospholide anion **46** and the electrophile results in the formation of neutral phosphole **48** with the 4π -electron diene system (**Scheme 24**).^[76,77,78]



Scheme 24. Synthesis of 1-R-monophospholes **48**.

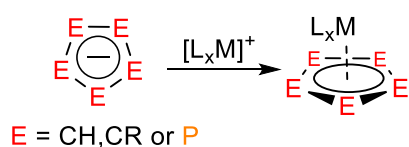
In the absence of sterically demanding substituents, diene systems with the P=P and P=C bonds undergo [4+2]^[79] (**Scheme 25**) or [2+2]^[80] (in special cases) cycloadditions, giving rise to cage polyphosphines.^[81]



Scheme 25. Reaction with aliphatic halides followed by [4+2] cycloaddition.

1.7 Phosphametallocenes

Similar to the cyclopentadienyl anion, $[\text{cyclo}-(\text{CR})_{5-n}\text{P}_n]^-$ are also capable of binding to transition-metal cations in a η^5 -fashion to form phosphametallocenes (**Scheme 26**).^[82,83]



Scheme 26. Synthesis of phosphametallocenes.

The energy decomposition analysis of the hypothetical η^5 - $[\text{cyclo-P}_5]_2\text{Fe}$ complex shows a covalent character of the Fe—L (L = $[\text{cyclo-P}_5]$) bonding, which is mainly implemented by the $\pi(\text{L}) \rightarrow \text{Fe}^{2+}$ donation.^[84] However, it is noteworthy that the π -donor strength of the phospholylic ligand $[\text{cyclo}-(\text{CR})_{5-n}\text{P}_n]$ decreases when the methine units are substituted by pnictogen atoms or CR (R = EWG).^[85,86] Therefore, the stability and redox properties of phosphametallocenes are well predictable which is essential for the design of target compounds with useful properties.

The distinctive feature of phosphametallocenes is the presence of energetically and sterically accessible lone pairs on each phosphorus atom. Thus, the chemistry of phosphametallocenes is significantly diversified compared to classical ferrocenes by the Lewis basicity of the P-atoms, and the η^1 -coordination *via* the phosphorus lone-pairs.^[87] The η^1 -coordination mode

of phosphametalloenes expands the scope of possible coordination motifs and leads to polynuclear complexes and supramolecular assemblies (**Figure 6**).^[47,83]

Complexes bearing phosphametalloenes as ligands were applied in catalytic Suzuki-cross coupling reactions and the polymerization of olefins.^[88,89,90] Recently, *Scheer et al.* reported that organophosphanes are accessible directly from P₄ in the pentaphosphaferrocene-mediated synthesis. In this particular case, pentaphosphaferrocene acts as a P-atom carrier.^[91] The Lewis basicity of phosphametalloenes was employed in the nucleophilic catalysis of the ring-opening reaction of epoxides.^[92,93] Phosphametalloene derivatives are especially interesting as ligands for asymmetrical catalysis.^[94,95]

In 2017, it was demonstrated by *Mills et al.* that the phosphadysprosocenium SMM (Single-Molecule Magnet) with Cp_{ttt} (Cp_{ttt} = C₅H₂^tBu₃-1,2,4) ligands shows a magnetic hysteresis at 60 K (which is close to the boiling point of N₂).^[96] This impressive result was achieved by a massive increase in the energy barrier to magnetic reversal (U_{eff}) caused by the combination of Dy³⁺ with the rigid and charge-dense π-aromatic phospholyl rings. Later, it was also predicted that the U_{eff} could be increased not only by replacement of CH by CR (R = alkyl) but also with P following different considerations.^[97] Thus, phosphametalloenium cations of lanthanides with SMM properties became target compounds.^[98]

1.8 Motivation of this study

The growing interest in aromatic polyphosphorus heterocycles^[99] requires to find simple and efficient pathways towards the barely explored [cyclo-(CR)_{5-n}P_n]⁻ species. The recent reports demonstrate that polyphosphides, easily accessible *via* P₄ activation (**Scheme 6**), react with electrophiles and electron-poor species to give valuable cyclic and acyclic organophosphorus compounds (**Scheme 6**, **Scheme 13**, **Scheme 14** and **Scheme 23**).

In this respect, [cyclo-P₅]⁻ deserves special attention, among various polyphosphides, for several reasons:

- 1) Two of the above-mentioned examples concerning the reactivity of Na[cyclo-P₅] towards unsaturated species show that the pentaphospholide anion can serve as a formal source of [P₁₋₂]⁻ fragments for the synthesis of the polyphospholide anions. Consequently, it can be assumed that the aromaticity is the driving force of [cyclo-P₅]⁻ transformations. Thus, it can

anticipated that it can also act as a source of $[P_{3-4}]^-$ fragments under the right reaction conditions.

2) The highly symmetric and aromatic nature of $[cyclo-P_5]^-$ makes it a relatively simple object for comprehensive studies. This would potentially allow controlling and predicting possible fragmentation pathways crucial for the synthesis of desired compounds.

3) $Na[cyclo-P_5]^-$ can be prepared directly from elemental sodium and P_4 . The compound is soluble in diglyme and, therefore, easy to monitor with routine spectroscopy methods.

The main goal is the in-depth study of the reactivity of $Na[cyclo-P_5]^-$ towards isoelectronic triple bond systems: alkynes, nitriles, phosphalkynes, and arsaalkynes. The success of this research project will potentially give rise to a library of novel and barely explored five-membered phosphorus-containing heterocycles. Particularly interesting is the synthesis of phosphorus heterocycles with the consecutive chain of P-atoms, which are complicated or even impossible to obtain using the traditional synthetic protocols involving PCl_3 .

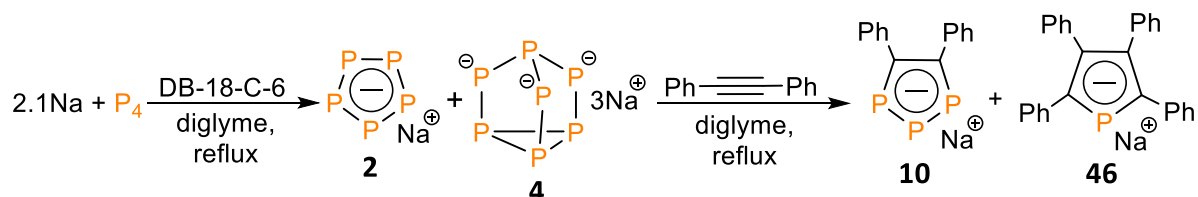
Taking into account an importance of phosphametalloenes in catalysis and in the design of new materials, the second goal is the synthesis and characterization of corresponding sandwich complexes with novel η^5 -coordinated polyphospholyl heterocycles.

Chapter 2. Reactivity of the pentaphospholide anion towards $C\equiv C$ triple bonds. Synthesis of 1,2,3-triphospholide anions.

2.1 Introduction.

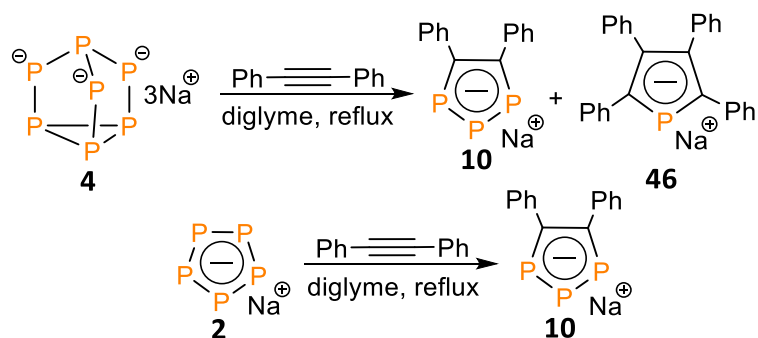
2.1.1 1,2,3-triphospholide anions

In 2017, it was reported that a mixture of polyphosphides in diglyme (**Scheme 7**), which mainly consists of Na[cyclo-P₅] (in the liquid phase) and Na₃[P₇] (in the solid phase), reacts with diphenylacetylene to give two products: sodium 4,5-diphenyl-1,2,3-triphospholide and 2,3,4,5-tetraphenyl-1-monophospholide (**Scheme 27**).*



Scheme 27. Synthesis of the mono- and 1,2,3-triphospholide anions **46** and **10**.

Test reactions with the isolated polyphosphides revealed that Na[cyclo-P₅] interacts with the alkyne to give **10** exclusively, while Na₃[P₇] leads to both compounds (**Scheme 28**). At the same time, *Goicoechea et al.* reported that pure K₃[P₇] reacts with the same alkyne in refluxing DMF to give potassium 4,5-diphenyl-1,2,3-triphospholide **10** (**Scheme 5**). Thus, it was concluded that 2,3,4,5-tetraphenyl-1-monophospholide anion was formed due to the contamination of Na₃[P₇] with higher polyphosphides.

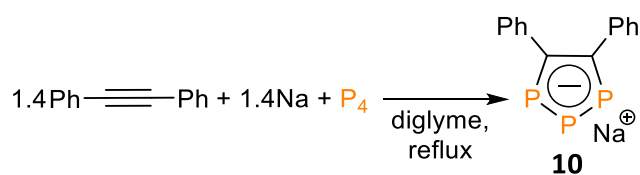


Scheme 28. Test reactions between the isolated [cyclo-P₅] **2**, [P₇]³⁻ **4** and diphenylacetylene.

The synthesis of sodium 4,5-diphenyl-1,2,3-triphospholide **10** was significantly improved when Na, P₄ and alkyne were loaded in one flask with diglyme and stirred under reflux

* The following paragraph is based on the results presented in the specialist degree thesis in June 2018 - Andrey Petrov.

conditions (**Scheme 29**). This *one-pot* procedure allows to obtain other sodium 4,5-diaryl-1,2,3-triphospholides in high yields as well (based on P₄).^[100]



Scheme 29. Synthesis of 1,2,3-triphospholide anion **10**.

Despite 1,2,3-triphospholides being studied for many years, the family of 1,2,3-[cyclo-(RC)₂P₃]⁻ is limited to several derivatives (R = H, Ph, Py, thiophenyl)^[30,31,32,99,100,101] which is in obvious contrast to the structurally more diverse 1,2,4-[cyclo-(RC)₂P₃]⁻ (R = Alk, -SiR₃, Ar, -OR) isomer.^[65,66,68,69,102] 1,2,3-triphospholides exhibit less sterically hindered P-atoms in comparison to the 1,2,4-triphospholide isomer and is therefore considered as interesting objects for coordination chemistry studies.^[103]

Preliminary studies show that Na[cyclo-P₅] may serve as a viable intermediate in the chemical transformation of P₄ into P-heterocycles. In contrast to the cage congener **4**, aromatic [cyclo-P₅]⁻ **2** is a soft and stabilized nucleophile. Thus, it was assumed that [cyclo-P₅]⁻ may also interact with electron-rich alkynes and give rise to the previously unknown 1,2,3-triphospholides featuring new types of substituents. The harsh conditions of the developed *one-pot* procedure might be incompatible with some more volatile alkynes and derivatives with multiple reactive centers. Therefore, the main focus of the following study is on the reactivity of Na[cyclo-P₅] towards C≡C triple bonds.

2.2 Results and discussion

2.2.1 Synthesis of sodium 4,5-dialkyl-1,2,3-triphospholides

P₄ reacts with two equivalents of Na in the presence of the phase-transfer agent (DB-18-C-6) under reflux conditions in diglyme to give an orange solution of Na[cyclo-P₅] and a dark green precipitate that mainly consists of Na₃[P₇] (**Scheme 7**).^[35] After a filtration, Na[cyclo-P₅] (**Figure 9**) was obtained in approximately 30 % analytical yield according to ³¹P NMR spectroscopy.

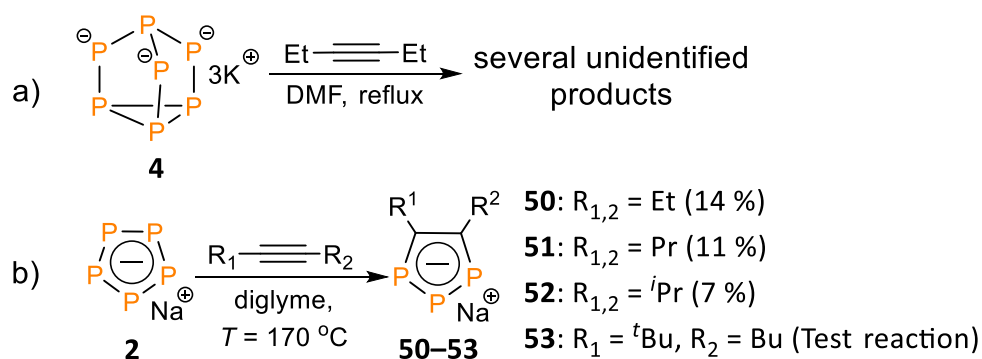
Based on the above considerations, it was interesting to investigate the reactivity of the Na[*cyclo*-P₅] towards aliphatic alkynes as a potential pathway to the otherwise elusive 4,5-dialkyl-1,2,3-triphospholide anions.



Figure 9. Freshly prepared diglyme solution Na[*cyclo*-P₅] **2**.

The previous attempt to access these species was based on K₃[P₇] functionalization with aliphatic alkynes (**Scheme 30a**) that yielded a mixture of several unidentified products.^[104] The unsatisfactory result of the proposed approach could be explained as an unfavored interaction between the electron-rich [P₇]³⁻ cage with an electron-rich alkyne. On the other hand, [*cyclo*-P₅]⁻ possesses a delocalized charge within the aromatic backbone, which may promote the synthesis of the desired species.

Commercially available 3-hexyne with a sterically accessible triple bond was used for the initial studies. One equivalent of 3-hexyne was added to a solution of Na[*cyclo*-P₅] in diglyme and stirred for 12 hours at 170 °C (**Scheme 30b**).



Scheme 30. Synthesis of 4,5-dialkyl-1,2,3-triphospholides **50–53**. In parentheses: the corresponding yield of the reaction.

A color change from orange to dark red and a formation of the precipitate was observed after several hours of reflux. The $^{31}\text{P}\{^1\text{H}\}$ NMR spectrum of the reaction mixture displays two resonances at $\delta = 241.8$ and 281.4 ppm as well as several low-intensity broad signals between $\delta = -150.0$ – 60.0 ppm typical for cage polyphosphides.^[105] The downfield shifted resonances represent an AB_2 spin system ($^1J_{\text{P-P}} = 473$ Hz) which is characteristic for the $1,2,3$ -[cyclo-(RC) $_2\text{P}_3$] $^-$ systems (**Figure 10**). The literature known 4,5-diphenyl-1,2,3-triphospholide anion **10** displays two resonances of the same multiplicity but slightly downfield shifted ($\delta = 272.2$ and 296.8 ppm)^[100] in comparison with the new species.

After the work up procedure, which includes a filtration and a removal of diglyme followed by washing of the residue with a THF:pentane mixture, the new compound was obtained as a dark red oil in 14 % yield. A detailed analysis of the new species revealed the presence the desired sodium 4,5-diethyl-1,2,3-triphospholide **50**. The ^1H NMR spectrum of **50** displays a triplet with the chemical shift at $\delta = 1.32$ ppm ($^3J_{\text{H-H}} = 8$ Hz) attributed to the CH_3 group and a low-intensity doublet-of-quartet signal at $\delta = 3.10$ ppm arising from the $^3J_{\text{H-H}}$ and $^3J_{\text{H-P}} = 12$ Hz coupling constants. The $\text{C}_{(\text{heterocycle})}$ nuclei were detected by $^{13}\text{C}\{^1\text{H}\}$ NMR as a multiplet resonance signal at $\delta = 177.5$ ppm.

4-Octyne also reacts with $\text{Na}[\text{cyclo-P}_5]$ under reflux conditions in diglyme to give the corresponding sodium 4,5-dipropyl-1,2,3-triphospholide **51** in 11 % yield (**Scheme 30**). The $^{31}\text{P}\{^1\text{H}\}$ NMR of **51** displays two downfield shifted multiplet resonances at $\delta(\text{ppm}) = 240.2$ and 280.5 forming an AB_2 spin system (**Figure 10**). Moreover, the concentrated sample reveals phosphorus-containing side-products as multiplets with resonances between $\delta = 258.0$ – 270.0 ppm. The ^1H NMR spectrum displays three resonances in the area between $\delta = 1.00$ – 3.03 ppm. The $\alpha\text{-CH}_2$ group protons were registered as a doublet-of-triplets with coupling constants of $^3J_{\text{H-H}} = 8$ Hz and $^3J_{\text{H-P}} = 12$ Hz. The $\text{C}_{(\text{heterocycle})}$ nuclei were observed in the $^{13}\text{C}\{^1\text{H}\}$ NMR spectrum at $\delta = 176.3$ ppm.

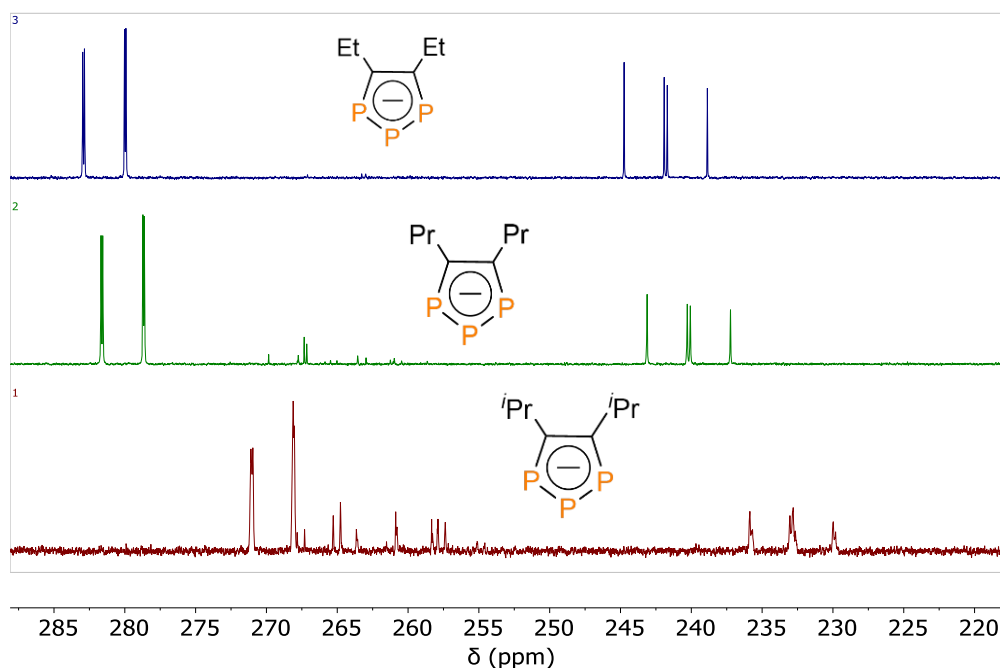
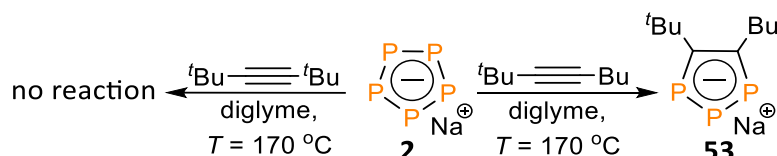


Figure 10. $^{31}\text{P}\{^1\text{H}\}$ NMR spectra of **50** (top, blue), **51** (middle, green), **52** (bottom, red).

Sterically more bulky 2,5-dimethylhex-3-yne (bis(isopropyl)acetylene) reacts with $\text{Na}[\text{cyclo-P}_5]$ to give the corresponding sodium 4,5-diisopropyl-1,2,3-triphospholide **52** in only 7 % yield (**Scheme 30**). The $^{31}\text{P}\{^1\text{H}\}$ NMR spectrum shows downfield shifted AB_2 multiplets ($\delta = 239.0$ and 276.0 ppm) and a phosphorus-containing side-product with a chemical shift between $\delta = 258.0$ – 270.0 ppm (**Figure 10**). The CH_3 group protons were detected by ^1H NMR spectroscopy at $\delta = 1.73$ ppm. Interestingly, the $^{13}\text{C}\{^1\text{H}\}$ NMR spectrum reveals the $\text{C}_{(\text{heterocycle})}$ nuclei as a multiplet resonance signal at $\delta = 185.0$ ppm, which is 10 ppm downfield compared to **51** ($\delta = 176.5$ ppm).

A gradual loss of the yield of the main product and the formation of additional side products were observed moving from 3-hexyne to more bulky 2,5-dimethylhex-3-yne. The $^{31}\text{P}\{^1\text{H}\}$ NMR spectroscopic monitoring of the mixture containing $\text{Na}[\text{cyclo-P}_5]$ and one equivalent of 2,2,5,5-tetramethylhex-3-yne (bis(*tert*-butyl)acetylene) did not show any reaction between the two species but rather the slow decomposition of $\text{Na}[\text{cyclo-P}_5]$ (**Scheme 31**). At the same time, the less bulky 4,4-dimethylpent-2-yne reacts with $\text{Na}[\text{cyclo-P}_5]$ to give the desired nonsymmetric 4-*tert*-butyl-5-methyl-1,2,3-triphospholide anion **53** (**Scheme 31**), which was shown as a downfield shifted AMX spin system pattern by $^{31}\text{P}\{^1\text{H}\}$ NMR spectroscopy.

These experiments indicate the importance of the accessibility of the C≡C triple bond (**Scheme 31**). The relatively low yield of these reactions is also due to the electron-donating nature of the alkyl groups that surround the C≡C triple bond. Moreover, all aliphatic 1,2,3-triphospholides **50–53** are very sensitive to air and moisture and readily decompose.



Scheme 31. Test reactions with 2,2,5,5-tetramethylhex-3-yne (left) and 4,4-dimethylpent-2-yne (right)

The proton-coupled ^{31}P NMR spectra of **50** (**Figure 11**) exhibit second order effects due to the $\text{AA}'\text{BX}_2\text{X}'_2$ spin system nature of these compounds. At the same time, the ^{31}P NMR spectrum of **52** (**Figure 12**) displays an $\text{AA}'\text{BXX}'$ spin system pattern. Both ^{31}P NMR spectra are in accordance with the proposed structure of these compounds and the expected number of $^3J_{\text{H-P}}$ couplings.

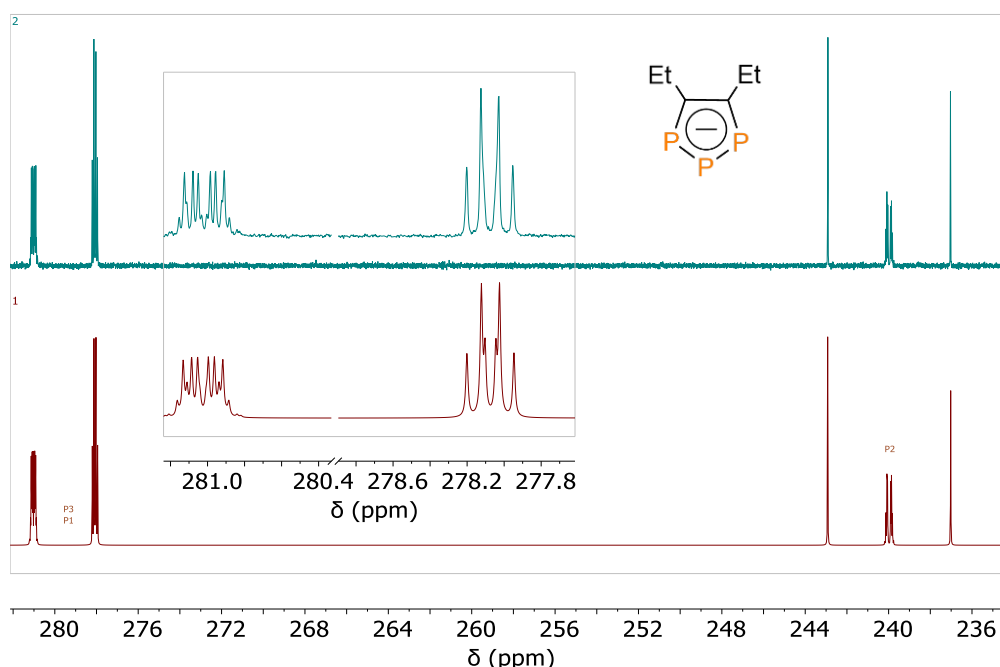


Figure 11. Experimental (top, blue) and simulated (bottom, red) ^{31}P NMR spectra of **50**.

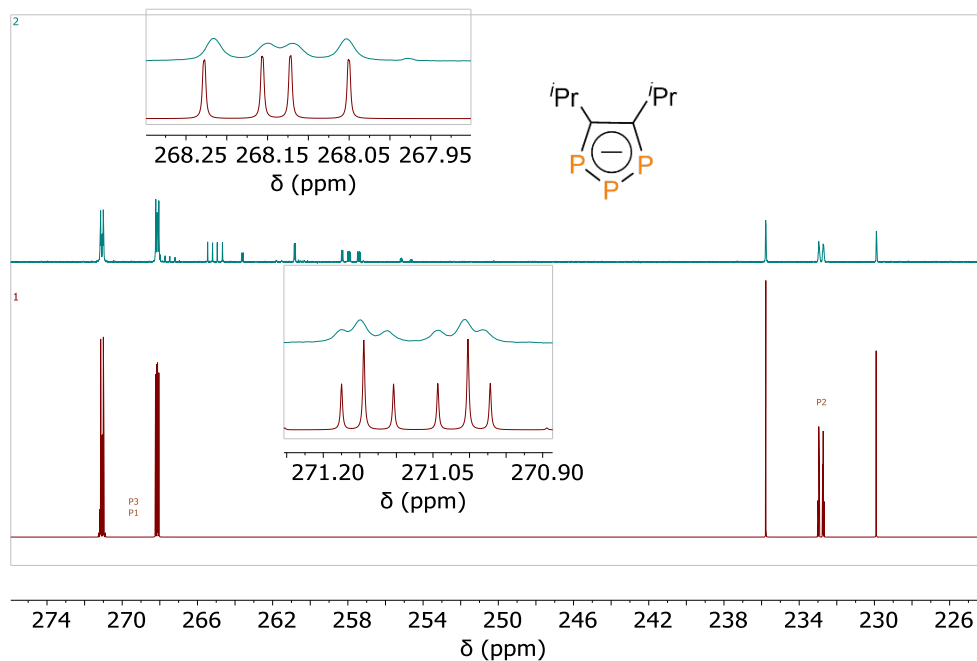


Figure 12. Experimental (top, blue) and simulated (bottom, red) ^{31}P NMR spectra of **52**.

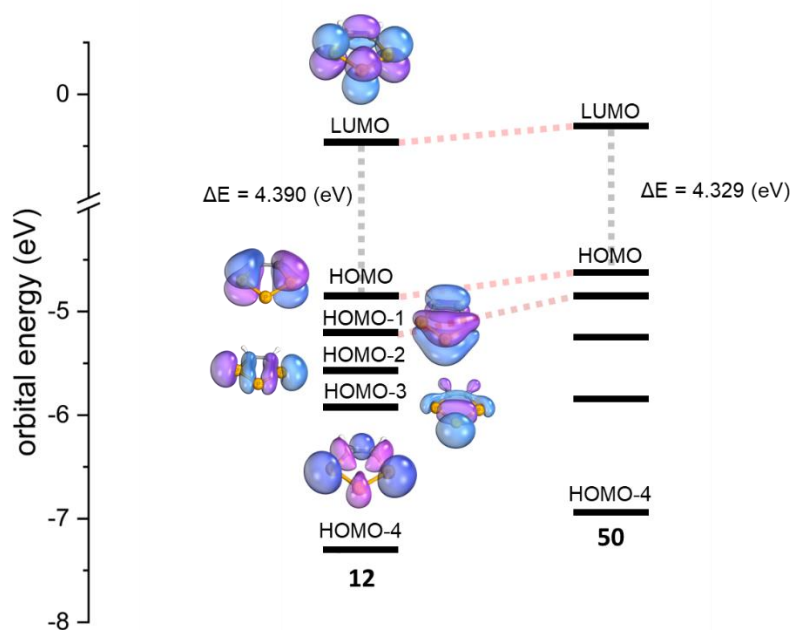


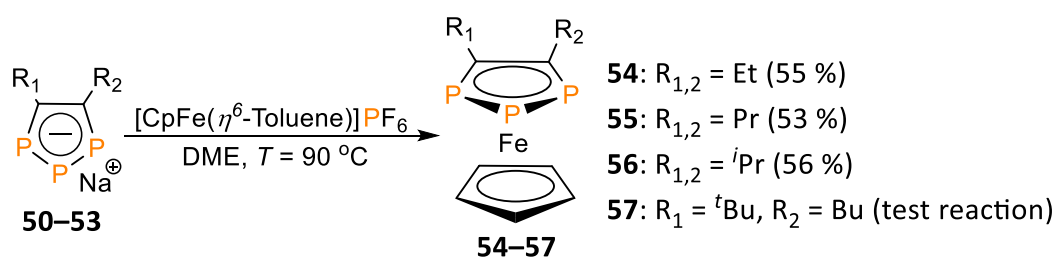
Figure 13. Frontier molecular orbitals of the parent 1,2,3-triphospholide anion **12** and the 3,5-diethyl-1,2,3-triphospholide anion **50**. Calculated at the B3LYP-D3/def2-TZVP level of theory.

The frontier molecular orbitals of the parent 1,2,3-triphospholide **12** and the ethyl derivative **50** (**Figure 13**) display two bonding π -orbitals (HOMO and HOMO-1) that are close in energy, while the antibonding π^* -orbital represents the LUMO in these species. The comparison reveals that the alkyl substituent leads to an increase in energy of the HOMO and LUMO in **50**. Therefore, the ethyl derivative of 1,2,3-triphospholide can be considered as the better π -donor than the parent 1,2,3-triphospholide.

Compounds **51** and **52** are also accessible in a *one-pot* procedure (analogous to **Scheme 29**) when *in situ* generated polyphosphides are directly reacted with alkynes. Although the method showed a high efficiency and selectivity in the synthesis of 4,5-diaryl-1,2,3-triphospholides (**Scheme 29**),^[100] this is not true for aliphatic alkynes. The *one-pot* reaction between sodium, P₄ and the aliphatic alkyne in diglyme under reflux conditions leads to a mixture of the desired species along with the parent 1,2,3-triphospholide **12**. It is most likely that a combination of the volatility of the alkyne and the steric hindrance of the C≡C triple bond leads to undesirable interactions of polyphosphides with diglyme resulting in the formation of **12** (analogous to **Scheme 6**).^[32]

2.2.2 Synthesis of 4,5-dialkyl-1,2,3-triphosphaferrocenes

The high sensitivity of the new species **50–53** towards moisture and air makes it necessary to stabilize them in the coordination sphere of a transition metal center. It was found that [CpFe(η^6 -Toluene)]PF₆ reacts with **50–53** in DME under reflux conditions to give 4,5-dialkyl-1,2,3-triphosphaferrocenes **54–57** (**Scheme 32**).



Scheme 32. Synthesis of 4,5-dialkyl-1,2,3-triphosphaferrocenes **54–57**. In parentheses: the corresponding yield of the reaction.

The ³¹P{¹H} NMR spectra of the reaction mixtures show a significant upfield shift of two multiplets corresponding to **54–56**, which appear between $\delta = -10.0$ – 60.0 ppm with a

preserved AB₂ spin system pattern, in line with the proposed η^5 -coordination of these ligands. The coupling constants are around $^1J_{P-P} \approx 420$ Hz and are smaller in comparison to the free ligands (**50**: $^1J_{P-P} = 473$ Hz), indicating a slight elongation of the interatomic bonds in the complexes.

The ^1H NMR spectra of **54–56** reveal the resonances assigned to the α -CH₂ (**54**, **55**) and β -CH₃ (**56**) protons as divided into two multiplets with the same integration between $\delta = 2.40$ – 2.80 ppm (**54**, **55**) (**Figure 14**) and between $\delta = 1.20$ – 1.60 ppm (**56**). This phenomenon implies the diastereomeric nature of the complexes **54–56**. VT (Variable Temperature) ^1H NMR spectroscopy experiment did not reveal the coalescence of these multiplets at elevated temperatures. The $^{13}\text{C}\{^1\text{H}\}$ NMR spectra of **54–56** display the C_(Heterocycle) nuclei as a multiplet with its signal at around $\delta \approx 120$ ppm.

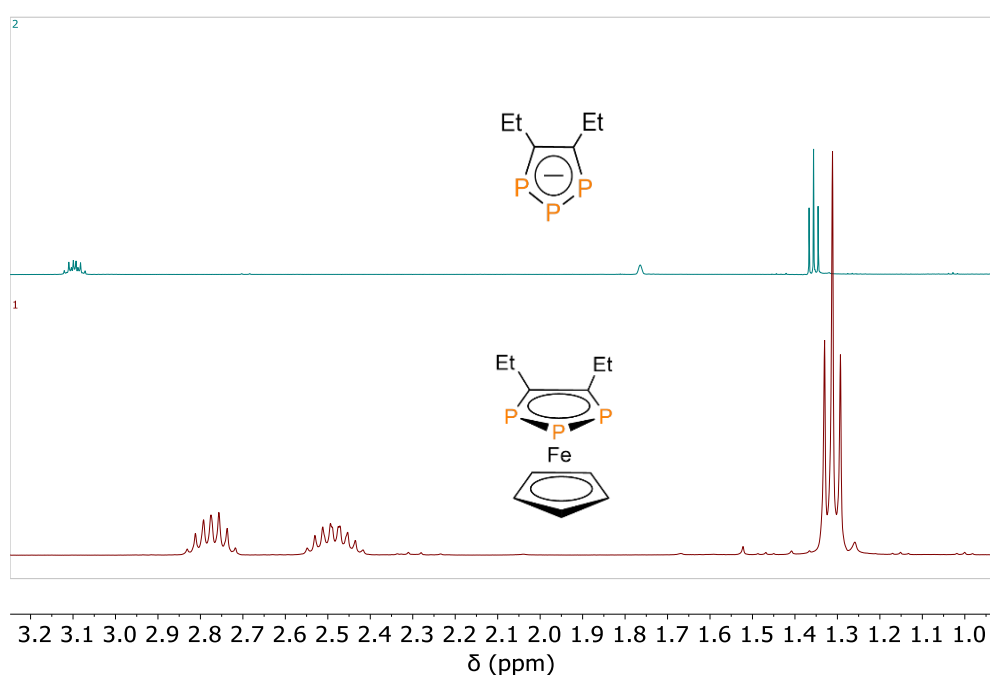


Figure 14. Comparison of the ^1H NMR spectra of **50** (top, blue), and **54** (bottom, red).

Compounds **54–56** possess a higher stability compared to the free ligands and can be purified either by column chromatography or by sublimation. Single crystals of the symmetric complexes **54–56** were obtained from the concentrated pentane solutions at $T = -36$ °C. Compounds **54** and **56** crystallize in the monoclinic space group $P2_1/n$, while **55** crystallizes in the monoclinic space group $P2_1/c$. The sandwich structure arrangement is confirmed in these

complexes (**Figure 15**). The η^5 -coordinated 1,2,3-triphospholyl and cyclopentadienyl rings are almost parallel to each other with a tilting angle of $177.80(8)^\circ$ for **54**, $179.15(4)^\circ$ for **55** and $179.18(2)^\circ$ for **56**. Complexes **54** and **55** slightly deviate from a perfect eclipsed conformation with interplanar angles of $2.82(19)^\circ$ and $2.95(9)^\circ$, respectively. At the same time, **56** has a staggered conformation with an interplanar angle of $21.47(6)^\circ$. The $[\text{C}_2\text{P}_3]_{\text{cent}}\text{—Fe}$ length value of $1.5973(10)$ Å for **54** is shorter than the $[\text{Cp}]_{\text{cent}}\text{—Fe}$ distance of $1.6736(15)$ Å, which serves as structural evidence of the π -acceptor nature of the 1,2,3-triphospholyl ligand.

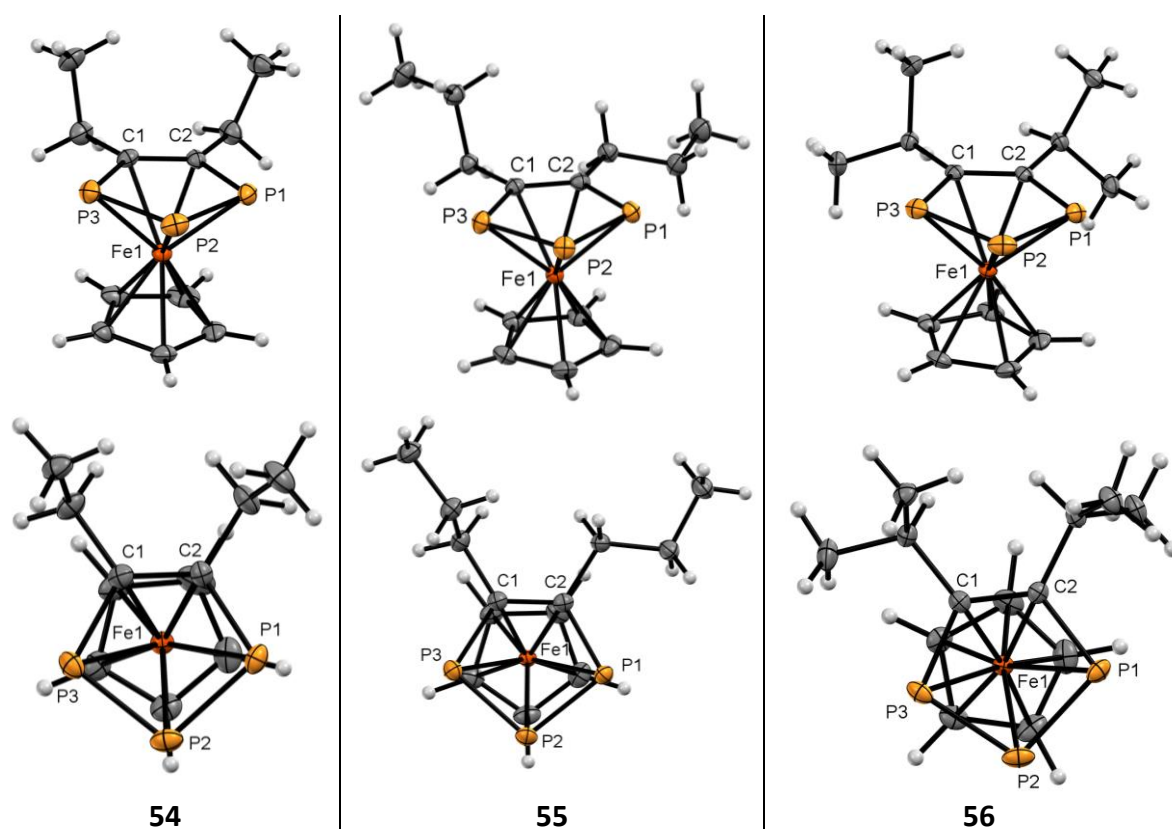


Figure 15. Molecular structures of **54–56** in the crystal. Ellipsoids are shown at 50 % probability level. Selected bond lengths (Å) and angles ($^\circ$): **54**: P1-P2: 2.1298(14); P2-P3: 2.1288(14); C1-C2: 1.412(5); C2-P1: 1.781(3); P1-P2-P3: 99.36(5); P1-C2-C1: 121.0(2); $[\text{Cp}]_{\text{cent}}\text{—Fe1}$: 1.6736(15); $[\text{C}_2\text{P}_3]_{\text{cent}}\text{—Fe1}$: 1.5973(10); **55**: P1-P2: 2.1267(6); P2-P3: 2.1286(5); C1-C2: 1.418(2); C2-P1: 1.7850(16); P1-P2-P3: 99.75(2); P1-C2-C1: 120.61(12). $[\text{Cp}]_{\text{cent}}\text{—Fe1}$: 1.6735(7); $[\text{C}_2\text{P}_3]_{\text{cent}}\text{—Fe1}$: 1.5996(5) **56**: P1-P2: 2.1261(4); C1-C2: 1.7885(10); C2-P1: 1.7885(10); P1-P2-P3: 99.560(15); P1-C2-C1: 120.49(7) $[\text{Cp}]_{\text{cent}}\text{—Fe1}$: 1.6778(7); $[\text{C}_2\text{P}_3]_{\text{cent}}\text{—Fe1}$: 1.6031(4).

Aliphatic substituents do not significantly affect the bond lengths and angles within the [Cp-Fe-C₂P₃] framework, as shown by the similarity with these values in the previously reported 4,5-diphenyl-1,2,3-triphosphaferrocene **58**.^[106] The P1—P2 and P2—P3 bond lengths are within the range of 2.1257(4)–2.1298(14) Å and lie in between the standard P—P single (2.20 Å) and the P=P double (2.00 Å) bond distances, which indicates a delocalization of the electron density in the heterocycle. Similar values for the C1—C2 bond lengths in **54–56** (1.412(5)–1.4219(13) Å) and in the previously reported 4,5-diphenyl-1,2,3-triphosphaferrocene **58** (1.426(8) Å)^[106] denote an absence of the strain caused by the branched alkyl substituents. The P3-C1-C2 and C1-C2-P1 angles are nearly 120°, while P-centered angles are closer to a value of 100°.

Phosphaferrocenes can also undergo one-electron oxidation to form kinetically unstable phosphaferrocenium cations. Replacing the CH unit in ferrocene with the isolobal P atom leads to increasingly positive oxidation potentials. Moreover, oxidation potentials are significantly depend on the nature of substituents that are attached to the phosphaferrocene scaffold: an electron-withdrawing substituent results in a cathodic shift, while an electron-donating substituent acts in the opposite manner.^[107]

The cyclic voltammogram of the complex **54** (**Figure 16**, right) shows an irreversible oxidation process at the peak potential of $E_{ox} = 0.56$ V (vs. Fc/Fc⁺) and at sweep rates of 25–500 mV/s. This value is close to the E_{ox} of the isomeric 3,5-bis(*tert*-butyl)-1,2,4-triphosphaferrocene **59** ($E_{ox} = 0.50$ V (vs. Fc/Fc⁺))^[107] and shifted anodically by 0.23 V compared to 4,5-diphenyl-1,2,3-triphosphaferrocene **58** ($E_{ox} = 0.79$ V (vs. Fc/Fc⁺)).^[106] The increase of the scan rate causes higher peak currents for the cathodic wave, along with a slight cathodic shift. Upon scanning anodically at a sweep rate of 100 mV/s (**Figure 16**, left), an irreversible reduction wave at the peak potential of $E_{red} = -2.80$ V (vs. Fc/Fc⁺) followed by two coupled anodic signals at -0.95 V and 0.32 V (vs. Fc/Fc⁺) was registered.

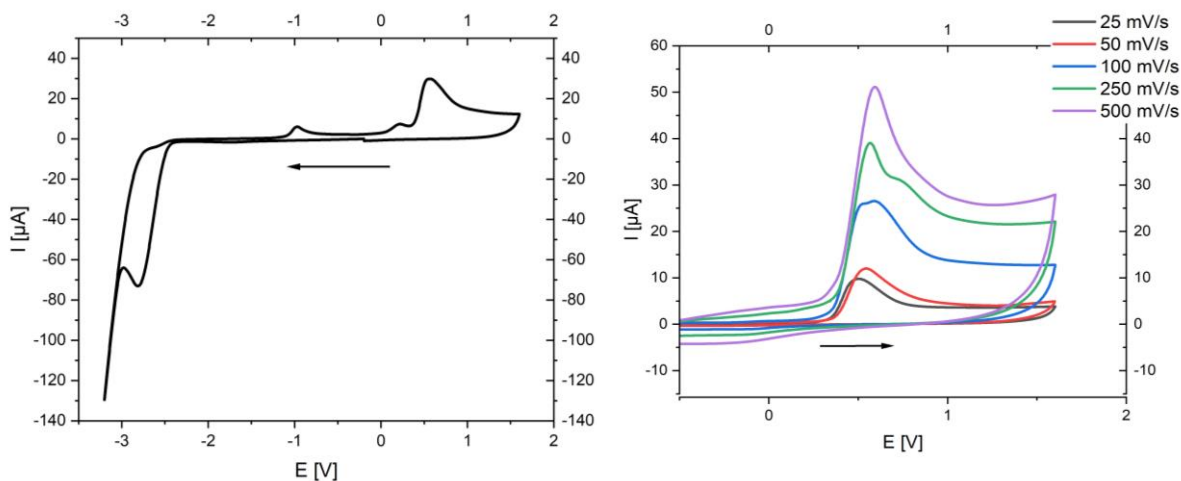


Figure 16. Cyclic voltammogram of **54** in DCM under an atmosphere of argon. Measurement conditions: $T = 20^{\circ}\text{C}$, scan rate: 100 mV/s (left), conducting salt: 0.1 M $[\text{NBu}_4]\text{PF}_6$. Potentials were referenced versus Fc/Fc^+ .

Compound	 54	 58	 59
$E_{\text{ox}}/E_{\text{red}}$ (V, vs Fc/Fc^+)	0.56/-2.80	0.79	0.5

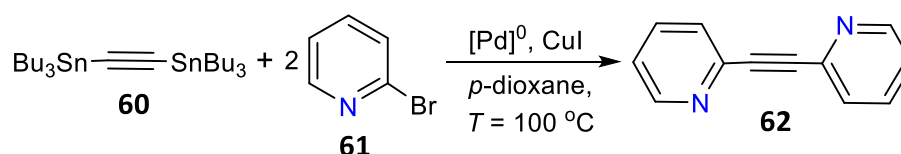
Table 1. Electrochemical parameters of triphosphaferrocenes.

The recorded redox properties of the 4,5-diethyl-1,2,3-triphosphaferrocene **54** are in line with the electronic properties of 1,2,3-phospholyl ligand discussed previously (**Figure 13**). The electron-donating nature of the ethyl substituents leads to a higher energy of the HOMO and thus weakens the π -acceptor capability of the ligand.

2.2.3 Synthesis of 1,2,3-triphospholides with the heteroatom-functionalized substituents

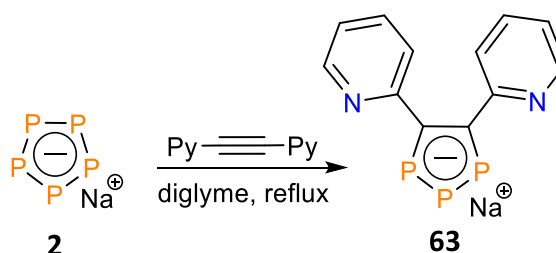
The progress in the synthesis of aliphatic derivatives of $1,2,3\text{-[cyclo-(RC)}_2\text{P}_3\text{]}^-$ raised the question, whether it is possible to incorporate heteroelements in the backbone of the substituents. To date, the list of corresponding derivatives only includes monopyridyl-^[104] and bistihiophenyl-functionalized^[100] $1,2,3\text{-[cyclo-(RC)}_2\text{P}_3\text{]}^-$.

The initial approach was to expand the library of characterized $1,2,3\text{-[cyclo-(RC)}_2\text{P}_3\text{]}^-$ by introducing P,N-substituents to enable a polydentate function of the heterocycle, making them more attractive for studying their coordination chemistry. First, di(pyridin-2-yl)ethyne (bispyridylacetylene) **62** was synthesized according to the literature procedure *via* a Stille cross-coupling reaction between 1,2-bis(tributylstannyl)ethyne **60** and bromopyridine **61** (Scheme 33).^[108]



Scheme 33. Synthesis of di(pyridin-2-yl)ethyne **62**.

Yellow crystals of 1,2-di(pyridin-2-yl)ethyne **62** were obtained by multiple extractions followed by sublimation. Indeed, $\text{Na[cyclo-P}_5\text{]}$ reacts with one equivalent of the alkyne to give sodium 4,5-bispyridyl-1,2,3-triphospholide **63** in 40 % yield (Scheme 34).



Scheme 34. Synthesis of sodium 4,5-bispyridyl-1,2,3-triphospholide **63**.

The $^{31}\text{P}\{^1\text{H}\}$ NMR spectrum of **63** displays resonance signals of an AB_2 spin system pattern at $\delta = 290.3$ and 300.5 ppm, which is more downfield shifted compared to the 4,5-diphenyl-1,2,3-triphospholide anion **10** ($\delta = 272.2$ and 296.6 ppm). The ^1H NMR spectrum reveals four resolved multiplets between $\delta = 6.90\text{--}8.10$ ppm which integrate in a 1:1:1:1 ratio and are attributed to the pyridyl substituents. The most downfield shifted resonance belongs to two protons next to the N-atom in the pyridine ring. The $\text{C}_{(\text{heterocycle})}$ nuclei registered at $\delta = 174.8$ ppm in the $^{13}\text{C}\{^1\text{H}\}$ NMR spectrum, which is close to the aliphatic derivatives ($\delta \approx 176$ ppm).

The new species **63** reacts with $[\text{CpFe}(\eta^6\text{-Toluene})]\text{PF}_6$ under reflux conditions in diglyme to give the corresponding 4,5-bispyridyl-1,2,3-triphosphaferrocene **64**, which can be easily

isolated by sublimation. The $^{31}\text{P}\{^1\text{H}\}$ NMR spectrum reveals resonance signals of an AB_2 spin system (for **64**: $\delta = 2.1$ and 77.2 ppm) which are significantly shielded in comparison to the free ligand (for **63**: $\delta = 290.3$ and 300.5 ppm). Single crystals were obtained by cooling the saturated acetonitrile solution of **64** down to $T = -36$ °C.

As it was expected, the molecular structure of **64** shows the $[\text{C}_2\text{P}_3]$ and $[\text{Cp}]$ rings coordinated in the η^5 -fashion to the iron center with a tilting angle of $178.92(4)^\circ$ (**Figure 17**). The new phosphoferrocene exhibits an eclipsed conformation (deviation angle is $9.35(10)^\circ$) in the crystal. The interatomic bond lengths and angles in **64** are similar to those observed in **54–56**. The repulsion between the two sterically demanding substituents results in a twist angle of $47.19(4)^\circ$ between the $[\text{C}_2\text{P}_3]$ and $[\text{Py}]$ rings, while the 4-*H*-5-pyridyl-1,2,3-triphospholyl ligand η^5 -coordinated to molybdenum is almost parallel (twist angle between $[\text{C}_2\text{P}_3]$ and $[\text{Py}]$ is 5.6°).^[101]

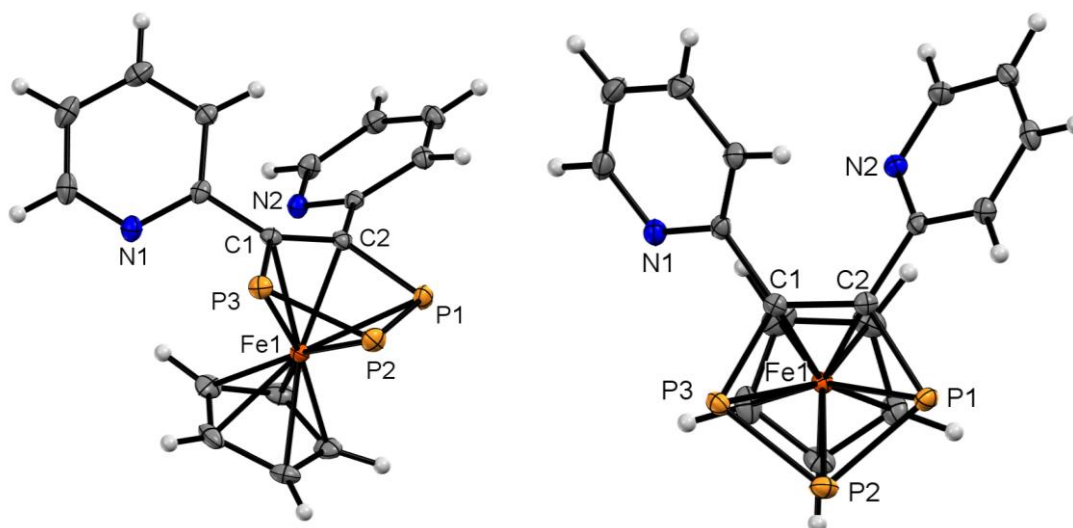
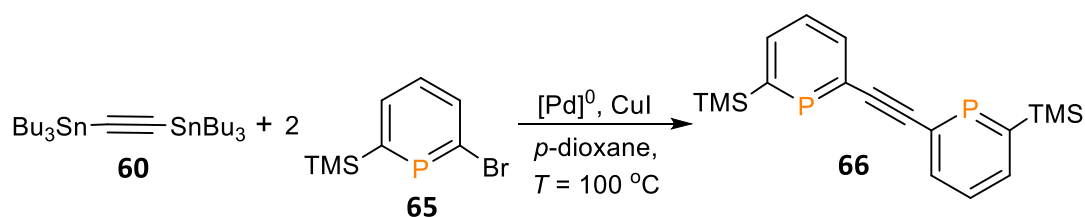


Figure 17. Molecular structure of **64** in the crystal. Ellipsoids are shown at 50 % probability level. Selected bond lengths (Å) and angles (°): **64**: P1-P2: 2.1244(6); P2-P3: 2.1269(6); C1-C2: 1.422(2); C2-P1: 1.7824(16); P1-P2-P3: 100.52(2); P1-C2-C1: 120.95(12). $[\text{Cp}]_{\text{cent}}\text{-Fe1-}[\text{C}_2\text{P}_3]_{\text{cent}}$: $178.92(4)$; interplanar angle: $9.35(10)^\circ$. $[\text{C}_2\text{P}_3]_{\text{cent}}\text{-Fe1-}[\text{Cp}]_{\text{cent}}\text{-Fe1}$: $1.6754(7)$.

The next goal was to synthesize an isoelectronic analog of bispyridylacetylene with two phosphinine substituents. Two equivalents of bromophosphinine **65**, synthesized according to the literature procedure,^[109] as well as bis(tributyl)tinacetylene **60**, a palladium catalyst,

and CuI were loaded in a Schlenk flask with dioxane as a solvent and stirred under reflux conditions (**Scheme 35**).



Scheme 35. Synthesis of bisphosphenylacetylene **66**.

The Stille cross-coupling reaction was monitored by means of the $^{31}\text{P}\{^1\text{H}\}$ NMR spectroscopy. Within 12 hours the singlet resonance at $\delta = 232.0$ ppm corresponding to the starting compound **65** had disappeared, while a new singlet formed at $\delta = 245.9$ ppm. The APCI-MS (Atmospheric Pressure Chemical Ionization Mass Spectrometry) spectrum taken from the reaction mixture reveals a molecular ion peak at $m/z = 359.1$ which was identified as a $[\text{M}+\text{H}]^+$ ion of the new alkyne **66**. The ^1H NMR spectrum of **66** displays resonance signals of the phosphinyl substituents between $\delta = 7.50\text{--}8.00$ ppm, while the CH_3 protons of the TMS group were detected at $\delta = 0.40$ ppm. The $^{13}\text{C}\{^1\text{H}\}$ NMR spectrum of **66** shows some characteristic resonance as doublets emerging from $^nJ_{\text{C-P}}$ ($n = 1\text{--}4$) coupling constants.

Unfortunately, it was not possible to isolate the new alkyne due to the low yield, volatility of the desired compound and a contamination with organotin compounds. The standard work up protocols were not suitable for the isolation of air- and moisture-sensitive products. The low yield of this reaction can be explained by the formation of relatively stable phosphinyl—Pd complexes with the stable Pd—P σ -bonds.

However, **66** reacts with two equivalents of CuBr at room temperature in DCM to give complex **67** with a characteristic a heterocubane-type $[\text{Cu}_4\text{Br}_4]$ cluster (**Figure 18**). The complexation results in an upfield shift of the singlet resonance to $\delta(\text{ppm}) = 199.2$ in the $^{31}\text{P}\{^1\text{H}\}$ NMR spectrum (**66**: $\delta = 245.9$ ppm).

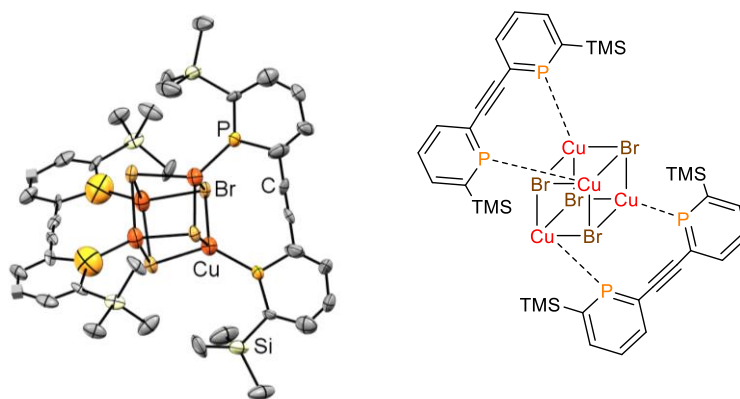
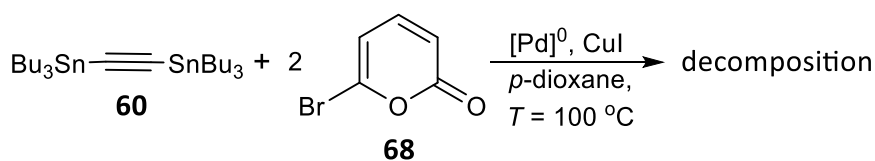


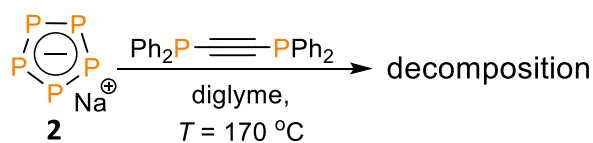
Figure 18. Connectivity of copper-bisphosphenylacetylene **67** complex in the crystal.

Another approach to this acetylene was based on the Stille cross-coupling reaction between 3-bromo-2-pyrone **68** and bis(tributyltin)acetylene **60** (Scheme 36). Bromopyrone **68**, a precursor in the synthesis of bromophosphinine **65**, is stable on air. Thus, it was presumed that the purification and isolation of the corresponding bis(pyrone)acetylene would be easier compared to **66**. However, suitable conditions to perform this cross-coupling reaction were not found.



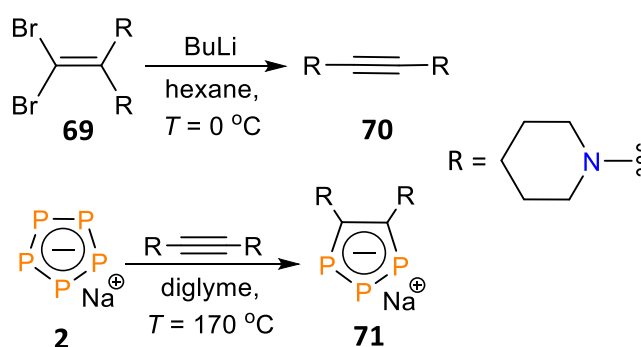
Scheme 36. Approach to bis(pyrone)acetylene via the Stille cross-coupling reaction.

Subsequently, acyclic alkynes with P,N-substituents were applied in the reaction with Na[cyclo-P₅]. One equivalent of bis(diphenylphosphino)acetylene was added to a solution of Na[cyclo-P₅] and the reaction mixture was stirred under reflux conditions for 12 hours (Scheme 37). Although there was visual evidence of a chemical reaction due to a color change and a formation of the precipitate, the ³¹P{¹H} NMR spectrum of the reaction mixture only revealed decomposition of Na[cyclo-P₅].



Scheme 37. Reaction between **2** and bis(diphenylphosphino)acetylene.

Next, the reaction with 1,1-dipiperidinoethyne **70** (**Scheme 38**) was performed. The alkyne was originally synthesized by *Tamm et al.* based on the Fritsch–Buttenberg–Wiechell (FBW) rearrangement of 2,2-dibromo-1,1-ethenediamine **69**.^[110] Diaminoacetylene **70** was reacted with a diglyme solution of Na[*cyclo*-P₅] under reflux conditions to give sodium 4,5-dipiperidino-1,2,3-triphospholide **71**. Interestingly, the ³¹P NMR spectrum shows an AB₂ spin system with two multiplets at δ = 198.4 and 229.5 ppm (¹J_{P-P} = 487 Hz) (**Figure 19**), which is substantially upfield shifted compared to other 1,2,3-triphospholide anions.



Scheme 38. Synthesis of 4,5-dipiperidino-1,2,3-triphospholide anion **71**.

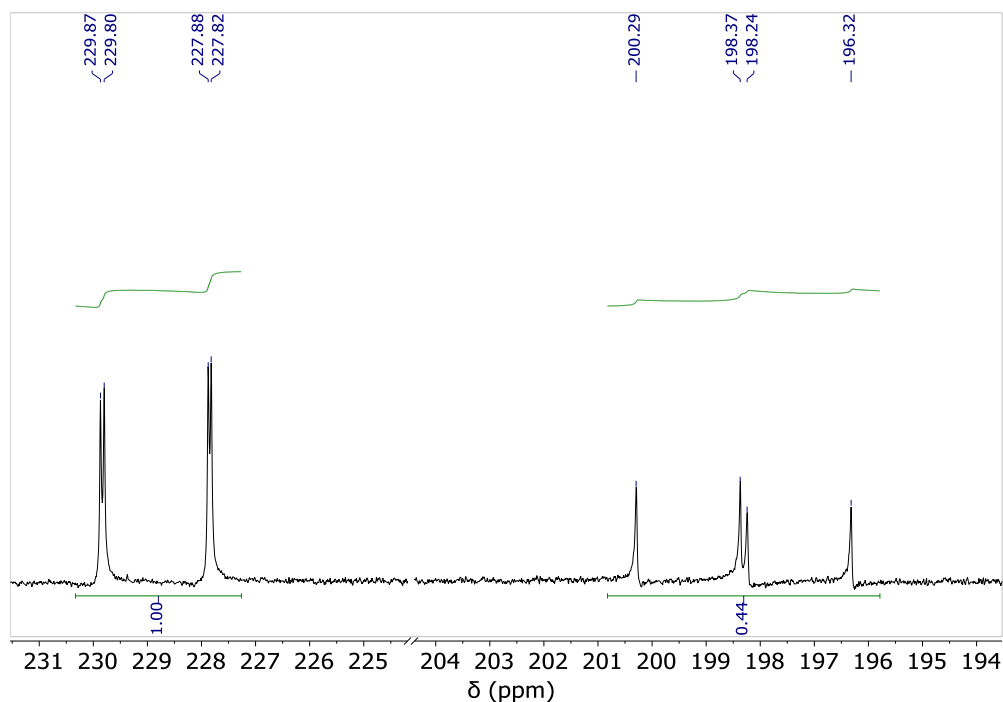


Figure 19. ³¹P NMR spectrum of sodium 4,5-dipiperidino-1,2,3-triphospholide **71**.

This observation is reminiscent of the electronic features of 2-aminophosphine reported by Müller *et al.*,^[111] and is indicative of an effective interaction between the lone pairs of the N-atoms and the triphospholide heterocycle (**Figure 20**).

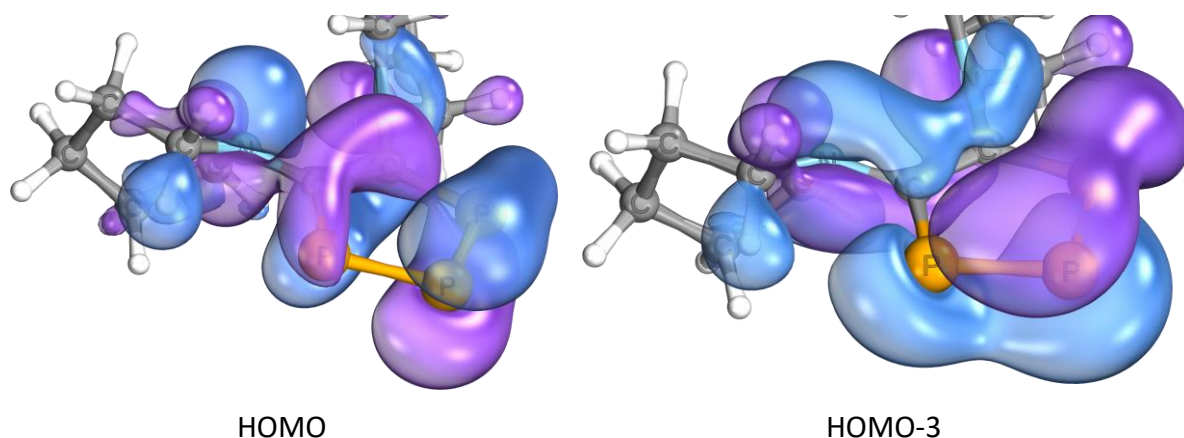
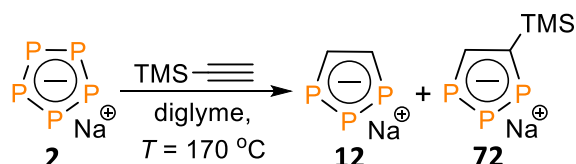


Figure 20. The HOMO and HOMO-3 orbitals of **71** showing $n(N)-\pi(C_2P_3)$ interactions.

Calculated at the B3LYP-D3/def2-TZVP level of theory.

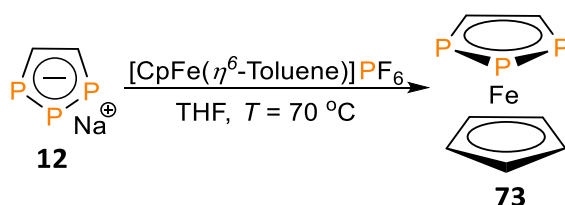
It was further attempted to examine silicon-substituted alkynes in the reaction with a diglyme solution of Na[*cyclo*-P₅] (**Scheme 39**). One equivalent of trimethylsilylacetylene was added to diglyme solution of Na[*cyclo*-P₅] and kept under reflux conditions for 12 hours. After several hours the orange-colored solution turned deep red. The ³¹P{¹H} NMR spectrum taken from the reaction mixture showed five multiplets with resonances between $\delta = 260.0$ – 300.0 ppm that were assigned to the parent 1,2,3-triphospholide **12** (2 multiplets of an AB₂ spin system at $\delta = 262.3$ and 273.7 ppm, ¹J_{P-P} = 490 Hz; which is the major product of the reaction) and 4-trimethylsilyl-1,2,3-triphospholide anion **72** (3 multiplets of an AMX spin system at $\delta = 277.1$ (d), 289.8 (dd), 301.4 (d) ppm, ¹J_{P-P} = 470 and 481 Hz; which is the minor product).



Scheme 39. Synthesis of the parent 1,2,3-triphospholide anion **12** and the 4-trimethylsilyl-5-H-1,2,3-triphospholide anion **72**.

It was assumed that the harsh reaction conditions lead to a protodesilylation of **72** in the presence of the basic Na[cyclo-P₅]. Indeed, the yield of **12** increases when the reaction between trimethylsilylacetylene and Na[cyclo-P₅] is performed in the presence CsF or KF. The ¹H NMR spectrum of the parent 1,2,3-triphospholide anion shows CH_(heterocycle) protons as a multiplet with a resonance at δ = 8.97 ppm, arising from ³J_{H-H} = 8 Hz, ²J_{H-P} = 46 Hz, and ³J_{P-P} = 17 Hz coupling constants. The C_(heterocycle) nuclei were detected at δ = 155.6 ppm in the ¹³C{¹H} NMR spectrum, which is about 20 ppm shifted upfield in comparison to the 4,5-diphenyl- and 4,5-diethyl-1,2,3-triphospholide anions **10** and **50**, respectively.

12 reacts with [CpFe(η⁶-Toluene)]PF₆ in THF under reflux conditions to give the parent 1,2,3-triphosphaferrocene **73** (Scheme 40). Pure crystalline powder of the new compound was collected in low 8 % yield after sublimation of a crude solid residue. The ³¹P{¹H} NMR spectrum exhibits signals of an AB₂ spin system at δ = 12.5 and 40.6 ppm (¹J_{P-P} = 409 Hz), which is significantly upfield shifted compared to **12** (δ = 262.3 and 273.7 ppm). The ¹H NMR reveals characteristic protons as a multiplet with resonances at δ = 6.15 ppm, which is approximately 3 ppm upfield shifted compared to **12**. The C_(heterocycle) nuclei of the ligand were detected in the ¹³C{¹H} NMR spectrum as a multiplet at δ = 99.2 ppm.



Scheme 40. Synthesis of parent 1,2,3-triphosphaferrocene **73**.

The single crystals of **73** were obtained from a concentrated pentane solution of the complex at T = -36 °C. The molecular structure of **73** in the crystal shows a sandwich complex with an eclipsed conformation, which deviates from the ideal conformation by 5.9(3)° (Figure 21). The juxtaposition of structural parameters of **73** with other 1,2,3-triphosphaferrocenes does not show any distinctive features. However, a detailed comparison with the free ligand **12**^[104] shows that all bonds in the η⁵-coordinated 1,2,3-triphosphyl ligand are slightly elongated.

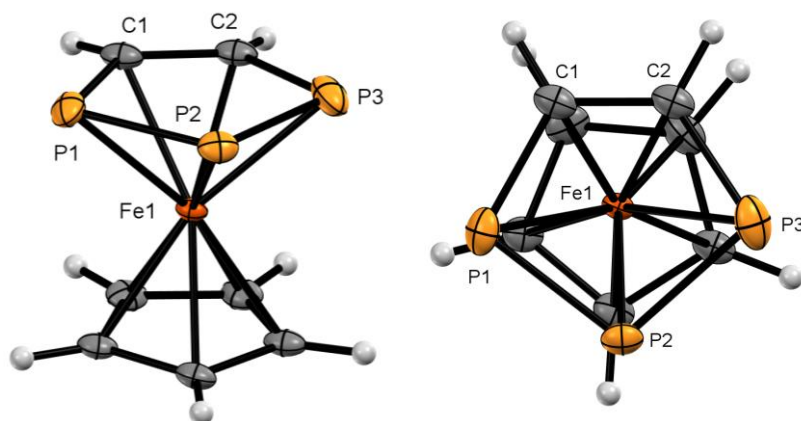


Figure 21. Molecular structure of **73** in the crystal. Ellipsoids are shown at 50 % probability level. Selected bond lengths (Å) and angles (°): **73**: P1-P2: 2.129(2); P2-P3: 2.115(2); C1-C2: 1.422(8); C1-P1: 1.797(6); P1-P2-P3: 100.49(9); P1-C1-C2: 119.2(4). $[\text{Cp}]_{\text{cent}}\text{-Fe1-}[\text{C}_2\text{P}_3]_{\text{cent}}$: 178.47(11); interplanar angle: 5.9(3); $[\text{C}_2\text{P}_3]_{\text{cent}}\text{-Fe1}$: 1.5986(17); $[\text{Cp}]_{\text{cent}}\text{-Fe1}$: 1.672(3).

2.3 Conclusions

In summary, it was shown that the aromatic $\text{Na}[\text{cyclo-P}_5]$ **2**, which is readily available from elemental sodium and P_4 , reacts with aliphatic alkynes to give sodium 3,5-dialkyl-1,2,3-triphospholides **50–53** (Scheme 30b), what is in contrast to the cage polyphosphide $\text{K}_3[\text{P}_7]$ **4** (Scheme 30a). It is assumed that the aromaticity of $[\text{cyclo-P}_5]^-$ plays an important role in the stabilization of intermediates and controls the reaction profile in general. It was found, that sterically demanding substituents surrounding the $\text{C}\equiv\text{C}$ triple bond hinders the desired interaction (Scheme 31).

At the same time, the interaction between alkynes with electron-withdrawing groups and $\text{Na}[\text{cyclo-P}_5]$ is more favored. In fact, $\text{Na}[\text{cyclo-P}_5]$ reacts with bispyridylacetylene **62** to give 3,5-bispyridyl-1,2,3-triphospholide **63** in good yield (Scheme 34). This compound is particularly interesting as a ligand in metallocene chemistry, due to its multidentate nature.

The approach to a P-analog of bispyridylacetylene resulted in the synthesis and characterization of the previously unknown bisphosphinylacetylene **66** via the Stille cross-coupling reaction between bromophosphinine **65** and bis(tetrabutyltin)acetylene **60** (Scheme 35). However, the desired product was collected in very low yield and was contaminated with tinorganyls, which could not be isolated. Nevertheless, it was demonstrated that the novel

bisphosphinylacetylene **66** undergoes coordination with two equivalents of CuBr in THF to form the heterocubane-cluster **67** (**Figure 18**).

Na[*cyclo*-P₅] reacts with dipiperidinoacetylene **70** to give the corresponding 4,5-dipiperidino-1,2,3-triphospholide anion **71** in moderate yield (**Scheme 38**). The distinguishing feature of **71** is the pronounced interaction of the strongly π -donating piperidine substituent with the aromatic system of the phosphorus heterocycle.

Interestingly, trimethylsilylacetylene reacts with Na[*cyclo*-P₅] to give the parent 1,2,3-triphospholide anion **12** as a major product, indicating protodesilylation of the corresponding alkyne under these conditions (**Scheme 39**). Previously, it was reported that the parent 1,2,3-triphospholide anion **12** is accessible *via* a reaction between K₃[P₇] and gaseous acetylene.^[30] The new method is considered to an easier route to the parent heterocycle because it does not require any corrosive and potentially explosive acetylene, as well as special laboratory equipment.

All new sodium 3,5-*R*-1,2,3-triphospholides react with [CpFe(η^6 -Toluene)]PF₆ to give the corresponding 3,5-*R*-1,2,3-triphosphaferrocenes in good yields (**Scheme 32**, **Scheme 40**). This reaction may serve as experimental evidence of the aromaticity of 3,5-*R*-1,2,3-triphospholyl rings. Novel phosphametallocenes were characterized *via* cyclic voltammetry (**Figure 16**) and SC-XRD analysis (**Figure 15**, **Figure 17** and **Figure 21**). The cyclic voltammograms of the selected species show the pronounced π -acceptor nature of the new heterocycles when compared to ferrocene.

2.4 Experimental part

2.4.1 General remarks

All reactions were performed under an argon atmosphere in oven-dried glassware using modified Schlenk techniques or in an MBraun glovebox unless otherwise stated. All common solvents and chemicals were commercially available. 3-Hexyne, 4-octyne, 2,2-dimethyloct-3-yne, ferrocene, alumina powder, 2-bromopyridine, trichloroethylene, AlCl₃, NH₄PF₆ and TBAPF₆ were commercially available. 3-Bromo-2H-pyran-2-one^[112] was available in the laboratory and initially it was synthesized according to the literature procedure. The synthesis of all other chemicals is discussed below. Commercially available chemicals were used

without further purification. All dry and deoxygenated solvents were prepared using standard techniques or were obtained from a MBraun solvent purification system. The ^1H , ^{31}P and $^{31}\text{P}\{^1\text{H}\}$ NMR spectra were recorded on a JEOL ECS400 spectrometer (^{31}P : 162 MHz, ^1H : 400 MHz). Some $^{31}\text{P}\{^1\text{H}\}$ NMR spectra were recorded on a Bruker AVANCE III 700 spectrometer (242 MHz). $^{13}\text{C}\{^1\text{H}\}$ spectra were recorded on a Bruker AVANCE III 700 spectrometer (176 MHz). All chemical shifts are reported relative to the residual resonance in the deuterated solvents. The ESI-TOF (Electron-Spray ionization Time-of-flight) Mass spectrometry measurements were performed on an Agilent 6230 ESI-TOF. Cyclic voltammograms were measured at room temperature with the substance (0.005 mmol) in DCM (5 mL) and 0.1 M TBAPF₆ added as an electrolyte at 25–250 mV/s under an argon atmosphere. Ferrocene was used as the internal standard. An Autolab PGSTAT302N potentiostat by Metrohm was used in combination with an in-house made, gas-tight glass cell equipped with a glassy carbon disk working electrode by Metrohm, a platinum wire as counter electrode and a leak-free Ag/AgCl reference electrode LF-2 by Innovative Instruments, Inc. Low-temperature diffraction data were collected on Bruker-AXS X8 Kappa Duo diffractometers with $l\mu\text{S}$ micro-sources, performing ϕ - and ω -scans. For the structures of compounds **54–56**, **64**, and **73** data were collected using a Photon 2 CPAD detector with Mo K_α radiation ($\lambda = 0.71073 \text{ \AA}$). For the structure of compound **67**, a Smart APEX2 CCD detector and Cu K_α radiation ($\lambda = 1.54178 \text{ \AA}$) was used. The structures were solved by dual-space methods using SHELXT^[113] and refined against F^2 on all data by full-matrix least squares with SHELXL-2017^[114] following established refinement strategies^[115]. The program Olex2^[116] was also used to aid in the refinement of the structures of compounds. All non-hydrogen atoms were refined anisotropically. All hydrogen atoms were included into the model at geometrically calculated positions and refined using a riding model. The isotropic displacement parameters of all hydrogen atoms were fixed to 1.2 times the U-value of the atoms they are linked to (1.5 times for methyl groups). DFT Calculations were carried out with the ORCA 5.0.3 program suite.^[117] Initial molecular structures were created in the program Avogadro^[118] or were based on crystal structures, if available. Geometry optimizations were then performed with the PBEh-3c method developed by Grimme and co-workers.^[119] Standardized convergence criteria were used for the geometry optimization (OPT). To confirm the nature of stationary points found by geometry optimizations analytical frequency calculations were carried out. The absence of imaginary vibrational frequencies indicated that the optimized structure is a local minimum.

Final single point calculations on the optimized structures were conducted with the B3LYP^[120] functional with def2-TZVP^[121] basis set and def2/J^[122] auxiliary basis set. Additionally, for all calculations the Dispersion Correction (D3)^[123] was used. For SCF-calculations an additional “tight” correlation was included (“TIGHTSCF”). Solvent effects were taken into account with the Conductor-like-Polarizable-Continuum-Modell (CPCM)^[124] for THF. Intrinsic bond orbital (IBO) analysis^[125] was carried out with the IBO module implemented in the ORCA program suite. Molecular orbitals and IBOs were visualized via the freely available IBOView v20150427.^[126]

2.4.2 Synthesis of alkynes

2,5-dimethylhex-3-yne

$i\text{Pr}-\text{C}\equiv\text{C}-i\text{Pr}$ This synthesis is based on the original manuscript by *Nicholas et al.*^[127] In a 250 mL Schlenk flask 3,6-dimethyl-4-octyne-3,6-diol 4.25 g (0.025 mol) and 100 mL of dichloromethane were mixed together. Then, 1 eq. of dicobalt octacarbonyl was added and the solution was allowed to stir at room temperature for 6 h. After this, the flask was cooled down to $T = 0\text{ }^{\circ}\text{C}$ in an ice bath and 2.8 g of sodium borohydride (0.08 mol) was added. To the resulting suspension, kept at $0\text{ }^{\circ}\text{C}$, 25 mL of trifluoroacetic acid was added. The organic layer was separated and washed several times with cold water. The complex was then demetalated by the addition of 38 g of FeNO_3 to the dichloromethane solution over 2 h, followed by an additional 4 h of stirring. The solution was decanted and dried under vacuum. The product was further purified by distillation at low-pressure. Yield: 1.56 g, 0.04 mol, 57 %.

$^1\text{H NMR (25 }^{\circ}\text{C, CDCl}_3) \delta \text{ (ppm) = 1.07 (d, } J_{\text{H-H}} = 7 \text{ Hz, 12H, CH}_3\text{), 3.06 (st, } ^3J_{\text{H-H}} = 8 \text{ Hz, 3H, CH).}$

2,2,5,5-tetramethylhex-3-yne

$t\text{Bu}-\text{C}\equiv\text{C}-t\text{Bu}$ This synthesis is based on the original manuscript by *Marcuzzi et al.*^[128] In a 250 ml Schlenk flask 1,2-bis(trimethylsilyl)ethyne 4 g (0.023 mol) and 2eq. of *tert*-butylchloride were dissolved in 100 ml of DCM. After the Schlenk flask was cooled down to $T = -30\text{ }^{\circ}\text{C}$, 0.3 g (0.002 mol) of AlCl_3 was added. The reaction was allowed to warm up to room temperature within 3 h. The organic phase was washed several times with water and dried

afterward. After DCM was removed under vacuum and the residue was distilled at low pressure to give the desired product as a colorless oil. Yield: 1.33 g, 9.6 mmol, 42 %.

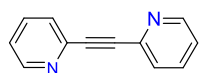
$^1\text{H NMR}$ (25 °C, CDCl_3) δ (ppm) = 1.17 (s, 18H, CH_3).

1,2-bis(tributylstannyl)ethyne (60)

$(\text{Bu})_3\text{Sn}-\text{C}\equiv\text{C}-\text{Sn}(\text{Bu})_3$ This synthesis is based on the original manuscript by *Eichler et al.*^[108] $n\text{-BuLi}$ (24 mL, 60.2 mmol, 3 eq.) was dissolved in a mixture of equal amounts of THF and Et_2O (50 mL). Then, the solution was cooled down to $T = -80$ °C and trichloroethylene (1.8 mL, 20 mmol, 1 eq.) was added dropwise with stirring. After the addition was complete, the reaction mixture was allowed to warm up to room temperature and stirred for 3 h. The suspension was cooled to $T = -80$ °C and tributyltin chloride (10.5 mL, 38.3 mmol, 1.9 eq.) was added dropwise. The suspension was stirred for 14 hours at room temperature and later it was quenched with a saturated ammonium chloride solution (40 mL). The aqueous layer was extracted with DCM (3 x 50 mL) and the organic layers were combined and washed with brine (2 x 50 mL). Then, the organic phase was dried over magnesium sulfate. DCM was removed under reduced pressure and the pale yellow oil was purified *via* fractional distillation under reduced pressure. Yield: 5.91 g, 9.8 mmol, 50 %.

$^1\text{H NMR}$ (25 °C, CDCl_3) δ (ppm) = 1.63–1.29 (m, 24 H), 1.20–0.72 (m, 30 H).

1,2-di(pyridin-2-yl)ethyne (62)

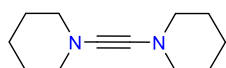


This synthesis is based on the original manuscript by *Eichler et al.*^[108] 1,2-bis(tributylstannyl)ethyne (6.4 g, 11 mmol, 1 eq.), 2-bromopyridine (2.1 mL, 22.1 mmol, 2 eq.) and $\text{Pd}(\text{PPh}_3)_4$ (220 mg, 1.5 mol%) were dissolved in dioxane (80 mL) and stirred at $T = 100$ °C for 15 h. The solvent was removed under reduced pressure and the oily residue was dissolved in 20 mL of DCM. The product was extracted with aqueous HCl (40 mL, 6 M). The aqueous layer was washed three times with 50 mL of DCM. Then, the aqueous layer was slowly added to 100 mL of 25 % solution of ammonia and extracted with DCM (3 x 25 mL). The organic layer was finally washed with a saturated solution of KF (20 mL) and brine (20 mL) and dried over MgSO_4 . The solvent was removed under reduced pressure to afford

yellow powder, which was further purified by sublimation to give pale yellow crystals of 1,2-di(pyridin-2-yl)ethyne. Yield: 1.13 g, 6.3 mmol, 57 %.

$^1\text{H NMR}$ (25 °C, CDCl_3) δ (ppm) = 8.60 (ddd, $^3J_{\text{H-H}} = 5$ Hz, $^4J_{\text{H-H}} = 2$ Hz, $^5J_{\text{H-H}} = 1.0$ Hz, 2H, CH), 7.67 (td, $^3J_{\text{H-H}} = 8$ Hz, $^4J_{\text{H-H}} = 2$ Hz, 2H, CH), 7.58 (dt, $^3J_{\text{H-H}} = 8$ Hz, $^4J_{\text{H-H}} = 1.0$, 2H, CH), 7.24 (ddd, $^3J_{\text{H-H}} = 8$ Hz, $^4J_{\text{H-H}} = 5$ Hz, $^5J_{\text{H-H}} = 1$ Hz, 2H, CH).

1,1-Dipiperidinoethene (70)

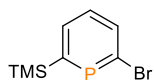


1,1-Dipiperidinoethene for the test reaction was synthesized in the group of Prof. Dr. Tamm (Institut für Anorganische und Analytische Chemie, Technische Universität Braunschweig).^[110]

Trimethylsilylphosphaalkyne (33)

See experimental part of **Chapter 4** for details.

6-bromo-2-(trimethylsilyl)phosphinine (65)

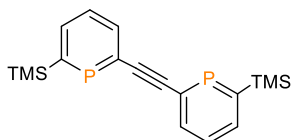


This synthesis is based on the original manuscript by Müller *et al.*^[109] A toluene solution of trimethylsilylphosphaalkyne (6.5 mmol, 75 mL) and 3-bromopyrone (6.5 mmol, 1.33 g) were added to the Schlenk flask and stirred under reflux for 24 hours. Then, the solvent was removed under reduced pressure to afford a black-colored oily residue. The desired product was isolated by column chromatography (10 cm silica layer, hexane as eluent) to afford a yellow oil of 6-bromo-2-(trimethylsilyl)phosphinine. Yield: 0.59 g, 2.4 mmol, 37 %.

$^1\text{H NMR}$ (25 °C, CDCl_3) δ (ppm) = 8.04 (dd, $^3J_{\text{H-H}} = 8.7$, $^3J_{\text{H-H}} = 4.1$ Hz, 1H, CH), 7.37 (dd, $^3J_{\text{H-H}} = 11.6$ Hz, $^3J_{\text{H-P}} = 7.6$ Hz, 1H, CH), 7.36 (ddd, $^3J_{\text{H-H}} = 8.5$ Hz, $^3J_{\text{H-H}} = 7.9$ Hz, $^3J_{\text{H-P}} = 4.1$ Hz, 1H, CH), 0.38 (s, 9 H, CH_3);

$^{31}\text{P}\{^1\text{H}\}$ NMR (25 °C, CDCl_3) δ (ppm) = 232.0 (s).

1,2-bis(6-(trimethylsilyl)phosphinin-2-yl)ethyne (66)



6-bromo-2-(trimethylsilyl)phosphinine (0.18 g, 0.905 mmol, 2 eq.), 1,2-bis(tributylstannyl)ethyne (0.27 g, 0.451 mmol, 1 eq.), tetrakis(triphenylphosphine)palladium(0) (0.052 g, 0.045 mmol)

and 10 mL of dioxane were added to the Schlenk flask. The reaction mixture was stirred at $T = 100\text{ }^{\circ}\text{C}$ for 14 hours. Then, the solvent was carefully removed under reduced pressure to afford black colored oily residue, which was dissolved in 3 mL of DCM. The solution was first filtrated through a small layer (0.5 cm) of celite. Then, the solution was filtrated through a silica layer (10 cm). 9:1 mixture of DCM and pentane was used as eluent. This procedure afforded a yellow-colored oil of the desired product contaminated with tinorganyls. Yield: not available.

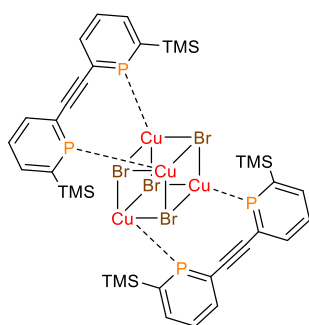
$^{31}\text{P}\{^1\text{H}\}$ NMR (25 $^{\circ}\text{C}$, CDCl_3) δ (ppm) = 245.9 (s);

^1H (25 $^{\circ}\text{C}$, CDCl_3) δ (ppm) = 8.04-7.96 (m, 2H, H-3, H-5), 7.59-7.54 (m, 1H, H-4), 0.38 (s, 9H, CH₃);

$^{13}\text{C}\{^1\text{H}\}$ (25 $^{\circ}\text{C}$, CDCl_3) δ (ppm) = 172.8 (d, $^1J_{\text{C-P}} = 80.6$ Hz, C), 152.1 (d, $^1J_{\text{C-P}} = 61.0$ Hz, C); 138.3 (d, $^3J_{\text{C-P}} = 4.0$ Hz, CH), 137.8 (br., CH), 129.6 (br., CH), 99.4 (d, $^2J_{\text{C-P}} = 33.0$ Hz, C), 0.1 (d, $^4J_{\text{C-P}} = 7.1$ Hz, CH₃);

APCI-MS (m/z): 359.1 [M+H]⁺.

1,2-bis(6-(trimethylsilyl)phosphinin-2-yl)ethyne copper bromide adduct (**67**)



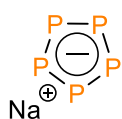
1,2-bis(6-(trimethylsilyl)phosphinin-2-yl)ethyne (2.2 mg, 6.1 μmol) and $[\text{Cu}(\text{Me}_2\text{S})]\text{Br}$ (2.4 mg, 12.2 μmol , 2 eq.) were loaded to a J. Young NMR-tube and dissolved in 1 mL of THF. The reaction was kept for one hour at room temperature. Then, the reaction mixture was transferred to a vial in the glove box and, subsequently, 10 mL of pentane was added. The formed precipitate was washed several

times with pentane to afford the desired product contaminated with tinorganyls as a yellow oil. Single crystals of the desired product were grown upon vapor diffusion of pentane into a vial with the concentrated DCM solution of **67**. Yield: not available.

$^{31}\text{P}\{^1\text{H}\}$ NMR (25 $^{\circ}\text{C}$, CD_2Cl_2) δ (ppm) = 199.2;

^1H NMR (25°C, CD_2Cl_2) δ (ppm) = 8.06–7.93 (m, 2H, CH), 7.59–7.46 (m, CH), 0.47 (s, 9H, CH_3).

2.4.3 Synthesis of sodium pentaphospholide $\text{Na}[\text{cyclo-P}_5]$ (2)

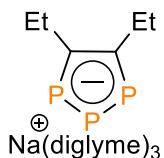


Sodium pentaphospholide was synthesized according to the literature procedure.^[35] P_4 (approx. 1.20 g), stored under water, was transferred to a pre-weighed 100 mL Schlenk flask, was washed with ethanol, acetone and ethyl ether and dried under vacuum for 30 min. After washing, the mass of P_4 was remeasured (1.04 g, 8.4 mmol, 1 eq.). Na (0.39 g, 16.9 mmol, 2.1 eq.), catalytic amounts of DB-18-C-6 (5 mg) and 30 mL of diglyme were added to the Schlenk flask containing P_4 . The reaction was stirred under reflux for 3 hours to afford an orange-colored solution. The solution was filtered *via* a cannula equipped with a microfiber glass filter. Yield: 2.5 mmol, 30 %.

$^{31}\text{P}\{^1\text{H}\}$ NMR (25°C, H_3PO_4 capillary) δ (ppm) = 468.7.

2.4.4 Synthesis of sodium 1,2,3-triphospholides

Sodium 4,5-diethyl-1,2,3-triphospholide (50)



3-Hexyne (0.2 g, 2.5 mmol, 1 eq.) was added to a diglyme solution of $\text{Na}[\text{cyclo-P}_5]$ (1 eq.) in a pressure-rated Schlenk flask. The reaction mixture was stirred at $T = 170$ °C for 12 h. Then, the solution was filtered *via* a cannula equipped with a microfiber glass filter and the solvent was removed under reduced pressure. The crude residue was washed three times with a THF:pentane (2 ml:40 ml) mixture and dried under vacuum for several hours to give **50** as a dark red oil. The composition of the cation solvate shell was calculated on the basis of the ^1H NMR spectroscopy. Yield: 210 mg, 0.3 mmol, 14 %.

$^{31}\text{P}\{^1\text{H}\}$ NMR (25 °C, THF- d_8) δ (ppm) = (AB₂ spin system) 241.8 (m, $^1J_{\text{P-P}} = 473$ Hz, P_A), 281.4 (m, $^1J_{\text{P-P}} = 473$ Hz, P_B);

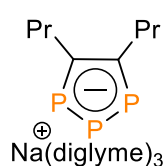
^{31}P NMR (25 °C, THF- d_8) δ (ppm) = (AA'BX₂X₂' spin system) 241.8 (m, $^1J_{\text{P-P}} = 473$ Hz, P_B), 281.4 (m, $^1J_{\text{P-P}} = 473$ Hz, $^2J_{\text{P-P}} = 17$ Hz, $^3J_{\text{H-P}} = 12$ Hz P_A/P_{A'});

^1H NMR (25°C, THF- d_8) δ (ppm) = 1.32 (t, $J^3_{\text{H-H}} = 8$ Hz, 6H, CH_3), 3.06 (dq, $^3J_{\text{H-P}} = 12$ Hz, $^3J_{\text{H-H}} = 8$ Hz, 4H, CH_2), 3.33 (s, 18H, $\text{CH}_3_{\text{diglyme}}$), 3.48 (m, 12H, $\text{CH}_2_{\text{diglyme}}$), 3.56 (m, 12H, $\text{CH}_2_{\text{diglyme}}$);

$^{13}\text{C}\{^1\text{H}\}$ NMR (25 °C, THF-*d*₈) δ (ppm) = 20.1 (d, $^3J_{\text{C-P}} = 4$ Hz, CH₃), 27.7 (m, CH₂), 59.3 (s, CH₃_{diglyme}), 70.9 (s, CH₂_{diglyme}), 72.6 (s, CH₂_{diglyme}), 177.5 (m, C_{heterocycle});

ESI- (m/z): 174.9987 (calc. 175.0001) [R₂C₂P₃⁻].

Sodium 4,5-dipropyl-1,2,3-triphospholide (51)



51 was synthesized according to the same procedure as the above-mentioned **50** using the solution of Na[cyclo-P₅] (2.5 mmol in 30 mL) and 4-octyne (2.5 mmol, 0.27 g). After the standard work up procedure **2.3** was collected as a dark red oil. The composition of the cation solvate shell was calculated on the basis of the ^1H NMR spectroscopy. Yield: 172 mg, 0.3 mmol, 11 %.

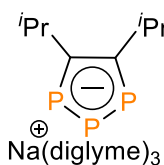
$^{31}\text{P}\{^1\text{H}\}$ NMR (25 °C, THF-*d*₈) δ (ppm) = (AB₂ spin system) 240.2 (m, $^1J_{\text{P-P}} = 473$ Hz, P_A), 280.5 (m, $^1J_{\text{P-P}} = 473$ Hz, P_B);

^1H NMR (25 °C, THF-*d*₈) δ (ppm) = 1.00 (t, $J^3_{\text{H-H}} = 8$ Hz, 6H, CH₃), 1.29 (br, 4H, CH₂), 3.03 (dq, $^3J_{\text{H-P}} = 12$ Hz, $^3J_{\text{H-H}} = 8$ Hz, 4H, CH₂), 3.31 (s, 18H, CH₃_{diglyme}), 3.48 (m, 12H, CH₂_{diglyme}), 3.57 (m, 12H, CH₂_{diglyme});

$^{13}\text{C}\{^1\text{H}\}$ NMR (25 °C, THF-*d*₈) δ (ppm) = 15.1 (s, CH₃), 29.1 (d, $^3J_{\text{C-P}} = 4$ Hz, CH₂), 37.3 (m, CH₂), 59.1 (s, CH₃_{diglyme}), 71.2 (s, CH₂_{diglyme}), 72.8 (s, CH₂_{diglyme}), 176.3 (m, C_{heterocycle});

ESI- (m/z): 203.0305 (calc. 203.0314) [R₂C₂P₃⁻].

Sodium 4,5-diisopropyl-1,2,3-triphospholide (52)



52 was synthesized according to the same procedure as the above-mentioned **50** using the solution of Na[cyclo-P₅] (2.5 mmol in 30 mL) and 2,5-dimethylhex-3-yne (2.5 mmol, 0.27 g). After the standard work up procedure **52** was collected as a dark red oil. Alternatively, **52** can be synthesized in a *one-pot* procedure: P₄ (1 g, 8.4 mmol, 1.0 eq.), Na (0.26 g, 11.3 mmol, 1.4 eq.), alkyne (1.0 eq.) and DB-18-C-6 (5 mg) were loaded to the Schlenk flask and stirred under reflux for 8 hours. After the standard work up procedure, the desired product **52** was collected as a dark red oil which was contaminated with the parent 1,2,3-triphospholide **12**. The composition of the cation

solvate shell was calculated on the basis of the ^1H NMR spectroscopy. Yield: 166 mg, 0.2 mmol, 6 % (via $\text{Na}[\text{cyclo-P}_5]$).

$^{31}\text{P}\{^1\text{H}\}$ NMR (25 °C, THF- d_8) δ (ppm) = (AB₂ spin system) 239.0 (m, $^1J_{\text{P-P}} = 473$ Hz, P_A), 276.0 (m, $^1J_{\text{P-P}} = 473$ Hz, P_B);

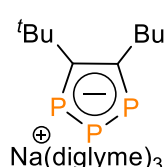
^{31}P NMR (25 °C, THF- d_8) δ (ppm) = (AA'BXX' spin system) 239.0 (m, $^1J_{\text{P-P}} = 473$ Hz, P_B), 276.0 (m, $^1J_{\text{P-P}} = 473$ Hz, $^2J_{\text{P-P}} = 17$ Hz, $^3J_{\text{H-P}} = 12$ Hz, P_A/P_{A'});

^1H NMR (25 °C, THF- d_8) δ (ppm) = 1.45 (d, $J^{\text{H-H}} = 8$ Hz, CH₃), 3.30 (s, 18H, CH₃_{diglyme}), 3.45 (m, 12H, CH₂_{diglyme}), 3.54 (m, 12H, CH₂_{diglyme});

$^{13}\text{C}\{^1\text{H}\}$ NMR (25 °C, THF- d_8) δ (ppm) = 29.4 (m, CH₃), 33.9 (m, CH), 59.1 (s, CH₃_{diglyme}), 71.2 (s, CH₂_{diglyme}), 72.8 (s, CH₂_{diglyme}), 185.0 (m, C_{heterocycle});

ESI- (m/z): 203.0348 (calc. 203.0314) [$\text{R}_2\text{C}_2\text{P}_3^-$].

Sodium 4-*tert*-butyl-5-butyl-1,2,3-triphospholide (53)

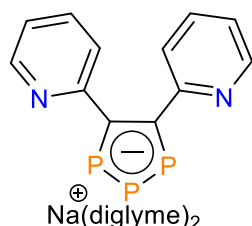


53 was synthesized according to the same procedure as the above-mentioned **50** but on a smaller scale as a test reaction using 2,2-dimethyloct-3-yne. 1,2,3-triphospholide **53** was not isolated from the reaction mixture. Yield: not available.

$^{31}\text{P}\{^1\text{H}\}$ NMR (25°C, THF- d_8) δ (ppm) = (AMX spin system) 237 (t, $^1J_{\text{P-P}} = 477$ Hz, P_A), 281 (dd, $^1J_{\text{P-P}} = 477$ Hz, $^2J_{\text{P-P}} = 11$ Hz, P_M), 298 (t, $^1J_{\text{P-P}} = 477$ Hz, $^2J_{\text{P-P}} = 11$ Hz, P_X);

ESI- (m/z): 231.0635 (calc. 231.0627) [$\text{R}_2\text{C}_2\text{P}_3^-$].

Sodium 4,5-bispyridyl-1,2,3-triphospholide (63)



1,2-di(pyridine-2-yl)ethyne **62** (0.45 g, 2.5 mmol, 1 eq.) was added to the diglyme solution of $\text{Na}[\text{cyclo-P}_5]$ (2.5 mmol in 30 mL). The reaction mixture was stirred under reflux for 8 hours. After the standard work up procedure, sodium 4,5-bispyridyl-1,2,3-triphospholide **63** was collected as a dark red oil. The composition of the cation solvate shell was calculated on the basis of the ^1H NMR spectroscopy. Yield: 606 mg, 1.1 mmol, 43 %.

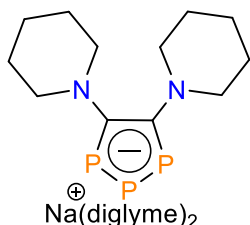
$^{31}\text{P}\{^1\text{H}\}$ NMR (25 °C, THF-*d*₈) δ (ppm) = (AB₂ spin system) 290.3 (m, $^1J_{\text{P-P}} = 482$ Hz, P_A), 300.5 (m, $^1J_{\text{P-P}} = 482$ Hz, P_B);

^1H NMR (25 °C, THF-*d*₈) δ (ppm) = 3.30 (s, 18H, CH₃_{diglyme}), 3.45 (m, 12H, CH₂_{diglyme}), 3.54 (m, 12H, CH₂_{diglyme}), 6.91 (m, 2H, CH), 7.29 (m, 2H, CH), 7.42 (m, 2H, CH), 8.18 (m, 2H, CH);

$^{13}\text{C}\{^1\text{H}\}$ NMR (25 °C, THF-*d*₈) δ (ppm) = 59.1 (s, CH₃_{diglyme}), 71.2 (s, CH₂_{diglyme}), 72.8 (s, CH₂_{diglyme}), 120.3 (s, CH), 126.1 (s, CH), 135.9 (s, CH), 147.9 (s, CH), 164.7 (m, *ipso*-C), 174.8 (m, C_(heterocycle));

ESI- (m/z): 272.9889 (calc. 272.9906) [R₂C₂P₃⁻].

Sodium 4,5-dipiperidino-1,2,3-triphospholide (71)



Dipiperidinoacetylene **70** (150 mg, 0.8 mmol, 1 eq.) was added to the diglyme solution of Na[*cyclo*-P₅] (0.8 mmol in 10 mL). The reaction mixture was stirred under reflux for 8 hours. After the standard work up procedure, sodium **71** was collected as an orange powder. The composition of the cation solvate shell calculated on the basis of the ^1H NMR spectroscopy.

Yield: 101 mg, 0.2 mmol, 22 %.

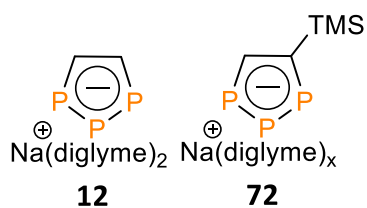
$^{31}\text{P}\{^1\text{H}\}$ NMR (25 °C, THF-*d*₈) δ (ppm) = (AB₂ spin system) 198.4 (m, $^1J_{\text{P-P}} = 487$ Hz, P_A), 229.5 (m, $^1J_{\text{P-P}} = 487$ Hz, P_B);

^1H NMR (25 °C, THF-*d*₈) δ (ppm) = 1.49–1.55 (br, 8H, CH₂), 1.69 (m, 8H, CH₂), 3.14–3.21 (br, 8H, CH₂), (3.29 (s, 12H, CH₃_{diglyme}), 3.45 (m, 8H, CH₂_{diglyme}), 3.54 (m, 8H, CH₂_{diglyme});

$^{13}\text{C}\{^1\text{H}\}$ NMR (25 °C, THF-*d*₈) δ (ppm) = 26.1 (s, CH₂), 28.6 (s, CH₂), 57.2 (t, $^3J_{\text{P-C}} = 7$ Hz, CH₂), 59.1 (s, CH₃_{diglyme}), 71.2 (s, CH₂_{diglyme}), 72.8 (s, CH₂_{diglyme}), 184.7 (m, C_(heterocycle));

ESI- (m/z): 285.0879 (calc. 285.0845) [R₂C₂P₃⁻].

Sodium 1,2,3-triphospholide (parent 1,2,3-triphospholide anion) (12) and sodium 4-trimethylsilyl-1,2,3-triphospholide and (72)



Ethynyltrimethylsilane (0.23 g, 2.5 mmol, 1 eq.) was added to a diglyme solution of Na[*cyclo*-P₅] (2.5 mmol in 30 mL) and stirred under reflux conditions for 14 hours. The standard work up procedure (see 50) afforded both **12** (major) and **72** (minor) products in a 5 : 1 ratio (according to the ³¹P NMR spectrum). Exclusive formation of **12** is achievable when the reaction is performed in the presence of CsF or KF (1 eq.). The composition of the cation solvate shell was calculated on the basis of the ¹H NMR spectroscopy. Yield: 276 mg, 0.7 mmol, 27 %.

12: ³¹P{¹H} NMR (242 MHz, 25 °C, THF-*d*₈) δ (ppm) = (AB₂ spin system) 262.3 (m, ¹J_{P-P} = 484 Hz, P_A), 273.7 (m, ¹J_{P-P} = 484 Hz, P_B);

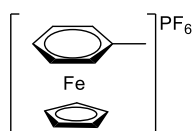
¹H NMR (25°C, THF-*d*₈) δ (ppm) = 3.27 (s, 12H, CH₃_{diglyme}), 3.44 (m, 8H, CH₂_{diglyme}), 3.53 (m, 8H, CH₂_{diglyme}), 9.03 (m, ³J_{H-H} = 8 Hz, ²J_{H-P} = 47 Hz, ³J_{H-P} = 18 Hz, ³J_{H-P} = 6 Hz, 2H, CH);

¹³C{¹H} NMR (25 °C, THF-*d*₈) δ (ppm) = 59.2 (s, CH₃_{diglyme}), 71.1 (s, CH₂_{diglyme}), 72.9 (s, CH₂_{diglyme}), 155 (m, CH).

72: ³¹P{¹H} NMR (242 MHz, 25 °C, THF-*d*₈) δ (ppm) = (AMX spin system) 278.1 (d, ¹J_{P-P} = 476 Hz, P_A), 290.4 (t, ¹J_{P-P} = 476 Hz, P_M), 301.8 (d, ¹J_{P-P} = 476 Hz, P_X).

2.4.5 Synthesis of 1,2,3-triphosphaferrocenes

Iron(II) η⁶-toluene-η⁵-cyclopentadienyl hexafluorophosphate ([CpFe(η⁶-Toluene)]PF₆)



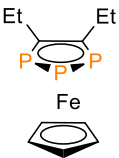
Ferrocene (10.0 g, 53 mmol), finely powdered alumina (1.4 g, 54 mmol, 1 eq.), AlCl₃ (7.15 g, 53 mmol 1 eq.) and toluene (150 mL) were loaded to the Schlenk flask. The reaction was stirred under reflux conditions for 14 hours.

The reaction mixture was cooled down to room temperature, the residue AlCl₃ was carefully quenched with 100 mL of water. The resulting water phase was separated from toluene and washed several times with DCM (50 mL). NH₄PF₆ (8.6 g, 53 mmol) was added to the water solution, which has produced a green precipitate of the desired product. The precipitate was isolated and washed several times with water. Crystalline powder of Iron(II) η⁶-toluene-η⁵-

cyclopentadienyl hexafluorophosphate was obtained after the recrystallization in acetone. Yield: 12.7 g, 35 mmol, 72 %.

^1H (25°C, DCM- d_2) δ (ppm) = 1.58 (s, 3H, CH₃), 5.29 (s, 5H, CH), 6.09–6.20 (br., 5H, CH).

4,5-diethyl-1,2,3-triphosphaferrocene (54)

 **50** (211 mg, 0.35 mmol), [CpFe(η^6 -Toluene)]PF₆ (125 mg, 0.35 mmol, 1 eq.) and 20 ml of DME were loaded into the Schlenk flask. The reaction was stirred under reflux conditions for 14 h. The solution was then filtered *via* a cannula equipped with a microfiber glass filter. DME was removed under reduced pressure. **54** was purified by sublimation ($T = 90$ °C, $1 \cdot 10^{-3}$ mbar) followed by filtration over a Pasteur pipette filled with silica (2 cm). Suitable crystals of **54** for the SC-XRD analysis were obtained from a saturated pentane solution at $T = -36$ °C. Yield: 57 mg, 0.2 mmol, 55 %.

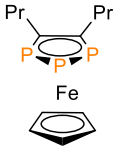
$^{31}\text{P}\{^1\text{H}\}$ NMR (25 °C, DCM- d_2) δ (ppm) = (AB₂ spin system) -13.6 (m, $^1J_{\text{P-P}} = 413$ Hz, P_A), 64.3 (m, $^1J_{\text{P-P}} = 413$ Hz, P_B);

^1H NMR (25 °C, DCM- d_2) δ (ppm) = 1.31 (t, $J^3_{\text{H-H}} = 8$ Hz, 6H, CH₃), 2.44-2.53 (m, 2H, CH₂), 2.74-2.81 (m, 2H, CH₂), 4.46 (s, 5H, CH);

$^{13}\text{C}\{^1\text{H}\}$ NMR (25 °C, THF- d_8) δ (ppm) = 18.9-19.0 (m, CH₃), 27.6–27.7 (m, CH₂), 75.0 (s, Cp), 125.2-125.7 (m, C_{Heterocycle});

Elemental analysis calculated (%) for C₁₁H₁₅FeP₃: C, 44.63; H, 5.11; **found**: C, 44.94; H, 5.20.

4,5-dipropyl-1,2,3-triphosphaferrocene (55)

 **55** was synthesized using **51** (172 mg, 0.3 mmol) according to the above-mentioned procedure for **54**. Single crystals of **55** suitable for the SC-XRD analysis were obtained from a saturated pentane solution at $T = -36$ °C. Yield: 51 mg, 0.2 mmol, 53 %.

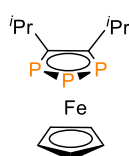
$^{31}\text{P}\{^1\text{H}\}$ NMR (25 °C, DCM- d_2) δ (ppm) = (AB₂ spin system) -13.6 (m, $^1J_{\text{P-P}} = 413$ Hz, P_A), 63.5 (m, $^1J_{\text{P-P}} = 413$ Hz, P_B);

^1H (25°C, DCM- d_2) δ (ppm) = 1.03 (t, $J^3_{\text{H-H}} = 8$ Hz, 6H, CH₃), 1.59-1.74 (m, 4H, CH₂), 2.38-2.49 (m, 2H, CH₂), 2.66-2.76 (m, 2H, CH₂), 4.45 (s, 5H, CH);

$^{13}\text{C}\{^1\text{H}\}$ (25°C, THF- d_8) δ (ppm) = 14.7 (s, CH₃), 28.0-28.1 (m, CH₂), 36.7-36.8 (m, CH₂), 75.2 (s, Cp), 123.3-123.8 (m, C_{Heterocycle}).

s.p.: $T = 110$ °C, $1 \cdot 10^{-3}$ mbar.

4,5-diisopropyl-1,2,3-triphosphaferrocene (56)



56 was synthesized using **52** (166 mg, 0.2 mmol) according to the above-mentioned procedure for **50**. Single crystals of **56** suitable for SC-XRD analysis were obtained from a saturated pentane solution at $T = -36$ °C. Yield: 36 mg, 0.1 mmol, 56 %.

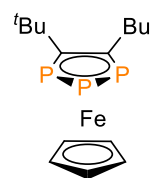
$^{31}\text{P}\{^1\text{H}\}$ NMR (25 °C, THF- d_8) δ (ppm) = (AB₂ spin system) -18.6 (m, $^1J_{\text{P-P}} = 413$ Hz, P_A), 57.9 (m, $^1J_{\text{P-P}} = 413$ Hz, P_B);

^1H NMR (25 °C, THF- d_8) δ (ppm) = 1.25 (d, $J^3_{\text{H-H}} = 7$ Hz, 6H, CH₃), 1.63 (d, $J^3_{\text{H-H}} = 7$ Hz, 6H, CH₃), 2.83-2.88 (m, 2H, CH), 4.61 (s, 5H, CH);

$^{13}\text{C}\{^1\text{H}\}$ NMR (25 °C, THF- d_8) δ (ppm) = 27.1-27.3 (m, CH₃), 29.3-29.4 (br, CH), 32.8-33.0 (m, CH₃), 74.4 (s, CH), 133.8-134.7 (m, C_{Heterocycle});

Elemental analysis calculated (%) for C₁₃H₁₉FeP₃: C, 48.18; H, 5.91; **found**: C, 48.53; H, 6.26; s.p.: $T = 110$ °C, $1 \cdot 10^{-3}$ mbar.

4-tert-butyl-5-butyl-1,2,3-triphosphaferrocene (57)

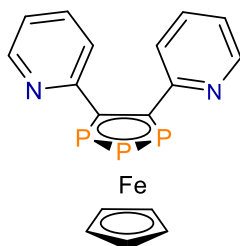


57 was synthesized using **53** according to the above-mentioned procedure for **50** on a small scale for a test reaction experiment.

$^{31}\text{P}\{^1\text{H}\}$ NMR (25°C, THF- d_8) δ (ppm) = (ABX spin system) -21.3 (t, $^1J_{\text{P-P}} = 403$ Hz, P_X), 78.5 (dd, $^1J_{\text{P-P}} = 403$ Hz, $^2J_{\text{P-P}} = 3$ Hz, P_A), 80.2 (dd, $^1J_{\text{P-P}} = 403$ Hz, $^2J_{\text{P-P}} = 3$ Hz, P_B);

^1H NMR (25°C, THF- d_8) δ (ppm) = 0.94 (t, $^3J_{\text{H-H}} = 8$ Hz, 3H, CH₃), 1.46 - 1.48 (br, 2H, CH₂), 1.50 (d, $^4J_{\text{H-P}} = 2$ Hz, 9H, CH₃), 1.70 - 1.75 (br, 2H, CH₂), 2.86 - 2.92 (br, 2H, CH₂).

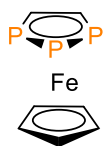
4,5-dipyridyl-1,2,3-triphosphaferrocene (**64**)



63 (500 mg, 0.9 mmol), [CpFe(η^6 -Toluene)]PF₆ (361 mg, 0.9 mmol, 1 eq.) and 20 ml of diglyme were loaded to the Schlenk flask. The reaction was stirred under reflux conditions for 14 h. The solution was then filtered *via* a cannula equipped with a microfiber glass filter. Diglyme was removed under high vacuum. **64** was purified by sublimation ($T = 180\text{ }^\circ\text{C}$, $1 \cdot 10^{-3}$ mbar) followed by filtration over a Pasteur pipette filled with silica (2 cm). Single crystals of **64** suitable for SC-XRD analysis were obtained from a saturated acetonitrile solution at $T = -36\text{ }^\circ\text{C}$. Yield: 166 mg, 0.4 mmol, 53 %.

³¹P{¹H} NMR (25 °C, THF-*d*₈) δ (ppm) = (AB₂ spin system) 2.1 (m, ¹J_{P-P} = 409 Hz, P_A), 77.2 (m, ¹J_{P-P} = 409 Hz, 2P_B).

1,2,3-triphosphaferrocene (**73**)



12 (0.5 g, 1.2 mmol), [CpFe(η^6 -Toluene)]PF₆ (0,43 g, 1.2 mmol, 1 eq.) and 20 mL of THF were loaded to the Schlenk flask. The reaction mixture was stirred under reflux conditions for 24 hours. After filtration and removal of the solvent under reduced pressure, the solid residue was sublimed ($T = 60\text{ }^\circ\text{C}$, $1 \cdot 10^{-3}$ mbar) to afford **73** as a red powder. Single crystals of **73** suitable for SC-XRD analysis were obtained from a saturated acetonitrile solution at $T = -36\text{ }^\circ\text{C}$. Yield: 23 mg, 0.1 mmol, 8 %.

³¹P{¹H} NMR (25 °C, THF-*d*₈) δ (ppm) = (AB₂ spin system) 12.5 (m, ¹J_{P-P} = 409 Hz, P_A), 40.5 (m, ¹J_{P-P} = 409 Hz, P_B);

¹H NMR (25 °C, THF-*d*₈) δ (ppm) = 4.55 (s, 5H, CH), 6.16 (m, 2H, CH);

¹³C{¹H} NMR (25 °C, THF-*d*₈) δ (ppm) = 72.3 (s, CH), 99.2 (m, CH).

2.4.6 Crystallographic data for all compounds

Identification code	54	55	56	64	73
Empirical formula	C ₁₁ H ₁₅ FeP ₃	C ₁₃ H ₁₉ FeP ₃	C ₁₃ H ₁₉ FeP ₃	C ₁₇ H ₁₃ FeN ₂ P ₃	C ₇ H ₇ FeP ₃
Formula weight	295.99	324.04	324.04	394.05	239.89
Temperature/K	106.6	100.1	100.0	100(2)	100(2)
Crystal system	monoclinic	monoclinic	monoclinic	monoclinic	orthorhombic

Space group	P2 ₁ /n	P2 ₁ /c	P2 ₁ /n	P2 ₁ /c	Pca2 ₁
a/Å	7.0636(7)	8.1286(4)	9.2932(2)	11.3225(4)	15.5069(2)
b/Å	15.7860(16)	13.0594(7)	14.3849(3)	7.0225(3)	10.7210(2)
c/Å	11.7056(12)	14.3065(8)	11.4045(3)	20.2845(8)	10.4784(2)
α/°	90	90	90	90	90
β/°	101.968(4)	103.755(2)	108.6780(10)	91.4980(10)	90
γ/°	90	90	90	90	90
Volume/Å ³	1276.9(2)	1475.15(14)	1444.28(6)	1612.32(11)	1742.03(5)
Z	4	4	4	4	8
ρ _{calc} /cm ³	1.540	1.459	1.490	1.623	1.829
μ/mm ⁻¹	1.521	1.324	1.352	1.231	2.207
F(000)	608.0	672.0	672.0	800.0	960.0
Crystal size/mm ³	0.679 × 0.332 × 0.212	0.354 × 0.265 × 0.133	0.555 × 0.126 × 0.066	0.42 × 0.12 × 0.07	0.19 × 0.14 × 0.02
Radiation	MoKα (λ = 0.71073)	MoKα (λ = 0.71073)	MoKα (λ = 0.71073)	MoKα (λ = 0.71073)	MoKα (λ = 0.71073)
2θ range for data collection/°	4.394 to 61.418	4.28 to 61.104	4.716 to 61.006	5.324 to 52.746	3.8 to 51.38
Index ranges	-9 ≤ h ≤ 10, -20 ≤ k ≤ 22, -16 ≤ l ≤ 16	-11 ≤ h ≤ 11, -18 ≤ k ≤ 17, -17 ≤ l ≤ 20	-12 ≤ h ≤ 13, -20 ≤ k ≤ 19, -16 ≤ l ≤ 16	-14 ≤ h ≤ 14, -8 ≤ k ≤ 8, - 25 ≤ l ≤ 25	-17 ≤ h ≤ 18, - 13 ≤ k ≤ 13, - 12 ≤ l ≤ 12
Reflections collected	28045	27621	33443	48301	27912
Independent reflections	3849 [R _{int} = 0.0509, R _{sigma} = 0.0330]	4369 [R _{int} = 0.0356, R _{sigma} = 0.0261]	4339 [R _{int} = 0.0298, R _{sigma} = 0.0167]	3294 [R _{int} = 0.0282, R _{sigma} = 0.0127]	3310 [R _{int} = 0.0245, R _{sigma} = 0.0136]
Data/restraints/parameters	3849/0/138	4369/0/156	4339/0/158	3294/0/208	3310/1/176
Goodness-of-fit on F ²	1.059	1.080	1.056	1.150	1.094
Final R indexes [I >= 2σ (I)]	R ₁ = 0.0532, wR ₂ = 0.1571	R ₁ = 0.0289, wR ₂ = 0.0622	R ₁ = 0.0202, wR ₂ = 0.0487	R ₁ = 0.0252, wR ₂ = 0.0628	R ₁ = 0.0294, wR ₂ = 0.0771
Final R indexes [all data]	R ₁ = 0.0613, wR ₂ = 0.1687	R ₁ = 0.0404, wR ₂ = 0.0696	R ₁ = 0.0224, wR ₂ = 0.0506	R ₁ = 0.0255, wR ₂ = 0.0630	R ₁ = 0.0297, wR ₂ = 0.0773
Largest diff. peak/hole / e Å ⁻³	1.51/-0.91	0.49/-0.39	0.39/-0.28	0.46/-0.26	1.44/-0.53

Chapter 3. Reactivity of the pentaphospholide anion towards $C\equiv N$ triple bonds. Synthesis of 1-aza-2,3,4-triphospholide anions.

3.1 Introduction.

3.1.1 Azaphospholide anions.

The isolobal relationship between a CH fragment and a N atom suggests an interaction of $[\text{cyclo-P}_5]^-$ with a $\text{C}\equiv\text{N}$ triple bond. A supposed reaction between $\text{Na}[\text{cyclo-P}_5]$ and nitriles would potentially lead to novel P,N-heterocycles. Although a substantial dipole moment of nitriles (in contrast to nonpolar alkynes) might seriously affect the reaction pathway, it was assumed that the stabilization through aromaticity is a prevailing factor that will result in the formation of the 6π electron five-membered ring, a so-called azaphospholide anion (**Figure 22**).

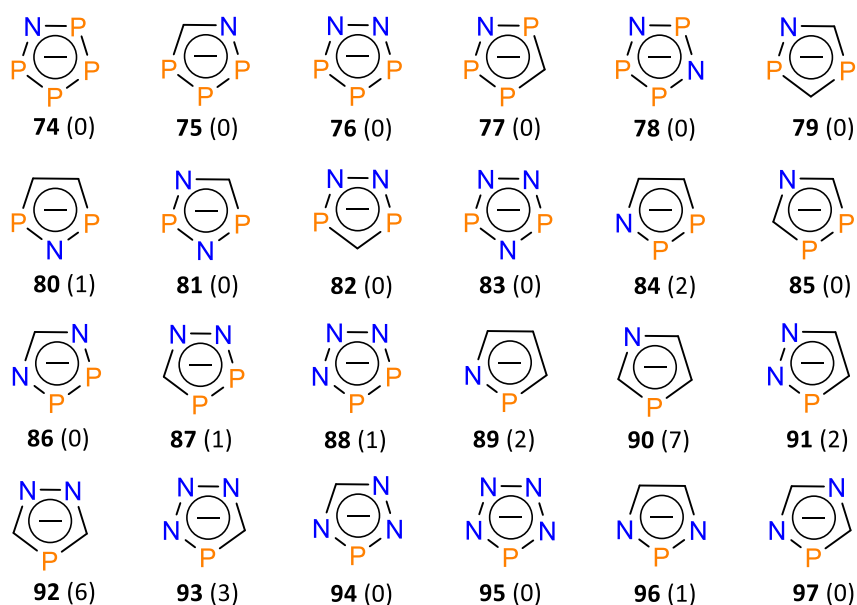


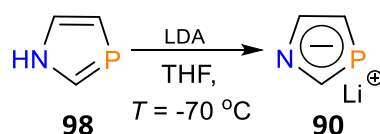
Figure 22. Representation of all possible isomers of azaphospholide anions. In parentheses: the amount of experimentally characterized derivatives of the corresponding isomer. Based on a Sci-Finder© inquiry on 31.03.2022.

Azaphospholide anions belong to a class of 6π electron aromatic P,N-heterocycles with the general formula $[\text{cyclo}-(\text{CR})_{5-x-y}\text{N}_y\text{P}_x]^-$ which are considered as isolobal analogs of $[\text{Cp}]^-$. The natural population analysis on the electron distribution in the azaphospholide rings reveals a substantial charge shift to the more electronegative N atom, since the electron density is higher in the bonds between lighter atoms.^[129] Moreover, a considerable contribution of canonical resonance structures that include charged N atoms has been reported.^[36] The

aromaticity of azaphospholides is of continuous fundamental interest since this feature was traditionally reserved for the domain of hydrocarbons. Thus, $[\text{cyclo}-(\text{CR})_{5-x-y}\text{N}_y\text{P}_x]^-$ are sometimes represented as a bridge between organic $[\text{Cp}]^-$ and its inorganic $[\text{cyclo-N}_5]^-/[\text{cyclo-P}_5]^-$ analogs.^[130] In a recent study, NICS values (the proton was placed in the middle of the ring system) were calculated for all possible $[\text{cyclo}-(\text{CH})_{5-x-y}\text{N}_y\text{P}_x]^-$ isomers. The study indicated that the aromaticity of P,N-heterocycles increases with the growing number of N/P atoms in the ring and the N—N, N—P, and P—P bonds in the following order.^[131]

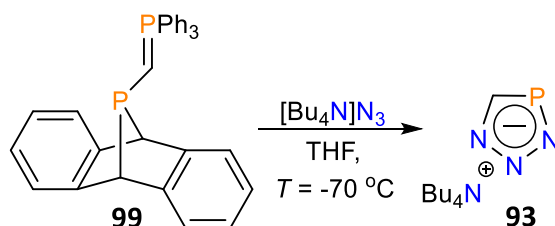
The library of possible $[\text{cyclo}-(\text{CH})_{5-x-y}\text{N}_y\text{P}_x]^-$ species is diverse and includes 24 unique anions (**Figure 22**). However, they are even more synthetically elusive than $[\text{cyclo}-(\text{CR})_{5-n}\text{P}_n]^-$ and, as a result, the scope of experimentally characterized species is very limited.

The main approach to azaphospholide anions (e.g. **90**) is based on the synthesis of the corresponding neutral azaphospholes (e.g. **98**) followed by a reaction with a strong base or alkali metal (**Scheme 41**). Azaphospholes, in turn, are feasible *via* [3+2] cycloaddition,^[132] cyclocondensation^[133,134] and ring-contraction reactions.^[135]



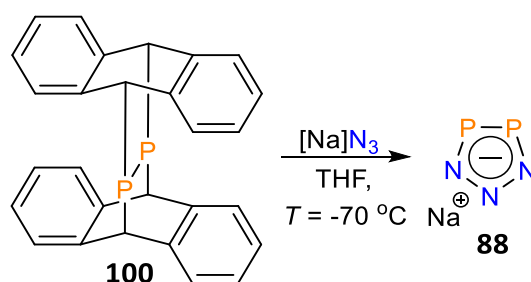
Scheme 41. Synthesis of 1,3-azaphospholide anion **90**.

Some azaphospholides are directly accessible *via* a click-reaction starting from inorganic azides. For instance, *Cummins et al.* reported that the parent 1,2,3,4- $[\text{cyclo}-(\text{CH})\text{N}_3\text{P}]^-$ **93** can be synthesized by thermal activation of dibenzo-7-phosphanorbornadiene **99** in the presence of $[\text{Bu}_4\text{N}][\text{N}_3]$ (**Scheme 42**). In this case, **99** acts as a molecular precursor for phosphacetyne ($\text{HC}\equiv\text{P}$) which undergoes a [3+2] cycloaddition with the azide.^[136]



Scheme 42. Synthesis of 1,2,3,4-triazaphospholide anion **93**.

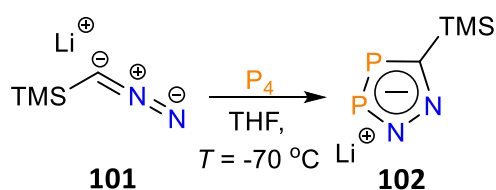
In a similar manner, combination of the anthracene-based masked source of diphosphorus [P≡P] **100** with Na[N₃] gives an access to 1,2,3,4,5-[cyclo-P₂N₃]⁻ **88** (Scheme 43).^[137]



Scheme 43. Synthesis of the 1,2,3-triaza-4,5-diphospholide anion **88**.

The aromaticity of the carbon-free 1,2,3-triaza-4,5-diphospholide 1,2,3,4,5-[cyclo-P₂N₃]⁻ **88** was supported by NRT (Natural Resonance Theory) and NICS calculations, which indicate an effective delocalization of π -electrons within the heterocycle moiety. Moreover, the formation of metallocenes with the η^5 -coordinated 1,2,3,4,5-[cyclo-P₂N₃]⁻ ligand was shown to be a thermodynamically favorable process due to the large negative values of the enthalpy and the free energy of formation.^[129]

The reaction between P₄ and (trimethylsilyl)diazomethanide **101** (a commonly used synthetic equivalent of an [RC]⁻ fragment) was originally intended by *Mathey et al.* as a simple route to 1,2,3,4-[cyclo-(CR)P₄]⁻, which, surprisingly, gave the 1,2,3,4-diazadiphospholide anion **102** (Scheme 44).^[138] The reaction could be described as a formal [3+2] cycloaddition between the diazomethyl anion and [P≡P].



Scheme 44. Synthesis of the 1,2,3,4-diazadiphospholide anion **102**.

The above-mentioned synthesis is a remarkable illustration of a rare direct P₄ transformation into P,N-rings. Moreover, this example highlights the scarcely studied potential of polyphosphorus species to build elusive heterocycles with several P—P and P—N bonds. Up

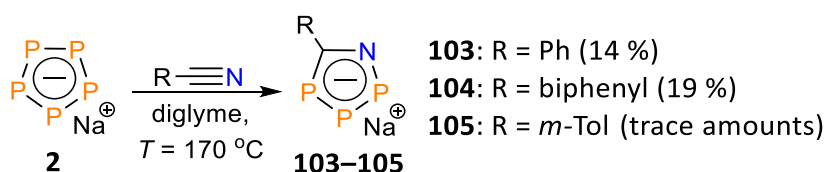
to a date, polyphosphide anions have never been used in the synthesis of P,N-heterocycles, although they also proved to be a valuable source of [P_n] fragments.

Although the η^5 -coordination mode of N-substituted cyclopentadienyls (pyrrolide) is considered as a global minimum according to DFT calculations,^[87,129] the corresponding azametallocene derivatives usually undergo ring-slippage resulting in an η^1 -binding,^[139] which is in contrast to the pronounced stability of phosphametallocenes. The localized orbital attributed to the lone pair of the N-atom exhibits a high p-character. Thus, while the diffuse and spherical P-atom lone pair (s-character) partly overlaps with the central metal, a more compact and directional N-atom lone pair interacts scarcely.^[87] Moreover, the spherical shape of the P-atom orbital in phosphametallocenes facilitates bonding to other transition metals or Lewis acids lying below or above the ring plane. At the same time, the energetically accessible N-atom lone pair of the azametallocene is constrained^[87] and undergoes η^1 ring-slippage if no kinetical stabilization of the pyrrolyl ligand is present.^[140,141] Up to date, only five azaphosphametallocenes with kinetically stabilized 1,2,4-diazaphospholyl ligand were isolated.^[142, 143, 144]

3.2 Results and discussion

3.2.1 Synthesis of sodium 1-aza-2,3,4-triphospholides

In the **Chapter 1**, it was demonstrated that electron-withdrawing and compact substituents around the C \equiv C triple bond facilitate reaction with [cyclo-P₅]⁻. Thus, aryl derivatives of nitriles were considered as the most suitable compounds for initial experiments. One equivalent of benzonitrile was added to a diglyme solution of Na[cyclo-P₅] and stirred under reflux for 12 hours (**Scheme 45**).



Scheme 45. Synthesis of sodium 1-aza-2,3,4-triphospholides **103–105**. In parentheses: the corresponding yield of the reaction.

The formation of a precipitate as well as a color change from orange to dark red were observed after several hours of reflux. The ^{31}P NMR spectrum taken from the crude reaction mixture reveals three resonances: two conjugated doublets-of-doublets at $\delta = 221.7$ and 325.2 ppm and a broad doublet at $\delta = 378.0$ ppm. The three resonances integrated in a 1:1:1 ratio. Large coupling constants ($^1J_{\text{P-P}} = 493$ and 438 Hz) indicate the presence of P—P bonds. A significant downfield shift of the doublet signal ($\delta = 378.0$ ppm) designates a direct bond between phosphorus and the highly electronegative nitrogen. The predicted ^{31}P chemical shifts of the parent 1-aza-2,3,4-triphospholide **75** ($\delta = 210.0, 333.0,$ and 352.0 ppm)^[131] match very well with the proposed structure of **103**. Thus, based on the analysis of the ^{31}P NMR spectrum (**Figure 23**), it can be concluded that the hitherto unknown 5-phenyl-1-aza-2,3,4-triphospholide anion **103** was formed in the reaction.

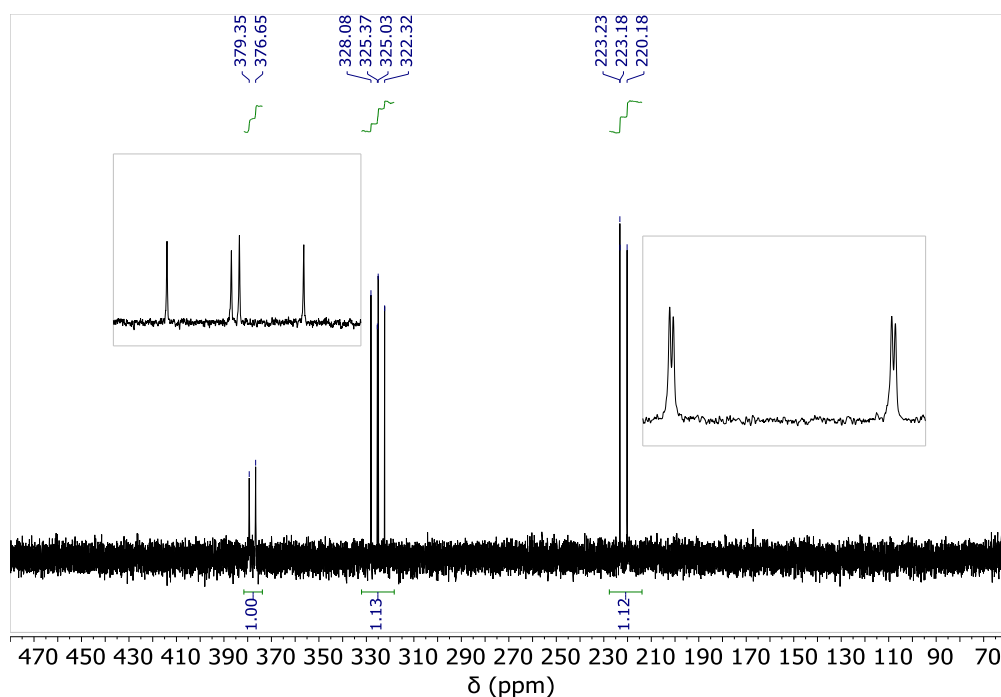


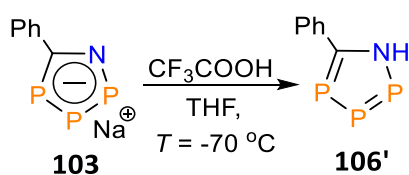
Figure 23. ^{31}P NMR spectrum of sodium 5-phenyl-1-aza-2,3,4-triphospholide **103**.

The work up procedure of **103** includes the filtration and removal of diglyme followed by washing of the residue with a THF:pentane mixture (1:10). The new compound was collected as a dark red oil, which is turned out to be very sensitive to air and moisture. The isolated yield was found to be 14 %. The ^1H and $^{13}\text{C}\{^1\text{H}\}$ NMR spectra confirmed the structure of the product. The proton NMR spectrum displays a set of three multiplets with the chemical shifts between $\delta = 7.00$ – 8.30 ppm which correspond to a phenyl ring. A downfield shifted resonance

at $\delta = 8.26$ ppm was assigned to the protons in *ortho* position of the phenyl ring. The three signals of diglyme in the solvate shell of the sodium cation appear between $\delta = 3.30$ – 3.60 ppm. The $^{13}\text{C}\{^1\text{H}\}$ NMR spectrum of **103** displays a carbon atom incorporated in the heterocycle as a deshielded multiplet resonance $\delta = 201.8$ ppm.

4-cyanobiphenyl also reacts with sodium pentaphospholide at elevated temperatures to give the 5-biphenyl-1-aza-2,3,4-triphospholide anion **104** in a slightly higher yield than benzonitrile (**Scheme 45**). Surprisingly, the presence of a methyl group in the phenyl ring of benzonitrile seriously affects the interaction between the nitrile and $\text{Na}[\text{cyclo-P}_5]$. The reaction between *m*-tolunitrile and $\text{Na}[\text{cyclo-P}_5]$ under reflux conditions leads only to trace amounts of the desired species **105**, while the addition of *p*-tolunitrile results in the decomposition of $\text{Na}[\text{cyclo-P}_5]$. Aliphatic nitriles, such as pivalonitrile and acetonitrile, cause the decomposition of $\text{Na}[\text{cyclo-P}_5]$ at high temperatures. Interestingly, benzonitrile derivatives with -F and -CF₃ groups in the phenyl backbone react rapidly with $\text{Na}[\text{cyclo-P}_5]$ in solution to give a grey-green precipitate and a colorless liquid phase.

In 1996 Mathey *et al.* demonstrated the first synthesis of a lithium salt of 1,2,3,4-diazadiphospholide and its conversion into a neutral 1,2,3,4-diazadiphosphole by treating the lithium salt with trifluoroacetic acid.^[138] To have an additional proof of the proposed structure of **103**, it was also treated with the same acid in a cold THF solution (**Scheme 46**).



Scheme 46. Synthesis of 1-*H*-5-phenyl-1-aza-2,3,4-triphosphole **106'**.

The addition of the acid resulted in an instant color change from dark red to yellow and formation of CF₃COONa as a white precipitate. However, the ^{31}P NMR spectrum, taken from the reaction mixture, did not reveal any significant changes other than a broadening of the doublet at $\delta = 378.0$ ppm, which may indicate some weak N—H interactions.

In the VT ^{31}P NMR spectroscopy experiment the resonance at $\delta = 378.0$ ppm transformed into a doublet of triplets with $^2J_{\text{H-P}} = 20$ Hz at $T = -100$ °C in THF-*d*₈ solution (**Figure 24**).

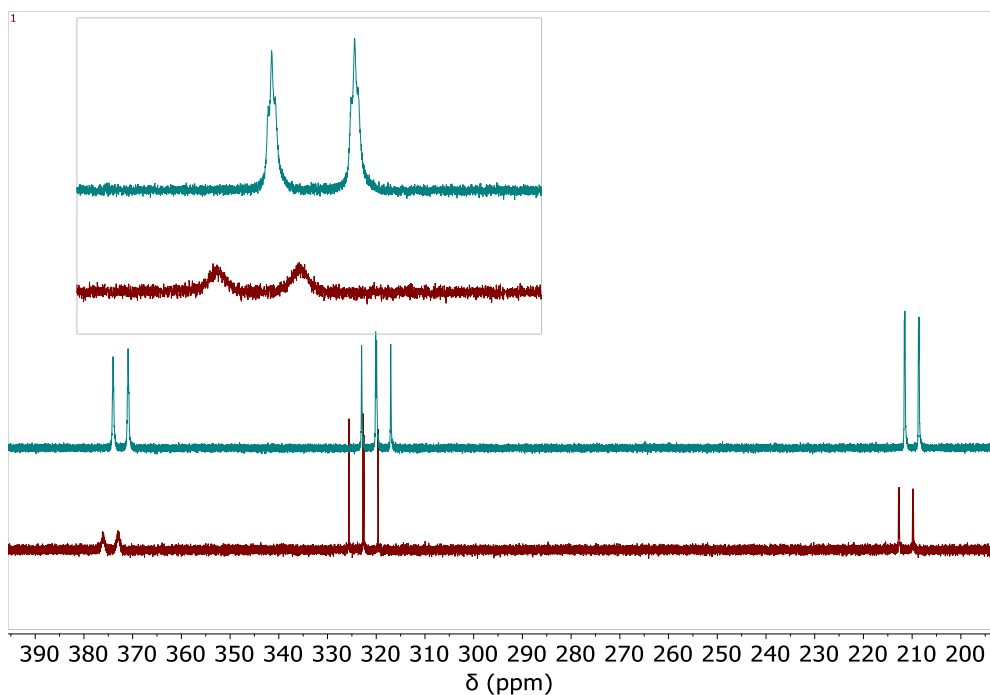
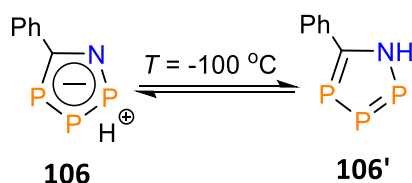


Figure 24. ^{31}P NMR of 1-aza-2,3,4-triphosphole **106** recorded at $-100\text{ }^\circ\text{C}$ (top, blue) and at room temperature (bottom, red).

The NMR experiment confirmed that **106** mainly retains the ionic structure of the 1-aza-2,3,4-triphospholide in solution at room temperature with the sigmatropic migration of the proton within the heterocyclic system. The equilibrium shifts towards the neutral 1-*H*-1-aza-2,3,4-triphosphole with the N—H σ -bond (**Scheme 47**) upon cooling of solution. The specific proton could be detected as a broad doublet at $\delta = 14.04\text{ ppm}$ ($^2J_{\text{H-P}} = 20\text{ Hz}$) in the ^1H NMR spectrum of **106** when recorded at $T = -100\text{ }^\circ\text{C}$ (**Figure 25**).



Scheme 47. Equilibrium between the ionic **106** and neutral forms **106'** of 1-aza-2,3,4-triphosphole.

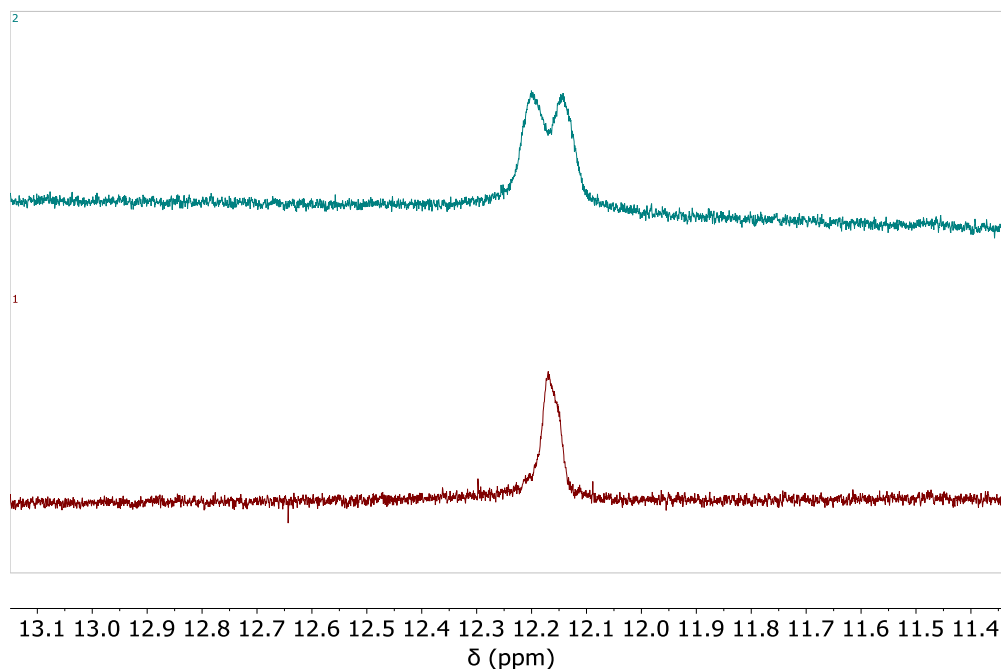


Figure 25. ^1H NMR (top, blue) and $^1\text{H}\{^{31}\text{P}\}$ NMR (bottom, red) spectra of **106**

recorded at $T = -100\text{ }^\circ\text{C}$.

The experimental data is consistent with the theoretical calculations carried out for the parent 1-aza-2,3,4-triphospholide **75** and for all possible tautomers of *H*-1-aza-2,3,4-triphosphole **75'A–D** (Figure 26). The tautomer **75'A** with the N–H bond was found to be substantially more stable than those with P–H bonds **75'B–D** by about 80-100 kJ/mol (Figure 26), due to stronger acid-base interactions. At the same time, the anion **75** exhibits a lower NICS value than the neutral **75'A**.^[131]

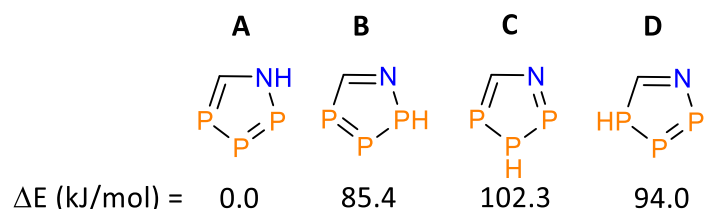
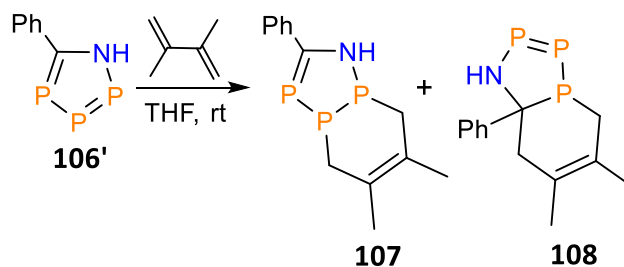


Figure 26. Relative energies of tautomers **75'A–D**.

5-phenyl-1-*H*-1-aza-2,3,4-triphosphole **106** is stable in THF or toluene solution. A yellow precipitate, that forms when the solvent is removed cannot be redissolved completely in the same or other solvent. Such behavior of **106** indicates oligomerization *via* numerous

cycloaddition reactions that are possible due to the accessibility of the highly reactive P=P and P=C bonds.^[145] The ability of **106** to undergo cycloaddition has been demonstrated in a test reaction with 2,3-dimethyl-1,3-butadiene (**Scheme 48**).



Scheme 48. Two proposed [4+2] cycloaddition reactions between **106'** and 2,3-dimethyl-1,3-butadiene.

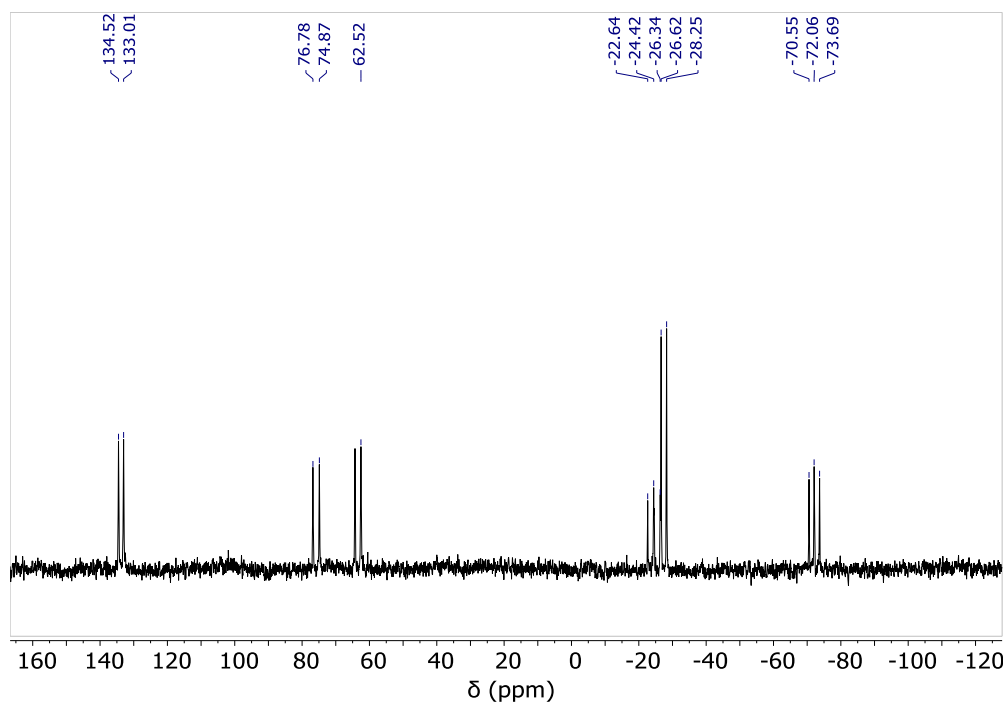


Figure 27. ³¹P{¹H} NMR spectrum of the reaction mixture containing **107** and **108**.

The analysis of the ³¹P{¹H} NMR spectrum of the crude reaction mixture revealed two sets of resonances consisting of 3 multiplet between δ = -80.0–150.0 ppm (**Figure 27**). Interestingly, 1-aza-2,3,4-triphosphole seems to act as a 2π electron component in two different [4+2] cycloadditions: *via* the P=C (**108**) and *via* the P=P (**107**) bonds. A substantial downfield shift of all signals in the ³¹P{¹H} NMR spectrum indicates a collapse of the aromatic system in the

heterocyclic moiety. Moreover, upon concentrating of the solution of two products, only decomposition was observed.

3.2.2 DFT study of the parent 1-aza-2,3,4-triphospholide anion

The parent 1-aza-2,3,4-triphospholide **75** anion was studied by means of quantum chemistry for the better understanding of the electronic properties of the novel heterocycle and to explore the possibility of using 1,2,3,4-[*cyclo*-(CR)NP₃]⁻ as a ligand.

The geometry optimization of **75** was performed with the PBEh-3c method, which showed a good correlation of the interatomic bond distances and angles in **75** compared to the other structurally characterized azaphospholide anions (**Figure 28**). The P—C, P—N and P—P bonds in the C_s-symmetrical structure of **75** are averaged in accordance with the delocalized bond structure expected for the aromatic compound.^[146]

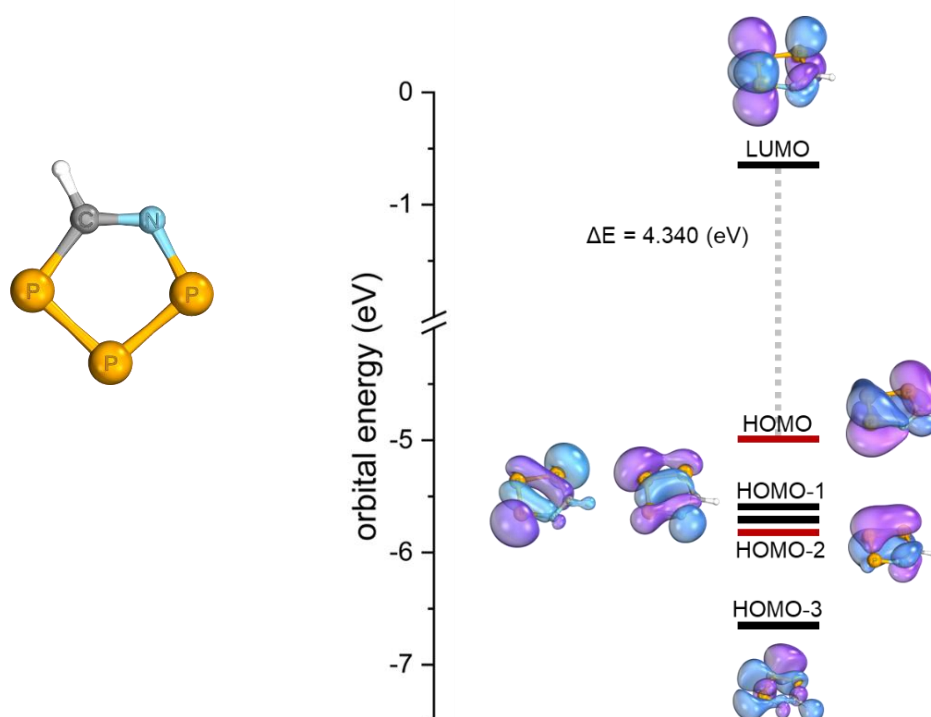


Figure 28. Optimized structure and frontier MOs of the parent 1-aza-2,3,4-triphospholide anion **75**. Calculated at the B3LYP-D3/def2-TZVP level of theory.

Molecular orbitals were calculated for the optimized structure using the B3LYP functional with the def2-TZVP basis set and def2/J auxiliary basis set. Interestingly, the frontier molecular orbitals of **75** (**Figure 28**) are in a different order compared to [*cyclo*-P₅]⁻ (**Figure 5**)

and the parent 1,2,3-triphospholide **12** (**Figure 13**), even though the HOMO and the LUMO of **75** are also represented by the π and π^* -orbitals, respectively. In contrast to the symmetrical tri- and pentaphospholide, two bonding π -orbitals in **75** can be found separately at the HOMO and HOMO-2 levels. The HOMO-1, in turn, is represented by two degenerate σ -orbitals formed from the in-plane p-orbitals (giving σ -bonds) and the lone pairs of the heteroatoms. The LUMO of **75** is 0.25 eV lower in energy than the same orbital of the parent 1,2,3-triphospholide anion **12**, indicating a stronger π -acceptor character of **75** compared to **12**. At the same time, it is anticipated that the η^5 -coordination mode of the $[\text{CNP}_3]^-$ ring is significantly less favored due to the large gap between the two binding π -orbitals and the contribution of the lone pairs in the shape HOMO-1. The energy gap between two π -bonding orbitals (at HOMO and HOMO-2 levels) in the structurally optimized **103** is even larger.

The nature of the bonding was analyzed using QTAIM (Quantum Theory of Atoms In Molecules),^[147] which has revealed five (3; -1) BCPs (Bond Critical Points) as well as the (3; +1) RCP (Ring Critical Point) (**Figure 29**). The Laplacian of the electron density $\nabla^2\rho_{\text{BCP}}$ as well as the energy density H_{BCP} values between all bonds are negative, which is typical for bonds with a covalent character.^[148]

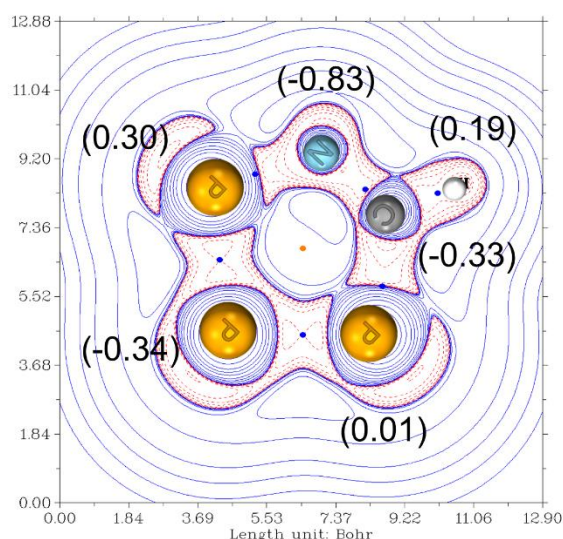


Figure 29. Contour plot of the Laplacian of the electron density in **75**; BCPs – blue dots; RCP – red dot. Positive contour lines are colored blue; negative contour lines are red. In parentheses: NPA charges.

The electron density $\rho(r_c)$ value is particularly high at the (3; -1) BCP between C and N compared to all the other bonds (**Figure 30**). A substantial localization of $\rho(r_c)$ in the space between C—N bond leads to the significant variation of partial charges on the atoms. As a result, a highly negative value of the (-0.83) natural charge at the N-atom was found from the NPA (Natural Population Analysis) (**Figure 29**). Following this considerations, **75** and the other 1,2,3,4-[*cyclo*-(CR)NP₃]⁻ anions can be represented as the N-centered nucleophiles, what has been proven experimentally in the reaction between **103** and CF₃COOH (**Scheme 46**).

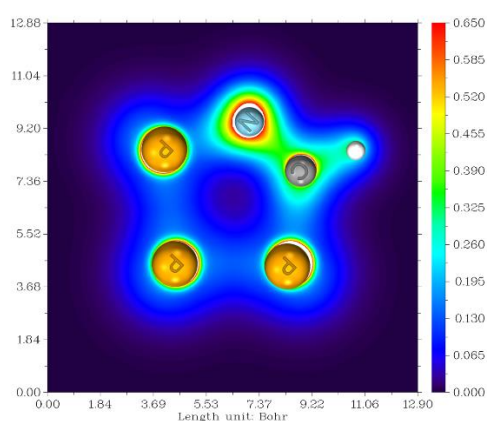


Figure 30. Color filled map of the electron density of **75**.

Covalency of the bonds of the heterocycle **75** is also evident from the plot of the electron localization function (**Figure 31**), which shows a substantial localization of the electron pairs between the atoms. Moreover, it confirms the localization of N and P lone pairs in the ring plane.

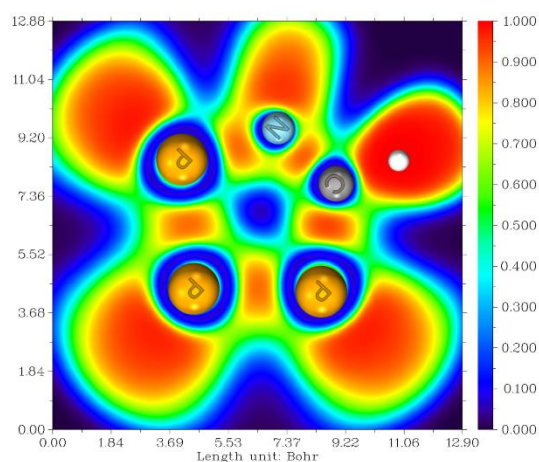
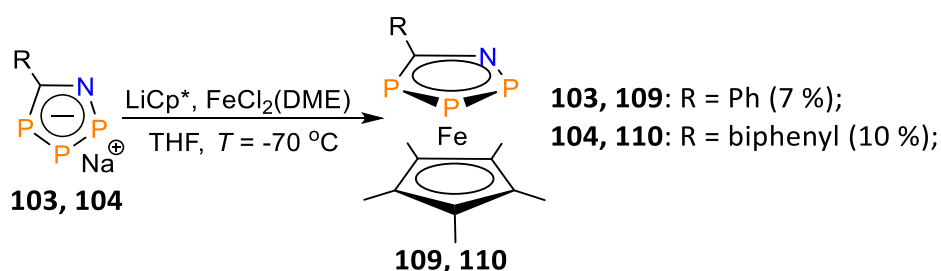


Figure 31. Color filled map of the electron localization function of **75**.

3.2.3 Synthesis of 1-aza-2,3,4-triphosphaferrocenes

The highly sensitive nature of the new species **103** and **104** towards moisture and air makes it necessary to find a way to stabilize them through coordination to a transition metal center. In contrast to 1,2,3-triphospholides **50–53**, the compounds **103** and **104** decompose when reacted with $[\text{CpFe}(\eta^6\text{-Toluene})]\text{PF}_6$. It is presumed that the sterically accessible nitrogen and the π -acceptor character of the ligand disfavor an η^5 -coordination through a $\pi(\text{L})\rightarrow\text{Fe}$ donation. Instead, a $n(\text{N})\rightarrow\text{Fe}$ donation plays the predominant role and facilitates an η^1 -coordination with the subsequent decomposition.^[87, 143] Thus, the electron-enriched $[(\eta^5\text{-Cp}^*)\text{Fe}]^+$ (Cp^* = pentamethylcyclopentadienyl) fragment was used as a stronger π -donor to direct the coordination in the desired fashion. Moreover, an increased electron density at the iron center impedes the $n(\text{N})\rightarrow\text{Fe}$ donation because of the electrostatic repulsion.

To prepare the 5-phenyl-1-aza-2,3,4-triphosphaferrocene **109**, a THF solution of lithium pentamethylcyclopentadienide (LiCp^*) was cooled down to $T = -70\text{ }^\circ\text{C}$. Then, a cold THF suspension of $\text{FeCl}_2(\text{DME})$ was added slowly *via* a cannula to give a black solution over some time. After two hours of stirring under the mild conditions, a cold solution of 1-aza-2,3,4-triphospholide **103** was added dropwise into the flask. The reaction mixture was allowed to warm up to room temperature and stirred for several hours (**Scheme 49**).



Scheme 49. Synthesis of 5-aryl-1-aza-2,3,4-triphosphaferrocenes **109** and **110**. In parentheses: the corresponding yield of the reaction.

The ^{31}P NMR spectrum taken from the crude reaction mixture displays three multiplet resonances of an ABX spin system, with the characteristic “roof” effect of the AB part (**Figure 32**). Two doublet-of-doublets signals appear in the range between $\delta = 30.0\text{--}50.0$ ppm, while the most deshielded doublet resonance was observed at $\delta = 142.6$ ppm. All resonance signals are significantly upfield shifted compared to the free ligand (for **103**: $\delta(\text{ppm}) = 221.7$ (dd),

325.2 (dd), 378.0 (br. d)) and exhibit large coupling constants of $^1J_{P-P} = 457$ and 345 Hz. Both the NMR spectrum pattern as well as the upfield chemical shifts indicate that the desired sandwich 5-phenyl-1-aza-2,3,4-triphosphaferrocene **109** was obtained (**Scheme 49**).

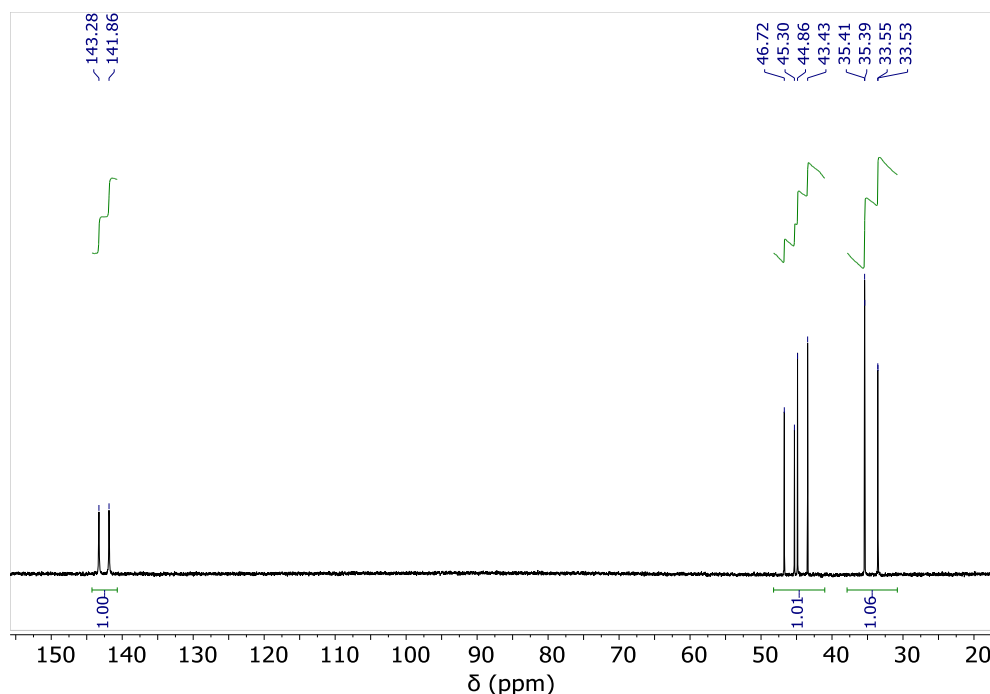


Figure 32. ^{31}P NMR spectrum of **109**.

Pure **109** was isolated from the reaction mixture as orange crystals after sublimation followed by a filtration over a small silica layer. The isolated yield of the new species was 7 %. The 1H NMR spectrum of the new complex reveals two overlapping multiplets at $\delta = 7.40$ ppm, which can be attributed to the *para*- and *meta*-CH protons of the phenyl ring, while the *ortho*-CH proton is downfield shifted to $\delta = 8.27$ ppm. An intense singlet signal at $\delta = 1.58$ ppm can be assigned to the methyl substituents of the cyclopentadienyl ring was observed. The $^{13}C\{^1H\}$ NMR spectrum of **109** displays $C_{(heterocycle)}$ nuclei at $\delta = 142.9$ ppm, which is substantially upfield shifted compared to the free ligand (**103**: $\delta(\text{ppm}) = 201.8$), but approximately 20 ppm downfield shifted when compared to 1,2,3-triphosphaferrocenes **54–56**, **64**.

Despite that **109** easily crystallizes from a concentrated ether solution at $T = -36$ °C, it was only possible to obtain single crystals of poor quality suitable for the determination of the connectivity. The solid state analysis confirms the proposed structure of the sandwich compound with the η^5 -coordinated 1,2,3,4-azatriphospholyl ligand.

To prepare 5-biphenyl-1-aza-2,3,4-triphosphaferrocene **110**, anion **104** was reacted with $\text{FeCl}_2(\text{DME})$ and LiCp^* according to the same protocol as used for the preparation of **109** (Scheme 49). The $^{31}\text{P}\{^1\text{H}\}$ NMR spectrum of **110** exhibits three multiplet resonances in the same area as **109**. The ^1H NMR spectrum shows four multiplet resonances attributed to the *para*-, *meta*- and *ortho*-CH protons of the biphenyl substituent between $\delta = 7.40\text{--}7.80$ ppm, while the *ortho*-CH was observed at $\delta = 8.27$ ppm. The $\text{C}_{(\text{heterocycle})}$ nucleus was detected by $^{13}\text{C}\{^1\text{H}\}$ NMR spectroscopy at $\delta = 142.7$ ppm.

Single crystals were obtained from a concentrated ether solution at $T = -36$ °C. Compound **110** crystallizes in the monoclinic space group $\text{P}2_1/\text{c}$ with two enantiomeric molecules in the unit cell and in a ratio of 85(A):15(B) (Figure 33). Due to the substantial disorder in the molecular structure of the minor enantiomer, only the main enantiomer **110(A)** will be discussed. The $[\text{Cp}^*]$ and $[1,2,3,4\text{-azatriphospholyl}]$ ligands are η^5 -coordinated to the Fe(II) ion with the respective $[\text{Cp}^*]_{\text{cent}}\text{-Fe-}[\text{CNP}_3]_{\text{cent}}$ tilting angle of $178.74(10)^\circ$. The interplanar angle between $[\text{Cp}^*]$ and $[\text{CNP}_3]$ is $19.04(13)^\circ$ (**110(B)**: $5.5(4)^\circ$). The P1—P2 bond ($2.1514(13)$ Å) is elongated compared to the P2—P3 bond ($2.1059(14)$ Å) due to the presence of the highly electronegative N-atom. The P1—N1 bond distance of $1.702(9)$ Å is close to the P—N bond distance ($1.670(1)$ Å) in the 1,2,3,4-diazadiphospholide-anion **102**.^[138] The C1-N1-P1 angle of $119.8(7)^\circ$ is in line with the sp^2 hybridization of the nitrogen atom. The found η^5 -coordination of the $[\text{RCNP}_3]$ ligand serves as the experimental (structural) proof of the aromaticity of the novel N,P-heterocycle. This is in line with the calculated NICS(0) and NICS(1) values for $[\text{cyclo}(\text{CH})\text{NP}_3]^-$.^[131]

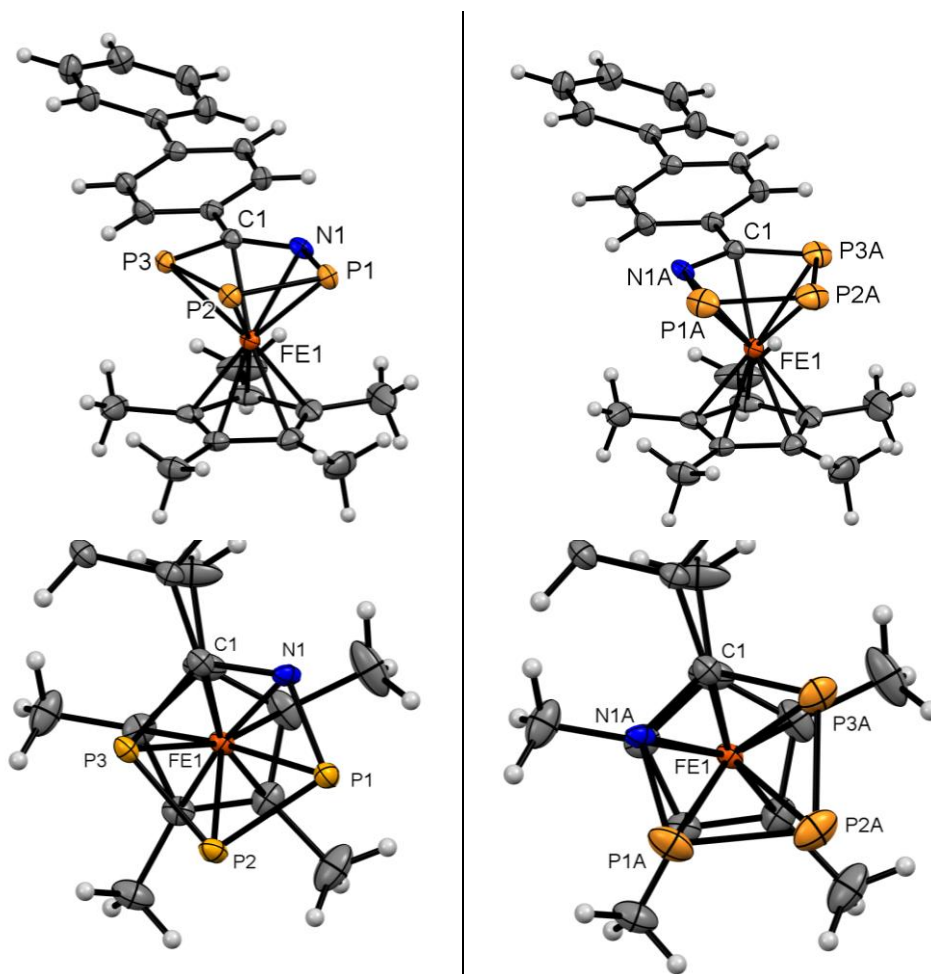


Figure 33. Molecular structure of **110(A)** (left) and **110(B)** (right) in the crystal. Ellipsoids are shown at 50 % probability level. Selected bond lengths (Å) and angles (°): **110(A)**: P1-P2: 2.1514(13); P2-P3: 2.1059(14); P1-N1: 1.702(9) C1-N1: 1.382(9); C1-P3: 1.813(2); P1-P2-P3: 97.37(5); P1-N1-C1: 119.8(7); P3-C1-N1: 122.3(5); [CNP₃]_{cent}-Fe1: 1.5995(4); [Cp*]_{cent}-Fe1: 1.6849(4).

The cyclic voltammogram of complex **110** at a sweep rate of 100 mV/s showed an irreversible oxidation process at $E_{\text{ox}} = 1.11$ V (vs. Fc*/Fc⁺) (Fc* = decamethylferrocene) (**Figure 34**, left) which is approximately at $E_{\text{ox}} = 0.56$ V vs. Fc/Fc⁺.^[149] The registered oxidation peak potential is 0.25 V shifted cathodically in comparison to 3,5-bis(*tert*-butyl)-1,2-diaza-4-phosphaferrocene **111** (**Table 2**). The electron-withdrawing biphenyl group and one extra heteroatom in the ligand result in a lower LUMO energy and, therefore, a stronger π -acceptor character of the 1-aza-2,3,4-triphospholyl ring.

At the same time, the E_{ox} value is reminiscent of the oxidation peak potential of pentaphosphaferrocene **13** ($E_{\text{ox}} = 0.6$ V vs. Fc/Fc⁺)^[150] (**Table 2**), which indicates a significant

impact of the highly electronegative N-atom to the redox properties of the novel 1-aza-2,3,4-triphosphaferrocene.

An increase of the scan rate causes higher peak currents for the cathodic wave along with a slight wave shift to more positive potentials (**Figure 34**, right). Upon scanning anodically at a sweep rate of 100 mV/s (**Figure 34**, left), an irreversible reduction wave at a peak potential of -2.0 V (vs. Fc^*/Fc^{*+}) without coupled anodic signals was registered.

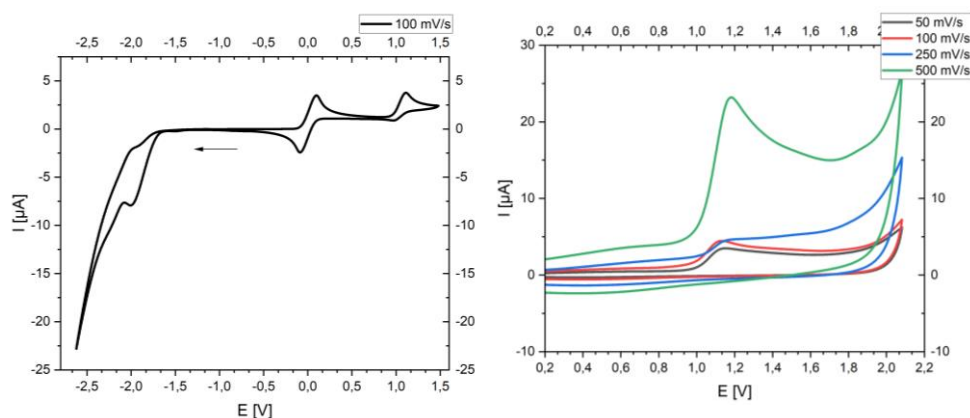


Figure 34. Cyclic voltammogram of **110** in DCM under an atmosphere of argon.

Measurement conditions: $T = 20\text{ }^{\circ}\text{C}$, scan rate: 100 mV/s (left), conducting salt: 0.1 M $[NBu_4]PF_6$. Potentials were referenced versus Fc^*/Fc^{*+} .

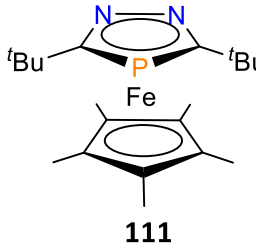
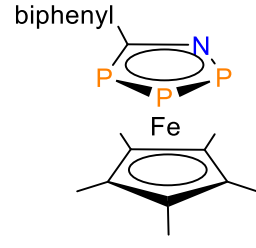
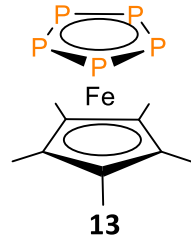
Compound	 <p style="text-align: center;">111</p>	 <p style="text-align: center;">110</p>	 <p style="text-align: center;">13</p>
E_{ox} / E_{red} (V, vs Fc/Fc^+)	$E_{ox} = 0.31^{[143]}$	0.56/-2.56	$E_{ox} = 0.60^{[150]}$

Table 2. Electrochemical parameters of the selected azaphosphaferrocenes.

3.3 Conclusions

It was demonstrated that $Na[cyclo-P_5]$ reacts with benzonitrile and 4-cyanobiphenyl to give the hitherto unknown P,N-heterocyclic anions: 5-phenyl-1-aza-2,3,4-triphospholide **103** and

5-biphenyl-1-aza-2,3,4-triphospholide **104** (Scheme 45). **103** reacted with trifluoroacetic acid affording 1-*H*-5-phenyl-1-aza-2,3,4-triphosphole **106**, which possesses an ionic structure with weak N—H interactions (sigmatropic shift of the proton) at room temperature (Scheme 46). The VT ³¹P NMR experiment revealed N—H bond formation and stabilization of the neutral 1-*H*-1-aza-2,3,4-triphosphole upon cooling a THF solution of **106** down to $T = -100$ °C (Figure 24). These observations are in line with the predicted thermodynamic stability and aromaticity of azatriphospholide and azatriphosphole (Figure 26). Furthermore, 1-*H*-1-aza-2,3,4-triphosphole **106** undergoes [4+2] cycloaddition with dipolarophiles yielding the corresponding Diels-Adler adducts **107** and **108** (Scheme 48).

The successful synthesis and the crystallographic characterization of 1-aza-2,3,4-triphosphaferrocenes **109** and **110** (Scheme 49) serves as the experimental (structural) evidence of the aromatic character of the novel 1,2,3,4-azatriphospholyl ring. The molecular structure of **110** in the crystal showed two enantiomers (Figure 33). The cyclic voltammogram of **110** (Figure 34) displays a substantial cathodic shift of the oxidation potential in comparison to phosphoferrocenes, which is due to the presence of a highly electronegative N-atom.

3.4 Experimental part

3.4.1 General remarks

All reactions were performed under an argon atmosphere in oven-dried glassware using modified Schlenk techniques or in an MBraun glovebox unless otherwise stated. All common solvents and chemicals were commercially available. Benzonitrile, 4-cyanobiphenyl, *p*-tolunitrile, *m*-tolunitrile, 4-(trifluoromethyl)benzonitrile, 4-fluorobenzonitrile, trifluoroacetic acid, 2,3-dimethyl-1,3-butadiene, pentamethylcyclopentadiene, butyllithium, decamethylferrocene and FeCl₂ were commercially available. Other chemicals were synthesized according to the literature procedures (see below). Liquid nitriles were stored with molecular sieves (3 Å) under argon. Solid nitriles were sublimed before use. Other commercially available chemicals were used without further purification. All dry and deoxygenated solvents were prepared using standard techniques or were obtained from a MBraun solvent purification system. The ¹H, ³¹P and ³¹P{¹H} NMR spectra were recorded on a JEOL ECS400 spectrometer (³¹P: 162 MHz, ¹H: 400 MHz). Some ³¹P{¹H} NMR spectra were recorded on a

Bruker AVANCE III 700 spectrometer (242 MHz). $^{13}\text{C}\{^1\text{H}\}$ spectra were recorded on a Bruker AVANCE III 700 spectrometer (176 MHz). All chemical shifts are reported relative to the residual resonance in the deuterated solvents. The ESI-TOF (Electron-Spray ionization Time-of-flight) Mass spectrometry measurements were performed on an Agilent 6230 ESI-TOF. Cyclic voltammograms were measured at room temperature with the substance (0.005 mmol) in DCM (5 mL) and 0.1 M TBAPF₆ added as an electrolyte at 25–500 mV/s under an argon atmosphere. Decamethylferrocene was used as the internal standard. An Autolab PGSTAT302N potentiostat by Metrohm was used in combination with an in-house made, gas-tight glass cell equipped with a glassy carbon disk working electrode by Metrohm, a platinum wire as counter electrode and a leak-free Ag/AgCl reference electrode LF-2 by Innovative Instruments, Inc. Low-temperature diffraction data were collected on Bruker-AXS X8 Kappa Duo diffractometers with $l\mu\text{S}$ micro-sources, performing ϕ - and ω -scans. For the structure of compounds **109** and **110**, a Smart APEX2 CCD detector and Cu K α radiation ($\lambda = 1.54178 \text{ \AA}$) were used. The structures were solved by dual-space methods using SHELXT^[113] and refined against F^2 on all data by full-matrix least squares with SHELXL-2017^[114] following established refinement strategies.^[115] The program Olex2^[116] was also used to aid in the refinement of the structures of compounds. All non-hydrogen atoms were refined anisotropically. All hydrogen atoms were included into the model at geometrically calculated positions and refined using a riding model. The isotropic displacement parameters of all hydrogen atoms were fixed to 1.2 times the U-value of the atoms they are linked to (1.5 times for methyl groups). DFT Calculations were carried out with the ORCA 5.0.3 program suite.^[117] Initial molecular structures were created in the program Avogadro^[118] or were based on crystal structures, if available. Geometry optimizations were then performed with the PBEh-3c method developed by Grimme and co-workers.^[119] Standardized convergence criteria were used for the geometry optimization (OPT). To confirm the nature of stationary points found by geometry optimizations analytical frequency calculations were carried out. The absence of imaginary vibrational frequencies indicated that the optimized structure is a local minimum. Final single point calculations on the optimized structures were conducted with the B3LYP^[120] functional with def2-TZVP^[121] basis set and def2/J^[122] auxiliary basis set. Additionally, for all calculations the Dispersion Correction (D3)^[123] was used. For SCF-calculations an additional “tight” correlation was included (“TIGHTSCF”). Solvent effects were taken into account with the Conductor-like-Polarizable-Continuum-Modell (CPCM)^[124] for THF. NBO population

analyses were performed with the NBO 7.0 module^[151] implemented in the ORCA program suite. The natural charges on atoms were calculated with the NPA. Intrinsic bond orbital (IBO) analysis^[125] was carried out with the IBO module implemented in the ORCA program suite. IBOs were visualized via the freely available IBOView v20150427.^[126] QTAIM analysis^[147] was conducted with the Multiwfn software (version 3.7)^[152] using the wave functions (.wfn) generated at the B3LYP/def2-TZVP level of theory.

3.4.2 Synthesis of sodium 1-aza-2,3,4-triphospholides

Synthesis of FeCl₂(DME)

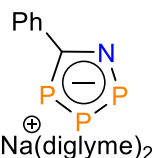
30 mL of DME were added to a Schlenk flask with 5 g of FeCl₂. The suspension was stirred under reflux conditions for 24 hours. Then, the solvent was decanted and the solid residue was washed three times with 10 mL of pentane and dried under reduced pressure to give FeCl₂(DME) in quantitative yield.

Synthesis of lithium pentamethylcyclopentadienyl (LiCp*)

Pentamethylcyclopentadiene (10 g, 73 mmol) was dissolved in 50 mL of hexane and cooled down to $T = -78$ °C. Then, butyllithium (73 mmol in hexane) was slowly added to the solution. Reaction mixture was allowed to slowly warm up to room temperature and stirred for 6 hours. After decantation of the solvent, the white solid residue was washed three times with hexane (20 mL) to give LiCp*. Yield: 7.4 g, 52 mmol, 72 %.

3.4.3 Synthesis of sodium 1-aza-2,3,4-triphospholides

Sodium 5-phenyl-1-aza-2,3,4-triphospholide (**103**)

 Benzonitrile (0.25 g, 2.5 mmol, 1 eq.) was added to a solution of Na[cyclo-P₅] in diglyme (2.5 mmol in 30 mL) in a Schlenk flask. The reaction mixture was stirred under reflux conditions for 14 h. Then, the solution was filtered *via* a cannula equipped with a microfiber glass filter and the solvent was removed under high vacuum. The reaction mixture was washed three times with a mixture of THF:pentane (2 ml: 40 ml) and dried on a high vacuum for several hours to give **103** as a dark red oil. A *one-pot* variation (as it was described for **55**) of the synthesis leads to the desired product in higher

yield, but is contaminated with multiple side-products that can be mainly removed. P₄ (0.81 g, 6.5 mmol), Na (0.32 g, 13.7 mmol, 2 eq.), benzonitrile (0.67 g, 6.5 mmol), DB-18-C-6 (5 mg) and diglyme were loaded to the Schlenk flask. The reaction was stirred under reflux conditions for 24 hours. Then, the reaction mixture was filtrated *via* a cannula and the solvent was removed under reduced pressure. The oily residue was redissolved in acetonitrile and cooled down to $T = -20$ °C. Then, isopropyl iodide (1 eq. based on the amount of used P₄) was added dropwise to the solution. The reaction was allowed to warm up slowly to room temperature within 2 hours. The solution was then filtered and acetonitrile was removed under vacuum. The solid residue was washed three times with THF:pentane (2 ml : 40 ml) mixture and dried under vacuum for several hours to give **103** as a dark red oil. The composition of the cation solvate shell was calculated on the basis of the ¹H NMR spectroscopy. Yield: 170 mg, 0.4 mmol, 14 %.

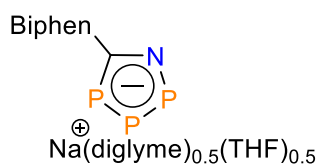
³¹P{¹H} NMR (25 °C, CD₃CN) δ (ppm) = (AMX spin system) 221.7 (dd, ¹J_{P-P} = 493 Hz, ²J_{P-P} = 8 Hz, P_A), 325.2 (dd, ¹J_{P-P} = 493 Hz, ¹J_{P-P} = 438 Hz, P_M), 378.0 (d, ¹J_{P-P} = 438 Hz, P_X);

¹H NMR (25 °C, CD₃CN) δ (ppm) = 3.30 (s, 12H, OCH₃), 3.47-3.48 (m, 8H, CH₂), 3.54-3.56 (m, 8H, CH₂), 7.22 (t, ³J_{H-H} = 7 Hz, 1H, *p*-CH), 7.35 (t, ³J_{H-H} = 7 Hz, 2H, *m*-CH), 8.26 (d, ³J_{H-H} = 7 Hz, 2H, *o*-CH);

¹³C{¹H} NMR (25 °C, CD₃CN) δ (ppm) = 59.0 (s, CH₃), 70.6 (s, CH₂), 72.3 (s, Ar), 127.00 (s, *p*-CH), 128.6 (m, *o*-CH), 129.1 (s, *m*-CH), 144.8 (m, *ipso*-C), 201.8 (m, C_{Heterocycle});

ESI- (m/z): 195.9622 (calc. 195.9640) [RCNP₃]⁻.

Sodium 5-biphenyl-1-aza-2,3,4-triphospholide (**104**)



104 was synthesized using 4-cyanobiphenyl according to the *via* Na[*cyclo*-P₅] (2.5 mmol solution of Na[*cyclo*-P₅] and 447 mg (2.5 mmol) of 4-cyanobiphenyl) procedure as described for **103**. The composition of the cation solvate shell was calculated on the basis of the ¹H NMR spectroscopy. Yield: 207 mg, 0.5 mmol, 19 %

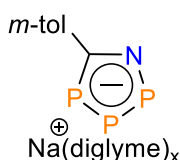
³¹P{¹H} NMR (25 °C, CD₃CN) δ (ppm) = (AMX spin system) 227.0 (dd, ¹J_{P-P} = 494 Hz, ²J_{P-P} = 8 Hz, P_A), 329.3 (dd, ¹J_{P-P} = 494 Hz, ¹J_{P-P} = 437 Hz, P_M), 382.4 (d, ¹J_{P-P} = 438 Hz, P_X);

^1H NMR (25 °C, CD_3CN) δ (ppm) = 1.75 (m, 2H, CH_2_{THF}), 3.29 (s, 3H, $\text{OCH}_3_{\text{diglyme}}$), 3.45 (m, 2H, $\text{CH}_2_{\text{diglyme}}$), 3.51 (m, 2H, $\text{CH}_2_{\text{diglyme}}$), 3.61 (m, 2H, CH_2_{THF}), 7.32 (t, $^3J_{\text{H-H}} = 8$ Hz, 1H, *p*-CH), 7.43 (t, $^3J_{\text{H-H}} = 8$ Hz, 2H, *m*-CH), 7.63 (d, $^3J_{\text{H-H}} = 8$ Hz, 2H, *o*-CH), 7.67 (d, $^3J_{\text{H-H}} = 8$ Hz, 2H, *m*-CH), 8.30 (d, $^3J_{\text{H-H}} = 8$ Hz, 2H, *o*-CH);

$^{13}\text{C}\{^1\text{H}\}$ NMR (25 °C, CD_3CN) δ (ppm) = 26.0 (s, CH_2_{THF}), 59.1 (s, $\text{CH}_3_{\text{diglyme}}$), 127.2-127.3 (m, *p*-CH), 127.4-127.5 (m, *m*-CH), 127.6-127.9 (m, *o*-CH), 128.6-128.9 (m, *o*-CH), 129.6-129.7 (m, *m*-CH), 139.0 (s, *ipso*-C), 141.4 (s, *ipso*-C), 143.5-143.8 (m, *ipso*-C), 201.2- 201.9 (m, $\text{C}_{\text{Heterocycle}}$);

ESI- (m/z): 271.9966 (calc. 271.9953) [RCNP_3] $^-$.

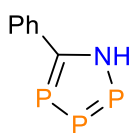
Sodium 5-(3-methylphenyl)-1-aza-2,3,4-triphospholide (105)



105 was synthesized using 2.5 mmol solution of $\text{Na}[\text{cyclo-P}_5]$ and *m*-tolunitrile (292 mg, 2.5 mmol) according to the procedure described for **103**. Yield: trace amounts detected by $^{31}\text{P}\{^1\text{H}\}$ NMR.

$^{31}\text{P}\{^1\text{H}\}$ NMR (25 °C, CD_3CN) δ (ppm) = (AMX spin system) 225.2 (dd, $^1J_{\text{P-P}} = 494$ Hz, $^2J_{\text{P-P}} = 8$ Hz, P_A), 328.4 (dd, $^1J_{\text{P-P}} = 494$ Hz, $^1J_{\text{P-P}} = 437$ Hz, P_M), 381.0 (d, $^1J_{\text{P-P}} = 438$ Hz, P_X).

5-phenyl-1-*H*-1-aza-2,3,4-triphosphole (106)



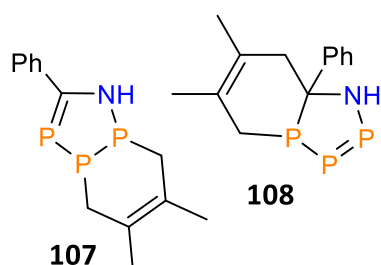
106 was synthesized by slow addition of trifluoroacetic acid (0.1 mL, 0.02 g, 0.2 mmol) *via* syringe to a cold ($T = -70$ °C) solution of **103** (0.1 g., 0.2 mmol) in THF. After the acid was added, the solution was allowed to slowly warm up to room

temperature and it was stirred for additional 14 h. Later, the solution was filtered *via* a cannula equipped with a microfiber glass filter to give a yellow-colored solution of **106**. Pure **106** was obtained after a filtration through a silica layer (10 cm) using toluene as the eluent. The removal of the solvent leads to the loss (decomposition) of **106**. Yield: 0.06 mmol, 34 % (based on the quantitative ^{31}P NMR spectrum).

$^{31}\text{P}\{^1\text{H}\}$ NMR (-100 °C, THF-d_8) δ (ppm) = (AMX spin system) 210.1 (dd, $^1J_{\text{P-P}} = 469$ Hz, $^2J_{\text{P-P}} = 20$ Hz, P_A), 320.0 (dd, $^1J_{\text{P-P}} = 498$ Hz, $^1J_{\text{P-P}} = 469$ Hz, P_M), 372.5 (broad dt, $^1J_{\text{P-P}} = 498$ Hz, $^2J_{\text{H-P}} = 19$ Hz, P_X);

^1H NMR (-100 °C, THF- d_8) δ (ppm) = 7.54-7.59 (m, *p*-CH), 7.93-7.95 (m, *m*-CH), 8.90-8.94 (m, *o*-CH), 14.04 (d, $^2J_{\text{H-P}} = 19$ Hz, NH).

[4+2] Diels-Alder adducts **107** and **108**



2,3-Dimethyl-1,3-butadiene (1 eq.) was added to the cold ($T = -70$ °C) THF solution of **106** (0.3 mmol). The reaction was allowed to slowly warm up to a room temperature. Monitoring of the reaction by $^{31}\text{P}\{^1\text{H}\}$ NMR revealed the instability of two products over the time. After 48 hours a full decomposition of products was observed. **107** and **108** are unstable upon concentration.

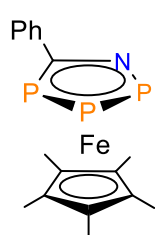
Yield: not available.

107: $^{31}\text{P}\{^1\text{H}\}$ NMR (-100 °C, THF) δ (ppm) = -72.2 (dd, $^1J_{\text{P-P}} = 244$ Hz, $^1J_{\text{P-P}} = 265$ Hz, 1P), -27.5 (d, $^1J_{\text{P-P}} = 244$ Hz, 1P), 63.2 ($^1J_{\text{P-P}} = 265$ Hz, 1P);

108: $^{31}\text{P}\{^1\text{H}\}$ NMR (-100 °C, THF) δ (ppm) = -24.5 (dd, $^1J_{\text{P-P}} = 309$ Hz, $^1J_{\text{P-P}} = 279$ Hz, 1P), 75.7 (d, $^1J_{\text{P-P}} = 309$ Hz, 1P), 133 (d, $^1J_{\text{P-P}} = 279$ Hz, 1P).

3.4.4 Synthesis of 1-aza-2,3,4-triphosphaferrocenes

5-phenyl-1-aza-2,3,4-triphosphaferrocene (**109**)



A pre-cooled ($T = -40$ °C) suspension of Cp^*Li (0.146 g, 1 mmol, 1 eq.) in 40 ml of THF was slowly added to the cold ($T = -40$ °C) suspension of $\text{FeCl}_2(\text{DME})$ (0.22 g, 1 mmol, 1 eq.) in 40 ml of THF. After the addition was complete, the reaction was stirred at $T = -40$ °C for two hours. Then, the cold ($T = -40$ °C) THF solution of **103** (0.5 g, 1 mmol, 1 eq.) was added dropwise to the reaction mixture. After

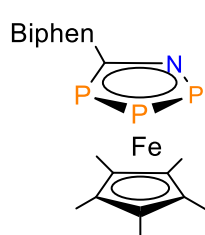
the addition was complete, the reaction was allowed to slowly warm up to room temperature. After 24 h of stirring at room temperature, resulting solution was filtered and the solvent was removed under reduced pressure. The crude black solid was sublimed ($T = 130$ °C, $1 \cdot 10^{-3}$ mbar) to give an orange crystalline powder of **109**. Prior to crystallization, **109** was dissolved in a pentane:toluene mixture (5:1) and filtered through a small (2 cm) layer of silica. Yield: 28 mg, 0.07 mmol, 7 %.

$^{31}\text{P}\{^1\text{H}\}$ NMR (25 °C, DCM- d_2) δ (ppm) = (ABX spin system) 34.5 (dd, $^1J_{\text{P-P}} = 451$ Hz, $^2J_{\text{P-P}} = 8$ Hz, P_A), 45.1 (dd, $^1J_{\text{P-P}} = 451$ Hz, $^1J_{\text{P-P}} = 346$ Hz, P_M), 142.6 (d, $^1J_{\text{P-P}} = 346$ Hz, P_X);

^1H NMR (25 °C, DCM- d_2) δ (ppm) = 1.54 (s, 15H, CH₃), 7.36-7.41 (m, 3H, CH), 8.22 (m, 2H, CH);

$^{13}\text{C}\{^1\text{H}\}$ NMR (25 °C, THF- d_8) δ (ppm) = 10.7 (s, CH₃), 90.2 (s, C), 128.7 (s, *p*-CH), 128.9 (s, *m*-CH), 130.0 (d, $^3J_{\text{C-P}} = 12$ Hz, *o*-CH), 139.0-139.3 (m, *ipso*-C), 142.5-143.4 (m, $\text{C}_{\text{Heterocycle}}$).

5-biphenyl-1-aza-2,3,4-triphosphaferrocene (**110**)



110 was synthesized using **104** (389 mg, 0.9 mmol) according to the procedure described for **109**. Single crystals suitable for the SC-XRD analysis were obtained from a concentrated ether solution at $T = -36$ °C. Yield: 42 mg, 0.09 mmol, 10 %.

$^{31}\text{P}\{^1\text{H}\}$ NMR (25 °C, DCM- d_2) δ (ppm) = (ABX spin system) 34.4 (dd, $^1J_{\text{P-P}} = 452$ Hz, $^2J_{\text{P-P}} = 8$ Hz, P_A), 45.3 (dd, $^1J_{\text{P-P}} = 452$ Hz, $^1J_{\text{P-P}} = 343$ Hz, P_M), 142.7 (dd, $^1J_{\text{P-P}} = 343$ Hz, $^2J_{\text{P-P}} = 8$ Hz, P_X);

^1H NMR (25 °C, DCM- d_2) δ (ppm) = 1.57 (s, 15H, CH₃), 7.37 (t, $^3J_{\text{H-H}} = 7$ Hz, 1H, *p*-CH), 7.46-7.49 (m, 2H, *m*-CH), 7.67-7.71 (m, 4H, *m*-CH/*o*-CH), 7.71-7.75 (m, 2H, *o*-CH), 8.29-8.31 (m, 2H, *o*-CH);

$^{13}\text{C}\{^1\text{H}\}$ NMR (25 °C, THF- d_8) δ (ppm) = 10.8 (s, CH₃), 90.2 (s, C), 127.1 (s, *p*-CH), 127.3 (s, *m*-CH), 127.9 (s, *m*-CH), 129.3 (s, *o*-CH), 130.4 (d, $^3J_{\text{C-P}} = 12$ Hz, *o*-CH), 138.3-138.5 (m, *ipso*-C), 140.8 (s, *ipso*-C), 141.1 (s, *p*-C), 142.3-143.0 (m, $\text{C}_{\text{Heterocycle}}$);

ESI+ (m/z): 464.0566 (calc. 464.0544) [MH^+];

Elemental analysis calculated (%) for $\text{C}_{23}\text{H}_{24}\text{FeNP}_3$: C, 59.64; H, 5.22; N, 3.02; **found**: C, 59.56; H, 5.25; N, 2.98;

s.p. $T = 180$ °C, $1 \cdot 10^{-3}$ mbar.

3.4.5 Crystallographic data for all compounds

Identification code	110
Empirical formula	$\text{C}_{23}\text{H}_{23}\text{FeNP}_3$

Formula weight	462.18
Temperature/K	101.3
Crystal system	monoclinic
Space group	P2 ₁ /c
a/Å	13.9512(7)
b/Å	7.5137(4)
c/Å	21.0754(10)
α/°	90
β/°	104.513(2)
γ/°	90
Volume/Å ³	2138.74(19)
Z	4
ρ _{calc} /cm ³	1.435
μ/mm ⁻¹	7.836
F(000)	956.0
Crystal size/mm ³	0.27 × 0.07 × 0.02
Radiation	CuKα (λ = 1.54178)
2θ range for data collection/°	6.544 to 150.124
Index ranges	-17 ≤ h ≤ 17, -9 ≤ k ≤ 9, -26 ≤ l ≤ 24
Reflections collected	34888
Independent reflections	4370 [R _{int} = 0.0652, R _{sigma} = 0.0349]
Data/restraints/parameters	4370/0/289
Goodness-of-fit on F ²	1.065
Final R indexes [I ≥ 2σ (I)]	R ₁ = 0.0392, wR ₂ = 0.0923
Final R indexes [all data]	R ₁ = 0.0434, wR ₂ = 0.0950
Largest diff. peak/hole / e Å ⁻³	0.49/-0.40

110: The compound crystallizes with one molecule per asymmetric unit. The CP3N ring bound to the Fe is disordered and modeled as two part. A thermal constraint was placed on the nitrogen atoms and the model was allowed to freely refine resulting in a 85:15 ratio.

Chapter 4. Reactivity of the pentaphospholide anion towards $C\equiv P$ and $C\equiv As$ triple bonds. Synthesis of 1,2,3,4-tetraphospholide anions.

4.1 Introduction.

4.1.1 Phosphaalkynes

Phosphaalkynes form a wide class of organophosphorus compounds containing a triple bond between the $\lambda^3\sigma^1$ -phosphorus and the sp-carbon atom with the general formula $R-C\equiv P$. For a long time it was considered that phosphorus cannot form multiple bonds with elements of the first period.^[153] Although there is an evidence of the phosphorus reluctance to participate in π -bonding, in fact, this only indicates that π -bonds are reactive in the absence of kinetically stabilizing substituents.^[136] Therefore, phosphaalkynes without sterically bulky substituents have rather short half-life times.^[154] The synthesis of kinetically stable phosphaalkyne with the bulky ^tBu substituent by *Uhl et al.* in 1981^[155] significantly increased the interest to these species.^[156,153,157,158]

The experiments,^[153,156,157,158] spectroscopic^[159] and theoretical studies^[160] confirm that the $C\equiv P$ triple bond is more similar to $C\equiv C$ than to an isoelectronic $C\equiv N$ triple bond. A comparison of the photoelectron spectra of $R-C\equiv E$ ($E = P, N$; $R = {}^t\text{Bu}, \text{Ph}$) reveals the increased $\pi(C\equiv P)-n(P)$ orbitals separation in the phosphaalkyne series as compared to that of nitriles.^[161] Therefore, the HOMO of $R-C\equiv P$ derivatives is mainly comprised of the π -orbitals of the $C\equiv P$ triple bond. An energetically reduced localized orbital representing the lone pair of phosphorus is reluctant to form σ -bonds.^[162] The resemblance between alkynes and phosphaalkynes is particularly noticeable when the shapes of their frontier MOs are compared. For instance, the frontier orbitals of $\text{Ph}-C\equiv\text{CH}$ and $\text{Tripp}-C\equiv\text{P}$ (Tripp = 1,3,5-tri(isopropyl)phenyl) are shown in **Figure 35**.

The electron density distribution (EDD) map of ^tBu- $C\equiv P$ obtained by special X-ray diffraction studies shows an excess of the electron density on the sp-hybridized carbon atom, while the P-atom holds a partial positive charge.^[163] Such polarization of the $C\equiv P$ triple bond is in contrast to the situation in $R-C\equiv N$, which is considered in the discussion of the chemical properties.

Similar to unsaturated hydrocarbons, phosphaalkynes are accessible *via* various 1,2-elimination reactions (**Scheme 50a-e**).^[156]

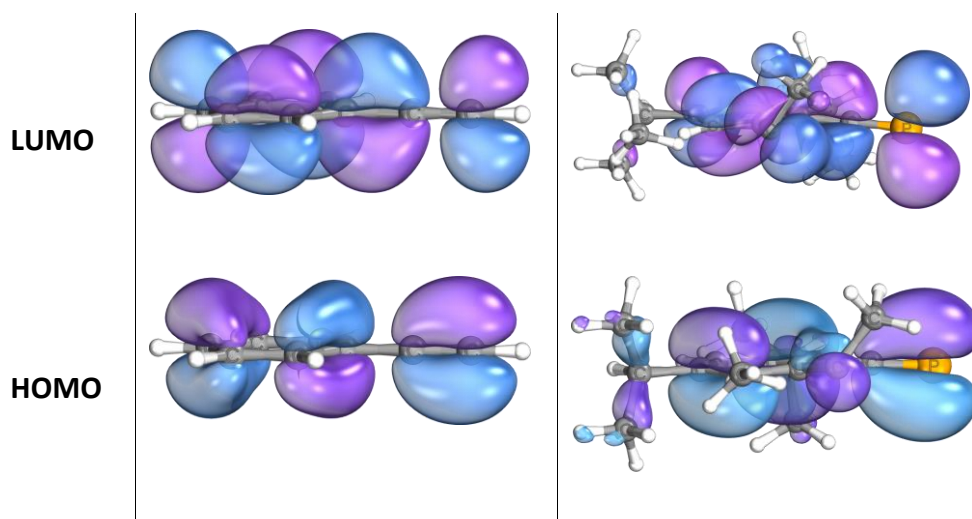
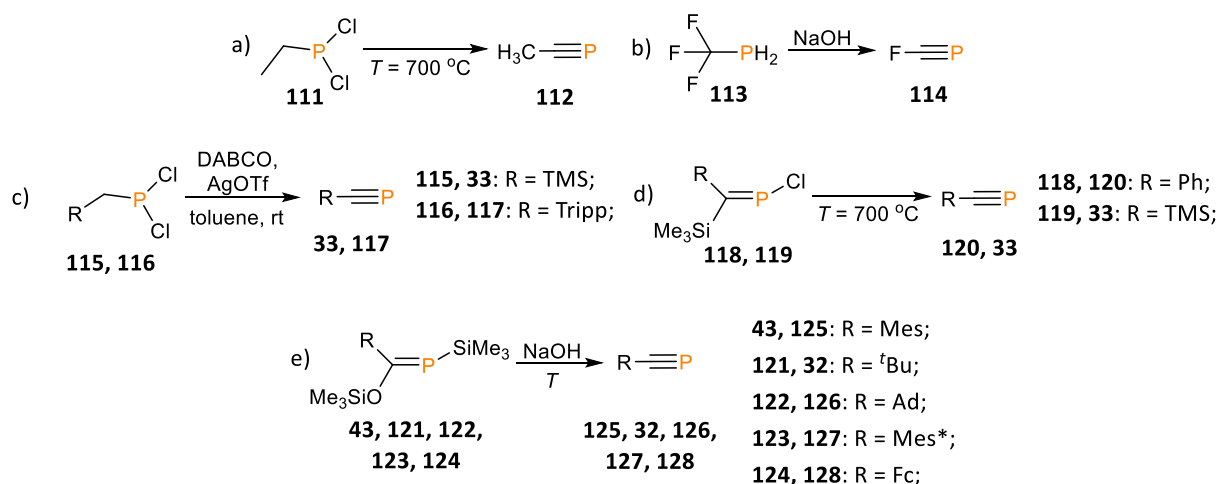


Figure 35. Frontier molecular orbitals of $\text{Ph}-\text{C}\equiv\text{CH}$ (left) and $\text{Tripp}-\text{C}\equiv\text{P}$ **117** (right).



Scheme 50. Synthesis of phosphalkynes.

Some $\text{R}-\text{C}\equiv\text{P}$ derivatives (**112**, **114**) were synthesized by a repeated dehydrohalogenation of dihalophosphines (**111**, **113**) promoted thermally ($T = 700\text{--}1000\text{ }^\circ\text{C}$)^[164] or by strong bases (**Scheme 50a-b**).^[165] Although these relatively straightforward methods are sufficient for the determination of the physical and spectral properties of volatile phosphalkynes, they are inappropriate for chemical studies due to a low selectivity and poor yields of the desired species. The dehydrohalogenation of dihalophosphanes was significantly improved when hydroxides were replaced by DABCO/AgOTf (**Scheme 50c**).^[166,167] Following this modification, phosphalkynes **33** and **117** become accessible on a multigram scale.

Appel *et al.* described a thermally induced elimination of Me_3SiCl from phosphalkenes **118** and **119** containing vicinal Cl and Me_3Si groups, which leads to phosphalkynes **33** and **120** in

almost quantitative yields. (**Scheme 50d**)^[168,169] Despite the efficiency of this method it requires special equipment, which is usually not available routinely in a laboratory setting. The “classical” elimination of hexamethyldisiloxane proved to be a reliable route to a library of phosphalkynes **32**, **125–128** containing aliphatic and aryl substituents.^[170,171,172]

The chemical behavior of phosphalkynes is reminiscent of alkynes and represented by electrophilic addition and cycloaddition reactions. The electrophilic addition reactions are inconsiderable in the chemistry of phosphalkynes, however, it is noteworthy that the reaction with hydrogen halides results in a protonation of the carbon atom^[173] (in accordance with the EDD maps),^[163] rather than of the P-atom.

On the other hand, various cycloaddition reactions with $R-C\equiv P$ are of significant value in preparative chemistry as a source of $[C=P]$ and $[C-P]$ units in the construction of heterocycles.^[154] Syntheses involving $R-C\equiv P$ are usually characterized by high selectivity and yields.^[136,174]

Phosphalkynes are particularly interesting in terms of the synthesis of phospholide anions as they have already been used for such purposes. Several examples of reactions that involve $R-C\equiv P$ derivatives for the synthesis of phospholide anions were discussed in **Chapters 1 and 3 (Scheme 17, Scheme 18, Scheme 19, Scheme 20 and Scheme 42)**.

4.1.2 1,2,3,4-tetraphospholide anions

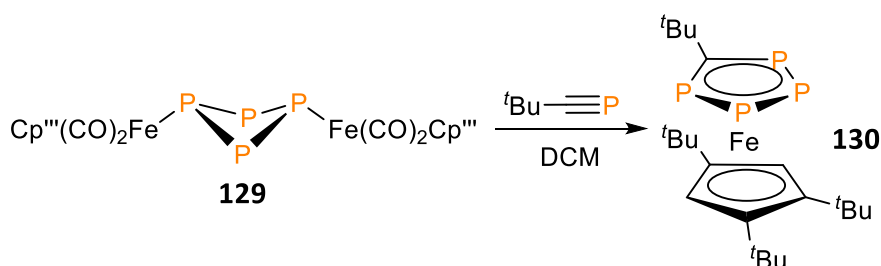
Taking into account the resemblance in the electronic structure between phosphalkynes and alkynes, it was anticipated that a reaction between $Na[cyclo-P_5]$ and $R-C\equiv P$ may give rise to the barely explored 1,2,3,4-tetraphospholide anions ($1,2,3,4-[cyclo-(CR)P_4]^-$).

$1,2,3,4-[cyclo-(CR)P_4]^-$ remain elusive, with only four isolated and characterized species up to date. In 1987, *Baudler et al.* reported the formation of the parent 1,2,3,4-tetraphospholide anion **11** as a minor by-product of the activation of P_4 by Na in boiling diglyme (**Scheme 6**).^[32] The detection of $1,2,3,4-[cyclo-(CH)P_4]^-$ among other products indicates an entangled mechanism in which diglyme acts as a source of the methine unit.

Ten years later, *Mathey et al.* proposed a seemingly straightforward route to $1,2,3,4-[cyclo-(CR)P_4]^-$ via a reaction of a synthetic equivalent of the $[RC]^-$ fragment with P_4 . Surprisingly, an

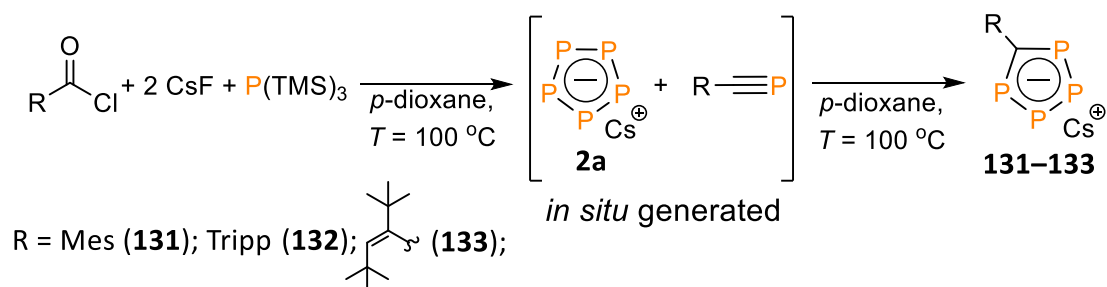
attempt to react lithium(trimethylsilyl)diazomethanide **101** with P_4 led to 1,2,3,4-diazadiphospholide anion **102** via formal [3+2] cycloaddition between $[P\equiv P]$ and $[CR=N=N]$ fragments (**Scheme 44**).^[138]

The substantial progress was achieved in 2005 when *Scheer et al.* obtained an iron complex containing η^5 -coordinated 5-*tert*-butyl-1,2,3,4-tetraphospholide **130** as one of the products in the reaction between $R-C\equiv P$ and the tetraphosphabicyclobutadiene complex **129** (**Scheme 51**).^[175]



Scheme 51. Synthesis of 1,2,3,4-tetraphosphaferrocene **130**.

A few years after, *Ionkin et al.* succeeded in the isolation of the free 1,2,3,4-[cyclo-(CR) P_4]⁻. The original procedure is a three-component *one-pot* reaction between acid chloride, CsF, and $P(\text{TMS})_3$ in boiling dioxane giving the desired product (**131–133**) after continuous reflux (up to 10 days) (**Scheme 52**).^[176,177,178]



Scheme 52. Synthesis of 5-*R*-1,2,3,4-tetraphospholide anions **131–133**.

Although the mechanism of this chemical transformation is rather obscure, it was assumed that $P(\text{TMS})_3$ could undergo several possible fluorodesilylation routes, yielding a highly reactive low-coordinate phosphorus species.^[177] The formation of 1,2,3,4-[cyclo-(CR) P_4]⁻ was

interpreted as a reaction between the *in situ* generated Cs[*cyclo*-P₅] **2a** and R—C≡P (**Scheme 52**).

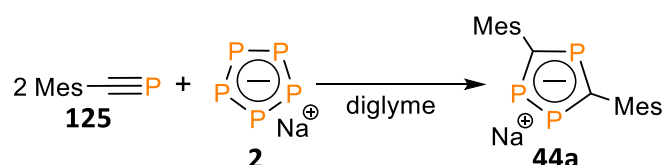
In order to examine the hypothesis of the 1,2,3,4-tetraphospholide anion formation proposed by Ionkin *et al.*, a comprehensive study on the reactivity of R—C≡P towards Na[*cyclo*-P₅] was performed.

4.2 Results and discussion

4.2.1 Synthesis of sodium 1,2,4-triphospholides and 1,2,3,4-tetraphospholides

In **Chapters 2** and **3** it was demonstrated that electron-withdrawing substituents at the C≡C and C≡N triple bonds facilitate the reaction with [*cyclo*-P₅]⁻. Thus, kinetically stabilized aryl derivatives of R—C≡P were selected for the initial experiments.

The addition of one equivalent of Mes—C≡P **125** to a solution of Na[*cyclo*-P₅] results in a rapid color change from orange to dark red with the subsequent formation of a solid precipitate. The ³¹P NMR spectrum taken from the reaction mixture displays the residual signal for [*cyclo*-P₅]⁻ at δ = 468.7 ppm as well as two multiplet resonances of an AX₂ spin system, a triplet at δ = 252.6 ppm and a doublet at δ = 263.2 ppm (²J_{P-P} = 38 Hz) in a 1:2 ratio. Based on the analysis of the NMR spectrum and the literature data^[69] it can be concluded that sodium 3,5-bismesityl-1,2,4-triphospholide **44a** was formed (**Scheme 53**). The maximal yield (19 % based on P₄) of the reaction is achievable when two equivalents of **125** were added.

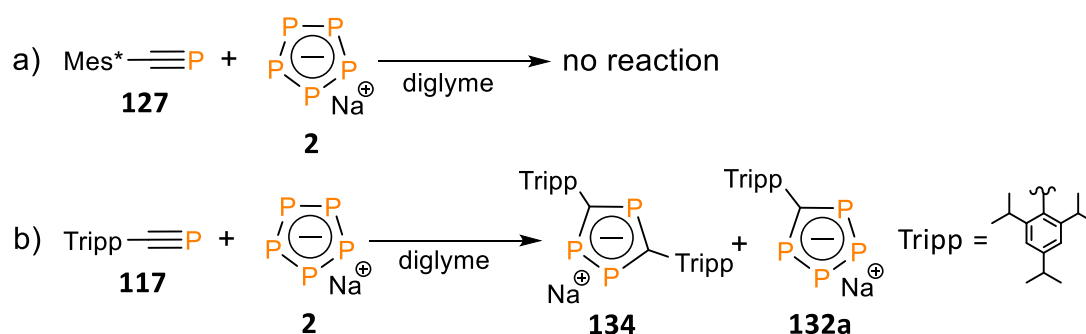


Scheme 53. Synthesis of 3,5-bismesityl-1,2,4-triphospholide anion **44a**.

The ¹H NMR spectrum reveals three singlets with chemical shifts at δ = 2.40, 2.48 and 6.97 ppm attributed to the mesityl substituents. The ¹³C{¹H} NMR spectrum displays the C_(heterocycle) nuclei as a multiplet resonance signal at δ = 190.6 ppm, which is approximately 10 ppm downfield shifted in comparison to 4,5-diethyl-1,2,3-triphospholide **50** (δ = 177.5 ppm).

In this reaction, Na[cyclo-P₅] acts as a source of [P]⁻ in a formal [2+2+1] cycloaddition which is reminiscent of the above-mentioned synthesis of 3,5-bis(trimethyl)silyl-1,2,4-triphospholide anion **35** in the reaction between triphosphapentadienide **40** with TMS—C≡P **33** (Scheme 19).^[66] Taking in account the mutuality between these two reactions it can be concluded that the general pathway to 1,2,4-triphospholides is the interaction of R—C≡P with a weak P-centered nucleophile.

It was hypothesized that the bulky Mes*—C≡P (Mes*: 1,3,5-tri(*tert*-butyl)phenyl) **127** cannot participate in a formal [2+2+1] cycloaddition because of the unfavored arrangement of two sterically demanding substituents and, therefore, may only interact in a desired [3+2] fashion. However, it was found that **127** does not react with Na[cyclo-P₅] even at elevated temperatures, indicating an increased steric hindrance of the C≡P triple bond for any interactions with Na[cyclo-P₅] (Scheme 54a).

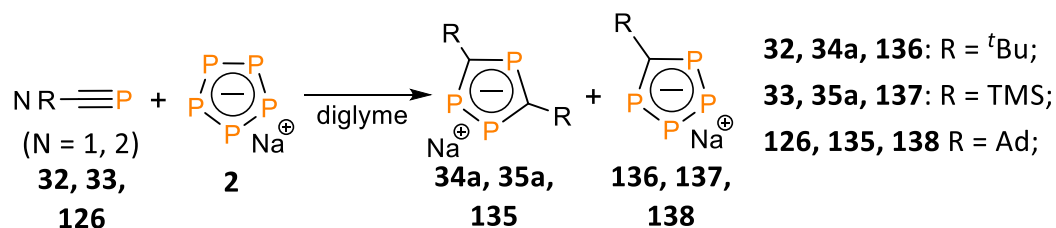


Scheme 54. Synthesis of sodium 3,5-bis(1,3,5-tri(isopropyl)phenyl)-1,2,4-triphospholide **134** and sodium 5-(1,3,5-tri(isopropyl)phenyl)-1,2,3,4-tetraphospholide **132a**.

At the same time, addition of the less bulky Tripp—C≡P (Tripp = 1,3,5-tri(isopropyl)phenyl) **117** to the Na[cyclo-P₅] solution results in a slowly developing reaction (Scheme 54b). The ³¹P NMR spectroscopic monitoring of the reaction mixture displays the formation of two sets of multiplet resonances in a 1:1 ratio. The doublet and triplet resonances between $\delta = 270.0$ – 274.0 ppm correspond to the 1,2,4-triphospholide anion **134**, while the resonances of an AA'MM' spin system at $\delta = 365.0$ – 373.0 ppm belong to the desired 1,2,3,4-tetraphospholide anion **132a** in accordance with the literature data.^[178] Due to the low yield (less than 5%, based on the **127**) of this reaction, it was impossible to isolate both products. Although these experiments highlight the importance of the steric hinderance around the C≡P triple bond,

they also indicative of that phosphalkynes with more electron-donating substituents are also reactive towards Na[cyclo-P₅].

One equivalent of TMS—C≡P **33** (in toluene) was added to a diglyme solution of Na[cyclo-P₅] (**Scheme 55**). The addition of the phosphalkyne resulted in a rapid color change from orange to dark red and the formation of a precipitate.



Scheme 55. Synthesis of sodium 1,2,4-triphospholides **34a**, **35a**, **135** and sodium 1,2,3,4-tetraphospholides **136**, **137**, **138**.

The ³¹P NMR spectrum taken from the reaction mixture reveals the presence of the residual Na[cyclo-P₅] as well as the 3,5-bis(trimethylsilyl)-1,2,4-triphospholide **35a** and the 5-trimethylsilyl-1,2,3,4-tetraphospholide anion **137** in a 7:1 ratio. **137** is represented with two downfield shifted multiplet resonances at δ = 373.3 and 399.6 ppm, which form a characteristic AA'MM' spin system (**Figure 36**) with large ¹J_{P-P} coupling constants of 481 and 491 Hz (simulated values). **35a** was detected as a simple AX₂ spin system consisting of a triplet at δ = 315.3 ppm and a doublet at δ = 324.9 ppm (²J_{P-P} = 32 Hz). After filtration, evaporation of solvents under high vacuum, and washing the residue with pentane, the mixture of **35a** and **137** was collected as a dark red oil. The ¹H NMR spectrum shows an intense singlet resonance at δ = 0.35 ppm which corresponds to the TMS groups of **35a**, while the same substituent in **137** occurs at δ = 0.48 ppm. The ¹³C{¹H} NMR spectrum revealed the most deshielded multiplet resonance at δ = 182.5 ppm, which was attributed to **35a**.

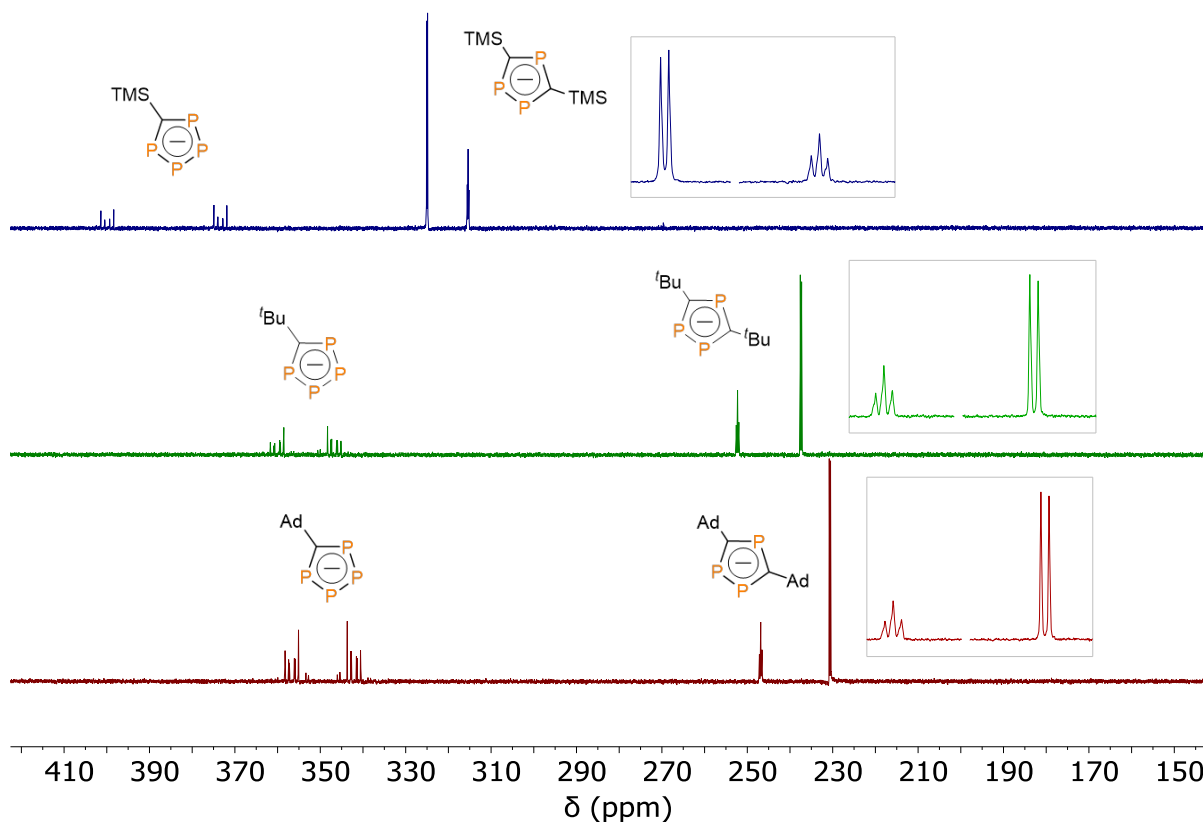


Figure 36. ^{31}P NMR spectra of mixtures **35a** and **137** (top, blue), **34a** and **136** (middle, green), **135** and **138** (bottom, red).

Aliphatic phosphalkynes such as $^t\text{Bu}-\text{C}\equiv\text{P}$ **32** and $\text{Ad}-\text{C}\equiv\text{P}$ **126** also react rapidly with the diglyme solution of $\text{Na}[\text{cyclo-P}_5]$ (Scheme 55). The reaction involving **32** results in the formation of sodium 3,5-bis(*tert*-butyl)-1,2,4-triphospholide **34a** and sodium 5-*tert*-butyl-1,2,3,4-tetraphospholide **136** in a 7:1 ratio respectively. The ^{31}P NMR spectrum reveals **136** as two resonances forming an $\text{AA}'\text{MM}'$ spin system at $\delta = 347.6$ and 358.6 ppm ($^1J_{\text{P-P}} = 494$ and 496 Hz), which are slightly upfield compared to **137** ($\delta = 373.3$ and 399.6 ppm). 1,2,4-triphospholide **34a** shows a doublet at $\delta = 237.4$ ppm and a triplet at $\delta = 252.3$ ppm ($^2J_{\text{P-P}} = 48$ Hz). The ^1H NMR spectrum displays a singlet with the chemical shift at $\delta = 1.50$ ppm and a seven times less intense singlet at $\delta = 1.74$ ppm which were attributed to the ^tBu groups of **34a** and **136**, respectively. A multiplet at $\delta = 206.8$ ppm in the $^{13}\text{C}\{^1\text{H}\}$ NMR spectrum was assigned to the $\text{C}_{(\text{heterocycle})}$ nuclei of **34a**.

The reaction between $\text{Na}[\text{cyclo-P}_5]$ and one equivalent of $\text{Ad}-\text{C}\equiv\text{P}$ **126** leads to sodium 3,5-bisadamantyl-1,2,4-triphospholide **135** and 5-adamantyl-1,2,3,4-tetraphospholide **138** in a

3:1 ratio. The ^{31}P NMR spectrum of **138** (Figure 36) reveals two resonances forming an AA'MM' spin system with the chemical shifts at $\delta = 343.5$ and 355.0 ppm. **135** is observed as a doublet at $\delta = 230.7$ ppm and a triplet at $\delta = 246.9$ ppm. In the ^1H NMR spectrum, the resonances at $\delta = 1.73$ – 2.48 ppm correspond to the Ad substituents.

Taking into account the difference in nucleophilicity of 1,2,4-triphospholides and 1,2,3,4-tetraphospholides,^[75] the chemical separation of the mixture of **135** and **138** was attempted. The approach was to find a suitable alkylhalide that will react with the more nucleophilic 1,2,4-triphospholide anion exclusively. All attempts are summarized in the Table 3.

R'	X	Solvent	T	t	result
benzyl	Cl	diglyme	RT	30 min	both reacted
tributyltin (TBT)	Cl	diglyme	RT	30 min	both reacted
ethane	Br	diglyme	RT	over night	both reacted
5-pentene	Br	diglyme	RT	30 min	both reacted
neopentyl	Cl	diglyme	60°C	overnight	no reaction
allyl	Br	diglyme	RT	30 min	both reacted
isopropyl	Br	diglyme	RT	30 min	no reaction
isopropyl	Br	diglyme	RT	overnight	decomposition
isopropyl	Br	diglyme	60°C	30 min	both reacted
isopropyl	Br	MeCN	60°C	30 min	both reacted

Table 3. Summarized data for attempts to separate **135** and **138** chemically.

The full conversion of $\text{Na}[\text{cyclo-P}_5]$ could be achieved after the addition of two equivalents of $\text{R}-\text{C}\equiv\text{P}$, which does not affect the ratio between the pairs of six compounds (Table 4). A slow, dropwise addition of $\text{R}-\text{C}\equiv\text{P}$ via a dropping funnel with intense stirring of the reaction mixture does not change the ratio between the two products substantially. A reverse addition of $\text{Na}[\text{cyclo-P}_5]$ to a $\text{R}-\text{C}\equiv\text{P}$ solution results in the exclusive formation of sodium 1,2,4-triphospholides **34a**, **35a**, **135** in low yields.

In summary, the experiments on the reactivity of $\text{R}-\text{C}\equiv\text{P}$ towards $\text{Na}[\text{cyclo-P}_5]$ show only a partial compatibility with the concept^[177] of a 1,2,3,4-tetraphospholide anion formation in the reaction between *in situ* generated $\text{Cs}[\text{cyclo-P}_5]$ and corresponding $\text{R}-\text{C}\equiv\text{P}$ (as showcased in Scheme 52).

Products	The respective ratio between two products	Combined yield, %
35a and 137	7:1	10
34a and 136	6:1	18
135 and 138	3:1	19

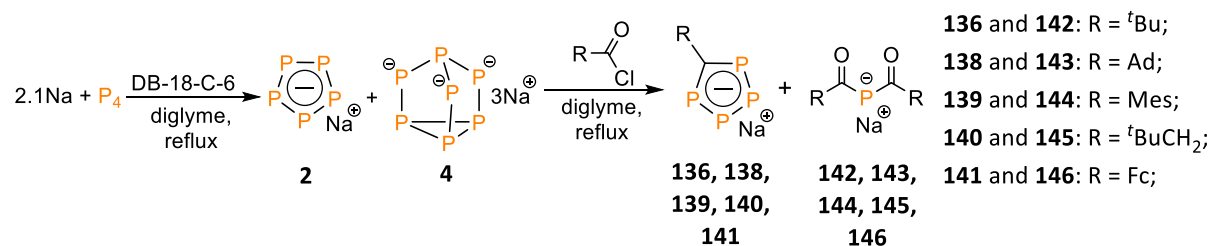
Table 4. Summarized data on ratio and yields (based on P_4) of products.

4.2.2 Synthesis of 1,2,3,4-tetraphospholide anions

Since the interaction between $R-C\equiv P$ and $[cyclo-P_5]^-$ (**Scheme 55**) did not fully explain the formation of $1,2,3,4-[cyclo-(CR)P_4]^-$ in the three-component reaction (**Scheme 52**),^[177] it was assumed that the interaction between acid chloride and *in situ* generated polyphosphides plays a more important role in the chemical transformation of $P(TMS)_3$ into $1,2,3,4-[cyclo-(CR)P_4]^-$. At the same time, the use of $P(TMS)_3$ for the building of scaffolds with several P-atoms is considered as ineffective. Thus, the next goal was to examine the reactivity of acid chlorides towards polyphosphides synthesized directly from P_4 .

The mixture of polyphosphides was synthesized based on the reaction between Na and P_4 in the presence of DB-18-C-6 under reflux conditions in diglyme (**Scheme 7**).^[35] The reaction leads to a mixture that mainly consists of $Na[cyclo-P_5]$ **2** (30 %, soluble in diglyme) and $Na_3[P_7]$ **4** (40 %, insoluble in diglyme). Preference was given to this procedure for two reasons: 1) the direct access to two of the most abundant polyphosphides 2) the mixture of polyphosphides is easy to separate by filtration.

The mixture of $Na[cyclo-P_5]$ and $Na_3[P_7]$ in diglyme was produced starting from 0.5 g of P_4 following the standard protocol. Subsequently, one equivalent of trimethylacetyl chloride (relative to the amount of P_4) was added to the mixture of sodium polyphosphides and the reaction mixture was stirred under reflux conditions for 3 hours (**Scheme 56**).



Scheme 56. Synthesis of sodium 1,2,3,4-tetraphospholide anions **136**, **138–141**.

Within one hour the green-yellow reaction mixture turned to dark red. The ^{31}P NMR spectrum taken from the reaction mixture after 3 hours of reflux displays singlet resonance signals at $\delta = 39.2$ ppm and two multiplets forming a characteristic AA'MM' spin system at $\delta = 347.6$ and 358.6 ppm which are attributed to sodium 5-*tert*-butyl-1,2,3,4-tetraphospholide **136** (Figure 37). The singlet resonance at $\delta = 39.2$ ppm corresponds to the bis(2,2-dimethylpropionyl)phosphide anion **142**.^[179]

136 was collected as a dark red oil in a yield of 24 %. The $\text{C}_{(\text{heterocycle})}$ nucleus of **136** was observed by $^{13}\text{C}\{^1\text{H}\}$ NMR spectroscopy as a multiplet resonance at $\delta = 228.0$ ppm.

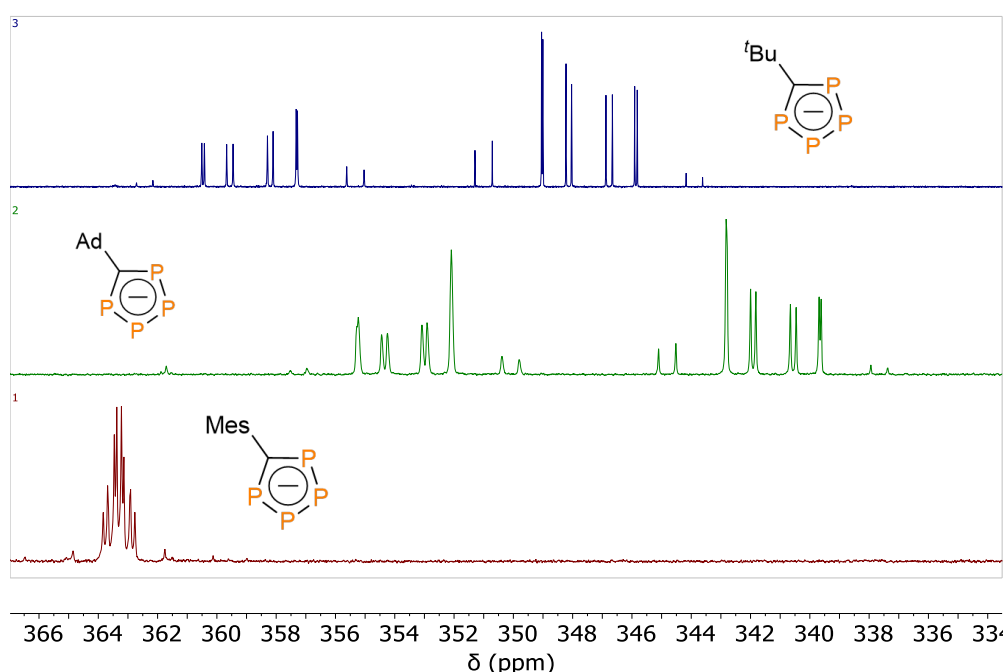
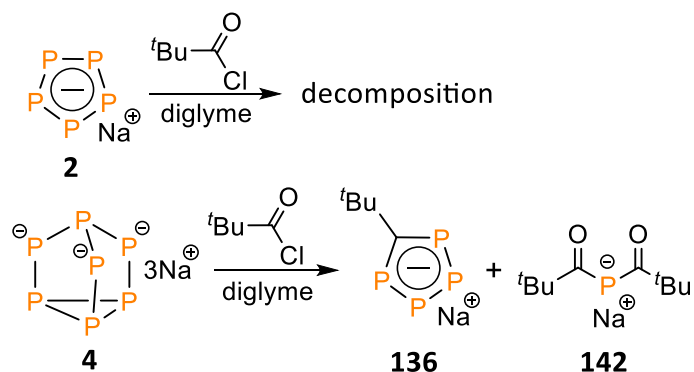


Figure 37. ^{31}P NMR spectra of the 5-R-1,2,3,4-tetraphospholide anions **136** (top, blue), **138** (middle, green) and **139** (bottom, red).

1-Adamantanecarbonyl chloride also reacts with the mixture of polyphosphides following the same protocol (Scheme 56). The $^{31}\text{P}\{^1\text{H}\}$ NMR spectrum reveals a singlet at $\delta = 39.2$ ppm and an AA'MM' multiplet for **138** at $\delta = 343.5$ and 355.0 ppm. After the standard workup procedure, **138** was collected as a dark red oil in 20 % yield. The ^1H NMR spectrum displays resonances for the adamantyl group in **138** as three broad resonances between $\delta = 1.50$ –2.80 ppm. The $\text{C}_{(\text{heterocycle})}$ nucleus was observed by $^{13}\text{C}\{^1\text{H}\}$ NMR spectroscopy as a multiplet resonance with the chemical shift at $\delta = 229.0$ ppm.

in diglyme leads to the formation of a deep red solution. After 3 hours of reflux, the desired 1,2,3,4-[cyclo-(CR)P₄]⁻ **136** along with bis(acyl)phosphide **142** was formed. Thus, it can be concluded that Na₃[P₇] plays an important role in the synthesis of the 1,2,3,4-tetraphospholide anions (**Scheme 58**).



Scheme 58. Reactivity of trimethylacetyl chloride towards Na[cyclo-P₅] and Na₃[P₇].

It was also discovered that the synthesis of 1,2,3,4-[cyclo-(CR)P₄]⁻ **136**, **138** and **139** can be modified to a simpler *one-pot* procedure. In this case, P₄, Na, acid chloride and diglyme were added into a Schlenk flask which was then stirred under reflux conditions for 3 hours. This method was considered as a rational approach towards the barely investigated 1,2,3,4-tetraphospholide anions.

In order to understand how substitution of nitrogen by a P-atom influences the electronic properties of polyphospholides, the frontier orbitals of the parent 1-aza-2,3,4-triphospholide anion **75** and the 1,2,3,4-tetraphospholide anion **11** were compared (**Figure 38**).

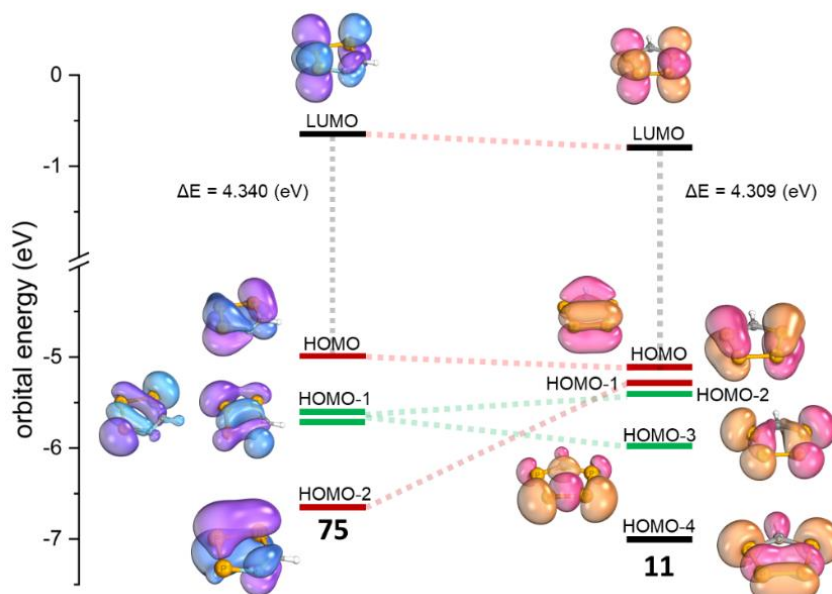
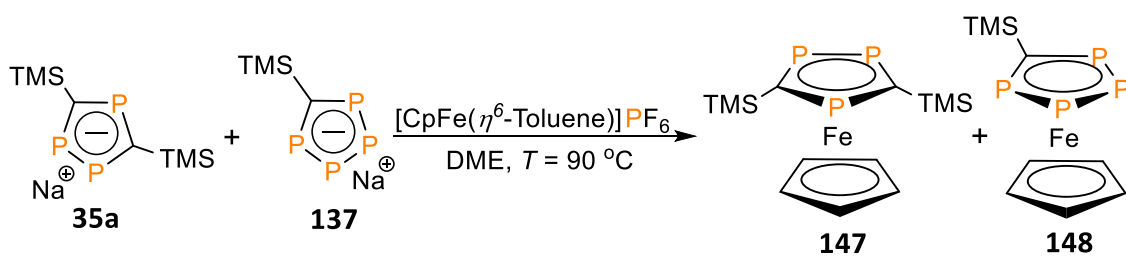


Figure 38. Frontier orbitals of the parent 1-aza-2,3,4-triphospholide **75** (left) and 1,2,3,4-tetraphospholide **11** (right). Calculated at the B3LYP-D3/def2-TZVP level of theory

In both species, the HOMO and LUMO are represented by π and π^* orbitals, respectively, while the order of the other bonding orbitals is different. Replacement of nitrogen by a P-atom results in an energy convergence of two bonding π -orbitals (HOMO/HOMO-2 of **75** and HOMO/HOMO-1 of **11**). At the same time, the degeneracy of two orbitals at HOMO-1 level (HOMO-1/HOMO-1' of **75**) is removed (HOMO-2/HOMO-3 of **11**). The energetically lowered LUMO of **11** as well as two energetically close-standing π -orbitals (HOMO and HOMO-1 of **11**) indicate better π -donation properties of tetraphospholide **11** and a preferential η^5 -coordination mode of this heterocycle.

4.2.3 Synthesis of 1,2,4-triphosphaferrocenes and 1,2,3,4-tetraphosphaferrocenes

A mixture of sodium 3,5-bis(trimethyl)silyl-1,2,4-triphospholide **35a** and 5-trimethylsilyl-1,2,3,4-tetraphospholide **137** reacts with $[\text{CpFe}(\eta^6\text{-Toluene})]\text{PF}_6$ in DME under reflux conditions to give the corresponding 1,2,4-tri- and 1,2,3,4-tetraphosphaferrocenes **147** and **148** (Scheme 59). Phosphaferrocenes **147** and **148** were sublimed to give a red powder with the combined yield of around 40 %.



Scheme 59. Synthesis of 3,5-bis(trimethyl)-1,2,4-triphenylferrocene **147** and 5-trimethyl-1,2,3,4-tetraphenylferrocene **148**.

The ^{31}P NMR spectrum displays two pairs of resonances forming an AX_2 ($\delta = 85.1$ (d) ppm, $t = 91.4$ (t) ppm, $^2J_{\text{P-P}} = 31$ Hz) and a slightly downfield shifted $\text{AA}'\text{MM}'$ ($\delta = 99.5$ (m) ppm, 135.4 (m) ppm) spin systems in a 23:1 ratio, respectively. A significant shielding of the resonance signals together with a retention of the spin systems (with respect to the free ligands **35a** and **137**) confirm the sandwich structure of **147** and **148**. The ^1H NMR spectrum reveals the TMS group as an intense and broadened singlet at $\delta = 0.34$ ppm. The $\text{C}_{(\text{heterocycle})}$ nuclei of **147** were registered by $^{13}\text{C}\{^1\text{H}\}$ NMR at $\delta = 111.6$ ppm.

Although 1,2,3,4-tetraphenylferrocene was synthesized in a negligible amount, single crystals suitable for the crystallographic characterization were obtained from a concentrated hexane solution at $T = -36$ °C. The molecular structure of **148** in the crystal is represented in **Figure 39**. Complex **148** crystallizes in the monoclinic $\text{P}2_1/\text{m}$ space group and reveals 5-trimethylsilyl-1,2,3,4-tetraphenylphospholyl and cyclopentadienyl ligands η^5 -coordinated to iron in an almost perfectly eclipsed conformation (the interplanar angle between the two rings is $1.23(7)^\circ$). The two rings are almost parallel to each other with the $[\text{CP}_4]_{\text{cent}}\text{-Fe-}[\text{Cp}]_{\text{cent}}$ angle of $179.14(3)^\circ$. P1—P1' bond ($2.1140(6)$ Å) in **148** is only slightly shorter than P1—P2 ($2.1277(4)$ Å).

3,5-bis(trimethylsilyl)-1,2,4-triphenylferrocene **147** was crystallized from a saturated acetonitrile solution at $T = -36$ °C. The twinned nature of the single crystals of **147** resulted in a substantial disorder of the molecular structure. **147** crystallizes in the orthorhombic $\text{P}2_12_12_1$ space group, the molecular structure in the crystal is shown in **Figure 39**. Two η^5 -coordinated ligands are arranged in a staggered conformation with the angle of $21.1(7)^\circ$. The impact of the P-atom on the π -acceptor character of the selected phospholyl ligand becomes evident

when $[C_{5-n}P_n]_{\text{centroid}}\text{-Fe}$ ($n = 3$ or 4) distances in **147** ($1.602(3)$ Å) and in **148** ($1.5777(4)$ Å) are compared to each other.

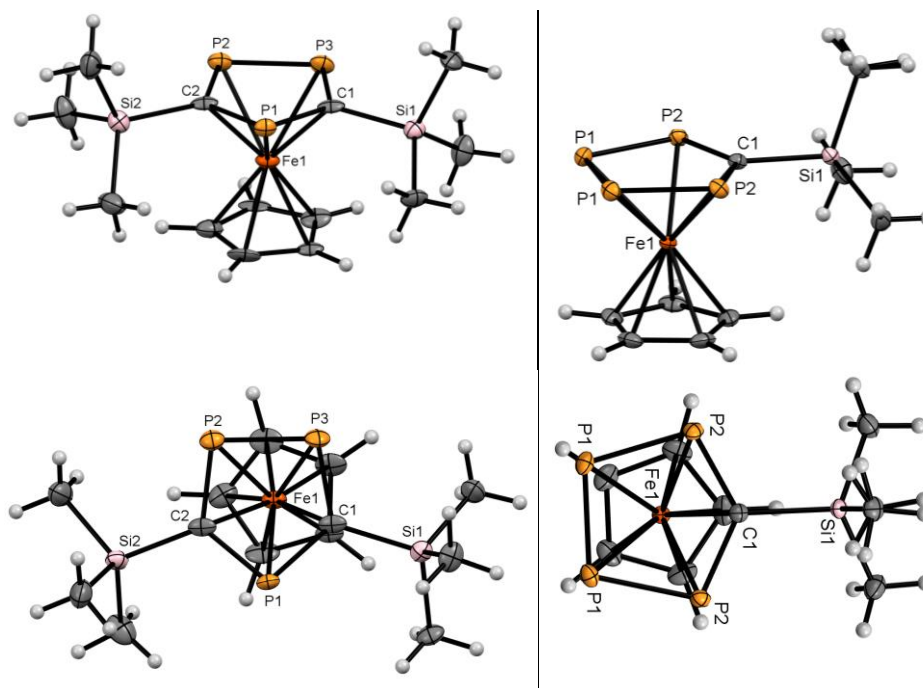
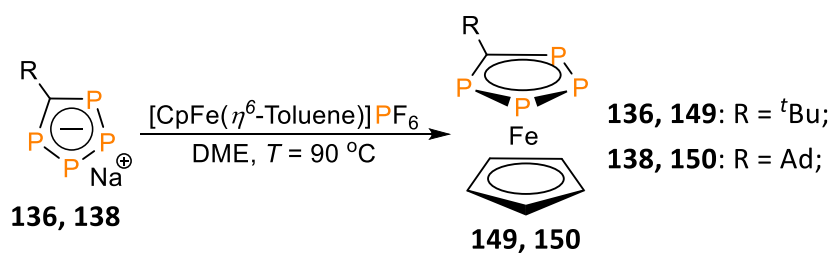


Figure 39. Molecular structure of **147** (left) and **148** (right) in the crystal. Ellipsoids are shown at 50 % probability level. Selected bond lengths (Å) and angles ($^{\circ}$) of **147**: P2-P3: 2.143(4); P1-C1: 1.763(10); P1-C2-P2: 121.8(6); C1-P1-C2: 98.7(4); C1-P2-P3: 98.9(4); $[Cp]_{\text{cent}}\text{-Fe1}$ - $[C_2P_3]_{\text{cent}}$: 179.8 (2); interplanar angle: 21.1(7). $[C_2P_3]_{\text{cent}}\text{-Fe1}$: 1.602(3); $[Cp]_{\text{cent}}\text{-Fe1}$: 1.684(5). Selected bond lengths (Å) and angles ($^{\circ}$) of **148**: P1-P1': 2.1140(6); P1-P2: 2.1277(4); P1-C2: 1.7622(7); C1-Si1: 1.8889(14); P1-P1'-P2: 104.113(10); C1-P2-P1: 102.43(4); P2-C1-P2': 126.81(8); $[Cp]_{\text{cent}}\text{-Fe1}$ - $[CP_4]_{\text{cent}}$: 179.14(3); interplanar angle: 1.23(7). $[CP_4]_{\text{cent}}\text{-Fe1}$: 1.5777(4); $[Cp]_{\text{cent}}\text{-Fe1}$: 1.6924(5).

The aliphatic derivatives of 1,2,3,4-tetraphospholides **136** and **138** also react with $[CpFe(\eta^6\text{-Toluene})]PF_6$ in DME to give the corresponding 1,2,3,4-tetraphosphaferrocenes **149** and **150** in 20 % yield (**Scheme 60**).



Scheme 60. Synthesis of 5-R-1,2,3,4-tetraphosphaferrocenes **149** and **150**.

Tetraphosphaferrocenes **149** and **150** exhibit two multiplet resonances between $\delta = 90.0$ – 110.0 ppm forming an AA'MM' spin system pattern. The resonances are upfield shifted by 20 ppm compared to the trimethylsilyl derivative **148**. The ^1H NMR spectra of these compounds reveal the resonance signals between $\delta = 1.20$ – 2.00 ppm attributed to the alkyl substituents. The correct assignment of the chemical shifts to the $\text{C}_{(\text{heterocycle})}$ nuclei of the shielded 1,2,3,4-tetraphospholyl rings is problematic, due to a possible overlap with other signals. However, the ^1H - ^{13}C HMBC NMR spectrum of **149** revealed a cross-peak between the CH_3 protons and the $\text{C}_{(\text{Heterocycle})}$ at $\delta = 165.3$ ppm.

Single crystals of compounds **149** and **150** were obtained from saturated acetonitrile solutions at $T = -36$ °C. The molecular structure of **149** in the crystal and the connectivity of **150** are represented in **Figure 40**. Both crystalize in the monoclinic $\text{P2}_1/\text{n}$ space group and reveal that the 1,2,3,4-tetraphospholyl and the cyclopentadienyl rings are coordinated in an η^5 -fashion to iron. The tilting angle in **149** ($177.83(5)^\circ$) is slightly larger than in **148** ($179.14(3)^\circ$). The conformation of **149** in the crystal deviates from the perfect eclipse by $4.86(7)^\circ$. The interatomic bond lengths and angles in **149** are similar to those observed in **148**.

The cyclic voltammogram of **149** at a sweep rate 25 mV/s showed an irreversible oxidation process at $E_{\text{ox}} = 1.21$ V (vs. $\text{Fc}^*/\text{Fc}^{**}$), which is approximately 0.67 V referenced vs. the half-wave potential of ferrocene (**Figure 41**). The registered E_{ox} of **149** is shifted anodically by 0.13 V compared to the parent pentaphosphaferrocene^[180], which is due to a weaker π -acceptor character of the 1,2,3,4-tetraphospholyl ligand. A reduction process at a peak potential $E_{\text{red}} = 1.70$ V (vs. $\text{Fc}^*/\text{Fc}^{**}$) was observed upon scanning anodically. A gradual increase of the sweep rate from 25 to 250 mV/s leads to a complication of the cyclic voltammogram and indicates a chemical decomposition of the non-stabilized 1,2,3,4-tetraphosphaferrocene **149**.

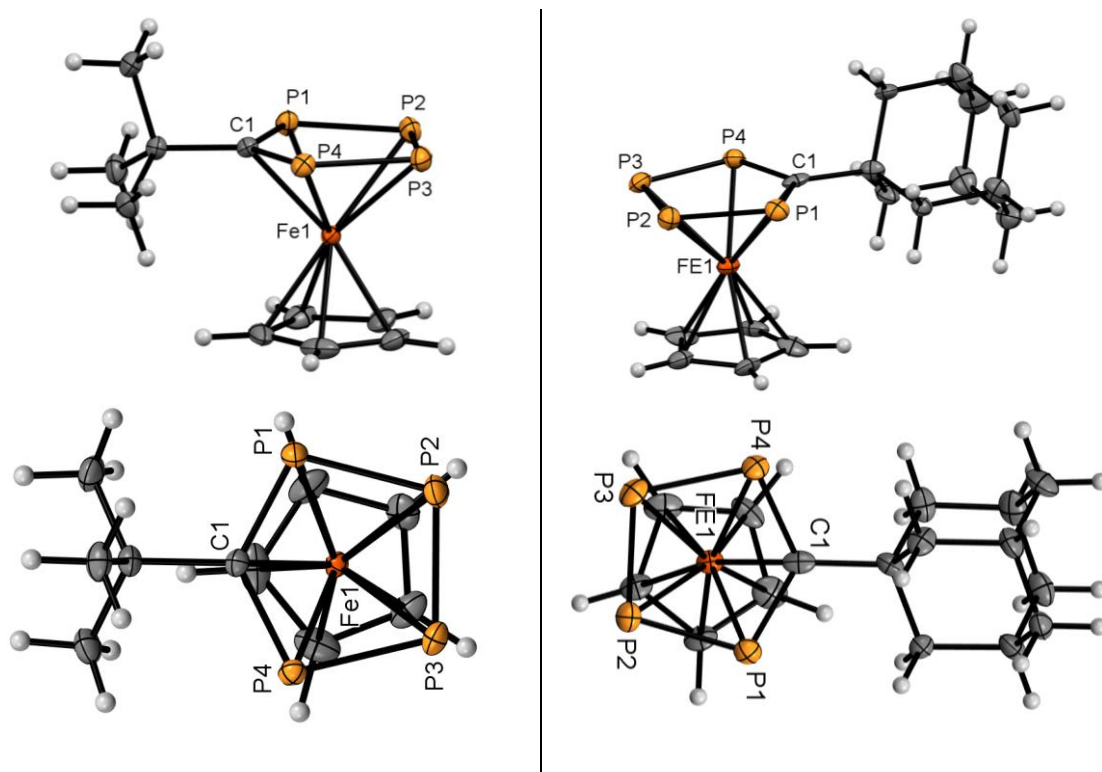


Figure 40. Molecular structure of **149** (left) and connectivity of **150** (right) in the crystal. Ellipsoids are shown at 50 % probability level. Selected bond lengths (Å) and angles (°) of **149**: P1-P2: 2.1165(5); P2-P3: 2.1236(5); P1-C1: 1.7690(12); P1-P2-P3: 104.147(19); P1-C1-P4: 125.23(7); [Cp]_{cent}-Fe1-[CP₄]_{cent}: 177.83(3); interplanar angle: 4.86(7). [CP₄]_{cent}-Fe1: 1.5790(4); [Cp]_{cent}-Fe1: 1.6868(7).

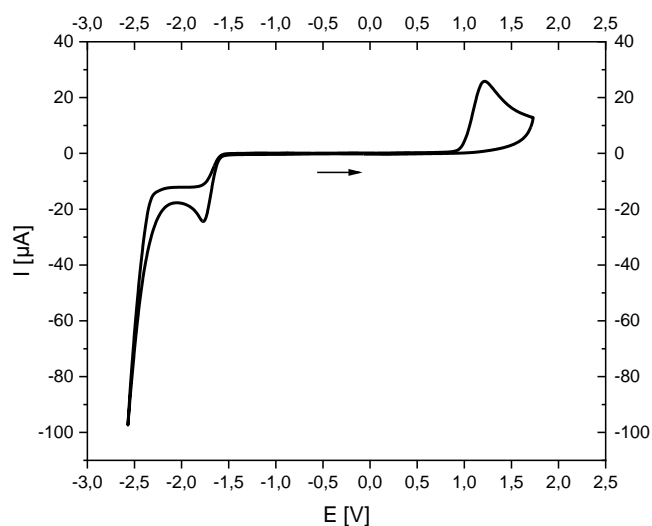
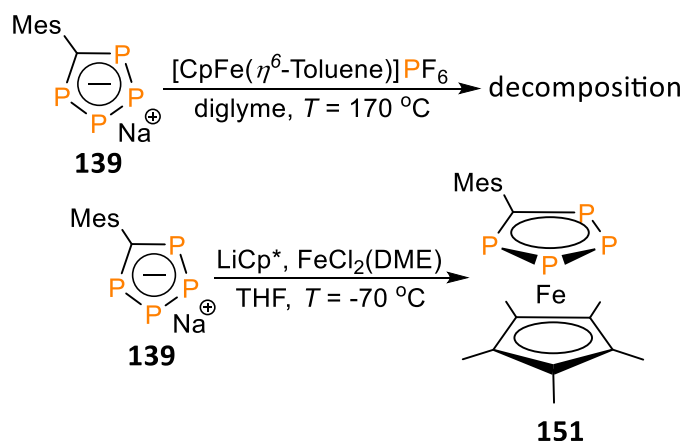


Figure 41. Cyclic voltammogram of **149** in DCM under an atmosphere of argon. Measurement conditions: $T = 20\text{ }^{\circ}\text{C}$, scan rate: 25 mV/s, conducting salt: 0.1 M [NBu₄]PF₆. Potentials were referenced versus Fc⁺/Fc⁰.

5-mesityl-1,2,3,4-tetraphospholide **139** does not react with $[\text{CpFe}(\eta^6\text{-Toluene})]\text{PF}_6$ even in refluxing diglyme, which was interpreted as a marker of the significant π -acceptor capacity. Instead, the sandwich complex **151** with an electron-rich Cp^* ring as a co-ligand was synthesized (**Scheme 61**) following the protocol for 5-aryl-1-aza-2,3,4-triphosphaferrocenes **109–110** (**Scheme 49**).



Scheme 61. Synthesis of 5-mesityl-1,2,3,4-tetraphosphaferrocene **151**.

It is noteworthy that the deep green color of the new complex is in contrast to all other species, which are red and olive-colored. The ^{31}P NMR spectrum of **151** exhibits an AA'MM' spin system with two multiplet resonances at $\delta = 86.6$ and 129.7 ppm.

Single crystals of **151** suitable for the crystallographic characterization were obtained from a saturated acetonitrile solution at $T = -36$ °C. **151** crystallizes in the monoclinic $\text{P2}_1/\text{n}$ space group and possesses two η^5 -coordinated ligands in the eclipsed conformation with an interplanar angle of $11.65(7)^\circ$ (**Figure 42**). While the interatomic bond lengths and angles in the $[\text{CP}_4]$ ring are similar to those observed in other 1,2,3,4-tetraphosphaferrocenes, the presence of the sterically demanding mesityl group seriously influences the shape of the molecular structure in general. The 1,2,3,4-tetraphospholyl ligand exhibits a large $[\text{CP}_4]_{\text{plane}}\text{-}[\text{Mes}]_{\text{plane}}$ twist angle of $58.66(3)^\circ$, which is due to a repulsion between the *ortho*- CH_3 groups of the mesityl and the lone-pairs of the P-atoms. Moreover, a constrained arrangement of the mesityl ring in the presence of the bulky $[\text{Cp}^*]$ ligand results in a larger deviation from the ideal sandwich complex with $[\text{CP}_4]_{\text{cent}}\text{-Fe-}[\text{Cp}]_{\text{cent}}$ tilting angle of $173.38(4)^\circ$ (**149**: $177.83(3)^\circ$). The carbon atom in the $[\text{CP}_4]$ ring is pushed out of the heterocycle plane and, therefore, the

C1—Fe bond length (**151**: 2.2295(14) Å) is approximately 0.12 Å elongated in comparison to other 1,2,3,4-tetraphosphaferrocenes (**148**: 2.1047(13) Å and **149**: 2.1193(12) Å).

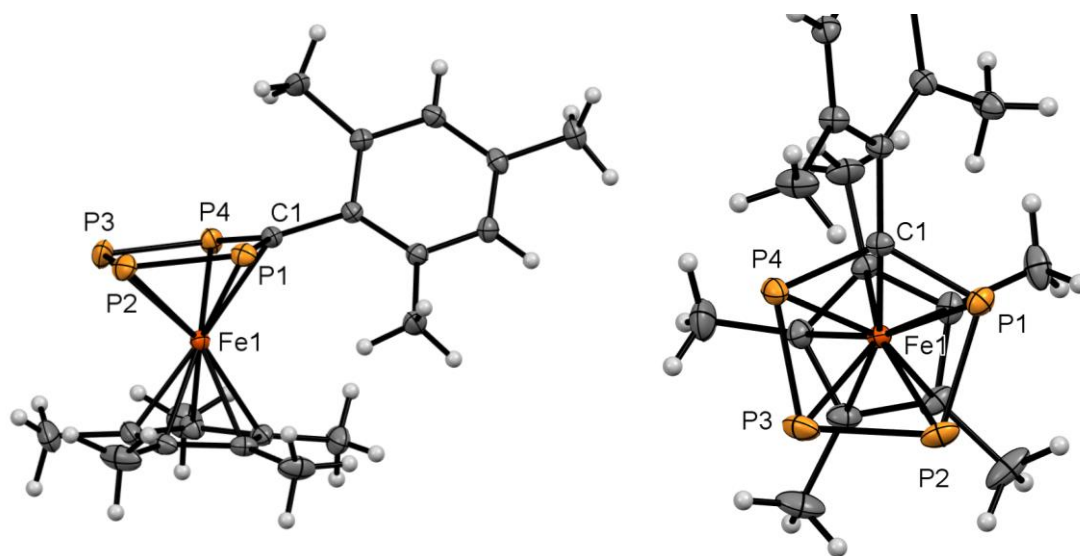


Figure 42. Molecular structure of **151** in the crystal. Ellipsoids are shown at 50 % probability level. Selected bond lengths (Å) and angles (°) of **151**: P1-P2: 2.1231(5); P2-P3: 2.1160(6) ; P1-C1: 1.7610(13); P1-P2-P3: 104.11(2); P1-C1-P4: 125.42(7); $[Cp]_{cent}-Fe1-[Cp_4]_{cent}$: 173.38(4); interplanar angle: 11.65(7). $[Cp_4]_{cent}-Fe1$: 1.6085(5); $[Cp]_{cent}-Fe1$: 1.7144(7).

The cyclic voltammogram of **151** at a sweep rate of 100 mV/s (**Figure 43**) shows an irreversible oxidation process at $E_{ox} = 0.51$ V followed by a coupled cathodic wave at a peak potential of 0.27 V. A reduction process at $E_{red} = -2.33$ V was registered upon scanning anodically. The E_{ox} value of complex **151** is 90 mV anodically shifted compared to pentaphosphaferrocene **112** (**Table 2**).^[150] This indicates that 1,2,3,4-tetraphospholyl ligand has weaker π -acceptor character compared to the pentaphospholyl ring.

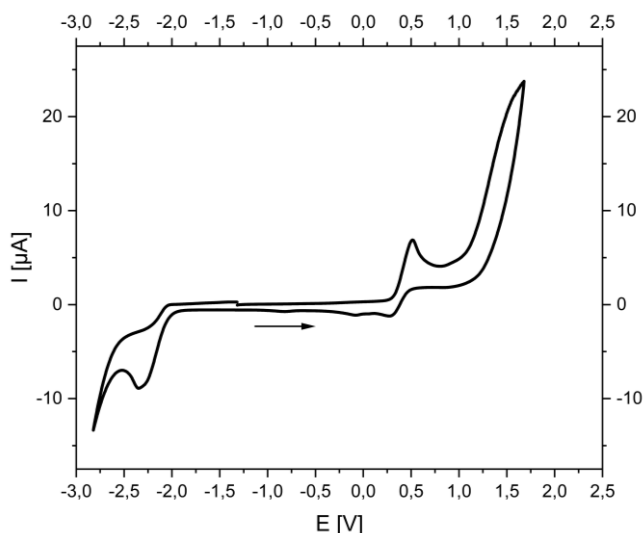
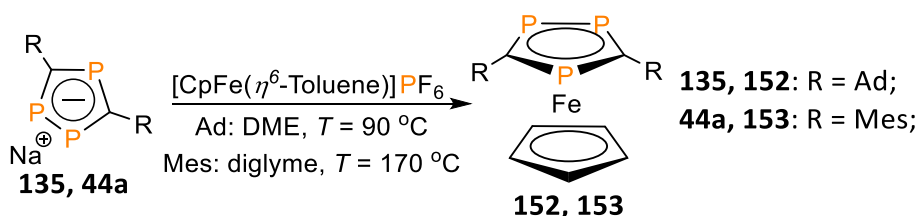


Figure 43. Cyclic voltammogram of **151** in DCM under an atmosphere of argon.

Measurement conditions: $T = 20\text{ }^{\circ}\text{C}$, scan rate: 100 mV/s (left), conducting salt: 0.1 M $[\text{NBu}_4]\text{PF}_6$. Potentials were referenced versus Fc/Fc^+ .

Sodium 3,5-adamantyl-1,2,4-triphospholide **135** reacts with $[\text{CpFe}(\eta^6\text{-Toluene})]\text{PF}_6$ in DME under reflux conditions, while the 3,5-mesityl-1,2,4-triphospholide anion **44a**, which is a stronger π -acceptor, reacts with the same iron precursor only at $T = 170\text{ }^{\circ}\text{C}$ in diglyme (**Scheme 62**).



Scheme 62. Synthesis of 3,5-R-1,2,4-triphosphaferrocenes **152** and **153**.

Similar to the free ligands, the $^{31}\text{P}\{^1\text{H}\}$ NMR spectra of 3,5-bisadamantyl-1,2,4-triphosphaferrocene **152** and 3,5-bismesityl-1,2,4-triphosphaferrocene **153** display AX_2 spin system patterns, although resonance signals are significantly upfield shifted (**152**: $\delta = 28.6$ (d) ppm, 31.1 (t) ppm, $^2J_{\text{P-P}} = 42\text{ Hz}$; **153**: $\delta = 57.3$ (t) ppm, 75.2 (d) ppm, $^2J_{\text{P-P}} = 33\text{ Hz}$). **153** reveals less shielded resonances compared to **152** and exhibits a smaller $^2J_{\text{P-P}}$ coupling constant due to the electron-withdrawing effect of the mesityl group. The $\text{C}_{(\text{heterocycle})}$ nuclei of **152** were registered by $^{13}\text{C}\{^1\text{H}\}$ NMR spectroscopy as a multiplet resonance at $\delta = 165.3$ ppm.

Single crystals of **152** and **153** were obtained from a saturated acetonitrile solution at $T = -36$ °C. The molecular structures of the new complexes in the crystals are represented in the **Figure 44**. **152** was crystallized in the monoclinic $P2_1/c$ space group and exhibits a staggered conformation with an interplanar angle of $31.30(11)^\circ$. The crystallographic analysis of **153** reveals two independent molecules in the asymmetric unit. Opposite to **152**, the iron complex **153** shows the eclipsed conformation of the two rings, with an interplanar angle of $0.19(6)^\circ$. The $[C_2P_3]$ -[Mes] twist angle of $47.78(8)^\circ$ is approximately 10° smaller than in 1,2,3,4-tetraphosphaferrocene **151**, which is considered as a result of the decreased steric repulsions in the system.

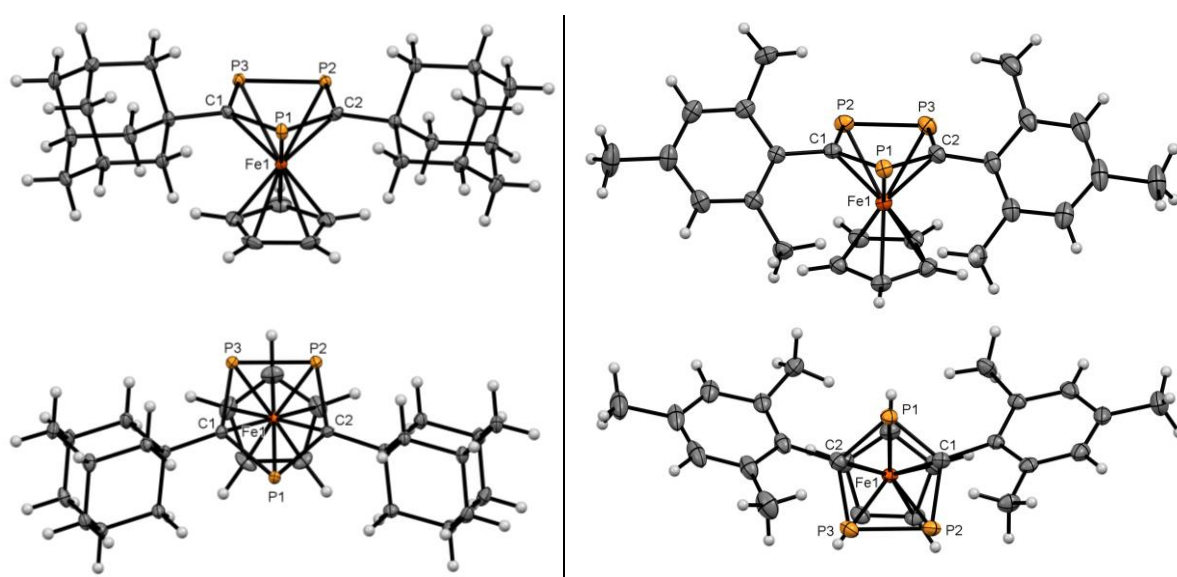


Figure 44. Molecular structure of **152** (left) and of **153** (right) in the crystal. Ellipsoids are shown at 50 % probability level. Selected bond lengths (Å) and angles ($^\circ$) of **152**: P2-P3: 2.1236(7); P1-C1: 1.7735(19); P1-C1-P2: 121.70(11); C1-P1-C2: 98.23(9); C1-P2-P3: 99.16(6); $[Cp]_{cent}-Fe1-[C_2P_3]_{cent}$: 178.86(5); interplanar angle: 31.30(11). $[C_2P_3]_{cent}-Fe1$: 1.6235(6); $[Cp]_{cent}-Fe1$: 1.6906(10). Selected bond lengths (Å) and angles ($^\circ$) of **153**: P2-P3: 2.1296(10); P1-C1: 1.761(2); P1-C1-P2: 121.67(14); C1-P1-C2: 98.91(12); C1-P2-P3: 98.86(9); $[Cp]_{cent}-Fe1-[C_2P_3]_{cent}$: 177.68(8); interplanar angle: 0.19(16). $[C_2P_3]_{cent}-Fe1$: 1.633(1); $[Cp]_{cent}-Fe1$: 1.6834(16).

The cyclic voltammogram of **153** at a sweep rate 100 mV/s (**Figure 45**) displays an irreversible oxidation process at $E_{ox} = 0.71$ V (vs. Fc/Fc^+). A reduction process at $E_{red} = 2.15$ V (vs. Fc/Fc^+) was detected upon scanning anodically. The registered E_{ox} for **153** is consistent with the data reported for 4,5-diphenyl-1,2,3-triphosphaferrocene **58** ($E_{ox} = 2.79$ V (vs. Fc/Fc^+)) (**Table 1**). A

small 80 mV anodic shift of the E_{ox} of **153** is explained as the influence of the mesityl substituents.

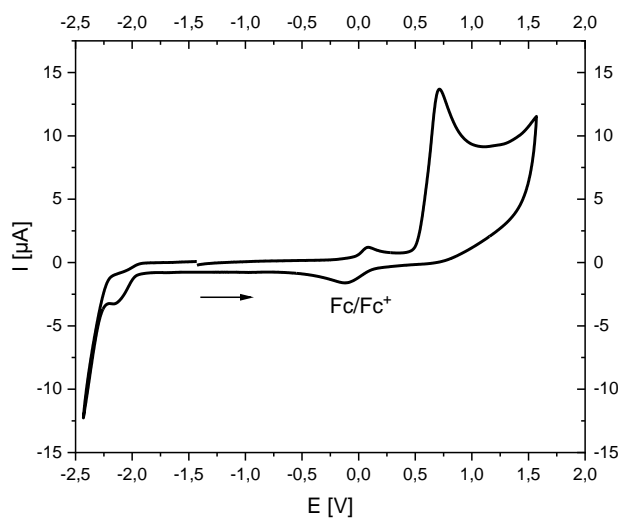
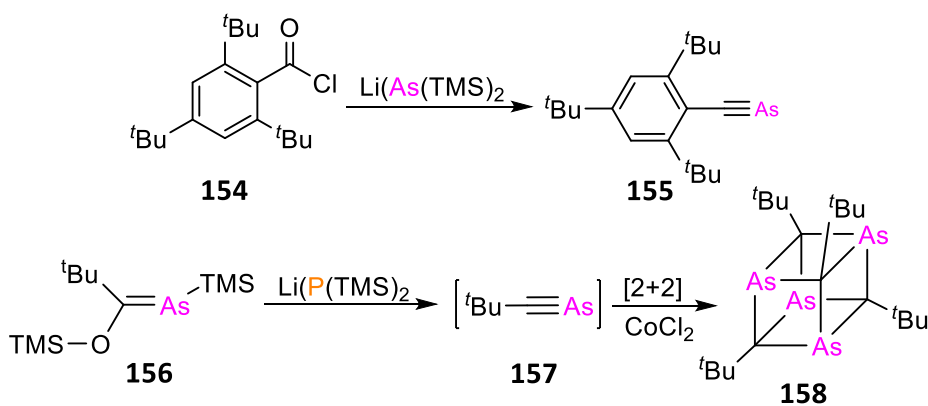


Figure 45. Cyclic voltammogram of **153** in DCM under an atmosphere of argon. Measurement conditions: $T = 20^{\circ}\text{C}$, scan rate: 100 mV/s. Conducting salt: 0.1 M [(*n*-Bu)₄N]PF₆. Potentials were referenced versus Fc/Fc⁺.

4.2.4 Arsaalkynes

Arsaalkynes represent a class of compounds containing a triple bond between the $\lambda^3\sigma^1$ -arsenic and the sp-carbon atom with the general formula of R—C≡As.^[181] Arsaalkynes possess even lower chemical stability than phosphalkynes and, therefore, the number of kinetically stabilized species is so far limited to only one representative: Mes*—C≡As **155**, which was first synthesized by *Nixon et al.* in 1994 (**Scheme 63**).^[182] In contradiction to the well-known ^tBu—C≡P **32**, the corresponding arsaalkyne **157** was only generated as a transient species in the Co-catalyzed synthesis of arsaalkynetetramer **158**, having a heterocubane structure (**Scheme 63**).^[183]

The pronounced reluctance of the arsenic atom to participate in π -bonding interactions becomes evident from the comparative analysis of electron density at the C—As bond BCP of the HC≡As and lighter congeners. It was found, that the subsequent formation of the double and triple C—As bonds does not result in a substantial increase of the electron density at the BCP between the C- and As-atoms.^[184]



Scheme 63. Synthesis of arsaalkynes.

Similar to alkynes and phosphalkynes, the HOMO of R—C≡As is represented by two degenerate π -orbitals of the triple bond. The localized orbital attributed to the lone pair of the As-atom was found to be 72 kcal/mol more stabilized with respect to the HOMO, which is due to the large 4s contribution to this orbital.^[185] Moreover, photoelectron spectroscopy and DFT calculations indicate a decreasing HOMO–LUMO gap moving from R—C≡P to R—C≡As congeners.^[186,185]

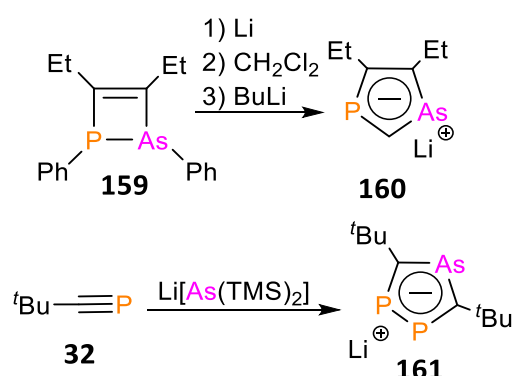
The general trends in the reactivity of R—C≡As derivatives are reminiscent of phosphalkynes. Müller *et al.* demonstrated that Mes*—C≡As **155** undergoes [3+2] cycloaddition reaction with organic azides^[187]. Additionally, **155** forms complexes with the η^2 -coordinated C≡As triple bond as showed by Nixon *et al.*^[182]

4.2.5 Arsaphospholides

Arsaphospholide anions form the class of 6π electron aromatic P,As-heterocycles with the general formula of [cyclo-(CR)_{5-x-y}As_yP_x][−], which are considered as isolobal analogs of [Cp][−].^[188,189] Although these species show a decreased stability compared to the P- and mixed P,N-congeners of [Cp][−], [cyclo-(CR)_{5-x-y}As_yP_x][−] also features aromaticity.^[190] This property was confirmed experimentally by building sandwich compounds with an η^5 -coordination of the arsaphospholyl ligands.^[191,192] The reluctance of arsenic to form π -bonds with carbon leads to a pronounced difference in stability between species containing only As—C delocalized bonds and those which are diversified by As—P and As—As delocalized bonds.^[193]

4,5-diethyl-1,3-arsaphospholide **160** was synthesized by Mathey *et al.* starting from 1,2-arsaphosphete **159** in a multistep ring expansion reaction (**Scheme 64**).^[194] 3,5-bis(*tert*-butyl)-

1-arsa-2,4-diphospholide **161** was synthesized by *Nixon et al.* via a formal [2+2+1] cycloaddition reactions between $t\text{Bu}-\text{C}\equiv\text{P}$ **32** and $\text{Li}[\text{As}(\text{TMS})_2]$ (**Scheme 64**).^[191]

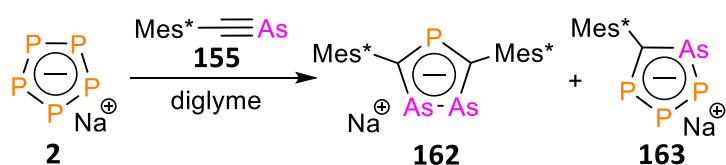


Scheme 64. Literature examples for the synthesis of arsaphospholides **160** and **161**.

Taking into account a certain similarity between $\text{R}-\text{C}\equiv\text{As}$ and $\text{R}-\text{C}\equiv\text{P}$ derivatives and the results of the previous studies it was anticipated that the reaction between $\text{Na}[\text{cyclo-P}_5]$ and $\text{Mes}^*-\text{C}\equiv\text{As}$ **155** may give rise to novel P,As-heterocycles by analogy with phosphalkynes (**Scheme 54**, **Scheme 55**): 3,5-bis(2,4,6-*tert*-butylphenyl)-1,2-diarsa-4-phospholide **162** or/and 5-(2,4,6-*tert*-butylphenyl)-1-arsa-2,3,4-triphospholide **163** anions (**Scheme 65**). Among them, the 5-(2,4,6-*tert*-butylphenyl)-1-arsa-2,3,4-triphospholide anion **163** is supposed to show a higher thermodynamic stability since it has only one C—As delocalized bond. However, the steric demand of $\text{Mes}^*-\text{C}\equiv\text{As}$ **155**, as in $\text{Mes}^*-\text{C}\equiv\text{P}$ **127**, must also be considered, since the $\text{C}\equiv\text{As}$ triple bond in this arsaalkyne (1.657(7) Å) is only 0.1 Å longer than in the corresponding phosphalkyne (1.545(3) Å).^[195]

4.2.6 Test reaction between $\text{Na}[\text{cyclo-P}_5]$ and supermesitylarsaalkyne

One equivalent of $\text{Mes}^*-\text{C}\equiv\text{As}$ was added to a diglyme solution of $\text{Na}[\text{cyclo-P}_5]$. After a few minutes, a rapid color change from orange to dark red along with an excessive precipitation of the green-grey solid (**Scheme 65**) was observed.



Scheme 65. Proposed products of the reaction between $\text{Na}[\text{cyclo-P}_5]$ and $\text{Mes}^*-\text{C}\equiv\text{As}$.

However, the $^{31}\text{P}\{^1\text{H}\}$ NMR spectrum taken directly from the reaction mixture did not reveal any resonances apart from a singlet at $\delta = 468.7$ ppm, that corresponds to $[\text{cyclo-P}_5]^-$. The reaction mixture was stirred for overnight. After 18 hours, the $^{31}\text{P}\{^1\text{H}\}$ NMR spectrum revealed the formation of several multiplet resonances in the range between $\delta = 280.0$ – 420.0 ppm (**Figure 46**). After 48 hours of stirring reaction mixture at room temperature, these new resonance signals reached a maximum intensity at the same time as the disappearance of the singlet at $\delta = 468.7$ ppm, indicating the completeness of the reaction (**Figure 46**).

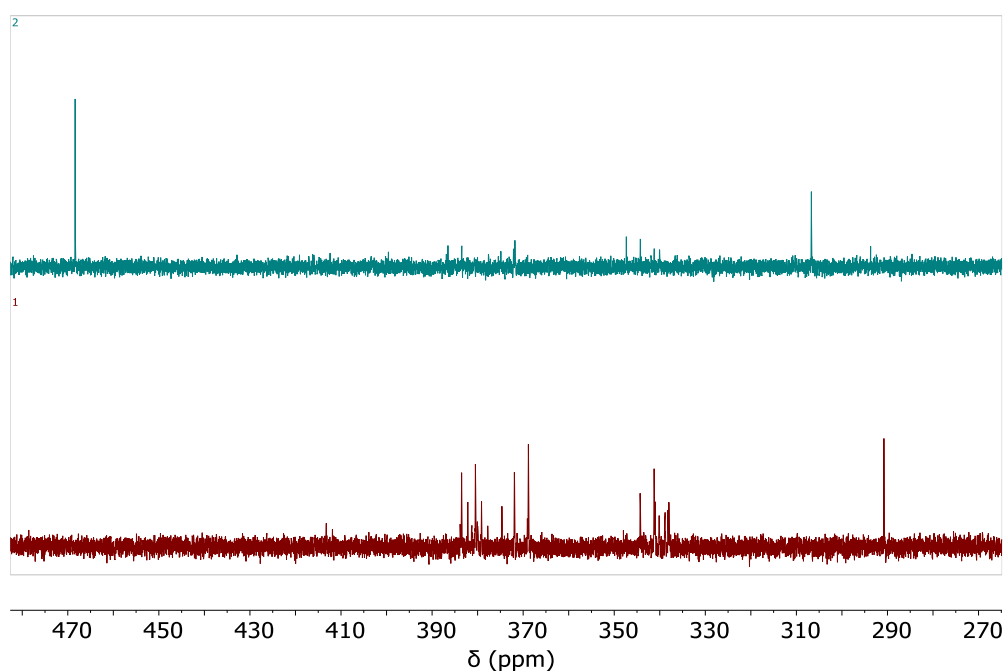


Figure 46. $^{31}\text{P}\{^1\text{H}\}$ NMR spectra of the reaction mixture containing $\text{Na}[\text{cyclo-P}_5]$ and $\text{Mes}^*-\text{C}\equiv\text{As}$: after 18 hours (top, blue); after 48 hours (bottom, red).

A significant downfield chemical shifts of the new resonances indicate that novel P,As-congeners of cyclopentadienyl were probably formed in this reaction (**Scheme 65**). A comparative analysis of the chemical shifts reported for other derivatives^[191] reveals some interesting features (**Table 5**). A singlet resonance at $\delta = 290.8$ ppm might be attributed to the 3,5-bis(2,4,6-*tert*-butylphenyl)-1,2-diarsa-4-phospholide anion **162**, which is supposed to be slightly downfield shifted compared to the literature known 1,2-diphospha-4-arsolide anion **161**.^[191] The area between $\delta = 340.0$ – 380.0 ppm consists of several multiplet resonances, among them, three relatively intense signals might be attributed to **163**, by analogy to 1,2,3,4- $[\text{cyclo}-(\text{CR})\text{P}_4]$ **136** and $[\text{cyclo}-(\text{CR})\text{NP}_3]^-$ **109**. Unfortunately, the low yield of

the reaction combined with the instability of the new species impede the proper isolation and characterization of new products.

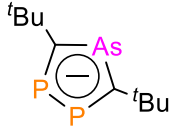
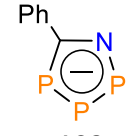
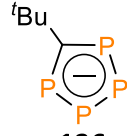
Compound	 161	 103	 136
³¹ P NMR chemical shifts	δ(ppm) = 246.0 (s) ^[191]	δ(ppm) = 221.7 (dd), 325.7 (dd), 378.0 (br. d)	δ(ppm) = 347.6 (m), 358.6 (m)

Table 5. A comparative table of ³¹P NMR chemical shifts for selected compounds.

4.3 Conclusions

It was demonstrated that R—C≡P (R = TMS, ^tBu, Ad, Tripp) reacts with Na[*cyclo*-P₅] to give a mixture of sodium 3,5-R-1,2,4-triphospholides **34a**, **35a**, **134**, **135** and 5-R-1,2,3,4-tetraphospholides **132a**, **136**, **137**, **138** (Scheme 54, Scheme 55). These syntheses nicely show that [*cyclo*-P₅][−] can act as a formal source of [P₃][−] and [P][−] units for the construction of new heterocycles. The ratio between two products is in favor of 3,5-R-1,2,4-triphospholides and substantially shifts towards 5-R-1,2,3,4-tetraphospholides when Ad—C≡P **126** and Tripp—C≡P **117** are used (Table 4). While Mes*—C≡P **127** does not interact with Na[*cyclo*-P₅] due to the sterically hindered triple bond, the less bulky Mes—C≡P **125** undergoes a formal [2+2+1] cycloaddition to give sodium 3,5-bismesityl-1,2,4-triphospholide **44a** exclusively (Scheme 53).

The study displays only a partial compatibility with the concept of the 1,2,3,4-tetraphospholide anion formation in the one-*pot* reaction between acid chlorides, P(TMS)₃ and CsF, which was explained by *lonkin et al.* as the interaction between *in situ* generated Cs[*cyclo*-P₅] and R—C≡P (Scheme 52).

Interestingly, It was found that acid chlorides with the electron-donating substituents (R = ^tBu, Ad, Mes) react with sodium polyphosphides to give the desired 5-R-1,2,3,4-tetraphospholide anions **136**, **138**, **139** (Scheme 56). The procedure was further modified to

a *one-pot* method, when P₄, Na and acid chloride are loaded to the Schlenk flask with diglyme and stirred under reflux conditions for several hours.

All 1,2,4-tri- and 1,2,3,4-tetraphospholide derivatives interact with iron (II) precursors affording 1,2,4-tri- and 1,2,3,4-tetraphosphaferrocenes in the good yields (**Scheme 59**, **Scheme 60**, **Scheme 62**). All new complexes were characterized by the SC-XRD analysis (**Figure 39**, **Figure 40**, **Figure 42**, **Figure 44**). The selected species were additionally characterized by cyclic voltammetry (**Figure 41**, **Figure 45**).

Monitoring the reaction mixture containing Mes*—C≡As **155** and Na[*cyclo*-P₅] (**Scheme 65**) by ³¹P{¹H} NMR spectroscopy (**Figure 46**) revealed that, the new phosphorus-containing products were formed. Taking into account the reported literature data, it was assumed that the novel P,As-heterocycles **162** and **163** were synthesized (**Scheme 65**).

4.4 Experimental part

4.4.1 General remarks

All reactions were performed under an argon atmosphere in oven-dried glassware using modified Schlenk techniques or in an MBraun glovebox unless otherwise stated. All common solvents, 2,2-dimethylpropanoyl chloride, magnesium chips, (chloromethyl)trimethylsilane, PCl₃, silver triflate, DABCO, 1-adamantanecarbonyl chloride, 2,4,6-trimethylbenzyl bromide, zinc powder, 2,4,6-tri(tert-butyl)benzoyl chloride, 3,3-dimethylbutyryl chloride and ferrocenecarboxylic acid were commercially available. P(TMS)₃,^[196] Tripp—C≡P^[171] and Li[As(TMS)₂]^[197] were available in the laboratory and initially were synthesized according to the literature procedures. The synthesis of other chemicals is described below. Commercially available chemicals were used without further purification. All dry and deoxygenated solvents were prepared using standard techniques or were obtained from a MBraun solvent purification system. The ¹H, ³¹P and ³¹P{¹H} NMR spectra were recorded on a JEOL ECS400 spectrometer (³¹P: 162 MHz, ¹H: 400 MHz). Some ³¹P{¹H} NMR spectra were recorded on a Bruker AVANCE III 700 spectrometer (242 MHz). ¹³C{¹H} spectra were recorded on a Bruker AVANCE III 700 spectrometer (176 MHz). All chemical shifts are reported relative to the residual resonance in the deuterated solvents. The ESI-TOF (Electron-Spray ionization Time-of-flight) Mass spectrometry measurements were performed on an Agilent 6230 ESI-TOF.

Cyclic voltammograms were measured at room temperature with the substance (0.005 mmol) in DCM (5 mL) and 0.1 M TBAPF₆ added as an electrolyte at 25–250 mV/s under an argon atmosphere. Ferrocene or decamethylferrocene were used as the internal standard. An Autolab PGSTAT302N potentiostat by Metrohm was used in combination with an in-house made, gas-tight glass cell equipped with a glassy carbon disk working electrode by Metrohm, a platinum wire as counter electrode and a leak-free Ag/AgCl reference electrode LF-2 by Innovative Instruments, Inc. Low-temperature diffraction data were collected on Bruker-AXS X8 Kappa Duo diffractometers with *l* μ S micro-sources, performing ϕ - and ω -scans. For the structures of compounds **147–152**, data were collected using a Photon 2 CPAD detector with Mo K_{α} radiation ($\lambda = 0.71073 \text{ \AA}$). The structures were solved by dual-space methods using SHELXT^[113] and refined against F^2 on all data by full-matrix least squares with SHELXL-2017^[114] following established refinement strategies.^[115] The program Olex2^[116] was also used to aid in the refinement of the structures of compounds. All non-hydrogen atoms were refined anisotropically. All hydrogen atoms were included into the model at geometrically calculated positions and refined using a riding model. The isotropic displacement parameters of all hydrogen atoms were fixed to 1.2 times the U-value of the atoms they are linked to (1.5 times for methyl groups). DFT Calculations were carried out with the ORCA 5.0.3 program suite.^[117] Initial molecular structures were created in the program Avogadro^[118] or were based on crystal structures, if available. Geometry optimizations were then performed with the PBEh-3c method developed by Grimme and co-workers.^[119] Standardized convergence criteria were used for the geometry optimization (OPT). To confirm the nature of stationary points found by geometry optimizations analytical frequency calculations were carried out. The absence of imaginary vibrational frequencies indicated that the optimized structure is a local minimum. Final single point calculations on the optimized structures were conducted with the B3LYP^[120] functional with def2-TZVP^[121] basis set and def2/J^[122] auxiliary basis set. Additionally, for all calculations the Dispersion Correction (D3)^[123] was used. For SCF-calculations an additional “tight” correlation was included (“TIGHTSCF”). Solvent effects were taken into account with the Conductor-like-Polarizable-Continuum-Modell (CPCM).^[124] Intrinsic bond orbital (IBO) analysis^[125] was carried out with the IBO module implemented in the ORCA program suite. IBOs were visualized via the freely available IBOView v20150427.^[126]

4.4.2 Synthesis of starting materials

Tert-butylphosphaalkyne (**32**)



2,2-dimethylpropanoyl chloride (pivaloyl chloride) (37.2 g, 309 mmol, 1.1 eq.) in pentane (100 mL) was added dropwise to a solution tris(trimethylsilyl)phosphane (69.9 g, 280 mmol, 1 eq.) in 200 ml pentane at room temperature. The reaction mixture was stirred for 24 hours. Later, the solvent was removed under vacuum to give yellow oil of (2,2-dimethyl-1-(trimethylsiloxy)propylidene)trimethylsilylphosphine **121**. Yield: 65 g, 278 mmol, 90 %.

A three-neck Schlenk flask with 3g of NaOH was equipped with dropping funnel and assembled with two consecutive traps. One trap was cooled down to $T = -80\text{ }^{\circ}\text{C}$ and the second one cooled with liquid nitrogen. (2,2-dimethyl-1-(trimethylsiloxy)propylidene)trimethylsilylphosphine (5 g, 19 mmol, 1 eq.) was added dropwise on to a powder of NaOH. **32** was collected in the first cooling trap as a colorless oil. Yield: 1.34 g, 14 mmol, 75 %.

$^{31}\text{P}\{^1\text{H}\}$ NMR (25 °C, DCM- d_2) δ (ppm) = -66.5;

^1H NMR (25 °C, DCM- d_2) δ (ppm) = 1.52 (s, 9H, ^tBu).

Trimethylsilylphosphaalkyne (**33**)



Magnesium (11 g, 460 mmol, 1.3 eq.) was added to a 500 ml Schlenk flask with stirring bar. Magnesium was activated mechanically overnight and 200 ml of Et₂O was added the next day. (Chloromethyl)trimethylsilane (50 ml, 254 mmol) was dissolved in 100 ml of dry Et₂O and added dropwise to a flask with magnesium. After the addition was complete, the reaction mixture was stirred at room temperature for 2 hours and filtrated *via* canula equipped with paper filter. Ether solution was cooled down to $T = -40\text{ }^{\circ}\text{C}$ and PCl₃ solution (16 ml, 1.4 eq.) in 150 ml of Et₂O was added dropwise. After the addition was complete, the reaction mixture was allowed to warm up to a room temperature and stirred for 1 hour. Later, 100 ml of a 2M HCl solution in ether was added to the reaction mixture. After 12 hours, the solution was filtrated over a 3 cm layer of dry silica. The solvent was removed under high vacuum to give dichloro-(trimethylsilylmethyl)phosphane as a pale yellow oil. Dichloro-(trimethylsilylmethyl)phosphane (7 g, 37 mmol, 1 eq.) was dissolved in 100 ml of toluene. Then, silver triflate (14.3 g, 85 mmol, 2.3 eq.) and, 10 minutes later, DABCO (9 g, 85 mmol,

2.3 eq.) was added to a toluene solution. The reaction mixture was stirred for 1 hour and then trap-to-trap condensation was performed. **32** was obtained as a colorless solution. Yield: 23 %, conc.: 8.6 mmol/L (based on the quantitative ^{31}P NMR spectrum with PPh_3 as the internal standard).

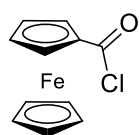
$^{31}\text{P}\{^1\text{H}\}$ NMR (25 °C, $\text{DCM-}d_2$) δ (ppm) = 97.4.

Lithium bis(trimethylsilyl)phosphide

$\text{Li}[\text{P}(\text{TMS})_2]$ Tris(trimethylsilyl)phosphine $\text{P}(\text{TMS})_3$ (15.5 g, 61.9 mmol, 1 eq.) in THF (75 mL) was cooled down to 0 °C. Then, MeLi (38.7 mL, 1.36 g, 61.9 mmol, 1 eq.) in Et_2O was added dropwise. The reaction mixture was warmed up slowly overnight to room temperature and all volatile substances were removed under reduced pressure. After drying under vacuum, lithium bis(trimethylsilyl)phosphide was obtained as a white crystalline powder. Yield: 9.69 g, 52 mmol, 85 %

$^{31}\text{P}\{^1\text{H}\}$ NMR (25 °C, $\text{THF-}d_8$) δ (ppm) = -305.2.

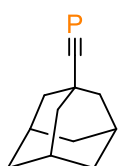
Ferrocenoyl chloride



To ferrocenecarboxylic acid (5 g, 22 mmol, 1 eq.) in 50 mL of DCM thionyl chloride (5 g, 44 mmol, 2 eq.) was added dropwise at 0 °C. The reaction was allowed to warm up to room temperature and stirred for 24 hours. Then, all volatile substances were removed under reduced pressure to afford the desired product in a quantitative yield.

^1H NMR (25 °C, $\text{DCM-}d_2$) δ (ppm) = 4.1 (s, 5H, CH), 4.5 (m, 2H, CH), 4.9 (m, 2H, CH).

Adamantylphosphaalkyne (126)



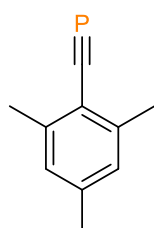
1-Adamantanecarbonyl chloride (1 g, 5 mmol, 1 eq.) was dissolved in 50 ml of pentane. The solution was cooled down to $T = -40$ °C and then pentane solution (50 ml) of $\text{LiP}(\text{TMS})_2$ (1 eq.) was added dropwise. After 2 hours reaction mixture was allowed to warm up to room temperature. The solution was filtrated *via* a canula. The solvent was removed under high vacuum. The residue was dissolved in 10 ml of DME. Then, 10 mg of NaOH (catalytic amount) was added. The reaction mixture was allowed to stir overnight for 12 h at room temperature. Schlenk flask with crude product was

assembled with two cooling traps: the first one was cooled down to $T = 0\text{ }^{\circ}\text{C}$, the second trap was cooled down to $T = -80\text{ }^{\circ}\text{C}$. Adamantylphosphaalkyne was collected in the first trap as a white solid. Yield: 300 mg, 1.7 mmol, 47 %.

$^{31}\text{P}\{^1\text{H}\}$ NMR (25 $^{\circ}\text{C}$, benzene- d_6) δ (ppm) = -67.2;

^1H NMR (25 $^{\circ}\text{C}$, benzene- d_6) δ (ppm) = 1.43–2.15 (m, 15H, Ad).

Mesitylphosphaalkyne (125)



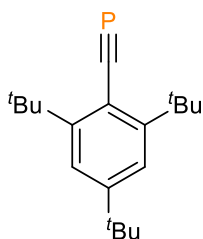
Zinc powder (9.85 g, 151 mmol, 2.0 eq) and 80 ml DME were placed in to the 250 ml Schlenk flask. The resulting suspension of zinc was stirred at room temperature in an ultrasonic bath for 4 hours. 2,4,6-trimethylbenzyl chloride (12.7 g, 75.3 mmol, 1.0 eq) was dissolved in 15 ml dry DME and dropwise added at $T = 10\text{--}12\text{ }^{\circ}\text{C}$ to the suspension and stirred for 2 hours. The reaction mixture was filtrated through a celite yielding (2,4,6-Trimethylbenzyl)zinc(II) chloride as a colorless solution. (2,4,6-Trimethylbenzyl)zinc(II) chloride (1 eq.) was added dropwise to a cold ($T = 0\text{ }^{\circ}\text{C}$) solution of PCl_3 (3.66 g, 42 mmol, 2 eq.) in 50 ml of DME. Resulting reaction mixture was allowed to warm up to a room temperature and stirred for 12 hours. Later, the solvent was removed under high vacuum and the residue was dissolved in pentane. The pentane solution was filtered through a silica pad. Then, the solvent was removed under high vacuum to give dichloro(2,4,6-trimethylbenzyl) phosphane as a pale yellow oil (2 g, 15 mmol, 40 % yield).

The freshly prepared dichloro(2,4,6-trimethylbenzyl)phosphane was dissolved in 150 ml of toluene. Then, silver triflate (8.49 g, 33.0 mmol, 2.2 eq) was added to the solution, followed by DABCO (3.71 g, 33.0 mmol, 2.2 eq) 10 minutes later. The reaction mixture stirred for an hour and filtrated through celite. After the toluene was removed under high vacuum, the residue was dissolved in pentane and purified by column chromatography. The product was obtained as a colorless fraction. After removal of the solvent mesitylphosphaalkyne was obtained as a colorless oil. Yield: 600 mg, 3.7 mmol, 28 %.

$^{31}\text{P}\{^1\text{H}\}$ NMR (25 $^{\circ}\text{C}$, $\text{DCM-}d_2$) δ (ppm) = 1.5

^1H NMR (25 $^{\circ}\text{C}$, $\text{DCM-}d_2$) δ (ppm) = 2.28 (s, 3H, CH_3), 2.47 (s, 6H, CH_3), 6.88 (s, 2H, CH).

Supermesitylphosphaalkyne (127)



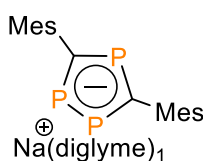
2,4,6-tri-tert-butylbenzoyl chloride (1.87 g, 6.1 mmol), Li(THF)₂P(TMS)₂ (2.03 g, 6.1 mmol, 1 eq.) and THF (50 mL) were mixed in the Schlenk flask and stirred for 24 h at room temperature. The solvent was removed at low pressure and the product was extracted from the crude solid residue with pentane. The resulting solution was purified by column chromatography to give supermesitylphosphaalkyne as a colourless crystals. Yield: 160 mg, 0.6 mmol, 10 %.

³¹P{¹H} NMR (25 °C, DCM-*d*₂) δ (ppm) = 34.7;

¹H NMR (25 °C, DCM-*d*₂) δ (ppm) = 1.24 (s, 9H, ^tBu), 1.73 (s, 18H, ^tBu), 7.43 (s, 2H, CH).

4.4.3 Synthesis of sodium 1,2,4-triphospholides and 1,2,3,4-tetraphospholides

Sodium 3,5-mesityl-1,2,4-triphospholide (44a)



Mes—C≡P **125** (400 mg, 2.5 mmol, 2 eq.) was added to the diglyme solution of Na[*cyclo*-P₅] (1.2 mmol in 30 mL). The reaction mixture stirred for 4 hours, followed by filtration through a canula equipped with microfiber glass filter. The solvent was removed under reduced pressure and the resulting oily residue was washed several times with a THF:pentane mixture (5 mL:40 mL) to afford a dark red oil of **44a**. The composition of the cation solvate shell was calculated on the basis of the ¹H NMR spectroscopy. Yield: 116 mg, 0.2 mmol, 19 %.

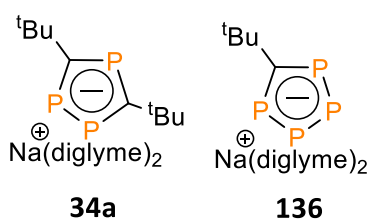
³¹P{¹H} NMR (25 °C, THF-*d*₈) δ (ppm) = 252.6 (t, ²J_{P-P} = 37 Hz, 1P), 263.2 (d, ²J_{P-P} = 37 Hz, 2P);

¹H NMR (25 °C, THF-*d*₈) δ (ppm) = 2.14 (s, 12H, CH₃), 2.19 (s, 6H, CH₃), 3.24 (s, 12H, CH₃), 3.40 (m, 4H, CH₂), 3.48 (m, 4H, CH₂), 6.72 (s, 4H, *m*-CH);

¹³C{¹H} NMR (25 °C, THF-*d*₈) δ (ppm) = 21.3 (s, CH₃), 22.9 (s, CH₃), 59.2 (s, CH₃), 70.9 (s, CH₂), 72.6 (s, CH₂), 127.8 (s, *m*-CH), 132.8 (s, *p*-C), 137.4 (*o*-C), 145.24 (m, *ipso*-C), 190.6 (m, C_{Heterocycle});

ESI- (*m/z*): 355.0923 (calc. 355.0939) [R₂C₂P₃⁻].

Synthesis of sodium 3,5-bis(*tert*-butyl)-1,2,4-triphospholide (34a**) and sodium 5-*tert*-butyl-1,2,3,4-tetraphospholide (**136**)**



*t*Bu—C≡P **32** (240 mg, 2.5 mmol, 2 eq.) was added to the diglyme solution of Na[*cyclo*-P₅] (1.2 mmol in 30 mL). The reaction was stirred for 4 hours and then it was filtered through a cannula equipped with a microfiber glass filter. The solvent was removed under reduced pressure and the resulting oily residue was washed several times with a THF:pentane mixture (5 mL:40 mL) to afford a dark red oil of **34a** and **136** in a 6:1 ratio (based on the quantitative ³¹P NMR spectrum). The composition of the cation solvate shell of **34a** was calculated on the basis of the ¹H NMR spectroscopy. Yield: 111 mg, 0.2 mmol, 18 % (combined).

34a: ³¹P{¹H} NMR (25 °C, THF-*d*₈) δ (ppm) = 237.4 (d, ²J_{P-P} = 48 Hz, 2P), 252.3 (t, ²J_{P-P} = 48 Hz, 2P);

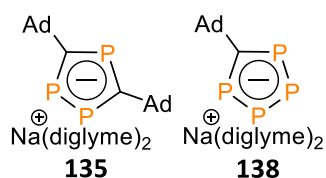
¹H (25°C, THF-*d*₈) δ (ppm) = 1.52 (s, 18H, CH₃), 3.24 (s, 12H, CH₃_{diglyme}), 3.41 (m, 8H, CH₂_{diglyme}), 3.49 (m, 8H, CH₂_{diglyme});

¹³C{¹H} NMR (25 °C, THF-*d*₈) δ (ppm) = 38.2 (m, CH₃), 39.6 (t, C), 59.2 (s, CH₃_{diglyme}), 71.0 (s, CH₂_{diglyme}), 72.7 (s, CH₂_{diglyme}), 206.8 (m, C_{Heterocycle});

ESI- (m/z): 231.0581 (calc. 231.0627) [R₂C₂P₃]⁻.

136: Full characterisation is given in the paragraph 4.4.4.

Sodium 3,5-bisadamantyl-1,2,4-triphospholide (135**) and sodium 5-adamantyl-1,2,3,4-tetraphospholide (**138**)**



135 and **138** were synthesized using Ad—C≡P **126** according to the procedure described for the synthesis of **34a** and **136**. The standard work up procedure afforded the dark red oil of **135** and **138** in a 3:1 ratio (based on the quantitative ³¹P NMR spectrum).

The composition of the cation solvate shell of **135** was calculated on the basis of the ¹H NMR spectroscopy. Yield: 150 mg, 0.2 mmol, 19 % (combined).

135: $^{31}\text{P}\{^1\text{H}\}$ NMR (25 °C, THF-*d*₈) δ (ppm) = 230.7 (d, $^2J_{\text{P-P}} = 48$ Hz, 2P), 246.9 (t, $^2J_{\text{P-P}} = 48$ Hz, 2P);

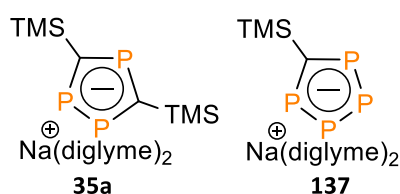
^1H NMR (25 °C, THF-*d*₈) δ (ppm) = 1.73 (m, 6H, Ad), 1.98 (s, 3H, Ad), 2.25 (d, $^4J_{\text{H-P}} = 2$ Hz, 6H, Ad); 3.27 (s, 12H, CH₃_{diglyme}), 3.44 (m, 8H, CH₂_{diglyme}), 3.52 (m, 8H, CH₂_{diglyme});

$^{13}\text{C}\{^1\text{H}\}$ NMR (25 °C, THF-*d*₈) δ (ppm) = 31.6 (s, Ad), 38.5 (s, Ad), 39.6 (t, C), 51.0 (m, $^3J_{\text{C-P}} = 2$ Hz, Ad), 52.4 (t, $^2J_{\text{C-P}} = 12$ Hz, Ad), 59.3 (s, CH₃_{diglyme}), 71.2 (s, CH₂_{diglyme}), 72.8 (s, CH₂_{diglyme}), 207.7 (m, C_{Heterocycle});

ESI- (m/z): 387.1582 (calc. 387.1566) [R₂C₂P₃]⁻.

138: Full characterisation is given in the paragraph 4.4.4.

Sodium 3,5-bis(trimethylsilyl)-1,2,4-triphospholide (**35a**) and sodium 5-trimethylsilyl-1,2,3,4-tetraphospholide (**137**)



35a and **137** were synthesized using TMS—C≡P **33** according to the procedure described for the synthesis of **34a** and **136**. The standard work up procedure afforded dark the red oil of **35a** and **137** in a 7:1 ratio (based on the quantitative ^{31}P NMR spectrum). The composition of the cation solvate shell of **35a** was calculated on the basis of the ^1H NMR spectroscopy. Yield: 65 mg, 0.1 mmol, 10 % (combined).

35a: $^{31}\text{P}\{^1\text{H}\}$ NMR (25 °C, THF-*d*₈) δ (ppm) = 315.3 (t, $^2J_{\text{P-P}} = 32$ Hz, 1P), 324.9 (d, $^2J_{\text{P-P}} = 32$ Hz, 2P);

^1H NMR (25 °C, THF-*d*₈) δ (ppm) = 0.35 (s, 18H, TMS), 3.31 (s, 12H, CH₃_{diglyme}), 3.46 (m, 8H, CH₂_{diglyme}), 3.54 (m, 8H, CH₂_{diglyme});

$^{13}\text{C}\{^1\text{H}\}$ NMR (25 °C, THF-*d*₈) δ (ppm) = 4.7 (s, TMS), 59.2 (s, CH₃_{diglyme}), 71.1 (s, CH₂_{diglyme}), 72.7 (s, CH₂_{diglyme}), 182.5 (m, C_{Heterocycle});

ESI- (m/z): 263.0151 (calc. 263.0165) [R₂C₂P₃]⁻;

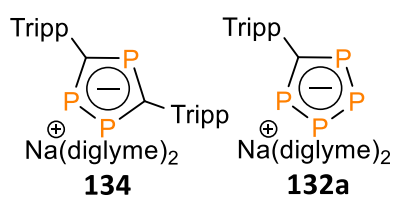
137: $^{31}\text{P}\{^1\text{H}\}$ NMR (25 °C, THF-*d*₈) δ (ppm) = (AA'MM' spin system) 373.3 (m, $^1J_{\text{P-P}} = 491$ Hz, $^1J_{\text{P-P}} = 481$, $^2J_{\text{P-P}} = 8$ Hz), P_A/P_{A'}) 399.6 (m, $^1J_{\text{P-P}} = 481$, $^2J_{\text{P-P}} = 44$ Hz, $^2J_{\text{P-P}} = 8$ Hz, P_M/P_{M'});

^1H (25 °C, THF-*d*₈) δ (ppm) = 0.45 (s, 9H, TMS), 3.31 (s, 12H, CH₃_{diglyme}), 3.46 (m, 8H, CH₂_{diglyme}), 3.54 (m, 8H, CH₂_{diglyme});

$^{13}\text{C}\{^1\text{H}\}$ NMR (25 °C, THF-*d*₈) δ (ppm) = 5.29 (s, TMS), 59.2 (s, CH₃_{diglyme}), 71.1 (s, CH₂_{diglyme}), 72.7 (s, CH₂_{diglyme}); 208.9441 (calc. 208.9429) [RCP₄]⁻.

ESI- (m/z): 208.9412 (calc. 208.9429) [RCP₄]⁻;

Sodium 3,5-bis(1,4,6-(triisopropyl)phenyl-1,2,4-triphospholide (134) and Sodium 5-(1,4,6-(triisopropyl)phenyl-1,2,3,4-tetraphospholide (132a)



Tripp—C≡P **117** (50 mg, 0.2 mmol, 1 eq.) was added to the diglyme solution of Na[*cyclo*-P₅] (0.2 mmol in 5 mL) and stirred for 48 hours to afford **134** and **132a** in a 1:1 ratio, (based on the quantitative ³¹P NMR spectrum). The

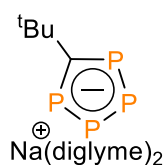
combined yield of the reaction does not exceed 5 % and it was not worked up further.

132a: $^{31}\text{P}\{^1\text{H}\}$ NMR (25 °C, THF-*d*₈) δ (ppm) = (AA'MM' spin system) 365.6 (m, $^1J_{\text{P-P}} = 488$ Hz, $^1J_{\text{P-P}} = 492$, $^2J_{\text{P-P}} = -1.6$ Hz, P_A/P_{A'}) 372.4 (m, $^1J_{\text{P-P}} = 492$, $^2J_{\text{P-P}} = 52$ Hz, $^2J_{\text{P-P}} = -1.6$ Hz, P_M/P_{M'});

134: $^{31}\text{P}\{^1\text{H}\}$ NMR (25 °C, THF-*d*₈) δ (ppm) = 270.5 (d, $^2J_{\text{P-P}} = 38$ Hz, 2P), 273.9 (t, $^2J_{\text{P-P}} = 38$ Hz, 1P).

4.4.4 Synthesis of sodium 5-R-1,2,3,4-tetraphospholides

Sodium 5-*tert*-butyl-1,2,3,4-tetraphospholide (136)



Route A: The mixture of polyphosphides Na[*cyclo*-P₅] and Na₃[P₇] (from 1 g of P₄) was prepared according to the procedure described in the section **2.4.3**, but was not separated by filtration. Instead, trimethylacetyl chloride (0.96 g, 8 mmol, based on P₄) was added directly to the mixture. The reaction was stirred under reflux conditions for 3 hours and later it was filtrated *via* a cannula equipped with a glass microfiber filter.

Route B: P₄ (1 g, 8 mmol), Na (0.38 g, 17 mmol, 2.1 eq.), trimethylacetyl chloride (0.96 g, 8 mmol, 1 eq.), DB-18-C-6 (5 mg, 0.1 mmol%) and 30 mL of diglyme were loaded to the Schlenk

flask. The reaction mixture was stirred under reflux conditions for 3 hours and later it was filtrated *via* a cannula equipped with a glass microfiber filter.

The work up procedure includes evaporation of the solvent under reduced pressure and re-dissolving of the oily residue in 15 mL of acetonitrile. The resulting solution was cooled down to $T = -20\text{ }^{\circ}\text{C}$ and treated with 1 eq. of isopropyl iodide (based on the amount of P_4). The reaction mixture was allowed to warm up to room temperature within 2 hours. The solution was filtrated *via* a cannula equipped with a glass microfiber filter and concentrated. The concentrated solution was filtered again to avoid a contamination with NaI. After the acetonitrile was completely removed under reduced pressure, the residue was washed three times with a THF:pentane mixture (5 mL:40 mL) affording **136** as the dark red oil. The maximum yield is achieved via *route B*. The composition of the cation solvate shell was calculated on the basis of the ^1H NMR spectroscopy. Yield: 1.13 g, 1.9 mmol, 24 %.

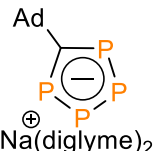
$^{31}\text{P}\{^1\text{H}\}$ NMR (25 $^{\circ}\text{C}$, THF- d_8) δ (ppm) = (AA'MM' spin system) 347.6 (m, $^1J_{\text{P-P}} = 494\text{ Hz}$, $^1J_{\text{P-P}} = 498$, $^2J_{\text{P-P}} = 5.4\text{ Hz}$), $\text{P}_A/\text{P}_{A'}$) 358.6 (m, $^1J_{\text{P-P}} = 498$, $^2J_{\text{P-P}} = 58\text{ Hz}$, $^2J_{\text{P-P}} = 5.4\text{ Hz}$, $\text{P}_M/\text{P}_{M'}$);

^1H NMR (25 $^{\circ}\text{C}$, THF- d_8) δ (ppm) = 1.82 (s, 9H, CH₃), 3.41 (s, 12H, CH₃_{diglyme}), 3.56 (m, 8H, CH₂), 3.64 (m, 8H, CH₂);

$^{13}\text{C}\{^1\text{H}\}$ NMR (25 $^{\circ}\text{C}$, THF- d_8) δ (ppm) = 37.2 (m, ^tBu), 38.6 (t, $^3J_{\text{C-P}} = 11\text{ Hz}$, ^tBu), 56.8 (s, CH₃_{diglyme}), 67.6 (s, CH₂_{diglyme}), 69.4 (s, CH₂_{diglyme}), 228.0 (m, C_{Heterocycle});

ESI- (m/z): 192.9683 (calc. 192.9660) [RCP_4]⁻.

Sodium 5-*tert*-butyl-1,2,3,4-tetraphospholide **138**

 **138** was synthesized according to the procedure described for **136**. Maximal yield is achieved via *route B* starting from P_4 (0.86 g, 6.9 mmol, 1 eq.), Na (0.33 g, 14.5 mmol, 2 eq.), 1-adamantanecarbonyl chloride (1.37 g, 6.9 mmol, 1 eq.), DB-18-C-6 (5 mg, 0.1 mmol%) and 30 mL of diglyme. The composition of the cation solvate shell was calculated on the basis of the ^1H NMR spectroscopy. Yield: 1.24 g, 2.2 mmol, 32 %.

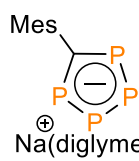
^{31}P NMR (25 $^{\circ}\text{C}$, THF- d_8) δ (ppm) = (AA'MM' spin system) 343.5 (m, $^1J_{\text{P-P}} = 494\text{ Hz}$, $^1J_{\text{P-P}} = 498$, $^2J_{\text{P-P}} = 5.4\text{ Hz}$, $\text{P}_A/\text{P}_{A'}$) 355.0 (m, $^1J_{\text{P-P}} = 498$, $^2J_{\text{P-P}} = 58\text{ Hz}$, $^2J_{\text{P-P}} = 5.4\text{ Hz}$, $\text{P}_M/\text{P}_{M'}$);

^1H NMR (25 °C, CD_3CN) δ (ppm) = 1.73 - 1.89 (br, 6H, CH_2), 2.09 (s, 3H, CH), 2.52 (s, 6H, CH_2), 3.41 (s, 12H, $\text{CH}_3_{\text{diglyme}}$), 3.56 (m, 8H, $\text{CH}_2_{\text{diglyme}}$), 3.64 (m, 8H, $\text{CH}_2_{\text{diglyme}}$);

$^{13}\text{C}\{^1\text{H}\}$ NMR (25 °C, CD_3CN) δ (ppm) = 28.7 (s, Ad), 35.4 (s, Ad), 42.4 (t, $^3J_{\text{C-P}} = 18$ Hz, Ad), 49.4 (t, $^4J_{\text{C-P}} = 11$ Hz, Ad), 56.8 (s, $\text{CH}_3_{\text{diglyme}}$), 67.6 (s, $\text{CH}_2_{\text{diglyme}}$), 69.4 (s, $\text{CH}_2_{\text{diglyme}}$), 229.0 (m, $\text{C}_{\text{Heterocycle}}$);

ESI- (m/z): 271.0122 (calc. 271.0130) $[\text{RCP}_4]^-$.

Sodium 5-mesityl-1,2,3,4-tetraphospholide (139)



139 was synthesized according to the procedure described for **136**. Maximal yield is achieved via *route B* starting from P_4 (0.64 g, 5.2 mmol, 1 eq.), Na (0.25 g, 10.8 mmol, 2 eq.), 2,4,6-trimethylbenzoyl chloride (0.93 g, 5.2 mmol, 1 eq.), DB-18-C-6 (5 mg, 0.1 mmol%) and 30 mL of diglyme. The Composition of the cation solvate shell was calculated on the basis of the ^1H NMR spectroscopy. Yield: 0.82 g, 1.5 mmol, 29 %.

$^{31}\text{P}\{^1\text{H}\}$ NMR (25 °C, $\text{THF-}d_8$) δ (ppm) = (AA'BB' spin system) 362.47 (m, $^1J_{\text{P-P}} = 484$ Hz, $^1J_{\text{P-P}} = 486$, $^2J_{\text{P-P}} = -1.6$ Hz), 2P) 358.6 (m, $^1J_{\text{P-P}} = 484$, $^2J_{\text{P-P}} = 58$ Hz, $^2J_{\text{P-P}} = -1.6$ Hz, 2P);

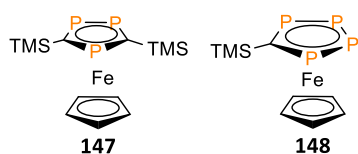
^1H NMR (25 °C, $\text{THF-}d_8$) δ (ppm) = 2.18 (s, 3H, CH_3), 2.26 (s, 6H, CH_3), 3.31 (s, 6H, $\text{CH}_3_{\text{diglyme}}$), 3.47 (m, 4H, $\text{CH}_2_{\text{diglyme}}$), 3.55 (m, 4H, $\text{CH}_2_{\text{diglyme}}$), 6.80 (s, 2H, CH);

$^{13}\text{C}\{^1\text{H}\}$ NMR (25°C, $\text{THF-}d_8$) δ (ppm) = 21.1 (s, CH_3), 21.3 (s, CH_3), 59.1 (s, $\text{CH}_3_{\text{diglyme}}$), 71.1 (s, $\text{CH}_2_{\text{diglyme}}$), 72.7 (s, $\text{CH}_2_{\text{diglyme}}$), 128.0 (s, CH), 209.0 (m, $\text{C}_{\text{Heterocycle}}$).

ESI- (m/z): 254.9798 (calc. 254.9817) $[\text{RCP}_4]^-$.

4.4.5 Synthesis of 1,3,4-triphosphaferrocenes and 1,2,3,4-tetraphosphaferrocenes

3,5-bis(trimethylsilyl)-1,2,4-triphosphaferrocene (147) and 5-trimethylsilyl-1,2,3,4-tetraphosphaferrocene (148)



Mixture of **35a** and **137** (145 mg, approx. 0.26 mmol, 1 eq.) and $[\text{CpFe}(\eta^6\text{-Toluene})]\text{PF}_6$ (92 mg, 0.26 mmol, 1 eq.) were loaded to the Schlenk flask and dissolved in 20 mL of THF. The reaction mixture was stirred under reflux conditions for 14 hours. Then, the solution was filtered *via* a cannula equipped with a microfiber filter and then the solvent was removed under reduced pressure. The solid residue was sublimed ($T = 120\text{ }^\circ\text{C}$, $1 \cdot 10^{-3}$ mbar) to afford the red crystalline powder of **147** and **148** in a 23:1 ratio (based on ^{31}P NMR spectrum). Single crystals of both species suitable for SC-XRD analysis were obtained from a concentrated pentane solution at $T = -36\text{ }^\circ\text{C}$. (**148** is olive green, while **147** is red). Yield: 63 mg, 0.15 mmol, 53 % (calculated for **147** solely).

147: $^{31}\text{P}\{^1\text{H}\}$ NMR (25 $^\circ\text{C}$, $\text{DCM-}d_2$) δ (ppm) = 85.1 (d, $^2J_{\text{P-P}} = 32$ Hz, 2P), 91.4 (t, $^2J_{\text{P-P}} = 32$ Hz, 1P);

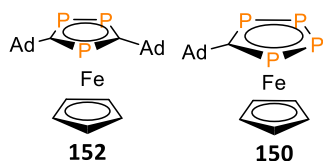
^1H NMR (25 $^\circ\text{C}$, $\text{DCM-}d_2$) δ (ppm) = 0.36 (s, 18H, TMS), 4.16 (s, 5H, CH);

$^{13}\text{C}\{^1\text{H}\}$ (25 $^\circ\text{C}$, $\text{DCM-}d_2$) δ (ppm) = 3.3 (s, TMS), 74.0 (s, CH).

148: $^{31}\text{P}\{^1\text{H}\}$ NMR (25 $^\circ\text{C}$, $\text{THF-}d_8$) δ (ppm) = (AA'MM' spin system) 99.55 (m, $^1J_{\text{P(A)}-\text{P(M)}} = -402.0$ Hz, $^2J_{\text{P(A)}-\text{P(A')}} = -33.7$, $^2J_{\text{P(A)}-\text{P(M')}} = 1.6$ Hz), 2P) 135.41 (m, $^1J_{\text{P(A')}-\text{P(M')}} = -402.0$, $^1J_{\text{P(M)}-\text{P(M')}} = -425.0$ Hz, $^2J_{\text{P(A')}-\text{P(M)}} = 1.6$ Hz, 2P);

^1H NMR (25 $^\circ\text{C}$, $\text{DCM-}d_2$) δ (ppm) = 0.41 (s, 18H, TMS), 4.28 (s, 5H, CH).

3,5-bisadamantyl-1,2,4-triphosphaferrocene (152) and 5-adamantyl-1,2,3,4-tetraphosphaferrocene (150)



The mixture of **152** and **150** was synthesized according to the procedure described for **147** and **148**, starting from the mixture of **135** and **138** (150 mg, 0.2 mmol (combined)). The ratio between **150** and **152** (based on the ^{31}P NMR spectrum) is 3:1. The two compounds could be separated by a sublimation. **150** sublimes at 100 °C as olive green crystals, while heavier **152** undergoes the sublimation at 150 °C ($1 \cdot 10^{-3}$ mbar). Single crystals suitable for the SC-XRD analysis were obtained from a concentrated pentane solution at $T = -36$ °C. Yield: 63 mg, 0.11 mmol, 58 % (combined).

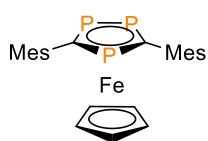
152: $^{31}\text{P}\{^1\text{H}\}$ NMR (25 °C, $\text{DCM-}d_2$) δ (ppm) = 28.6 (d, $^2J_{\text{P-P}} = 43$ Hz, 2P), 31.1 (t, $^2J_{\text{P-P}} = 43$ Hz, 1P);

^1H NMR (25 °C, $\text{DCM-}d_2$) δ (ppm) = 1.90-2.03 (m, Ad), 2.25 (s, Ad), 4.7 (s, 5H, CH);

$^{13}\text{C}\{^1\text{H}\}$ NMR (25 °C, $\text{DCM-}d_2$) δ (ppm) = 31.0 (s, Ad), 37.8 (s, Ad), 50.1 (m, $^3J_{\text{C-P}} = 2$ Hz, Ad), 52.3 (t, $^2J_{\text{C-P}} = 12$ Hz, Ad), 74.2 (s, CH), 145.3 (m, $\text{C}_{\text{Heterocycle}}$).

4.23: See paragraph 4.4.5.

3,5-mesityl-1,2,4-triphosphaferrocene (153)



153 was synthesized according to the procedure described for **64**, starting from **44a** (116 mg, 0.2 mmol). The sublimation (180 °C, $1 \cdot 10^{-3}$ mbar) affords the red crystalline powder of **153**. Single crystals suitable for the SC-XRD analysis were obtained from a concentrated pentane solution at $T = -36$ °C. Yield: 12 mg, 0.03 mmol, 13 %.

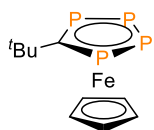
$^{31}\text{P}\{^1\text{H}\}$ NMR (25 °C, $\text{DCM-}d_2$) δ (ppm) = 57.3 (d, $^2J_{\text{P-P}} = 37$ Hz, 2P), 75.2 (t, $^2J_{\text{P-P}} = 37$ Hz, 1P);

^1H NMR (25 °C, $\text{DCM-}d_2$) δ (ppm) = 2.23 (s, 6H, CH₃), 2.60 (s, 12H, CH₃), 4.66 (s, 5H, CH), 6.88 (s, 4H, CH);

$^{13}\text{C}\{^1\text{H}\}$ NMR (25 °C, DCM- d_2) δ (ppm) = 20.8 (s, CH₃), 24.3 (s, CH₃), 76.5 (s, CH_{Cp}), 130.2 (s, CH_{mesityl}), 134.4 (s, *ipso*-C), 136.0 (s, C_{mesityl}), 137.2 (s, C_{mesityl}).

4.4.6 Synthesis 5-R-1,2,3,4-tetraphosphaferrocenes

5-*tert*-butyl-1,2,3,4-tetraphosphaferrocene (149)



34a (100 mg, 0.2 mmol, 1 eq.) and [CpFe(η^6 -Toluene)]PF₆ (73 mg, 0.2 mmol, 1 eq.) were loaded in the Schlenk flask and dissolved in 20 mL of DME. The reaction mixture was stirred under reflux for 14 hours. Later, the solution was filtered *via* a cannula equipped with a microfiber filter and the solvent was removed under reduced pressure. Solid residue was sublimed (100 °C, $1 \cdot 10^{-3}$ mbar) affording olive green crystalline powder of **149**. Single crystals suitable for SC-XRD analysis were obtained from a concentrated pentane solution at $T = -36$ °C. Yield: 20 mg, 0.06 mmol, 32 %.

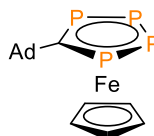
$^{31}\text{P}\{^1\text{H}\}$ NMR (25 °C, CD₃CN) δ (ppm) = (AA'MM' spin system) 87.96 (m, $^1J_{\text{P(A)}-\text{P(M)}} = -428.0$ Hz, $^2J_{\text{P(A)}-\text{P(A')}} = -57.7$, $^2J_{\text{P(A)}-\text{P(M')}} = 9.4$ Hz), 2P) 108.07 (m, $^1J_{\text{P(A')}-\text{P(M')}} = -428.0$, $^1J_{\text{P(M)}-\text{P(M')}} = -425.0$ Hz, $^2J_{\text{P(A')}-\text{P(M)}} = 9.4$ Hz, 2P);

^1H NMR (25 °C, CD₃CN) δ (ppm) = 1.64 (s, 9H, CH₃), 4.68 (s, 5H, CH);

$^{13}\text{C}\{^1\text{H}\}$ NMR (25 °C, CD₃CN) δ (ppm) = 37.7 (t, $^3J_{\text{C-P}} = 9$ Hz, CH₃), 40.1 (t, $^2J_{\text{C-P}} = 16$ Hz, C), 75.7 (s, CH);

Elemental Analysis calculated for C₁₀H₁₄FeP₄: C, 38.26 %; H, 4.49 %; **found**: C, 38.45 %; H, 4.51 %.

5-adamantyl-1,2,3,4-tetraphosphaferrocene (150)



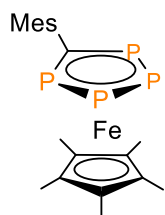
150 was synthesized according to the procedure described for **149**, starting from **135** (142 mg, 0.25 mmol). Single crystals suitable for SC-XRD analysis were obtained from a concentrated pentane solution at $T = -36$ °C. Yield: 35 mg, 0.09 mmol, 36 %.

^{31}P (25°C, DCM- d_2) δ (ppm) = (AA'MM' spin system) 83.53 (m, $^1J_{\text{P(A)}-\text{P(M)}} = -428.0$ Hz, $^2J_{\text{P(A)}-\text{P(A')}} = -57.7$, $^2J_{\text{P(A)}-\text{P(M')}} = 9.4$ Hz), 2P) 103.64 (m, $^1J_{\text{P(A')}-\text{P(M')}} = -428.0$, $^1J_{\text{P(M)}-\text{P(M')}} = -425.0$ Hz, $^2J_{\text{P(A')}-\text{P(M)}} = 9.4$ Hz, 2P);

^1H (25°C, DCM- d_2) δ (ppm) = 1.79 (s, 6H, CH₂), 2.09 - 2.12 (br. 3H, CH), 2.22 (s, 6H, CH₂) 4.61 (s, 5H, CH);

$^{13}\text{C}\{^1\text{H}\}$ (25°C, DCM- d_2) δ (ppm) = 30.8 (s, CH), 37.1 (s, CH₃), 43.0 - 43.4 (t, $^2J_{\text{C-P}} = 14$ Hz, C), 50.0 (t, $^3J_{\text{C-P}} = 9$ Hz, C), 75.8 (s, CH).

5-mesityl-1,2,3,4-tetraphosphaferrocene (**151**)



A pre-cooled ($T = -40$ °C) suspension of Cp*Li (0.146 g, 1 mmol, 1 eq.) in 40 ml of THF was slowly added to the cold ($T = -40$ °C) suspension of FeCl₂(DME) (0.22 g, 1 mmol, 1 eq.) in 40 ml of THF. After the addition was complete, the reaction mixture was stirred under -40 °C for two hours. Then, the cold ($T = -40$ °C) THF solution of **139** (0.41 g, 1 mmol, 1 eq.) was added dropwise to the reaction mixture. After the addition was complete, the reaction was allowed to slowly warm up to room temperature. After 24 h of stirring at room temperature, the resulting solution was filtered and the solvent was removed under reduced pressure. The crude black solid was sublimed ($T = 180$ °C, $1 \cdot 10^{-3}$ mbar) to give an orange crystalline powder of **151**. Single crystals suitable for the SC-XRD analysis were obtained from a concentrated pentane solution at $T = -36$ °C. Yield: 37 mg, 0.07 mmol, 7 %.

$^{31}\text{P}\{^1\text{H}\}$ NMR (25 °C, DCM- d_2) δ (ppm) = (AA'MM' spin system) 86.61 (m, $^1J_{\text{P(A)}-\text{P(M)}} = -403.0$ Hz, $^2J_{\text{P(A)}-\text{P(A')}} = -47.5$, $^2J_{\text{P(A)}-\text{P(M')}} = -1.1$ Hz), 2P) 129.67 (m, $^1J_{\text{P(A')}-\text{P(M')}} = -403.0$, $^1J_{\text{P(M)}-\text{P(M')}} = -416.0$ Hz, $^2J_{\text{P(A')}-\text{P(M)}} = -1.1$ Hz, 2P);

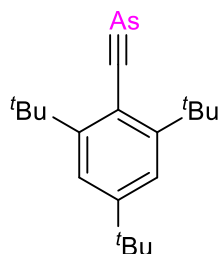
^1H NMR (25 °C, DCM- d_2) δ (ppm) = 1.66 (s, 15H, CH₃), 2.24 (s, 3H, CH₃), 2.30 (s, 6H, CH₃), 6.87 (s, 2H, CH);

$^{13}\text{C}\{^1\text{H}\}$ NMR (25 °C, DCM- d_2) δ (ppm) = 11.44 (s, CH₃), 20.38 (s, CH₃), 24.47 (s, CH₃), 89.6 (s, C), 129.2 (s, *m*-CH), 130.1 (t, $^2J_{\text{C-P}} = 17$ Hz, *ipso*-C), 135.7 (s, *p*-C), 137.1 (t, $^3J_{\text{C-P}} = 4$ Hz, *o*-C), Yield: 37 mg (7 %).

Elemental Analysis calculated for C₂₀H₂₆FeP₄: C, 53.84 %; H, 5.87%; **found**: C, 54.21 %; H, 4.60 %.

4.4.7 Test reaction with supermesitylarsaalkyne

Supermesitylarsaalkyne (155)



A solution of 2,4,6-tri(*tert*-butyl)benzoyl chloride (4.0 g, 13 mmol, 1 eq.) in 45 ml of THF was added dropwise to a solution of lithium bis(trimethylsilyl)arsenide (3.0 g, 13 mmol, 1 eq.) in 45 ml THF. The reaction mixture was stirred for 16 hours protected from the light. Then, the solvent was removed under reduced pressure, the solid residue was transferred on a column filled with silica (15 cm layer). The column chromatography was performed with the use of pentane as an eluent. The colorless pentane fraction was collected. A removal of the solvent gives supermesitylarsaalkyne **155** as a pale yellow powder. Yield: 0.98 g, 3.1 mmol, 24 %.

$^1\text{H NMR}$ (25 °C, DCM-d_2) δ (ppm) = 1.30 (s, 9H, *t*Bu), 1.72 (s, 18H, *t*Bu), 7.25 (s, 2H, CH).

Test reaction between supermesitylphosphaalkyne (155) and Na[*cyclo*-P₅]

155 (250 mg, 0.7 mmol) was added to the Schlenk flask with the diglyme solution of Na[*cyclo*-P₅] (0.7 mmol in 10 mL). The reaction was stirred at room temperature for 48 hours.

Compound **A** (proposed **162**): $^{31}\text{P}\{^1\text{H}\}$ NMR (25 °C, diglyme) δ (ppm) = 290.8 (s) (referenced with respect to [*cyclo*-P₅]);

Compound **B** (proposed **163**): $^{31}\text{P}\{^1\text{H}\}$ (25 °C, diglyme) δ (ppm) = 342.9 (d, $J = 486$ Hz), 370.1 (d, $J = 486$ Hz), 380.5 (d, $J = 470$ Hz) (referenced with respect to [*cyclo*-P₅]).

4.4.8 Crystallographic data for all compounds

3,5-*R*-1,2,4-triphosphaferrocenes **147**, **152**, **153**.

Identification code	147	152	153
Empirical formula	C ₁₃ H ₂₃ FeP ₃ Si ₂	C _{4.32} H _{5.6} Fe _{0.16} P _{0.48}	C ₁₀₅ H ₁₂₀ Fe ₄ P ₁₂
Formula weight	384.25	81.33	1977.04
Temperature/K	100(2)	100.00	119.7

Crystal system	orthorhombic	monoclinic	triclinic
Space group	P2 ₁ 2 ₁ 2 ₁	P2 ₁ /c	P-1
a/Å	6.9651(2)	11.1299(4)	9.0005(6)
b/Å	12.1211(3)	11.7427(5)	15.1395(9)
c/Å	21.5685(6)	17.6217(7)	18.8254(12)
α/°	90	90	73.302(2)
β/°	90	93.174(2)	81.272(2)
γ/°	90	90	89.480(2)
Volume/Å ³	1820.91(9)	2299.54(16)	2427.0(3)
Z	4	25	1
ρ _{calc} /cm ³	1.402	1.468	1.353
μ/mm ⁻¹	1.209	7.322	0.831
F(000)	800.0	1072.0	1034.0
Crystal size/mm ³	0.3 × 0.27 × 0.08	0.5 × 0.114 × 0.105	0.367 × 0.227 × 0.169
Radiation	MoKα (λ = 0.71073)	CuKα (λ = 1.54178)	MoKα (λ = 0.71073)
2θ range for data collection/°	3.854 to 51.488	9.054 to 144.268	4.104 to 61.268
Index ranges	-8 ≤ h ≤ 7, -14 ≤ k ≤ 14, -26 ≤ l ≤ 26	-13 ≤ h ≤ 13, -14 ≤ k ≤ 13, -21 ≤ l ≤ 21	-12 ≤ h ≤ 12, -21 ≤ k ≤ 21, -21 ≤ l ≤ 26
Reflections collected	69202	32905	100973
Independent reflections	3476 [R _{int} = 0.0660, R _{sigma} = 0.0214]	4515 [R _{int} = 0.0554, R _{sigma} = 0.0328]	14896 [R _{int} = 0.0446, R _{sigma} = 0.0319]
Data/restraints/parameters	3476/0/167	4515/0/280	14896/0/582
Goodness-of-fit on F ²	1.284	1.030	1.112
Final R indexes [I >= 2σ(I)]	R ₁ = 0.0641, wR ₂ = 0.1516	R ₁ = 0.0308, wR ₂ = 0.0742	R ₁ = 0.0520, wR ₂ = 0.1194
Final R indexes [all data]	R ₁ = 0.0647, wR ₂ = 0.1519	R ₁ = 0.0352, wR ₂ = 0.0772	R ₁ = 0.0638, wR ₂ = 0.1257
Largest diff. peak/hole / e Å ⁻³	1.05/-1.32	0.41/-0.31	1.45/-0.56

153: The asymmetric unit contains two molecules of the iron triphospholide complex and half a molecule of disordered pentane. The pentane shows translational disorder across a special position.

5-R-1,2,3,4-tetraphosphaferrocenes 148, 149, 151

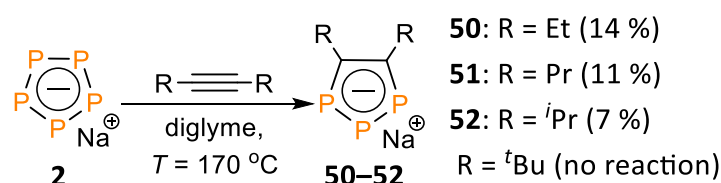
Identification code	149	148	151
Empirical formula	C ₁₀ H ₁₄ FeP ₄	C ₉ H ₁₄ FeP ₄ Si	C ₂₀ H ₂₆ FeP ₄
Formula weight	313.94	330.02	446.14
Temperature/K	110.00	100	150(2)
Crystal system	monoclinic	monoclinic	monoclinic
Space group	P2 ₁ /n	P2 ₁ /m	P2 ₁ /n
a/Å	6.5504(2)	6.8854(2)	8.45090(10)
b/Å	16.6879(6)	10.9108(3)	30.7816(4)
c/Å	11.9223(4)	9.1464(3)	8.73600(10)
α/°	90	90	90
β/°	94.5160(10)	97.2850(10)	115.1282(4)
γ/°	90	90	90
Volume/Å ³	1299.21(8)	681.58(4)	2057.44(4)
Z	4	2	4
ρ _{calc} /cm ³	1.605	1.608	1.440
μ/mm ⁻¹	1.618	1.629	1.045
F(000)	640.0	336.0	928.0
Crystal size/mm ³	0.664 × 0.201 × 0.137	0.319 × 0.166 × 0.15	0.47 × 0.45 × 0.06
Radiation	MoKα (λ = 0.71073)	MoKα (λ = 0.71073)	MoKα (λ = 0.71073)
2θ range for data collection/°	5.966 to 61.236	4.49 to 66.298	5.486 to 59.216
Index ranges	-8 ≤ h ≤ 9, -21 ≤ k ≤ 23, -16 ≤ l ≤ 17	-9 ≤ h ≤ 10, -16 ≤ k ≤ 16, -14 ≤ l ≤ 13	-11 ≤ h ≤ 11, -42 ≤ k ≤ 42, -9 ≤ l ≤ 12
Reflections collected	33863	17986	46277
Independent reflections	3968 [R _{int} = 0.0375, R _{sigma} = 0.0205]	2669 [R _{int} = 0.0256, R _{sigma} = 0.0179]	5745 [R _{int} = 0.0318, R _{sigma} = 0.0175]
Data/restraints/parameters	3968/0/139	2669/0/78	5745/0/234
Goodness-of-fit on F ²	1.081	1.051	1.152
Final R indexes [I ≥ 2σ(I)]	R ₁ = 0.0216, wR ₂ = 0.0440	R ₁ = 0.0208, wR ₂ = 0.0470	R ₁ = 0.0274, wR ₂ = 0.0653
Final R indexes [all data]	R ₁ = 0.0284, wR ₂ = 0.0480	R ₁ = 0.0247, wR ₂ = 0.0482	R ₁ = 0.0283, wR ₂ = 0.0658
Largest diff. peak/hole / e Å ⁻³	0.43/-0.33	0.51/-0.54	0.43/-0.28

148: The asymmetric unit contains half an equivalent of the complex.

Summary

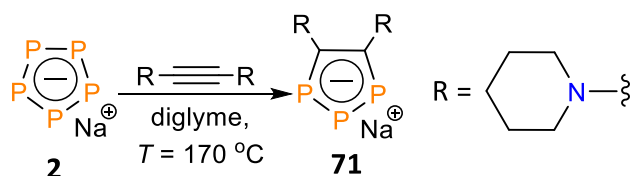
Sodium pentaphospholide (Na[*cyclo*-P₅]) **2**, which is readily available from P₄ and sodium, is reactive towards R—C≡E (E = C(R'), N, P, As). The pentaphospholide anion serves as a source of [P₁₋₃]⁻ fragments in the synthesis of different five membered heterocycles.

In **Chapter 2** the reactivity of Na[*cyclo*-P₅] towards alkynes is discussed. Na[*cyclo*-P₅] reacts with the aliphatic alkynes to give sodium 3,5-dialkyl-1,2,3-triphospholides **50–52** (**Scheme 66**). Sterically demanding substituents at the C≡C triple bond hinder the desired interaction between [*cyclo*-P₅]⁻ and the alkyne.



Scheme 66. Synthesis of sodium 4,5-*R*-triphospholides **50–52**. In parentheses: the corresponding yield of the reaction.

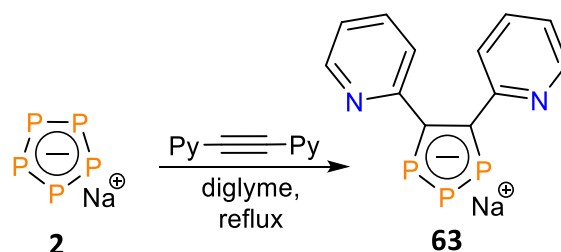
Apart from the aliphatic alkynes, Na[*cyclo*-P₅] also reacts with dipiperidinoacetylene. The reaction leads to the corresponding 4,5-dipiperidino-1,2,3-triphospholide anion **71** in 22 % yield (**Scheme 67**).



Scheme 67. Synthesis of sodium 4,5-dipiperidino-1,2,3-triphospholide **71**.

The distinguishing feature of **71** is a significant upfield shift of the corresponding resonances in the ³¹P NMR spectrum, due to the conjugation of the π-donating piperidine groups with the aromatic system of the phosphorus heterocycle.

The reaction between alkynes with electron-withdrawing groups and Na[*cyclo*-P₅] is more favored. In fact, Na[*cyclo*-P₅] reacts with bispyridylacetylene to give sodium 3,5-bispyridyl-1,2,3-triphospholide **63** in 40 % yield (**Scheme 68**). This compound is particularly interesting as a ligand in the metallocene chemistry, due to its multidentate nature.



Scheme 68. Synthesis of sodium 4,5-bispyridyl-1,2,3-triphospholide **63**.

Bisphosphinylacetylene **66** can be synthesized *via* the Stille cross-coupling reaction. It is demonstrated that the novel bisphosphinylacetylene **66** undergoes coordination with two equivalents of CuBr in THF affording complex **67** with the heterocubane-type [Cu₄Br₄] cluster (**Figure 47**).

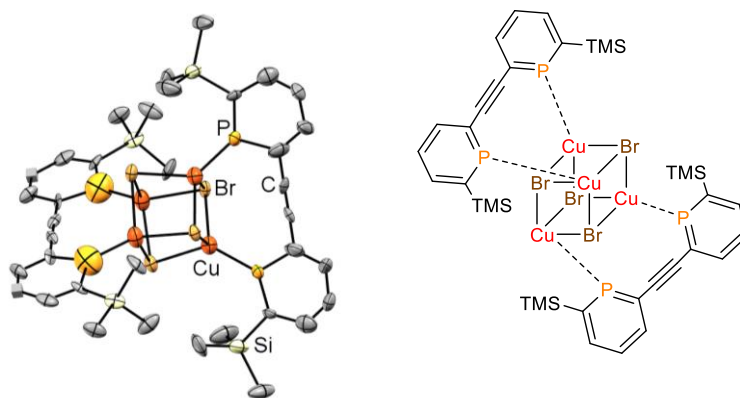
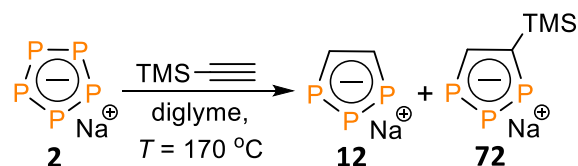


Figure 47. Connectivity of **67** in the crystal.

Trimethylsilylacetylene reacts with Na[*cyclo*-P₅] to give the parent 1,2,3-triphospholide anion **12** as a major product (in 27 % yield), indicating protodesilylation of the corresponding alkyne under these conditions (**Scheme 69**).



Scheme 69. Synthesis of the parent sodium 1,2,3-triphospholide **12** (major product) and sodium 4-trimethylsilyl-1,2,3-triphospholide **72** (minor product).

All new sodium 3,5-*R*-1,2,3-triphospholides react with [CpFe(η^6 -Toluene)]PF₆ to give the corresponding 3,5-*R*-1,2,3-triphosphaferrocenes (**Figure 48**) in around 50 % yields.

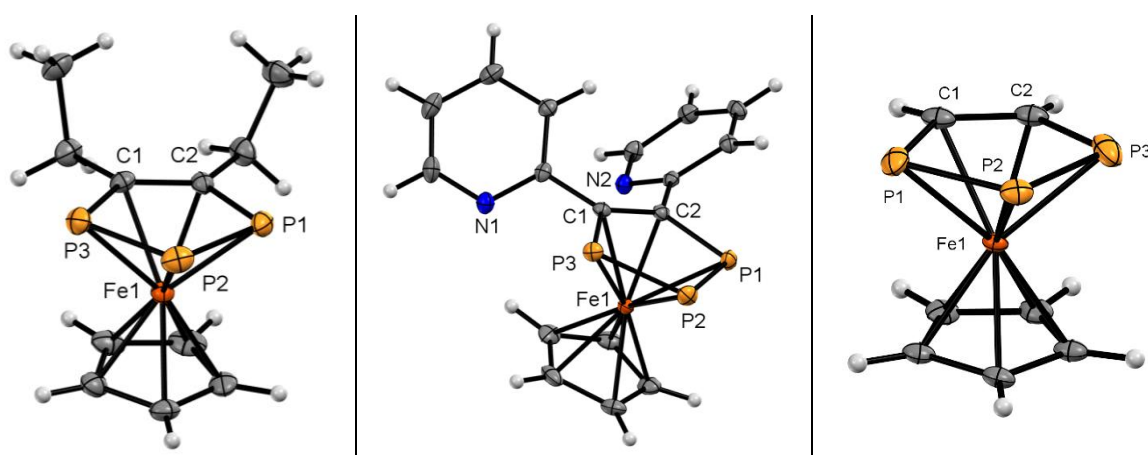
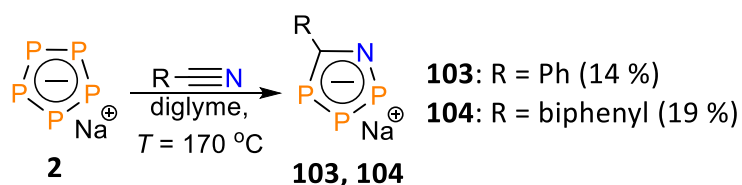


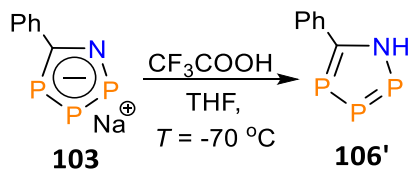
Figure 48. Molecular structures of 4,5-*R*-1,2,3-triphosphaferrocenes **54** (left), **64** (middle), and **73** (right).

In **Chapter 3** the reactivity of Na[cyclo-P₅] towards nitriles is described. It is demonstrated that Na[cyclo-P₅] reacts with benzonitrile and 4-cyanobiphenyl to give the hitherto unknown P,N-heterocyclic anions: 5-phenyl-1-aza-2,3,4-triphospholide **103** and 5-biphenyl-1-aza-2,3,4-triphospholide **104** (**Scheme 70**).



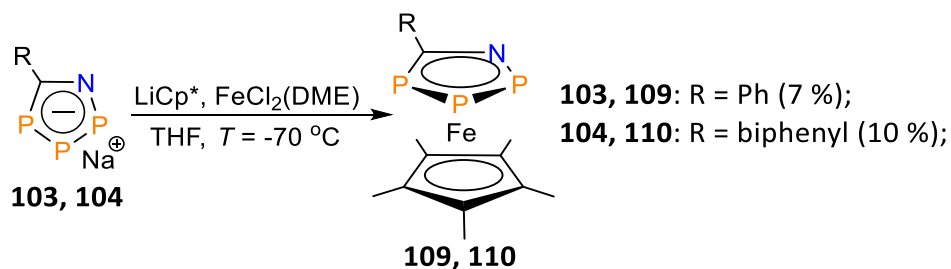
Scheme 70. Synthesis of sodium 5-*R*-1-aza-2,3,4-triphospholides **103** and **104**. . In parentheses: the corresponding yield of the reaction.

DFT calculations show that the 1-aza-2,3,4-triphospholide anions predominately act as the N-centered nucleophiles. Indeed, treating of **103** with CF₃COOH leads to the corresponding 1-H-1-aza-2,3,4-triphosphole **106'** (Scheme 71).



Scheme 71. Synthesis of 1-H-5-phenyl-2,3,4-triphosphole **106'**.

The aromaticity of the novel P,N-heterocycles **103** and **104** is proven by the synthesis of the corresponding 1-aza-2,3,4-triphosphaferrocenes **109** and **110** (Scheme 72, Figure 49).



Scheme 72. Synthesis of 5-R-1-aza-2,3,4-triphosphaferrocenes **109** and **110**. In parentheses: the corresponding yield of the reaction.

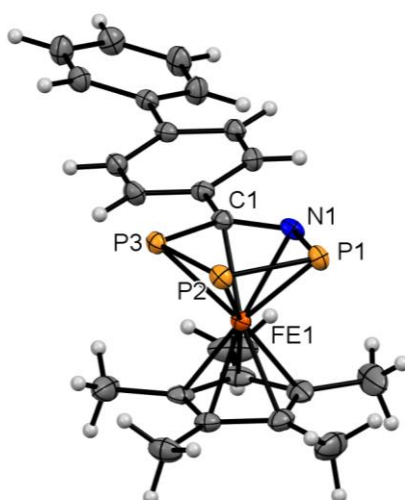
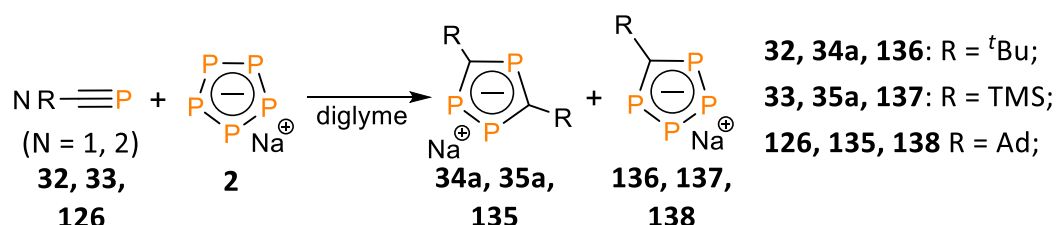


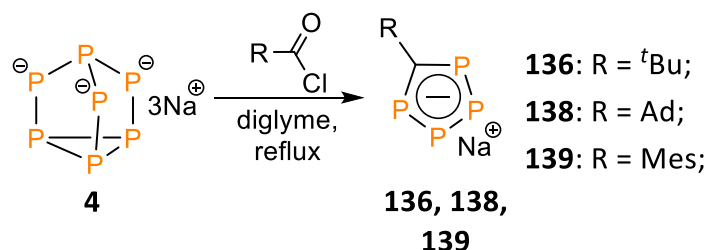
Figure 49. Molecular structure of 5-biphenyl-1-aza-2,3,4-triphosphaferrocene **110**.

In **Chapter 4** the reactivity of Na[*cyclo*-P₅] towards phospho- and arsaalkynes is discussed. It is demonstrated that R—C≡P (R = TMS, ^tBu, Ad,) reacts with Na[*cyclo*-P₅] affording a mixture of sodium 3,5-R-1,2,4-triphospholides **34a**, **35a**, **135** and 5-R-1,2,3,4-tetraphospholides **136**, **137**, **138** (**Scheme 73**). The ratio between two products is in favor of 3,5-R-1,2,4-triphospholides.



Scheme 73. Synthesis of sodium 3,5-R-1,2,4-triphospholides **34a**, **35a**, **135** and 5-R-1,2,3,4-tetraphospholides **136**, **137**, **138**.

Interestingly, it is found that acid chlorides with electron-donating (R = ^tBu, Ad) or mesityl substituents react with sodium heptaphosphide **4** to give the desired 5-R-1,2,3,4-tetraphospholide anions **136**, **138**, and **139** in around 20–30 % yield based on P₄ (**Scheme 74**).



Scheme 74. Synthesis of sodium 1,2,3,4-tetraphospholides **136**, **138** and **139**.

All 1,2,4-tri- and 1,2,3,4-tetraphospholide derivatives react with iron (II) precursors affording 1,2,4-tri- and 1,2,3,4-tetraphosphaferrocenes (**Figure 50**) in the good yields.

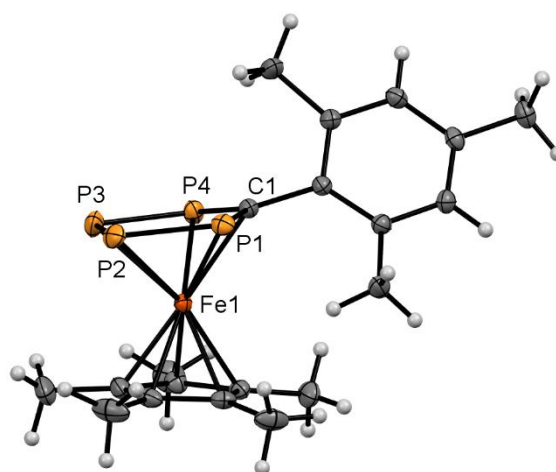
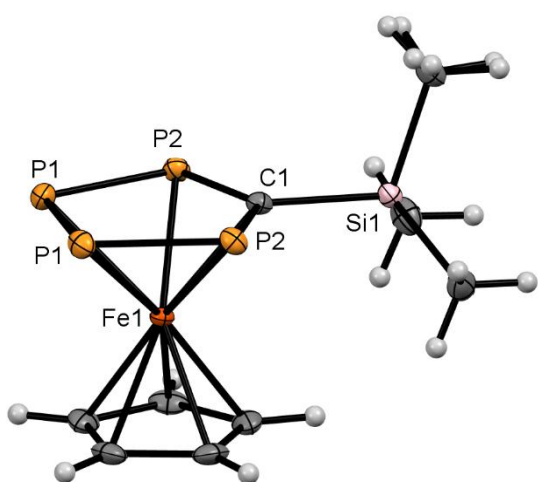
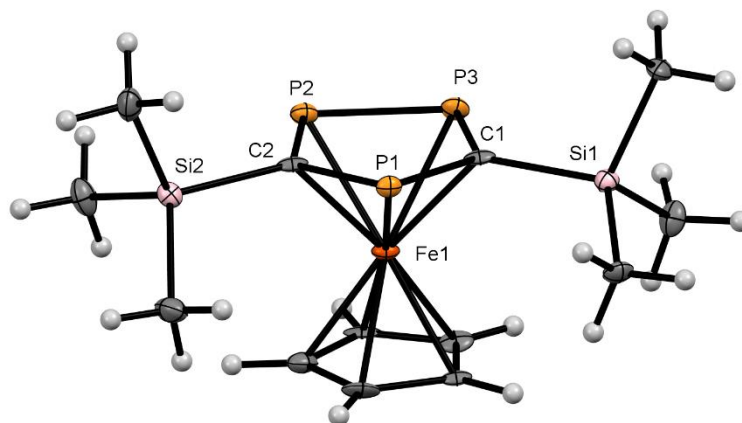
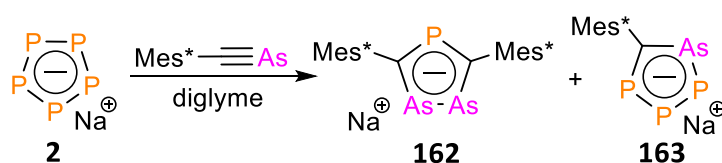


Figure 50. Molecular structures of 3,5-R-1,2,4-triphosphaferrocene **147** (top) and 5-R-1,2,3,4-tetraphosphaferrocenes **148** (left, bottom), **151** (right, bottom).

Monitoring the reaction mixture that contains $\text{Mes}^*-\text{C}\equiv\text{As}$ and $\text{Na}[\text{cyclo-P}_5]$ by $^{31}\text{P}\{^1\text{H}\}$ NMR spectroscopy revealed, that the new phosphorus-containing products are formed. Based on the relevant literature data, it is assumed that the novel P,As-heterocycles **162** and **163** are synthesized (**Scheme 75**).



Scheme 75. Synthesis of sodium 1,2-diarsa-4-phosphide **162** and sodium 1-arsa-2,3,4-triphospholide **163**.

List of abbreviations

Ad	adamantyl
AIM	atoms in molecule
Alk	alkyl
Å	ångström
Ar	aryl
BCP	bond critical point
biphen	biphenyl
Bu	butyl
BuLi	butyllithium
°C	temperature in celsius degree
Cp	cyclopentadienyl
Cp ^{ttt}	1,2,4-tritertbutylcyclopentadienyl
Cp*	pentamethylcyclopentadienyl
CV	cyclic voltammetry
δ	chemical shift
Δ	delta (shift or gap)
d	doublet
DABCO	1,4-diazabicyclo[2.2.2]octane
DCM	dichloromethane
DFT	density functional theory
DME	dimethoxyethane
DMF	n,n-dimethylformamide
dq	doublet of quartets
E	energy
e	electron
E _{ox}	oxidation at a peak potential
E _{red}	reduction at a peak potential
E _{1/2}	half wave potential
Ed	editor
EDD	electron density distribution
ELF	electron localization function
ESI-TOF	electron-spray ionization time-of-flight
Et	ethyl
eV	electronvolt
Fc	ferrocene/ ferrocenyl
Fc ⁺	ferrocenium cation
h	hour
Hal	halide
HOMO	highest occupied molecular orbital
Hz	herz
I	current

ⁱ Pr	isopropyl
J	joule
<i>J</i>	coupling constant
kcal	kilocalories
kJ	kilojoule
λ	wavelength
L	ligand
LUMO	lowest unoccupied molecular orbital
M	metal
m	mass
<i>m</i> -	meta
mbar	millibar
Me	methyl
MeCN	acetonitrile
Mes	mesityl
Mes*	supermesityl
MHz	megahertz
MO	molecular orbital
<i>m</i> -Tol	3-methylphenyl
N, n	natural numbers
NICS	nucleus independent chemical shift
NMR	nuclear magnetic resonance
NPA	natural population analysis
<i>o</i> -	ortho
Ortep	oak ridge thermal ellipsoid plot
<i>p</i> -	para
π	electrons at π orbital
Ph	phenyl
ppm	parts per million
Pr	propyl
Py	pyridyl
q	quartet
$\rho(r_c)$	electron density
R	substituent
RCP	ring critical point
r.t.	room temperature
s	singlet
SC-XRD	single crystal X-ray diffraction
SMM	single molecule magnet
T	temperature
t	triplet
TBAPF ₆	tetrabutylammonium hexafluorophosphate
^t Bu	<i>tert</i> -butyl
THF	tetrahydrofuran

TMS	trimethylsilyl
Tripp	2,4,6-triisopropylphenyl
UV	ultraviolet
V	volt
VT	variable temperature
[X] ⁻	anion
XRD	X-ray diffraction

References

- [1] D. E. C. Corbridge, *Phosphorus: An Outline of its Chemistry, Biochemistry and Technology*, 5th ed., Elsevier, Amsterdam, **1995**.
- [2] L. Maier, *Top. Curr. Chem.* **1971**, *19*, 95.
- [3] D. E. C. Corbridge, *Phosphorus 2000*, Elsevier, Amsterdam, **2000**.
- [4] M. B. Geeson, C. C. Cummins, *Science* **2018**, *359*, 1383–1385.
- [5] M. B. Geeson, C. C. Cummins, *ACS Cent. Sci.* **2020**, *6*, 848–860.
- [6] C. M. Hoidn, D. J. Scott, R. Wolf, *Chem. Eur. J.* **2021**, *27*, 1886–1902.
- [7] J. E. Borger, A. W. Ehlers, J. C. Sloopweg, K. Lammertsma, *Chem. Eur. J.* **2017**, *23*, 11738–11746.
- [8] B. M. Cossairt, N. A. Piro, C. C. Cummins, *Chem. Rev.* **2010**, *110*, 4164–4177.
- [9] M. Scheer, G. Balázs, A. Seitz, *Chem. Rev.* **2010**, *110*, 4236–4256.
- [10] V. A. Milyukov, Yu. H. Budnikova, O. G. Sinyashin, *Russ. Chem. Rev.* **2005**, *74*, 781–805.
- [11] A. Simon, H. Borrmann, H. Craubner, *Phosphorus, Sulfur Silicon Relat. Elem.* **1987**, *30*, 507–510.
- [12] L. R. Maxwell, S. B. Hendricks, V. M. Mosley, *J. Chem. Phys.* **1935**, *3*, 699.
- [13] N. J. Brassington, H. G. M. Edwards, D. A. Long, *J. Raman Spectrosc.* **1981**, *11*, 346–348.
- [14] G. Trinquier, J.-P. Malrieu, J.-P. Daudey, *Chem. Phys. Lett.* **1981**, *80*, 552–557.
- [15] B. M. Cossairt, C. C. Cummins, A. R. Head, D. L. Lichtenberger, R. J. F. Berger, S. A. Hayes, N. W. Mitzel, G. Wu, *J. Am. Chem. Soc.* **2010**, *132*, 8459–8465.
- [16] A. Hirsch, Z. Chen, H. Jiao, *Angew. Chem. Int. Ed.* **2001**, *40*, 2834–2838.

- [17] E. Fluck, C. M. E. Pavlidou, R. Janoschek, *Phosphorus, Sulfur Silicon Relat. Elem.* **1979**, *6*, 469–474.
- [18] A. Wiesner, S. Steinhauer, H. Beckers, C. Muller, S. Riedel, *Chem. Sci.* **2018**, *9*, 7161–7288.
- [19] V. A. Miluykov, Y. G. Budnikova, O. G. Sinyashin, *Russ. Chem. Rev.* **2005**, *74*, 781–805.
- [20] V. G. Tsirelson, N. P. Tarasova, M. F. Bobrov, Yu. V. Smetannikov, *Heteroat. Chem.* **2006**, *17*, 572–578.
- [21] H. G. Von Schnering, W. Hoenle, *Chem. Rev.* **1988**, *88*, 243–273.
- [22] A. P. Ginsberg in *Inorganic Syntheses* (Eds.: G. Becker, H. Schmidt, G. Uhl, W. Uhl), John Wiley & Sons, Inc., **1990**, pp. 243–249.
- [23] M. Baudler, D. Düster, J. Germeshausen, *Z. Anorg. Allg. Chem.* **1986**, *534*, 19–26.
- [24] M. Cicač-Hudi, J. Bender, S. H. Schlindwein, M. Bispinghoff, M. Nieger, H. Grützmacher, D. Gudat, *Eur. J. Inorg. Chem.* **2016**, *2016*, 649–658.
- [25] F. Kraus, J. C. Aschenbrenner, N. Korber, *Angew. Chem. Int. Ed.* **2003**, *42*, 4030–4033.
- [26] T. Hanauer, J. C. Aschenbrenner, N. Korber, *Inorg. Chem.* **2006**, *45*, 6723–6727.
- [27] G. Fritz, H.-W. Schneider, *Z. Anorg. Allg. Chem.* **1990**, *584*, 12–20.
- [28] N. K. Gusarova, S. F. Malysheva, S. N. Arbusova, B. A. Trofimov, *Russ. Chem. Bull.* **1998**, *47*, 1645–1652.
- [29] A. R. Jupp, J. M. Goicoechea, *Angew. Chem. Int. Ed.* **2013**, *52*, 10064–10067.
- [30] R. S. P. Turbervilla, J. M. Goicoechea, *Chem. Commun.* **2012**, *48*, 6100–6102.
- [31] C. P. Butts, M. Green, T. N. Hooper, R. J. Kilby, J. E. McGrady, D. A. Pantazis, C. A. Russell, *Chem. Commun.* **2008**, *7*, 856–858.
- [32] M. Baudler, D. Düster, D. Ouzounis, *Z. Anorg. Allg. Chem.* **1987**, *544*, 87–94.

- [33] C. Zhang, C. Sun, B. Hu, C. Yu, M. Lu, *Science* **2017**, *355*, 374–376.
- [34] M. Baudler, S. Akpapoglou, D. Ouzounis, F. Wasgestian, B. Meinigke, H. Budzikiewicz, H. Münster, *Angew. Chem. Int. Ed.* **1988**, *27*, 280–281.
- [35] V. A. Milyukov, A. V. Kataev, O. G. Sinyashin, E. Hey-Hawkins, *Russ. Chem. Bull.* **2006**, *55*, 1297–1299.
- [36] A. S. Nizovtsev, *Phys. Chem. Chem. Phys.* **2016**, *18*, 16084–16087.
- [37] Q. Jin, B. Jin, W. G. Xu, W. Zhu, *J. Mol. Struct. THEOCHEM.* **2005**, *713*, 113–117.
- [38] M. N. Glukhovtsev, P. v. R. Schleyer, C. Maerker, *J. Phys. Chem.* **1993**, *97*, 8200–8206.
- [39] R. Gupta, P. Maheshwari, M. Kour, *Comput. Theor. Chem.* **2015**, *1060*, 10–16.
- [40] I. A. Bezkishko, A. A. Zagidullin, V. A. Milyukov, O. G. Sinyashin, *Russ. Chem. Rev.* **2014**, *83*, 555–574.
- [41] V. A. Miluykov, O. G. Sinyashin, O. Scherer, E. Hey-Hawkins, *Mendeleev Commun.* **2002**, *12*, 1–2.
- [42] A. R. Kudinov, D. A. Loginov, Z. A. Starikova, P. V. Petrovskii, M. Corsini, P. Zanello, *Eur. J. Inorg. Chem.* **2002**, *2002*, 3018–3027.
- [43] E. Urnežius, W. W. Brennessel, C. J. Cramer, J. E. Ellis, P. V. R. Schleyer, *Science* **2022**, *295*, 832–834.
- [44] M. E. Moussa, S. Welsch, M. Lochner, E. V. Peresyphina, A. V. Virovets, M. Scheer, *Eur. J. Inorg. Chem.* **2018**, *2018*, 2689–2694.
- [45] C. Heindl, E. V. Peresyphina, A. V. Virovets, W. Kremer, M. Scheer, *J. Am. Chem. Soc.* **2015**, *137*, 10938–10941.
- [46] M. Scheer, L. J. Gregoriades, A. V. Virovets, W. Kunz, R. Neueder, I. Krossing, *Angew. Chem. Int. Ed.* **2006**, *45*, 5689–5693.

- [47] J. Bai, A. V. Virovets, M. Scheer, *Science* **2003**, *300*, 781–783.
- [48] M. Scheer, J. Bai, B. P. Johnson, R. Merkle, A. V. Virovets, C. E. Anson, *Eur. J. Inorg. Chem.* **2005**, *2005*, 4023–4026.
- [49] H. Brake, E. Peresyphkina, C. Heindl, A. V. Virovets, W. Kremer, M. Scheer, *Chem. Sci.* **2019**, *10*, 2940–2944.
- [50] A. A. Zagidullin, A. V. Petrov, I. A. Bezkishko, V. A. Miluykov, *Russ. Chem. Bull.* **2021**, *70*, 1260–1268.
- [51] C. Riesinger, G. Balázs, M. Bodensteiner, M. Scheer, *Angew. Chem. Int. Ed.* **2020**, *59*, 23879–23884.
- [52] R. Yadav, T. Simler, S. Reichl, B. Goswami, C. Schoo, R. Köppe, M. Scheer, P. W. Roesky, *J. Am. Chem. Soc.* **2020**, *142*, 1190–1195.
- [53] R. Yadav, T. Simler, B. Goswami, C. Schoo, R. Köppe, S. Dey, P. W. Roesky, *Angew. Chem. Int. Ed.* **2020**, *59*, 9443–9447.
- [54] R. Yadav, B. Goswami, T. Simler, C. Schoo, S. Reichl, M. Scheer, P. W. Roesky, *Chem. Commun.* **2020**, *56*, 10207–10210.
- [55] H. Brake, E. Peresyphkina, A. V. Virovets, M. Piesch, W. Kremer, L. Zimmermann, C. Klimas, M. Scheer, *Angew. Chem. Int. Ed.* **2020**, *59*, 16241–16246.
- [56] V. Miluykov, A. Kataev, O. Sinyashin, P. Lönnecke, E. Hey-Hawkins, *Organometallics* **2005**, *24*, 2233–2236.
- [57] I. Bezkishko, A. Zagidullin, A. Petrov, V. Miluykov, O. Sinyashin, *Phosphorus Sulfur Silicon Relat. Elem.* **2016**, *191*, 1425–1426.
- [58] A. Dransfeld, L. Nyulászi, P. v. R. Schleyer, *Inorg. Chem.* **1998**, *37*, 4413–4420.
- [59] E. H. Braye, I. Caplier, R. Saussez, *Tetrahedron* **1971**, *27*, 5523–5537.
- [60] N. Maigrot, N. Avarvari, C. Charrier, F. Mathey, *Angew. Chem. Int. Ed.* **1995**, *34*, 590–592.

- [61] R. Bartsch, J. F. Nixon, *Polyhedron* **1989**, *8*, 2407.
- [62] S. M. Mansell, M. Green, R. J. Kilby, M. Murray, C. A. Russell, *C. R. Chim.* **2010**, *13*, 1073–1081.
- [63] F. G. N. Cloke, P. B. Hitchcock, J. F. Nixon, D. J. Wilson, *Organometallics* **2000**, *19*, 219–220.
- [64] J. Steinbach, P. Binger, M. Regitz, *Synthesis* **2003**, *17*, 2720–2724.
- [65] S. B. Clendenning, P. B. Hitchcock, M. F. Lappert, P. G. Merle, J. F. Nixon, L. Nyulászi, *Chem. - Eur. J.* **2007**, *13*, 7121–7128.
- [66] V. Thelen, D. Schmidt, M. Nieger, E. Niecke, W. W. Schoeller, *Angew. Chem. Int. Ed.* **1996**, *35*, 313–315.
- [67] T. Wettling, R. Schneider, F. Zurmühlen, U. Bergsträsser, J. Hoffmann, G. Maas, M. Regitz, P. Binger, *Angew. Chem. Int. Ed.* **1991**, *30*, 207–210.
- [68] D. Heift, Z. Benkő, H. Grützmaker, *Chem. Eur. J.* **2014**, *20*, 11326–11330.
- [69] C. Heindl, A. Schindler, M. Bodensteiner, E. V. Peresykina, A. V. Virovets, M. Scheer, *Phosphorus Sulfur Silicon Relat. Elem.* **2015**, *190*, 397–403.
- [70] D. Rottschafer, S. Blomeyer, B. Neumann, H.-G. Stammler, R. S. Ghadwal, *Chem. Sci.* **2019**, *10*, 11078–11085.
- [71] D. Tofan, C. C. Cummins, *Angew. Chem. Int. Ed.* **2010**, *49*, 7516–7518.
- [72] L. Xu, Y. Chi, S. Du, W.-X. Zhang, Z. Xi, *Angew. Chem. Int. Ed.* **2016**, *55*, 9187–9190.
- [73] A. A. Zagidullin, M. N. Khrizanforov, I. A. Bezkishko, P. Lönnecke, E. Hey-Hawkins, V. A. Miluykov, *J. Organomet. Chem.* **2021**, *956*, 122122.
- [74] I. A. Bezkishko, A. A. Zagidullin, V. A. Milyukov, O. G. Sinyashin, *Russ. Chem. Rev.* **2014**, *83*, 555.
- [75] R. Gupta, P. Maheshwari, M. Kour, *Comput. Theor. Chem.* **2015**, *1060*, 10–16.

- [76] C. Thoumazet, M. Melaimi, L. Ricard, F. Mathey, P. L. Floch, *Organometallics* **2003**, *22*, 1580–1581.
- [77] J. Hydrio, M. Gouygou, F. Dallemer, J.-C. Daran, G. G. A. Balavoine, *Tetrahedron Asymmetry* **2002**, *13*, 1097–1102.
- [78] E. Mattmann, F. Mercier, L. Ricard, F. Mathey, *J. Org. Chem.* **2002**, *67*, 5422–5425.
- [79] A. Zagidullin, V. Miluykov, E. Oshchepkova, A. Tufatullin, O. Kataeva, O. Sinyashin, *Beilstein J. Org. Chem.* **2015**, *11*, 169–173.
- [80] V. A. Miluykov, A. V. Kataev, O. G. Sinyashin, P. Lönnecke, E. Hey-Hawkins, *Mendeleev Commun.* **2006**, *16*, 204–206.
- [81] A. A. Zagidullin, I. A. Bezkishko, V. A. Miluykov, O. G. Sinyashin, *Mendeleev Commun.* **2013**, *23*, 117–130.
- [82] D. Carmichael, F. Mathey, in *New Aspects in Phosphorus Chemistry I* (Eds.: J. P. Majoral) Springer, Berlin, **2002**, pp. 27–51.
- [83] I. A. Bezkishko, A. A. Zagidullin, V. A. Miluykov, O. G. Sinyashin, *Russ. Chem. Bull.* **2014**, *83*, 555–574.
- [84] M. Lein, J. Frunzke, G. Frenking, *Inorg. Chem.* **2003**, *42*, 2504–2511.
- [85] R. Bartsch, F. G. N. Cloke, J. C. Green, R. M. Matos, J. F. Nixon, R. J. Suffolk, J. L. Suter, D. J. Wilson, *J. Chem. Soc., Dalton Trans.* **2001**, 1013–1022.
- [86] F. G. N. Cloke, J. C. Green, J. R. Hanks, J. F. Nixon, J. L. Suter, *J. Chem. Soc., Dalton Trans.* **2000**, 3534–3536.
- [87] G. Frison, F. Mathey, A. Sevin, *J. Phys. Chem. A* **2002**, *106*, 5653–5659.
- [88] X. Sava, L. Ricard, F. Mathey, P. L. Floch, *Organometallics* **2000**, *19*, 4899–4903.
- [89] M. Melaimi, F. Mathey, P. L. Floch, *J. Organomet. Chem.* **2001**, *640*, 197–199.

- [90] E. J. M. Boer, I. J. Gilmore, F. M. Korndorffer, A. D. Horton, A. v. d. Linden, B. W. Royan, B. J. Ruisch, L. Schoon, R. W. Shaw, *J. Mol. Catal. A: Chem.* **1998**, *128*, 155–165.
- [91] S. Reichl, E. Mädl, F. Riedlberger, M. Piesch, G. Balázs, M. Seidl, M. Scheer, *Nat Commun.* **2021**, *12*, 5774.
- [92] L.-S. Wang, T. K. Hollis, *Org. Lett.* **2003**, *5*, 2543–2545.
- [93] C. E. Garrett, G. C. Fu, *J. Org. Chem.* **1997**, *62*, 4534–4535.
- [94] H. Willms, W. Frank, C. Ganter, *Organometallics* **2009**, *28*, 3049–3058.
- [95] D. Carmichael, G. Goldet, J. Klankermayer, L. Ricard, N. Seeboth, M. Stankevič, *Chem. Eur. J.* **2007**, *13*, 5492–5502.
- [96] C. A. P. Goodwin, F. Ortu, D. Reta, N. F. Chilton, D. P. Mills, *Nature* **2017**, *548*, 439–442.
- [97] P. Evans, D. Reta, G. F.S. Whitehead, N. F. Chilton, D. P. Mills, *J. Am. Chem. Soc.* **2019**, *141*, 19935–19940.
- [98] D. P. Mills, P. Evans, *Chem.Eur.J.* **2021**, *27*, 6645–6665.
- [99] K. Ota, R. Kinjo, *Chem. Soc. Rev.* **2021**, *50*, 10594–10673.
- [100] I. A. Bezkishko, A. A. Zagidullin, A. V. Petrov, V. A. Miluykov, T. I. Burganov, S. A. Katsyuba, O. G. Sinyashin, *J. Organomet. Chem.* **2017**, *844*, 1–7.
- [101] R. S. P. Turbervill, J. M. Goicoechea, *Inorg. Chem.* **2013**, *52*, 5527–5534.
- [102] C. Müller, R. Bartsch, A. Fischer, P. G. Jones, R. Schmutzler, *J. Organomet. Chem.* **1996**, *512*, 141–148.
- [103] S. Deng, C. Schwarzmaier, M. Zabel, J. F. Nixon, A. Y. Timoshkin, M. Scheer, *Organometallics* **2009**, *28*, 1075–1081.
- [104] R. S. P. Turbervill, A. R. Jupp, P. S. B. McCullough, D. Ergöçmen, J. M. Goicoechea, *Organometallics* **2013**, *32*, 2234–2244.

- [105] M. Baudler, *Angew. Chem. Int. Ed.* **1987**, *26*, 419–441.
- [106] A. V. Petrov, A. A. Zagidullin, I. A. Bezkishko, M. N. Khrizanforov, K. V. Kholin, T. P. Gerasimova, K. A. Ivshin, R. P. Shekurov, S. A. Katsyuba, O. N. Kataeva, Y. H. Budnikova, V. A. Miluykov, *Dalton Trans.* **2020**, *49*, 17252–17262.
- [107] R. Bartsch, S. Datsenko, N. V. Ignatiev, C. Müller, J. F. Nixon, C. J. Pickett, *J. Organomet. Chem.* **1997**, *529*, 375–378.
- [108] A. E. Brown, B. E. Eichler, *Tetrahedron Lett.* **2011**, *52*, 1960–1963.
- [109] M. H. Habicht, F. Wossidlo, M. Weber, C. Müller, *Chem. Eur. J.* **2016**, *22*, 12877–12883.
- [110] A. R. Petrov, C. G. Daniliuc, P. G. Jones, M. Tamm, *Chem. Eur. J.* **2010**, *16*, 11804–11808.
- [111] S. Giese, K. Klimov, A. Mikeházi, Z. Kelemen, D. S. Frost, S. Steinhauer, P. Müller, L. Nyulászi, C. Müller, *Angew. Chem. Int. Ed.* **2020**, *60*, 3581–3586.
- [112] S. I. Kotretsou, M. P. Georgiadis, *Org. Prep. Proced. Int.* **2000**, *32*, 161–167.
- [113] G. M. Sheldrick, *Acta Cryst. A* **2015**, *A71*, 3-8.
- [114] G. M. Sheldrick, *Acta Cryst. C* **2015**, *71*, 3-8.
- [115] P. Müller, *Crystallogr. Rev.* **2009**, *15*, 57–83.
- [116] O. V. Dolomanov, L. J. Bourhis, R. J. Gildea, J. A. K. Howard, H. Puschmann, *J. Appl. Cryst.* **2009**, *42*, 339–341.
- [117] F. Neese, F. Wennmohs, U. Becker, C. Riplinger, *J. Chem. Phys.* **2020**, *152*, 224108–224126.
- [118] Avogadro: an open-source molecular builder and visualization tool. Version 1.2.0.
- [119] S. Grimme, J. G. Brandenburg, C. Bannwarth, A. Hansen, *J. Chem. Phys.* **2015**, *143*, 54107–54127.
- [120] A. D. Becke, *J. Chem. Phys.* **1993**, *98*, 5648–5652.
- [121] F. Weigend, R. Ahlrichs, *Phys. Chem. Chem. Phys.* **2005**, *7*, 3297–3305.

- [122] F. Weigend, *Phys. Chem. Chem. Phys.* **2006**, *8*, 1057–1065.
- [123] S. Grimme, J. Antony, S. Ehrlich, H. Krieg, *J. Chem. Phys.* **2010**, *132*, 154104.
- [124] A. Klamt, G. Schüürmann, *J. Chem. Soc., Perkin Trans.* **1993**, *2*, 799–805.
- [125] G. Knizia, *J. Chem. Theory Comput.* **2013**, *9*, 4834–4843.
- [126] G. Knizia, J. E. M. N. Klein, *Angew. Chem. Int. Ed.* **2015**, *54*, 5518–5522.
- [127] K. M. Nicholas, J. Siegel, *J. Am. Chem. Soc.* **1985**, *107*, 4999–5001.
- [128] G. Cappozzi, G. Romeo, F. Marcuzzi, *J. Chem. Soc., Chem. Commun.* **1982**, 959–960.
- [129] S. Mandal, S. Nandi, A. Anoop, P. Kumar Chattaraj, *Phys. Chem. Chem. Phys.* **2016**, *18*, 11738–11745.
- [130] A. Velian, C. C. Cummins, *Science* **2015**, *348*, 1001–1004.
- [131] I. Alkorta, J. Elguero, *Struct. Chem.* **2016**, *27*, 1531–1542.
- [132] W. Rösch, M. Regitz, *Angew. Chem.* **1984**, *96*, 898–899.
- [133] J. Heinicke, *Tetrahedron Lett.* **1986**, *27*, 5699–5702.
- [134] D. Schmid, S. Loscher, D. Gudat, D. Bubrin, I. Hartenbach, T. Schleid, Z. Benkőb, L. Nyulászi, *Chem. Commun.* **2009**, 830–832.
- [135] L. Lopez, J.-P. Majoral, A. Meriem, T. N'Gando M'Pondo, J. Navech, J. Barrans, *J. Chem. Soc., Chem. Commun.* **1984**, 183–185.
- [136] W. J. Transue, A. Velian, M. Nava, M.-A. Martin-Drumel, C. C. Womack, J. Jiang, G.-L. Hou, X.-B. Wang, M. C. McCarthy, R. W. Field, C. C. Cummins, *J. Am. Chem. Soc.* **2016**, *138*, 6731–6734.
- [137] A. Velian, C. C. Cummins, *Science* **2015**, *348*, 1001–1004.
- [138] C. Charrier, N. Maignot, L. Ricard, P. L. Floch, F. Mathey, *Angew. Chem. Int. Ed.* **1996**, *35*, 2133–2134.

- [139] A. Efraty, N. Jubran, A. Goldman, *Inorg. Chem.* **1982**, *21*, 868–873.
- [140] N. Kuhn, K. Jendral, R. Boese, D. Bläser, *Eur. J. Inorg. Chem.* **1991**, *124*, 89–91.
- [141] M. Kreye, D. Baabe, P. Schweyen, M. Freytag, C. G. Daniliuc, P. G. Jones, M. D. Walter, *Organometallics* **2013**, *32*, 5887–5898.
- [142] W. Zheng, G. Zhang, K. Fan, *Organometallics* **2006**, *25*, 1548–1550.
- [143] L. Duan, X. Zhanga, W. Zheng, *Dalton Trans.* **2017**, *46*, 8354–8358.
- [144] C. Pi, L. Wan, Y. Gu, W. Zheng, L. Weng, Z. Chen, L. Wu, *Inorg. Chem.* **2008**, *47*, 9739–9741.
- [145] V. Caliman, P. B. Hitchcock, J. F. Nixon, *J. Organomet. Chem.* **1997**, *536–537*, 273–279.
- [146] L. Nyulaszi, T. Veszpremi, J. Reffy, B. Burkhardt, M. Regitz, *J. Am. Chem. Soc.* **1992**, *114*, 9080–9084.
- [147] R. F. W. Bader, *Acc. Chem. Res.* **1985**, *18*, 9–15.
- [148] D. Cremer, E. Kraka, *Angew. Chem. Int. Ed.* **1984**, *23*, 627–628.
- [149] M. A. Bennett, S. K. Bhargava, A. M. Bond, I. M. Burgar, S.-X. Guo, G. Kar, S. H. Privér, J. Wagler, A. C. Willis, A. A. J. Torriero, *Dalton Trans.* **2010**, *39*, 9079–9090.
- [150] R. F. Winter, W. E. Geiger, *Organometallics* **1999**, *18*, 1827–1833.
- [151] E. D. Glendening, J. K. Badenhoop, A. E. Reed, J. E. Carpenter, J. A. Bohmann, C. M. Morales, P. Karafiloglou, C. R. Landis, F. Weinhold, NBO 7.0, Madison, 2018.
- [152] T. Lu and F. W. Chen, *J. Comput. Chem.* **2012**, *33*, 580–592.
- [153] R. Appel, F. Knoll, I. Ruppert, *Angew. Chem. Int. Ed.* **1981**, *20*, 731–744.
- [154] A. Chirila, R. Wolf, J. C. Slootweg, K. Lammertsma, *Coord. Chem. Rev.* **2014**, *270–271*, 57–74.
- [155] G. Becker, G. Gresser, W. Uhl, *Z. Naturforsch. B* **1981**, *36*, 16–19.

- [156] L. N. Markovski, V. D. Romanenko, *Tetrahedron* **1989**, *45*, 6019–6090.
- [157] J. F. Nixon, *Coord. Chem. Rev.* **1995**, *145*, 201–258.
- [158] M. Regitz, *Chem. Rev.* **1990**, *90*, 191–213.
- [159] J. C. Duchamp, M. Pakulski, A. H. Cowley, K. W. Zilm, *J. Am. Chem. Soc.* **1990**, *112*, 6803–6809.
- [160] M. F. Lucas, M. C. Michelini, N. Russo, E. Sicilia, *J. Chem. Theory Comput.* **2008**, *4*, 397–403.
- [161] J. C. T. R. Burckett-St. Laurent, M. A. King, H. W. Kroto, J. F. Nixon, R. J. Suffolk, *J. Chem. Soc., Dalton Trans.* **1983**, 755–759.
- [162] P. B. Hitchcock, M. J. Maah, J. F. Nixon, J. A. Zora, G. J. Leigh, M. A. Bakar, *Angew. Chem. Int. Ed.* **1987**, *26*, 474–475.
- [163] M. Yu. Antipin, A. N. Chernega, K. A. Lysenko, Y. T. Struchkov, J. F. Nixon, *J. Chem. Soc., Chem. Commun.* **1995**, 505–506.
- [164] M. J. Hopkinson, H. W. Kroto, J. F. Nixon, N. P. C. Simmons, *Chem. Phys. Lett.* **1976**, *42*, 460–461.
- [165] H. W. Kroto, J. F. Nixon, N. P. C. Simmons, N. P. C. Westwood, *J. Am. Chem. Soc.* **1978**, *100*, 446–448.
- [166] T. Görlich, D. S. Frost, N. Boback, N. T. Coles, B. Dittrich, P. Müller, W. D. Jones, C. Müller, *J. Am. Chem. Soc.* **2021**, *143*, 19365–19373.
- [167] S. M. Mansell, M. Green, R. J. Kilby, M. Murray, C. A. Russell, *C. R. Chim.* **2010**, *13*, 1073–1081.
- [168] R. Appel, G. Maier, H. Peter Reisenauer, A. Westerhaus, *Angew. Chem. Int. Ed.* **1981**, *20*, 197–197.
- [169] R. Appel, A. Westerhaus, *Tetrahedron Lett.* **1981**, *22*, 2159–2160.

- [170] T. Allspach, M. Regitz, G. Becker, W. Becker, *Synthesis* **1986**, 31–36.
- [171] A. Mack, E. Pierron, T. Allspach, U. Bergsträßer, M. Regitz, *Synthesis* **1998**, 9, 1305–1313.
- [172] A. Grünhagen, U. Pieper, T. Kottke, H. W. Roesky, *Z. Anorg. Allg. Chem.* **1994**, 620, 716–722.
- [173] R. Appel, G. Maier, H. P. Reisenauer, A. Westerhaus, *Angew. Chem. Int. Ed.* **1981**, 20, 197.
- [174] J. A. W. Sklorz, S. Hoof, M. G. Sommer, F. Weißer, M. Weber, J. Wiecko, B. Sarkar, C. Müller, *Organometallics* **2014**, 33, 511–516.
- [175] M. Scheer, S. Deng, O. J. Scherer, M. Sierka, *Angew. Chem. Int. Ed.* **2005**, 44, 3755–3758.
- [176] A. S. Ionkin, W. J. Marshall, B. M. Fish, A. A. Marchione, L. A. Howe, F. Davidson, C. N. McEwen, *Eur. J. Inorg. Chem.* **2008**, 2008, 2386–2390.
- [177] A. S. Ionkin, W. J. Marshall, B. M. Fish, M. F. Schiffhauer, F. Davidson, C. N. McEwen, *Organometallics* **2009**, 28, 2410–2416.
- [178] C. Heindl, E. V. Peresykina, A. V. Virovets, G. Balázs, M. Scheer, *Chem. Eur. J.* **2016**, 22, 1944–1948.
- [179] G. Becker, M. Rössler, G. Uhl, *Z. Anorg. Allg. Chem.* **1982**, 495, 73–88.
- [180] C. Heinl, E. Peresykina, G. Balázs, E. Mädl, A. V. Virovets, M. Scheer, *Chem. Eur. J.* **2021**, 27, 7542–7548.
- [181] L. Weber, *Eur. J. Inorg. Chem.* **1996**, 129, 367–379.
- [182] P. B. Hitchcock, C. Jones, J. F. Nixon, *J. Chem. Soc., Chem. Commun.* **1994**, 2061–2062.
- [183] P. B. Hitchcock, J. A. Johnson, J. F. Nixon, *Angew. Chem. Int. Ed.* **1993**, 32, 103–104.
- [184] T. Marino, M. C. Michelini, N. Russo, E. Sicilia, M. Toscano, *Theor. Chem. Acc.* **2012**, 131, 1141.
- [185] K. D. Dobbs, J. E. Boggs, A. H. Cowley, *Chem. Phys. Lett.* **1987**, 141, 372–375.

- [186] V. Metail, A. Senio, L. Lassalle, J.-C. Guillemin, G. Pfister-Guillouzo, *Organometallics* **1995**, *14*, 4732–4735.
- [187] G. Pfeifer, M. Papke, D. Frost, J. A. W. Sklorz, M. Habicht, C. Müller, *Angew. Chem. Int. Ed.* **2016**, *55*, 11760–11764.
- [188] F. Mathey, in *Phosphorus-Carbon Heterocyclic Chemistry The Rise of a New Domain* (Eds.: A. Schmidpeter), Elsevier, Amsterdam, **2001**, pp. 363–461.
- [189] F. Mathey, *J. Organomet. Chem.* **1994**, *475*, 25–30.
- [190] W. R. Rocha, L. W. M. Duarte, W. B. De Almeida, V. Caliman, *J. Braz. Chem. Soc.* **2002**, *13*, 597–605.
- [191] S. S. Al-Juaid, P. B. Hitchcock, J. A. Johnson, J. F. Nixon, *J. Organomet. Chem.* **1994**, *480*, 45–50.
- [192] R. Bartsch, P. S. Hitchcock, J. A. Johnson, R. M. Matos, J. F. Nixon, *Phosphorus Sulfur Silicon Relat. Elem.* **1993**, *77*, 45–48.
- [193] R. Ghiasi, *Main Group Chem.* **2006**, *5*, 153–161.
- [194] M. L. Sierra, C. Charrier, L. Ricard, F. Mathey, *Bull. Soc. Chim. Fr.* **1993**, *130*, 521–526.
- [195] A. M. Arif, A. R. Barron, A. H. Cowley, S. W. Hall, *J. Chem. Soc., Chem. Commun.* **1988**, 171–172.
- [196] G. Becker, G. Gutekunst, H. J. Wessely, *Z. Anorg. Allg. Chem.* **1980**, *462*, 113–129.
- [197] R. L. Wells, M. F. Self, J. D. Johansen, J. A. Laske, S. R. Aubuchon, L. J. Jones, A. H. Cowley, S. Kamepalli in *Inorganic Syntheses* (Eds.: A. H. Cowley), John Wiley & Sons, Inc., New York, **1996**, pp. 150–158.